

THESE DE DOCTORAT DE L'UNIVERSITE DE STRASBOURG

DISCIPLINE : CHIMIE-PHYSIQUE
SPECIALITE : PHYSICO-CHIMIE DES POLYMERES

**SUPRAMOLECULAR SYSTEMS BASED ON α -CYCLODEXTRINS
AND POLY(ETHYLENE OXIDE) : STRUCTURE AND PROPERTIES OF
PSEUDO-POLYROTAXANES, POLYROTAXANES AND SLIDING GELS**

PRESENTEE PAR

CHRISTOPHE TRAVELET

INGENIEUR ECPM STRASBOURG
CHIMISTE TU DRESDE (ALLEMAGNE)

POUR OBTENIR LE GRADE DE DOCTEUR DE L'UNIVERSITE DE STRASBOURG

SOUTENUE PUBLIQUEMENT A STRASBOURG LE MARDI 16 JUN 2009 A 14 HEURES
DEVANT LE JURY COMPOSE DE :

M. LE DOCTEUR CARLOS MARQUES	DIRECTEUR DE RECHERCHE AU CNRS, ICS STRASBOURG PRESIDENT DU JURY DE THESE, RAPPORTEUR INTERNE
M. LE DOCTEUR LOÏC AUVRAY	DIRECTEUR DE RECHERCHE AU CNRS, LMPI EVRY RAPPORTEUR EXTERNE
M. LE PROFESSEUR SEBASTIEN LECOMMANDOUX	PROFESSEUR DES UNIVERSITES A L'UNIVERSITE DE BORDEAUX RAPPORTEUR EXTERNE
M. LE DOCTEUR ALAIN LAPP	INGENIEUR AU COMMISSARIAT A L'ENERGIE ATOMIQUE, LLB SACLAY EXAMINATEUR
M. LE PROFESSEUR GEORGES HADZIIOANNOU	PROFESSEUR DES UNIVERSITES A L'UNIVERSITE DE BORDEAUX CO-DIRECTEUR DE THESE
M. LE PROFESSEUR GUY SCHLATTER	PROFESSEUR DES UNIVERSITES A L'UNIVERSITE DE STRASBOURG CO-DIRECTEUR DE THESE
M. LE DOCTEUR PASCAL HÉBRAUD	CHARGE DE RECHERCHE AU CNRS (HDR), IPCMS STRASBOURG MEMBRE INVITE

LABORATOIRE D'INGENIERIE DES POLYMERES POUR LES HAUTES TECHNOLOGIES (LIPHT)
25, RUE BECQUEREL – 67087 STRASBOURG CEDEX 2 – FRANCE

THESE DE DOCTORAT DE L'UNIVERSITE DE STRASBOURG

DISCIPLINE : CHIMIE-PHYSIQUE
SPECIALITE : PHYSICO-CHIMIE DES POLYMERES

**SUPRAMOLECULAR SYSTEMS BASED ON α -CYCLODEXTRINS
AND POLY(ETHYLENE OXIDE) : STRUCTURE AND PROPERTIES OF
PSEUDO-POLYROTAXANES, POLYROTAXANES AND SLIDING GELS**

PRESENTEE PAR

CHRISTOPHE TRAVELET

INGENIEUR ECPM STRASBOURG
CHIMISTE TU DRESDE (ALLEMAGNE)

POUR OBTENIR LE GRADE DE DOCTEUR DE L'UNIVERSITE DE STRASBOURG

SOUTENUE PUBLIQUEMENT A STRASBOURG LE MARDI 16 JUN 2009 A 14 HEURES
DEVANT LE JURY COMPOSE DE :

M. LE DOCTEUR CARLOS MARQUES	DIRECTEUR DE RECHERCHE AU CNRS, ICS STRASBOURG PRESIDENT DU JURY DE THESE, RAPPORTEUR INTERNE
M. LE DOCTEUR LOÏC AUVRAY	DIRECTEUR DE RECHERCHE AU CNRS, LMPI EVRY RAPPORTEUR EXTERNE
M. LE PROFESSEUR SEBASTIEN LECOMMANDOUX	PROFESSEUR DES UNIVERSITES A L'UNIVERSITE DE BORDEAUX RAPPORTEUR EXTERNE
M. LE DOCTEUR ALAIN LAPP	INGENIEUR AU COMMISSARIAT A L'ENERGIE ATOMIQUE, LLB SACLAY EXAMINATEUR
M. LE PROFESSEUR GEORGES HADZIIOANNOU	PROFESSEUR DES UNIVERSITES A L'UNIVERSITE DE BORDEAUX CO-DIRECTEUR DE THESE
M. LE PROFESSEUR GUY SCHLATTER	PROFESSEUR DES UNIVERSITES A L'UNIVERSITE DE STRASBOURG CO-DIRECTEUR DE THESE
M. LE DOCTEUR PASCAL HÉBRAUD	CHARGE DE RECHERCHE AU CNRS (HDR), IPCMS STRASBOURG MEMBRE INVITE

LABORATOIRE D'INGENIERIE DES POLYMERES POUR LES HAUTES TECHNOLOGIES (LIPHT)
25, RUE BECQUEREL – 67087 STRASBOURG CEDEX 2 – FRANCE

à Monsieur Robert TRAVELET,

Madame Claudette TRAVELET 

et Monsieur Romain TRAVELET

Ce travail de thèse de doctorat a été réalisé entre le 01 janvier 2006 et le 31 décembre 2008 au sein du Laboratoire d'Ingénierie des Polymères pour les Hautes Technologies (LIPHT) de Strasbourg alors dirigé par Monsieur le Professeur Georges HADZIIOANNOU.

J'adresse mes sincères remerciements à Monsieur le Professeur Georges HADZIIOANNOU, co-directeur de thèse, professeur des universités à l'université de Bordeaux et membre de l'institut universitaire de France, et à Monsieur le Professeur Guy SCHLATTER, co-directeur de thèse, professeur des universités à l'université de Strasbourg et directeur adjoint du LIPHT, pour leur écoute et leurs conseils que je me suis efforcé de suivre au plus près. Leur aide m'a été précieuse et m'a soutenu tout au long de mes travaux de recherche et de rédaction.

J'adresse mes sincères remerciements à Monsieur le Docteur Pascal HÉBRAUD, chargé de recherche au centre national de la recherche scientifique, titulaire d'une habilitation à diriger des recherches, pour m'avoir aidé aux différentes étapes de la recherche et conseillé aux moments difficiles.

Je tiens à remercier Monsieur le Docteur Cyril BROCHON, maître de conférences à l'université de Strasbourg, titulaire d'une habilitation à diriger des recherches, du soin constant qu'il a su si discrètement me témoigner.


Je tiens également à remercier Monsieur le Docteur Alain LAPP (SANS à Saclay), Monsieur le Docteur Stephen KING et Monsieur le Docteur Richard HEENAN (SANS à Didcot, Grande-Bretagne), Monsieur le Docteur Peter LINDNER (SANS à Grenoble), Monsieur le Docteur Dimitri IVANOV et Monsieur le Docteur Denis ANOKHIN (WAXS à Grenoble), Monsieur le Docteur Pascal HÉBRAUD (SLS et DLS à Strasbourg), Monsieur le Docteur Lionel ALLOUCHE (LS-NOESY et LS-DOSY à Strasbourg), Monsieur le Docteur Jésus RAYA (HRMAS-NOESY à Strasbourg) et Monsieur le Docteur Cédric GAILLARD (TEM à Nantes) pour leurs conseils dans leurs domaines de prédilection respectifs.

J'exprime ma profonde gratitude à Monsieur le Docteur Carlos MARQUES, président du jury de thèse et directeur de recherche au centre national de la recherche scientifique,

à Monsieur le Docteur Loïc AUVRAY, directeur de recherche au centre national de la recherche scientifique, à Monsieur le Professeur Sébastien LECOMMANDOUX, professeur des universités à l'université de Bordeaux et membre de l'institut universitaire de France, à Monsieur le Docteur Alain LAPP, ingénieur au commissariat à l'énergie atomique, ainsi qu'à Monsieur le Professeur Georges HADZIIOANNOU, à Monsieur le Professeur Guy SCHLATTER et à Monsieur le Docteur Pascal HÉBRAUD d'avoir accepté d'être membres du jury de thèse.

Par ailleurs, je remercie Monsieur Christophe MÉLART, Monsieur Christophe SUTTER, Monsieur le Docteur Sébastien GALLET, Mademoiselle Chheng NGOV et Madame Catherine KIENTZ, personnels du LIPHT, pour leur soutien d'ordre technique, logistique et administratif.

Je tiens à remercier Monsieur le directeur général du centre national de la recherche scientifique et Monsieur le président du conseil régional d'Alsace pour leur soutien financier dans le cadre d'une bourse de doctorat pour ingénieur, ainsi que l'agence nationale de la recherche pour le financement du projet SUPRAGEL (JC05_50625).

Je tiens aussi à remercier mes parents, Monsieur Robert TRAVELET et Madame Claudette TRAVELET , ainsi que mon frère, Monsieur Romain TRAVELET, pour le soutien et l'attention constants qu'ils ont sus si chaleureusement et si généreusement dispenser.

Strasbourg, le vendredi 10 juillet 2009

Christophe TRAVELET

Titre français :

Systèmes supramoléculaires à base d' α -cyclodextrines et de poly(oxyéthylène) :
structure et propriétés des pseudo-polyrotaxanes, polyrotaxanes et gels glissants

Cette thèse de doctorat a été rédigée en utilisant, pour chaque chapitre, le format habituellement adopté dans les articles scientifiques paraissant dans des revues à comité de lecture. L'indulgence du lecteur est ainsi sollicitée pour les répétitions et redites nécessairement inhérentes à la forme de rédaction choisie.

Le présent mémoire de thèse a été rédigé en langue anglaise, conformément à l'autorisation délivrée par Monsieur le Professeur Eric WESTHOF, professeur des universités à l'université de Strasbourg et vice-président de l'université de Strasbourg chargé de la recherche et de la formation doctorale, le 08 juillet 2008.

Introduction et résumé (en Français).....	15
Abbreviations, acronyms and symbols.....	23
General introduction.....	27
<u>Chapter 1: An introduction to pseudo-polyrotaxanes, polyrotaxanes and sliding gels.....</u>	33
1.1. Supramolecular chemistry.....	35
<i>Catenanes, rotaxanes, knots and Borromean rings</i>	
1.2. Cyclodextrins and their inclusion complexes: catenanes, rotaxanes and derivatives.....	38
1.2.1. Cyclodextrins: genesis and bacterial synthesis.....	38
1.2.2. Cyclodextrins and their inclusion complexes: catenanes, rotaxanes and derivatives.....	41
1.2.2.1. Cyclodextrins: structure and amphiphilic character.....	41
1.2.2.2. Cyclodextrin-based inclusion complexes: pseudorotaxanes.....	44
1.2.2.3. Catenanes and their derivatives.....	46
1.2.2.4. Rotaxanes and their derivatives.....	46
<i>Sliding gels</i>	
1.2.3. Applications of cyclodextrin-based rotaxanes and polyrotaxanes.....	53
1.3. Poly(ethylene oxide) and its inclusion complexes.....	55
1.3.1. Poly(ethylene oxide): synthesis and properties.....	55
1.3.2. Poly(ethylene oxide)-based inclusion complexes.....	59
<u>Chapter 2: Formation and self-organization of pseudo-polyrotaxanes in water.....</u>	63
2.1. Introduction.....	68
2.2. Experimental section.....	72
2.2.1. Materials.....	72
2.2.2. Synthesis.....	72
2.2.3. Characterization methods.....	73
2.3. Results and discussion.....	75
2.3.1. Interactions between α -cyclodextrins and poly(ethylene oxide): threading mechanism.....	75
2.3.2. Pseudo-polyrotaxane formation, aggregation and precipitation at 30 °C.....	84
<i>"Consumption" of unthreaded α-cyclodextrins</i>	
<i>Formation of threaded α-cyclodextrin-based nano-cylinders</i>	
2.3.3. Pseudo-polyrotaxane formation, aggregation and precipitation at various temperatures.....	93
2.3.4. Pseudo-polyrotaxane formation, aggregation and precipitation at various N values.....	96
2.4. Conclusion.....	98
Annexes.....	99

Annexe 2.a: Sensitivity of small-angle neutron scattering measurements in deuterated water.....	99
Annexe 2.b: Influence of the poly(ethylene oxide) terminal group on the kinetics of gelation.....	100

Chapter 3: Physical gels based on polyrotaxanes in dimethyl sulfoxide.....105

3.1. Physical gels based on polyrotaxanes: kinetics of the gelation, and relative contributions of α-cyclodextrin and poly(ethylene oxide) to the gel cohesion.....	109
3.1.1. Introduction.....	110
3.1.2. Experimental section.....	110
3.1.2.1. Materials and polyrotaxane synthesis.....	110
3.1.2.2. Characterization methods.....	111
3.1.3. Results and discussion.....	113
3.1.3.1. Macroscopic signature of the gelation.....	113
3.1.3.2. Role of α -cyclodextrin and poly(ethylene oxide) in the gelation.....	116
3.1.4. Conclusion.....	124
Annexe 3.1.a: Influence of the polyrotaxane concentration on the gelation.....	125
3.2. Structure of physical gels based on polyrotaxanes: multiblock copolymer behaviour and nano-scale self-organization.....	131
3.2.1. Introduction.....	131
3.2.2. Experimental section.....	134
3.2.2.1. Materials.....	134
3.2.2.2. Polyrotaxane synthesis.....	134
3.2.2.3. Characterization method.....	135
3.2.3. Results and discussion.....	136
3.2.3.1. Structure of polyrotaxanes in concentrated solution at high temperature.....	137
3.2.3.2. Structure formation with time of polyrotaxanes in concentrated solution at room temperature.....	141
<i>At lower complexation degree N</i>	
<i>At higher complexation degree N</i>	
3.2.4. Conclusion.....	148
Annexes.....	150
Annexe 3.2.a: Sensitivity of small-angle neutron scattering measurements in deuterated dimethyl sulfoxide.....	150
Annexe 3.2.b: Transmission electron microscopy and atomic force microscopy observations.....	151

Chapter 4: Chemical gels based on polyrotaxanes in dimethyl sulfoxide and water: "sliding gels".....155

4.1. Introduction.....	159
4.2. Experimental section.....	161

4.2.1. Material preparation, polyrotaxane precursor synthesis and sliding gel formation.....	161
4.2.2. Characterization methods.....	162
4.3. Results.....	163
4.3.1. Influence of the cross-linker fraction K in water.....	164
4.3.2. Influence of the complexation degree N in water.....	173
4.3.3. Influence of the cross-linker fraction K in dimethyl sulfoxide.....	175
4.4. Discussion.....	178
4.5. Conclusion.....	184
Annexe 4.a: Materials, polyrotaxane precursor synthesis and sliding gel formation....	185

Chapter 5: Static and dynamic behaviour of polyrotaxanes in solution

<u>in dimethyl sulfoxide</u>	189
5.1. Introduction.....	193
5.2. Experimental section.....	194
5.2.1. Material preparation and polyrotaxane synthesis.....	194
5.2.2. Characterization methods.....	195
5.3. Results and discussion.....	196
5.3.1. Static behaviour of polyrotaxanes in solution.....	196
5.3.2. Dynamic behaviour of polyrotaxanes in solution.....	200
5.4. Conclusion.....	204
General conclusion and perspectives	207
Curriculum vitae succinct.....	217

La science des polymères s'est considérablement développée depuis le premier quart du 20^{ème} siècle, époque où le scientifique allemand Staudinger démontra l'existence de longues chaînes constituées de la répétition de petites unités liées entre elles par liaisons covalentes, appelées "macromolécules" (Makromoleküle dans la version originale) alors que beaucoup pensaient qu'il s'agissait simplement d'agrégats d'entités de faible masse moléculaire.^[A,B,C] Macromolécules et "polymères" sont synonymes^[D] et définis comme "des molécules de relativement haute masse moléculaire, dont la structure comprend essentiellement la répétition multiple d'unités dérivées, réellement ou conceptuellement, de molécules de relativement faible masse moléculaire."^[D] Le mot polymère provient de mots grecs signifiant plusieurs et parties ; il a été inventé en 1833 par le chimiste suédois Berzelius bien longtemps avant les recherches de Staudinger et possédait alors un sens relativement différent de sa définition actuelle.^[E] Staudinger a mené des recherches pionnières dans le domaine des polymères ce qui lui valut le prix Nobel de chimie en 1953.

Les scientifiques ont développé au cours du temps des molécules de polymère possédant des architectures de plus en plus complexes allant de simples polymères linéaires à des polymères en peigne (greffés), doublement greffés, en étoile, en brosse (en tant qu'homopolymères, ou bien en tant que copolymères statistiques, alternés, diblocs ou multiblocs).^[F,G] Certains d'entre eux possèdent des propriétés et des fonctionnalités élaborées telles des propriétés de libération de médicaments, d'adhésion, de croissance cellulaire, d'auto-organisation, de reconnaissance moléculaire, de biocompatibilité ou de biodégradabilité. De telles structures sont basées sur des interactions covalentes, c'est-à-dire sur des molécules de polymère résultant d'interactions covalentes entre sous-unités plus petites. Ces sous-unités sont habituellement de petites molécules bifonctionnelles. Cependant, il est possible de polymériser des sous-unités constituées de deux composants élémentaires liés entre eux

[A] H. Staudinger, *Berichte der Deutschen Chemischen Gesellschaft*, **1920**, 53, 1073-1085.

[B] H. Staudinger et J. Fritschi, *Helvetica Chimica Acta*, **1922**, 5, 785-806.

[C] R. Mülhaupt, *Angewandte Chemie International Edition English*, **2004**, 43, 1054-1063.

[D] A. Jenkins, P. Kratochvíl, R. Stepto et U. Suter, *Pure and Applied Chemistry*, **1996**, 68, 2287-2311 (disponible sur Internet à l'adresse <http://media.iupac.org/publications/pac/1996/pdf/6812x2287.pdf>).

[E] J. Berzelius, *Jahresbericht über die Fortschritte der Physischen Wissenschaften*, **1833**, 12, 63-67 (disponible sur Internet à l'adresse

<http://books.google.fr/books?id=eXs1AAAcAAJ&printsec=titlepage#PPP1,M1>) (en Allemand).

[F] A. Grosberg et A. Khokhlov, *Giant Molecules: Here, There and Everywhere*, Academic Press, San Diego (Etats-Unis d'Amérique), **1997**.

[G] K. Matyjaszewski et T. Davis, *Handbook of Radical Polymerization*, Wiley, Hoboken (Etats-Unis d'Amérique), **2002**.

par une interaction faible comme par exemple l'interaction hôte-invité^[H] abondamment utilisée dans le domaine de la chimie supramoléculaire.^[I,J] De cette manière, des structures en forme de collier peuvent être obtenues.



Figure 1. Exemple d'un collier de perle.

Nonobstant l'existence d'une grande variété de structures supramoléculaires pouvant être obtenue en utilisant les préceptes de la chimie supramoléculaire, nous nous sommes exclusivement intéressés au cours de ce travail de thèse aux colliers de perle. Exactement de la même manière que leurs analogues macroscopiques, les colliers de perle mésoscopiques possèdent les trois éléments qui suivent (Figure 1) :

- des perles,
- des colliers,
- des fermoirs.

Les perles sont combinées avec les colliers par complexation de nombreuses perles creuses sur les colliers. Puis, les colliers ainsi obtenus sont fermés aux deux extrémités en utilisant des fermoirs. En tant que perle, n'importe quelle molécule torique peut être utilisée en théorie. Il en va de même pour le collier (respectivement le fermoir) où toute molécule de polymère téléchélique (respectivement toute molécule fonctionnelle ayant un encombrement stérique suffisant) convient théoriquement. Présentement, des cyclodextrines (CD) et plus particulièrement les α -cyclodextrines (α -CD) sont choisies

[H] M. van den Boogaard, G. Bonnet, P. van't Hof, Y. Wang, C. Brochon, P. van Hutten, A. Lapp et G. Hadziioannou, *Chemistry of Materials*, **2004**, 16, 4383-4385.

[I] D. Amirsakis, M. Garcia-Garibay, S. Rowan, J. Stoddart, A. White et D. Williams, *Angewandte Chemie International Edition English*, **2001**, 40, 4256-4261.

[J] M. Miyauchi, Y. Takashima, H. Yamaguchi et A. Harada, *Journal of the American Chemical Society*, **2005**, 127, 2984-2989.

comme perles (Figure 2a). De plus, le poly(oxyéthylène) (PEO) (Figure 2b) ou plus précisément ses dérivés téléchéliques (dérivés hydroxylés, aminés et carboxylés) sont utilisés comme colliers. De plus, le 2,4-dinitro-1-fluorobenzène (DNFB) et le 1-aminoadamantane sont choisis comme fermoirs.

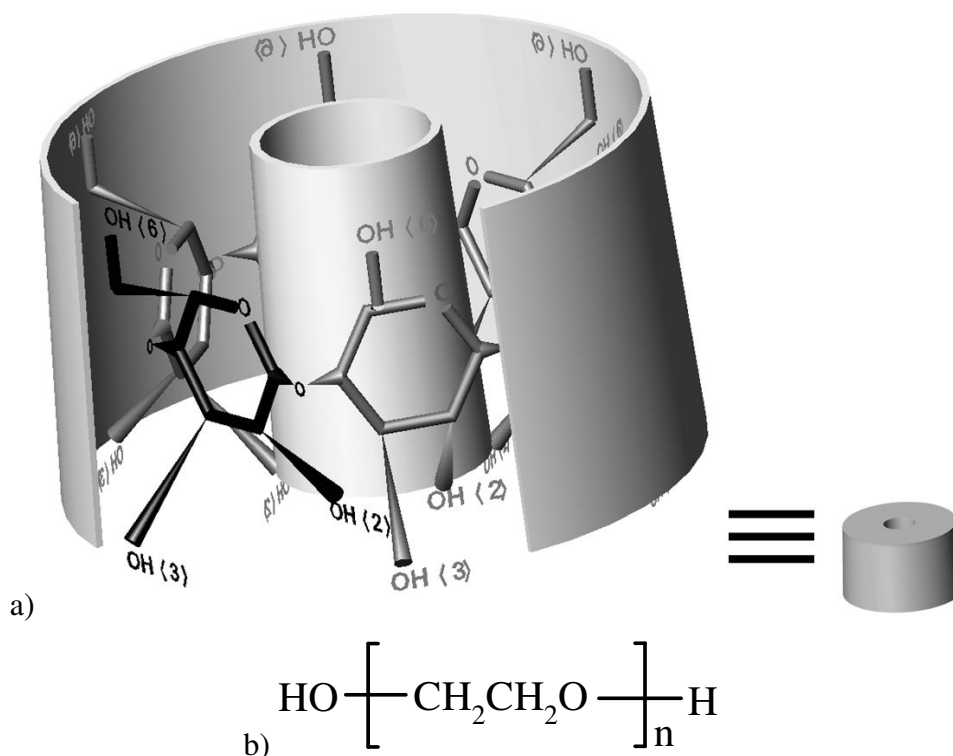


Figure 2. a) Représentations schématiques d'une molécule d' α -CD et b) représentation schématique d'une molécule de PEO ou plus précisément d'une molécule de PEO hydroxytéléchélique, où n représente le degré de polymérisation.

Les α -CD ont la forme d'un cône tronqué qui consiste en la répétition de 6 unités de D-glucose, chacune de ces unités comportant 3 fonctions hydroxyles (une fonction hydroxyle primaire et deux fonctions hydroxyles secondaires) (Figure 2a). Cette forme conique tronquée induit une séparation topologique entre l'intérieur et l'extérieur des α -CD. La répartition spatiale des groupements hydroxyles vers l'extérieur, des atomes d'oxygène interglucosidiques et d'atomes d'hydrogène vers l'intérieur rend la cavité des α -CD moins hydrophile que l'extérieur. Ceci donne la possibilité aux α -CD de complexer des molécules invitées telles que le PEO dont l'hydrophilie est connue pour être fortement dépendante de la température en solution aqueuse. C'est ainsi que le PEO a la capacité d'être encapsulé par les α -CD, formant ce qui s'appelle des complexes d'inclusion (Figure 3).

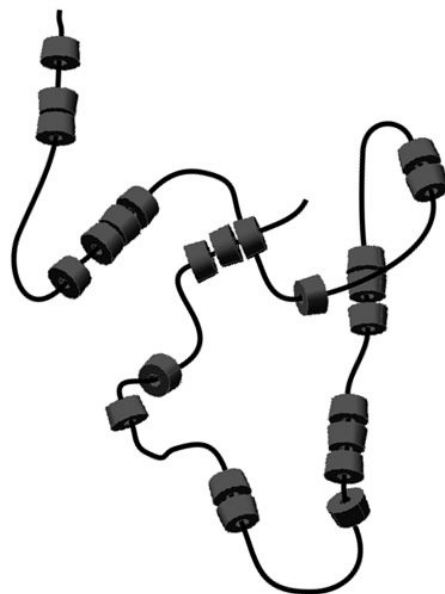


Figure 3. Représentation schématique d'un complexe d'inclusion à base d' α -CD et de PEO montrant des tubes d' α -CD et des segments de PEO nus.

Au cours de ce travail de thèse, nous avons étudié le processus de complexation entre les α -CD et le PEO dans l'eau, conduisant ainsi à la formation de complexes d'inclusion appelés pseudo-polyrotaxanes (PPR) (Figure 3) (**Chapitre 2**).^[K] Les nanostructures résultant de l'auto-organisation des PPR ont été également investiguées *in situ*. Partant d'un mélange liquide α -CD/PEO dans l'eau à une fraction massique totale de 15 w/w% à 70 °C, la formation des PPR au cours du temps à plus basse température (typiquement sur une plage de température allant de 5 °C à 30 °C) induit la formation au cours du temps d'un gel physique de couleur blanche. Une séparation de phase est observée. Nous avons établi à l'aide de méthodes de caractérisation complémentaires de résonance magnétique nucléaire que les molécules de PPR se trouvent exclusivement dans la phase précipitée alors que les molécules d' α -CD non complexées et les chaînes de PEO non complexées sont présentes dans la phase liquide. A 30 °C, la formation du gel physique est bien plus lente qu'à 5 °C. Ainsi, à 30 °C, nous avons établi par le biais de diffusion des neutrons aux petits angles et d'analyse rhéologique dynamique que, dans une première étape, les α -CD complexent les chaînes de PEO, formant des molécules de PPR (Figure 3) qui ne sont pas totalement solubles dans l'eau. A plus grande échelle, une agrégation rapide des molécules de PPR a lieu et des nano-cylindres à base d' α -CD complexées se forment (longueur du cylindre $L = 5.7$ nm et rayon du

[K] C. Travelet, G. Schlatter, P. Hébraud, C. Brochon, A. Lapp et G. Hadziioannou, *Langmuir*, **2009**, doi: 10.1021/la900070v.

cylindre $R = 4.7 \text{ nm}$) (Figure 4a). A plus grande échelle encore, les nano-cylindres à base d' α -CD s'associent de manière gaussienne (Figure 4b), engendrant la formation de domaines précipités lesquels sont responsables de l'importante turbidité du système étudié. A la fin de cette première étape (c'est-à-dire après un temps caractéristique de 20 min), le système demeure encore liquide et les PPR sont totalement formés. Ensuite, dans une seconde étape (c'est-à-dire après un temps caractéristique de 150 min), le système subit une auto-réorganisation caractérisée par une augmentation de la compacité des domaines précipités, et il forme un gel physique.

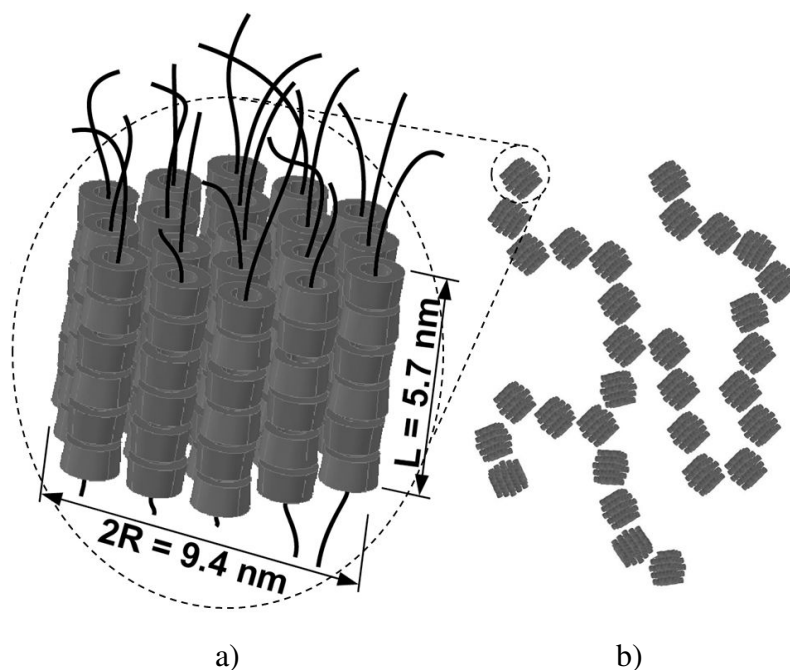


Figure 4. Représentation schématique de : a) un nano-cylindre à base d' α -CD complexées sur des chaînes de PEO et b) de nano-cylindres à base d' α -CD complexées sur des chaînes de PEO organisés de manière gaussienne (par souci de clarté, les α -CD libres et les segments de PEO nus qui connectent les nano-cylindres ne sont pas représentés).

Nous avons ensuite investigué les polyrotaxanes (PR), c'est-à-dire les PPR à base d' α -CD et de PEO bouchonnés stériquement aux extrémités à l'aide de DNFB, en solution concentrée dans le diméthylsulfoxyde (DMSO). Il a été établi par le biais d'analyse rhéologique dynamique que les PPR ont la particularité de former des gels physiques au cours du temps en l'absence de cisaillement à température ambiante (typiquement $21 \text{ }^{\circ}\text{C}$) (**Chapitre 3**). D'un point de vue macroscopique, ce comportement de gélification physique est réversible puisque le mélange redevient liquide par chauffe modérée (typiquement $43 \text{ }^{\circ}\text{C}$) (Figure 5).

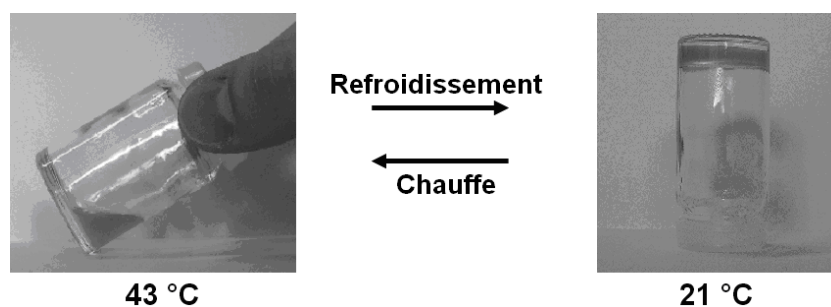


Figure 5. Gélification physique thermo-réversible de PR à base d' α -CD et de PEO à 19.6 w/w% dans le DMSO : état liquide à 43 °C et état gélifié après 24 h à 21 °C.

Nous avons déterminé à l'aide de méthodes de caractérisation complémentaires (calorimétrie différentielle à balayage, diffusion des rayons X aux grands angles, résonance magnétique nucléaire et diffusion des neutrons aux petits angles) que l'origine moléculaire de l'auto-organisation est (Figure 6) :

- d'une part, la cristallisation des segments de PEO nus (c'est-à-dire les unités oxyéthylène des chaînes de PEO qui ne sont pas couvertes par des α -CD),
- d'autre part, l'agrégation régulière des α -CD complexées provenant de liaisons hydrogène intra- et inter-moléculaires par l'intermédiaire de leurs groupements hydroxyles.

La première contribution à la cohésion du gel physique domine pour de basses valeurs du degré de complexation (c'est-à-dire le nombre d' α -CD complexées par chaîne de PEO) alors que la seconde est présente pour de hautes valeurs du degré de complexation.

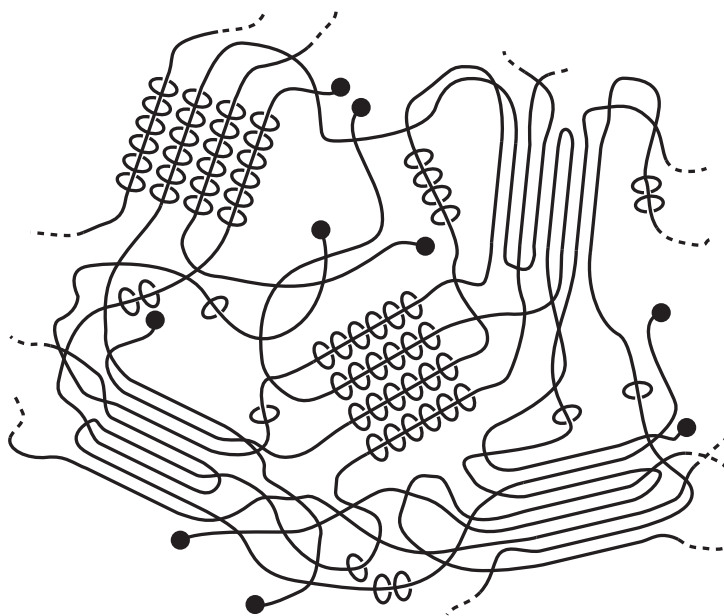


Figure 6. Vue schématique du gel physique à base de PR montrant les deux sortes de domaines réticulés : les cristaux de segments de PEO nus et les agrégats d' α -CD organisés plus ou moins gonflés dans le DMSO. Les domaines réticulés physiquement sont séparés par des domaines amorphes constitués de blocs rotaxane non agrégés ou de PEO nu immergés dans le DMSO.

Ensuite, nous avons étudié les gels chimiques obtenus par réticulation des PR par l'intermédiaire de leurs α -CD de manière intra- et inter-moléculaire à l'aide de divinylsulfone (DVS) (**Chapitre 4**).^[L] La réticulation chimique intramoléculaire conduit à la formation de tubes d' α -CD correspondant à l'empilement d' α -CD le long des chaînes de PEO tandis que la réticulation chimique intermoléculaire engendre la formation du réseau tridimensionnel (Figure 7). A température ambiante, les gels ainsi obtenus gonflent dans l'eau et le DMSO, et se révélèrent être plus hétérogènes dans l'eau. Dans le DMSO, les gels font montre par analyse mécanique dynamique d'une faible dissipation visqueuse à basse fréquence de sollicitation indiquant un mécanisme de relaxation des chaînes efficace. Du fait de l'existence d'un mode de relaxation à basse fréquence de sollicitation, nous pouvons raisonnablement conclure que les gels chimiques gonflés dans le DMSO possèdent des points de réticulation glissants, c'est-à-dire que les α -CD peuvent librement glisser le long des chaînes de PEO. Ainsi, ils sont appelés "gels glissants". Ce comportement n'a pas été observé dans l'eau étant donné que dans ce solvant de gonflement le nombre de points de réticulation physiques augmente drastiquement comparé au DMSO, empêchant ledit glissement.

[L] G. Fleury, G. Schlatter, C. Brochon, C. Travelet, A. Lapp, P. Lindner et G. Hadziioannou, *Macromolecules*, **2007**, 40, 535-543.

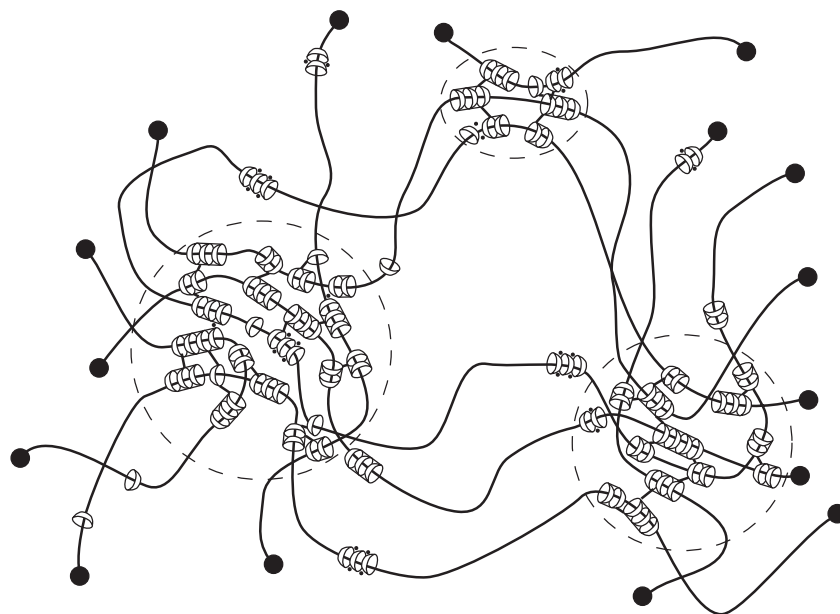


Figure 7. Vue schématique du gel chimique à base de PR gonflé montrant des hétérogénéités structurelles, en l'occurrence des domaines plus réticulés que d'autres.

Pour finir, nous avons investigué si le glissement des α -CD le long des chaînes de PEO peut également être observé au sein des précurseurs des gels glissants, c'est-à-dire les PR, en solution diluée dans le DMSO (**Chapitre 5**). Le DMSO est habituellement considéré comme un bon solvant pour les PR à base d' α -CD et de PEO,^[M] et devrait ainsi diminuer les interactions faibles intra- et inter-moléculaires entre PR et favoriser le glissement des α -CD. Cependant, de gros agrégats de PR possédant une taille caractéristique de 320-500 nm et contenant des tubes d' α -CD correspondant à l'empilement par liaison faible d' α -CD le long des chaînes de PEO ont été trouvés par le biais de diffusion statique de la lumière et de diffusion des neutrons aux petits angles dans les solutions de PR, et ce même en chauffant à 43 °C et en diluant à 0,02 w/w%. La présence d'agrégats empêche l'observation à l'aide de diffusion dynamique de la lumière d'un éventuel glissement des α -CD le long des chaînes de PEO. Un tel glissement a été rapporté ailleurs dans le cas de PR dissout dans une solution aqueuse de soude.^[N] Cependant, dans le DMSO, seules l'auto-diffusion de gros agrégats de PR et l'auto-diffusion de molécules de PR presque indépendantes ont été observées. De plus, le mode de relaxation relatif aux α -CD complexées, aux segments de PEO nus ou bien aux deux espèces a été également raisonnablement attribué.

[M] A. Harada, J. Li et M. Kamachi, *Journal of the American Chemical Society*, **1994**, 116, 3192-3196.

[N] C. Zhao, Y. Domon, Y. Okumura, S. Okabe, M. Shibayama et K. Ito, *Journal of Physics: Condensed Matter*, **2005**, 17, S2841-S2846.

Greek alphabet

α -CD	α -Cyclodextrin
β -CD	β -Cyclodextrin
γ -CD	γ -Cyclodextrin
Γ^{-1}	Decay time
δ	Chemical shift <i>or</i> scattering length density <i>or</i> loss angle
ΔH	Dissolution enthalpy
θ	Observation angle
λ	Wavelength of the used radiation
ξ <i>or</i> Ξ	Correlation lengths
τ	Characteristic time
Φ	Mass fraction <i>or</i> parameter representing the sharpness of the crossover region
ω	Angular frequency

Roman alphabet

a	Coherent diffusion length
AFM	Atomic force microscopy
BA-PEO <i>or</i> PEO _{NH2}	α,ω -Bis-amine-terminated poly(ethylene oxide)
C	Concentration
CD	Cyclodextrin
D	Diffusion coefficient
D _h	Hydrodynamic diameter
DMF	N,N-Dimethylformamide
DMSO	Dimethyl sulfoxide
DMSO-d ₆	Deuterated dimethyl sulfoxide
DNFB	2,4-Dinitro-1-fluorobenzene
DOSY	Diffusion ordered spectroscopy
DSC	Differential scanning calorimetry
DVS	Divinyl sulfone
E'	Elastic Young modulus
E''	Loss Young modulus
E ^{app}	Apparent activation energy
G	Decay time distribution function

G'	Elastic shear modulus
G''	Loss shear modulus
g_2-1	Time-intensity correlation function
GPC	Gel permeation chromatography
GxRy	Sliding gel synthesized with polyrotaxanes having the complexation degree x, y designating the cross-linker volume (in μL) incorporated in the pre-gel solution
hkl	Miller indices
$^1\text{H NMR}$	^1H Nuclear magnetic resonance
HRMAS $^1\text{H NMR}$	High-resolution magic angle spinning ^1H nuclear magnetic resonance
I	Scattering intensity
J_1	First-order Bessel function
K	Cross-linker fraction
L	Length
LS $^1\text{H NMR}$	Liquid-state ^1H nuclear magnetic resonance
m	Mass
n	Refractive index <i>or</i> mole number <i>or</i> polymerization degree
N	Complexation degree
N_A	Avogadro constant
NOESY	Nuclear Overhauser enhancement spectroscopy
P	Form factor
PEO	Poly(ethylene oxide)
PEO_{COOH}	α,ω -Bis-carboxyl-terminated poly(ethylene oxide)
PEO_{NH_2} <i>or</i> BA-PEO	α,ω -Bis-amine-terminated poly(ethylene oxide)
PEO_{OH}	Dihydroxy-terminated poly(ethylene oxide)
PPR	Pseudo-polyrotaxane
PR	Polyrotaxane
q	Modulus of the scattering vector
Q	Heat flow <i>or</i> swelling volume ratio
R	Radius <i>or</i> gas constant
RDA	Rheological dynamic analysis
R_g	Gyration radius
S	Structure factor <i>or</i> swelling degree

SANS	Small-angle neutron scattering
t	Time
T	Temperature
t _a	Aging time
TEM	Transmission electron microscopy
V	Volume <i>or</i> molar volume
v _b	Contrast length density
WAXS	Wide-angle X-ray scattering
w/w%	Weight to weight percentage
[Z]	Concentration of the species Z

GENERAL INTRODUCTION

"Dans la mesure où la rusticité est reconnue pour être une ignorance de ce qui est contraire aux convenances, le rustre est ainsi fait qu'il avale son brouet à la menthe avant de se rendre à l'assemblée, et à ceux de ses voisins que dérange l'odeur, il soutient qu'il n'est rien comme la senteur du thym pour fleurir délicatement. Il porte des chaussures trop grandes pour son pied, et parle d'une voix forte ; n'a confiance ni en ses amis ni en sa famille."

Théophraste (372 - 288 avant J.-C.), Caractères

Polymer science has considerably developed since the time when the German scientist Staudinger demonstrated in 1920 the existence of long chains of short repeating units linked by covalent bonds called "macromolecules" (Makromoleküle in the original German version).^[O,P,Q] Macromolecules and "polymers" are synonyms^[R] and are defined as "molecules of high relative molecular mass, the structure of which essentially comprises the multiple repetition of units derived, actually or conceptually, from molecules of low relative molecular mass."^[R] The word polymer is derived from Greek words meaning many and parts, was coined in 1833 by the Swedish chemist Berzelius a long time before the research by Staudinger and had quite a different meaning from the actual definition.^[S] Staudinger carried out pioneering research on polymers and was awarded with the chemistry Nobel Prize in 1953.

Scientists developed with time polymer molecules possessing more and more complex architectures going from simple linear polymers to comb-like grafted, double-grafted, star-like, brush-like polymers (as homopolymers, or as random, diblock or multiblock copolymers).^[T,U] Some of them possess elaborated properties and functionalities such as drug or gene delivery, adhesion, cell growth, self-organisation, molecular recognition,

[O] H. Staudinger, *Berichte der Deutschen Chemischen Gesellschaft*, **1920**, 53, 1073-1085.

[P] H. Staudinger and J. Fritsch, *Helvetica Chimica Acta*, **1922**, 5, 785-806.

[Q] R. Mülhaupt, *Angewandte Chemie International Edition English*, **2004**, 43, 1054-1063.

[R] A. Jenkins, P. Kratochvíl, R. Stepto and U. Suter, *Pure and Applied Chemistry*, **1996**, 68, 2287-2311 (available via the Internet at <http://media.iupac.org/publications/pac/1996/pdf/6812x2287.pdf>).

[S] J. Berzelius, *Jahresbericht über die Fortschritte der Physischen Wissenschaften*, **1833**, 12, 63-67 (available via the Internet at

<http://books.google.fr/books?id=eXs1AAAcAAJ&printsec=titlepage#PPP1,M1>) (in German).

[T] A. Grosberg and A. Khokhlov, *Giant Molecules: Here, There and Everywhere*, Academic Press, San Diego (USA), **1997**.

[U] K. Matyjaszewski and T. Davis, *Handbook of Radical Polymerization*, Wiley, Hoboken (USA), **2002**.

biocompatibility or biodegradability. Such structures are based on covalent interactions, *i.e.* on polymer molecules made from covalent interactions between smaller subunits. These subunits are usually small bifunctional molecules. But, we can realise polymerisation between subunits made of two elementary components bound with a weak interaction such as host-guest interaction as found in the supramolecular chemistry field.^[V] This way, we can obtain necklace structures.



Figure 8. Example of a pearl necklace.

In the present PhD work, we focus on pearl necklaces although a wide variety of other supramolecular structures can be obtained using the precepts of supramolecular chemistry. Exactly as their macroscopic analogues, mesoscopic pearl necklaces possess the three following parts: pearls, necklaces and clasps (Figure 8). The pearls are combined with the necklaces by threading numerous holed pearls onto the necklaces. Then, the necklaces are closed at both ends using the clasps. As pearl, every ring molecule can be theoretically used. Presently, cyclodextrins (CDs) and more particularly α -cyclodextrins (α -CDs) are taken. Indeed, they are biodegradable, have a truncated cone shape, possess a cavity which is less hydrophilic than the exterior and can thus encapsulate more hydrophobic molecules. Moreover, every polymer chain can be used in theory as necklace. Poly(ethylene oxide) (PEO) is chosen for its capability to be encapsulated by α -CDs, thus forming inclusion complexes.

After a bibliography on CDs, PEO and the diverse supramolecular structures which can be obtained using these compounds (**Chapter 1**), the process of encapsulation, also

[V] M. van den Boogaard, G. Bonnet, P. van't Hof, Y. Wang, C. Brochon, P. van Hutten, A. Lapp and G. Hadziioannou, *Chemistry of Materials*, **2004**, 16, 4383-4385.

called threading, between α -CDs and PEO in water and the resulting nanostructures are studied (**Chapter 2**). Then, α -CD/PEO-based pearl necklaces which are also called more scientifically polyrotaxanes (PRs) are investigated in concentrated solution in dimethyl sulfoxide (DMSO) (**Chapter 3**). Their self-organisation involving interactions between threaded α -CDs and between naked PEO segments (*i.e.* the ethylene oxide units of the PEO chains which are not covered by α -CDs) leads to a physical gelation of the system with time at room temperature. Moreover, PRs can be chemically cross-linked *via* the α -CDs thus forming gels which swell in water and DMSO (**Chapter 4**). This material is permanent compared to the one obtained in chapter 3 and exhibits particular mechanical properties from which we can reasonably think that the α -CDs are able to slide along the PEO chains when the gel is swollen in DMSO. Such chemical gels are called "sliding gels". To finish, it is investigated whether the α -CD sliding along the PEO chains can be observed in PRs in dilute solution in DMSO (**Chapter 5**).

CHAPTER 1

**An introduction to pseudo-polyrotaxanes,
polyrotaxanes and sliding gels**

An introduction to pseudo-polyrotaxanes, polyrotaxanes and sliding gels

1.1. Supramolecular chemistry

The 1987 chemistry Nobel laureate Jean-Marie Lehn awarded for his research in the field of supramolecular chemistry describes this area as follows:^[1] "Beyond molecular chemistry based on the covalent bond, supramolecular chemistry aims at developing highly complex chemical systems from components interacting through non-covalent intermolecular forces." Supramolecular chemistry is thus a broad field dealing with molecular assemblies which are built up from components interacting together through specific non-covalent interactions.

Historically, the existence of non-covalent forces was postulated by Van der Waals in the late 19th century. They were named after him and consist in intra- and/or inter-molecular forces other than those due to covalent bond formation or to electrostatic interaction of ions or of ionic groups with one another or with neutral molecules. Such non-covalent forces can be attractive or repulsive and include permanent dipole - permanent dipole forces, permanent dipole - induced dipole forces and instantaneous induced dipole - induced dipole (London forces). More precisely, the different types of non-covalent interactions used in the field of supramolecular chemistry are the following:

- Belonging to the Van der Waals forces, hydrogen bonds were described in the first quarter of the 20th century.^[2] They consist in non-covalent attractive forces between one electronegative atom and a hydrogen covalently bonded to another electronegative atom. They are directional, involve a limited number of interaction partners and can be strong with bond energies in the range from 5 to 155 kJ mol⁻¹. Thus, knowing that carbon-carbon single bonds have a typical energy of 350 kJ mol⁻¹, hydrogen bonds possess some characteristics of covalent bonds.
- Aromatic interactions, also called π - π stacking, consist in non-covalent interactions between compounds containing aromatic moieties. They originate from the overlapping of p-orbitals of the planar cyclic conjugated systems

[1] J.-M. Lehn, *Science*, **2002**, 295, 2400-2403.

[2] W. Latimer and W. Rodebush, *Journal of the American Chemical Society*, **1920**, 42, 1419-1433.

having $(4n + 2)$ π -electrons where n is a positive integer. In practice, most of the aromatic interactions are intermolecular although intramolecular π - π stacking is also reported.^[3] π - π stacking corresponds to face-to-face interactions and is found in DNA, RNA and proteins. Edge-to-face interactions as for them, also called T-stacking, are characterized by weaker energies compared to face-to-face interactions and result from the interaction between a partially positively charged hydrogen atom of one aromatic system pointing perpendicularly towards the centre of an aromatic plane of the other aromatic system.^[4,5] Moreover, interactions between a cation and an aromatic system called cation- π stacking are known. Recently, anion- π stacking was also reported.^[6]

- The proximity of electric charges with the same sign or not induces the formation of electrostatic forces between them whose magnitude, direction and sense are given by the Coulomb law. Such ionic interactions concern ion pairs and also ion/dipole pairs, and are mainly studied in biological systems.^[7,8]
- When non-polar molecules are present in a polar medium such as water, hydrophobic interactions appear, leading to the formation of intra- and/or inter-molecular associations of the non-polar molecules.^[9] Such non-covalent interactions contribute together with hydrogen bonding to the protein folding.^[10,11] When molecules are partially non-polar, they are amphiphilic and known to associate in solution as spheres, cylinders or other distorted structures in given concentration and temperature conditions.
- The last category of non-covalent interactions is of a complete different nature from those mentioned above. Fischer proposed in the late 19th century that the interactions between enzyme and substrate take the form of a lock and a key which fit together, and distinguished between a special key and a master

[3] A. Fernández-Botello, A. Holý, V. Moreno, B. Operschall and H. Sigel, *Inorganica Chimica Acta*, **2009**, 362, 799-810.

[4] M. Egli, V. Tereshko, G. Mushudov, R. Sanishvili, X. Liu and F. Lewis, *Journal of the American Chemical Society*, **2003**, 125, 10842-10849.

[5] C. Chipot, R. Jaffe, B. Maigret, D. Pearlman and P. Kollman, *Journal of the American Chemical Society*, **1996**, 118, 11217-11224.

[6] C. Garau, A. Frontera, D. Quiñonero, P. Ballester, A. Costa and P. Deyà, *Journal of Physical Chemistry A*, **2004**, 108, 9423-9427.

[7] T. Begenisich and P. de Weer, *Nature*, **1977**, 269, 710-711.

[8] V. Tōugu and T. Kesvatera, *Biochimica et Biophysica Acta: Protein Structure and Molecular Enzymology*, **1996**, 1298, 12-30.

[9] D. Chandler, *Nature*, **2005**, 437, 640-647.

[10] C. Tanford, *Journal of the American Chemical Society*, **1962**, 84, 4240-4247.

[11] G. Rose, P. Fleming, J. Banavar and A. Maritan, *Proceedings of the National Academy of Sciences of the United States of America*, **2006**, 103, 16623-16633.

key.^[12,13] Although this concept appeared later not to be truly valid for all enzymatic reactions, the lock and key principle remains founder of molecular recognition and host-guest chemistry where the host is represented by the lock and the guest by the key. Thus, mechanically interlocking a host with a guest creates interactions which are not of a covalent nature and are called topological interactions.

Supramolecular chemistry goals at rationally designing self-assembling supramolecular systems involving one or more types of the diverse above mentioned non-covalent interactions and especially topological interactions. The design of the desired more or less complex structures having the wished properties requires an enhanced understanding of the relationships between molecular geometry, non-covalent interactions and macroscopic characteristics. Supramolecular chemistry finds applications in the field of molecular recognition and transport (*e.g.* catalysis, molecular wires and ion channels).^[14] The activities in supramolecular chemistry are widespread as shown by the following families that emerged and have been widely studied.

Catenanes and rotaxanes

The supramolecular structures "catenanes" and "rotaxanes" are discussed in sections 1.2.2.3 and 1.2.2.4 respectively.

Knots

"Knots", also called "knotanes", are mechanically-interlocked molecular architectures that are analogous to macroscopic knots we find in daily life.^[15] They are synthesized using templation and folding routes mainly based on metal coordination or hydrogen bonding patterns. Knots in trefoil knot configurations are chiral, having at least two enantiomers.^[16] Naturally knotted forms of DNA and proteins^[17] are known. It was recently discovered that naturally knotted molecules can have sizes of several nanometers and possess quite unusual biochemical activities.

[12] J. Hepburn, *Journal of the Franklin Institute*, **1910**, 170, 85-116.

[13] F. Cramer, *Pharmaceutica Acta Helvetiae*, **1995**, 69, 193-203.

[14] J.-M. Lehn, *Angewandte Chemie International Edition English*, **1990**, 29, 1304-1319.

[15] O. Lukin and F. Vögtle, *Angewandte Chemie International Edition English*, **2005**, 44, 1456-1477.

[16] J.-P. Sauvage, *Accounts of Chemical Research*, **1990**, 23, 319-327.

[17] C. Liang and K. Mislow, *Journal of the American Chemical Society*, **1994**, 116, 11189-11190.

Borromean rings

"Borromean rings" are mechanically-interlocked structures in which at least three macrocycles are interlocked in such a way that breaking any macrocycle allows the others to disassociate.^[18,19] The name Borromean rings comes from their use in the coat of arms of the medieval aristocratic Borromeo family in northern Italy.^[20] Although their organic synthesis seems to be complex, it can be in reality fairly simple as suggested by a classroom experiment on a gram-scale.^[21]

Other types of supramolecular structures having the shape of crinkled tapes or rosettes can be obtained.^[22] As building blocks for supramolecular assemblies, poly(ethylene oxide) (PEO) and cyclodextrins (CDs) can be successfully used.

1.2. Cyclodextrins and their inclusion complexes: catenanes, rotaxanes and derivatives

1.2.1. Cyclodextrins: genesis and bacterial synthesis

CDs were mentioned for the first time by the French scientist Villiers in the late 19th century (Figure 1).^[23,24] They result from the digest of potato starch by the bacterium *bacillus amylobacter* and are obtained as byproduct (0.3 g for 100 g of potato starch). Villiers himself called them cellulose and was able to distinguish between two types of crystalline byproducts which are now thought to be the α -cyclodextrin (α -CD) and the β -cyclodextrin (β -CD).

[18] K. Chichak, S. Cantrill, A. Pease, S.-H. Chiu, G. Cave, J. Atwood and J. Stoddart, *Science*, **2004**, 304, 1308-1312.

[19] A. Peters, K. Chichak, S. Cantrill and J. Stoddart, *Chemical Communications*, **2005**, 27, 3394-3396.

[20] A. Lakshminarayan, *Resonance (Indian Academy of Sciences)*, **2007**, 12, 41-47 (available via the Internet at <http://www.ias.ac.in/resonance/May2007/p41-47.pdf>).

[21] C. Pentecost, N. Tangchaivang, S. Cantrill, K. Chichak, A. Peters and J. Stoddart, *Journal of Chemical Education*, **2007**, 84, 855-859.

[22] J. Zerkowski, C. Seto and G. Whitesides, *Journal of the American Chemical Society*, **1992**, 114, 5473-5475.

[23] A. Villiers, *Comptes Rendus de l'Académie des Sciences*, **1891**, 112, 435-437 (available via the Internet at <http://visualiseur.bnf.fr/ark:/12148/bpt6k3068q>) (in French).

[24] A. Villiers, *Comptes Rendus de l'Académie des Sciences*, **1891**, 112, 536-538 (available via the Internet at <http://visualiseur.bnf.fr/ark:/12148/bpt6k3068q>) (in French).

CHIMIE ORGANIQUE. — *Sur la transformation de la fécule en dextrine par le ferment butyrique.* Note de M. A. VILLIERS.

« Ayant entrepris l'étude de l'action des ferments figurés sur les hydrates de carbone, dans des conditions diverses, je donnerai ici les premiers résultats relatifs à l'action du *ferment butyrique* (*Bacillus amylobacter*) sur la fécule de pomme de terre.

» Il est facile de transformer la matière amylacée en dextrine sous l'action de ce ferment.

[...]

» Le bacille se présente, au début, sous la forme de bâtonnets rectilignes, très mobiles. A la fin de la fermentation, il s'est transformé en bâtonnets épaissis uniformément à leur extrémité, en forme caractéristique de têtard : ils sont alors complètement immobiles. A partir de ce moment, les produits de la fermentation ne sont plus modifiés.

» De petites bulles gazeuses se dégagent pendant cette transformation de la fécule; mais la quantité de gaz dégagé est si faible, qu'il est impossible d'en recueillir.

» Le liquide ainsi obtenu est très légèrement acide et présente nettement l'odeur de l'acide butyrique, mais ne renferme qu'une quantité insignifiante de ce dernier (environ 0,3 parties pour 100 de fécule).

» Outre certains corps qui se forment aussi en très petite quantité, et sur lesquels je reviendrai prochainement, les produits principaux de la fermentation sont constitués par des dextrines, non attaquables par le *Bacillus amylobacter*, du moins en présence des autres produits qui sont formés simultanément.

Figure 1. Beginning of the paper by Villiers mentioning for the first time what is nowadays called CD.^[23]

Schardinger, as for him, showed that the bacterial strain *aerobacillus macerans* leads also to the formation of crystalline CDs.^[25,26,27] He distinguished between the two types of CDs, α -CD and β -CD, because of their ability to form crystalline adducts of different colours in presence of iodine solution. Moreover, he completed the first observations by Villiers and showed that CDs can be obtained from starch of different sources, such as potato, rice or wheat, thanks to the exploration of various types of bacteria. Historically, different terms were used to designate what is currently called CD: cellulosine,^[24] afterwards crystalline dextrin (krystallisiertes Dextrin in the original German version)^[28] and then Schardinger dextrin in his honour.

The two types of CDs obtained by Villiers and Schardinger, α -CD and β -CD, were later identified as ring structures consisting of the repetition of 6 (Figure 2) and 7 D-glucose

[25] F. Schardinger, *Zentralblatt für Bakteriologie und Parasitenkunde, 2. Abteilung*, **1908**, 22, 98.

[26] F. Schardinger, *Zentralblatt für Bakteriologie und Parasitenkunde, 2. Abteilung*, **1911**, 29, 188-197.

[27] E. Tilden and C. Hudson, *Journal of the American Chemical Society*, **1939**, 61, 2900-2902.

[28] F. Schardinger, *Zeitschrift für Untersuchung der Nahrungs- und Genußmittel*, **1903**, 6, 865-880.

units respectively.^[29,30,31] γ -cyclodextrin (γ -CD) was discovered by Freudenberg^[32] and its ring structure consisting of the repetition of 8 D-glucose units was elucidated later.^[33] Thus, α -CD, β -CD and γ -CD were also commonly named cyclomaltohexaose, cyclomaltoheptaose and cyclomaltooctaose respectively. Larger CDs having up to more than 100 D-glucose units in the ring also exist.^[34,35] CDs result from the degradation through an intramolecular transglycosylation reaction of starch or starch derivatives by the enzyme cyclodextrin glucanotransferase (CGTase)^[36] which is from bacterial origin (*Bacillus amylobacter*, *Aerobacillus macerans*, *Bacillus clausii*...). The ratio of the quantity of amylose (*i.e.* the linear polysaccharide fraction) and amylopectin (*i.e.* the branched polysaccharide fraction) present in the starch is an important parameter regarding the bacterial CD production.^[37] During the degradation, the helicoidal structure of amylose with loops of 6 to 7 D-glucose units disappears forming macrocyclic structures.^[38] CDs obtained by a bacterial path consist of a mixture of CDs with different numbers of D-glucose units in which the α -CD, β -CD and γ -CD are generally the most abundant forms. Thus, the obtention yield of larger CDs remains low and their purification is not cost-effective what make them inappropriate for large-scale use.

[29] K. Freudenberg and M. Meyer-Delius, *Berichte der Deutschen Chemischen Gesellschaft*, **1938**, 71, 1596-1600.

[30] K. Freudenberg, E. Schaaf, G. Dumpert and T. Ploetz, *Naturwissenschaften*, **1939**, 27, 850-853.

[31] D. French and R. Rundle, *Journal of the American Chemical Society*, **1942**, 64, 1651-1653.

[32] K. Freudenberg and R. Jacobi, *Liebigs Annalen der Chemie*, **1935**, 518, 102-108.

[33] K. Freudenberg and F. Cramer, *Zeitschrift für Naturforschung*, **1948**, 3b, 464.

[34] W. Saenger, J. Jacob, K. Gessler, T. Steiner, D. Hoffmann, H. Sanbe, K. Koizumi, S. Smith and T. Takaha, *Chemical Reviews*, **1998**, 98, 1787-1802.

[35] J. Jacob, K. Gessler, D. Hoffmann, H. Sanbe, K. Koizumi, S. Smith and T. Takaha and W. Saenger, *Angewandte Chemie International Edition English*, **1998**, 37, 605-609.

[36] A. Nakamura, K. Haga, S. Ogawa, K. Kuwano, K. Kimura and K. Yamane, *FEBS Letters*, **1992**, 296, 37-40.

[37] H. Alves-Prado, A. Carneiro, F. Pavezzi, E. Gomes, M. Boscolo, C. Franco and R. da Silva, *Applied Biochemistry and Biotechnology*, **2008**, 146, 3-13.

[38] H. Bender, *Advances in Biotechnological Processes*, **1986**, 6, 31-71.

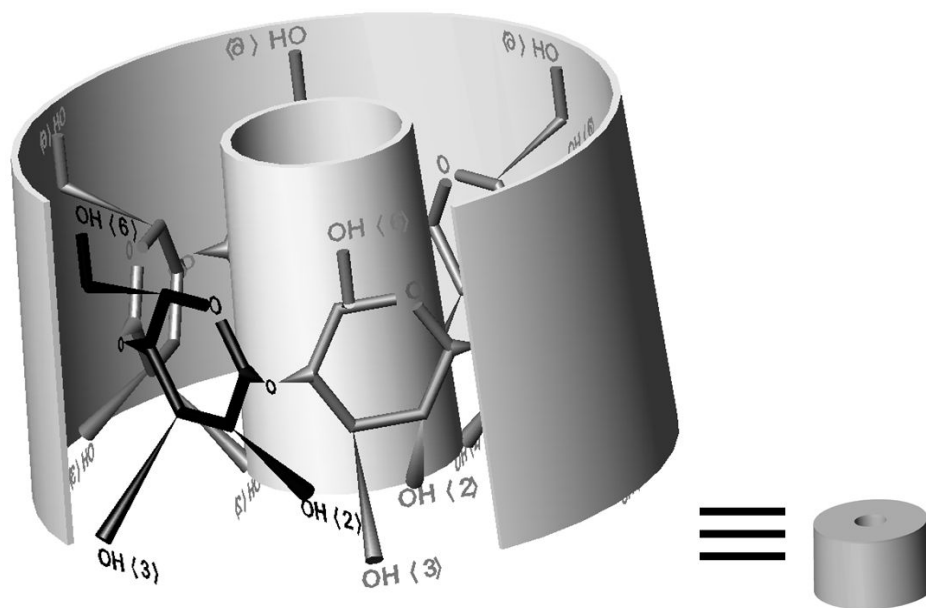


Figure 2. Schematic representations of an α -CD molecule.

In the 1950's, high interest was paid on the ability of CDs to form inclusion complexes with various compounds^[39] as shown by the publication of the first patent related to the CD-based inclusion complexes in 1953.^[40] Since the 1950's, research in the field of CDs has developed and remains at the present time a hot domain as shown by the 1537 publications having the word "cyclodextrin" in their title, abstract or keywords issued in the year 2008.^[41] Thus, CDs and CD-based inclusion complexes, and their related applications have attracted the attention of numerous scientists.

1.2.2. Cyclodextrins and their inclusion complexes: catenanes, rotaxanes and derivatives

1.2.2.1. Cyclodextrins: structure and amphiphilic character

CD structure was resolved using X-ray diffraction investigations.^[42,43] Complementarily, neutron diffraction studies were used to determine the accurate

[39] F. Cramer, *Einschlußverbindungen*, Springer, Berlin (Germany), **1954**.

[40] K. Freudenberg, F. Cramer and H. Plieninger, *Verfahren zur Herstellung von Einschlußverbindungen Physiologisch Wirksamer Organischer Verbindungen*, Knoll A.-G. Chemische Fabriken, German Patent Number 895769, November **1953** (available via the Internet at http://gb.espacenet.com/search97cgi/s97_cgi.exe?Action=FormGen&Template=gb/en/advanced.hts) (in German).

[41] Search carried out on the worldwide website <http://www.scopus.com/scopus/search/form.url>.

[42] P. Manor and W. Saenger, *Journal of the American Chemical Society*, **1974**, 96, 3630-3639.

[43] P. Manor and W. Saenger, *Nature*, **1972**, 237, 392-393.

positions of the hydrogen atoms.^[44] It appears that the CDs constituted by a moderate number of D-glucose units like α -CD, β -CD and γ -CD are organized as a truncated cone, each D-glucose unit having a 4C_1 chair conformation (Figure 3). On the contrary, CDs with a higher number of D-glucose units in the ring form cylinders without revolution symmetry.^[34,35] As far as concerns α -CD, β -CD and γ -CD, the secondary hydroxyl groups OH(2) and OH(3) are situated on the large rim of the truncated cone whereas the primary hydroxyl groups OH(6) are on the small rim. Thus, for α -CD, 12 hydroxyl groups are on the large rim and 6 hydroxyl groups are on the small rim (Figure 2). On the one hand, all the hydroxyl groups are in contact with the exterior of the CD, what confers the CD exterior its hydrophilic character. Thus, the hydroxyl groups which are potentially in contact with surrounding water molecules are responsible for the CD water solubility. On the other hand, the repartition of the interglucosidic oxygen atoms towards the CD interior, combined with the presence of hydrogen atoms in the cavity, give the CD interior its hydrophobic or at least less hydrophilic character. CDs can form intramolecular hydrogen bonds between the hydroxyl groups OH(2) belonging to a D-glucose unit and OH(3) belonging to a neighbouring D-glucose unit. These bonds are geometrically favoured in the case of β -CD, contrary to α -CD and γ -CD. As a consequence, they confer β -CD a very rigid structure and decrease its ability to form hydrogen bonds with surrounding water molecules. Thus, the water solubility is lower for β -CD than for the other common CDs as shown in Table 1 together with other physico-chemical data concerning α -CD, β -CD and γ -CD.

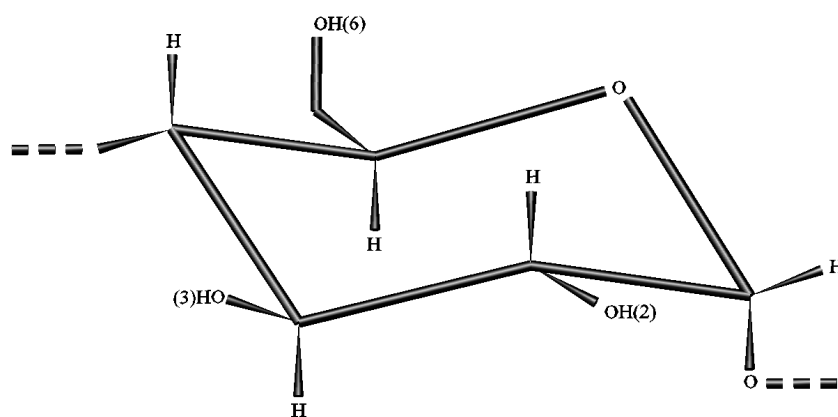


Figure 3. Schematic representation of the 4C_1 chair conformation of a D-glucose unit.

[44] B. Klar, B. Hingerty and W. Saenger, *Acta Crystallographica, Section B*, **1980**, 36, 1154-1165.

Table 1. Physico-chemical data concerning the most common CDs.^[34,45]

	α -CD	β -CD	γ -CD
Number of D-glucose units	6	7	8
Molecular formula	C ₃₆ H ₆₀ O ₃₀	C ₄₂ H ₇₀ O ₃₅	C ₄₈ H ₈₀ O ₄₀
Molecular weight [g mol ⁻¹]	972	1135	1297
Solubility in water at room temperature [g L ⁻¹]	145	18.5	232
Number of hydration water molecules	6 - 8	11 - 12	13 - 14
Cavity external diameter [nm]	1.46 ± 0.04	1.54 ± 0.04	1.75 ± 0.04
Cavity internal diameter (small rim - large rim) [nm]	0.47 - 0.53	0.60 - 0.65	0.75 - 0.83
Height of truncated cone [nm]	0.79 ± 0.01	0.79 ± 0.01	0.79 ± 0.01
Cavity volume [nm ³]	0.174	0.262	0.427
pK _a in water at room temperature †	12.33	12.20	12.08

†: determined by potentiometric method

Due to the presence of numerous CD hydroxyl groups, water molecules favourably bind to CDs. Thus, native α -CD with its 18 hydroxyl groups per molecule weakly links to 6 up to 8 water molecules. Among them, two water molecules are included within the α -CD cavity.^[46] Native CDs are known to adopt a cage structure, also called herringbone structure, in which both ends of the CD cavity are blocked by adjacent molecules (Figure 4).

[45] J. Szejtli, *Chemical Reviews*, **1998**, 98, 1743-1753.

[46] J. Szejtli, T. Osa and J.-M. Lehn, *Comprehensive Supramolecular Chemistry. Cyclodextrins*, Pergamon, Oxford (Great Britain), **1996**, volume 3.

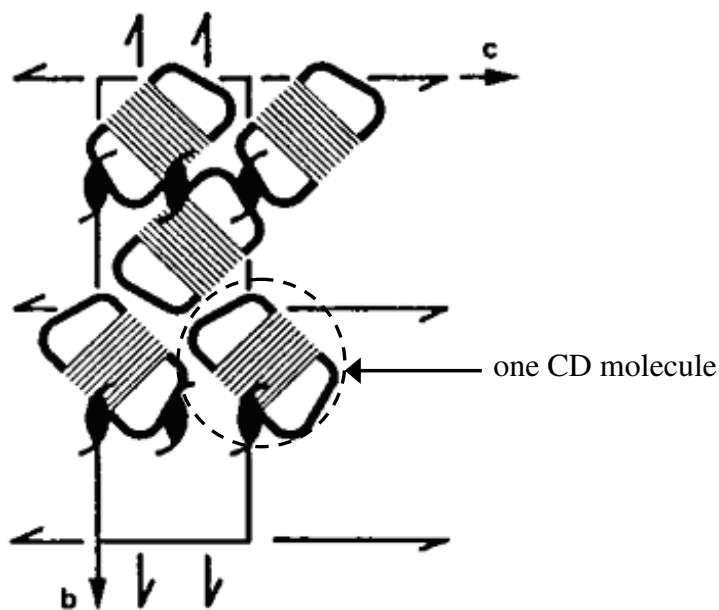


Figure 4. Schematic representation of the cage structure, also called herringbone structure (reproduced from reference 47).

The topological separation between the CD interior and exterior induced by the truncated cone shape of the most common CDs (Figure 2) and the less hydrophilic CD cavity compared to the exterior give the possibility to CDs to form inclusion complexes with guest molecules.

1.2.2.2. Cyclodextrin-based inclusion complexes: pseudorotaxanes

Low and high molecular weight compounds can form inclusion complexes with CDs.^[48,49] They are called "pseudorotaxanes" and "semirotaxanes", the latter term being however in practice less frequently used, and are obtained most of the time in water. Conditions for complexation to occur are not obvious and most of the time empirically determined. In presence of low molecular weight non-ionic compounds, CDs adopt the cage structure (Figure 4), *e.g.* α -CD with water^[42,50] or methanol,^[51] or the brick structure, also called layer structure (Figure 5a), *e.g.* α -CD with *p*-nitrophenol^[52] or 2-pyrrolidone.^[53] When higher molecular weight compounds are threaded by CDs, the

[47] J. Atwood, J. Davies and D. MacNicol, *Inclusion Compounds. Structural Aspects of Inclusion Compounds Formed by Organic Host Lattices*, Academic Press, London (Great Britain), **1984**, volume 2.

[48] M. Rekharsky and Y. Inoue, *Chemical Reviews*, **1998**, 98, 1875-1917.

[49] G. Wenz, B.-H. Han and A. Müller, *Chemical Reviews*, **2006**, 106, 782-817.

[50] K. Harata, *Chemical Reviews*, **1998**, 98, 1803-1827.

[51] B. Hingerty and W. Saenger, *Journal of the American Chemical Society*, **1976**, 98, 3357-3365.

[52] K. Harata, *Bulletin of the Chemical Society of Japan*, **1977**, 50, 1416-1424.

[53] K. Harata, *Bulletin of the Chemical Society of Japan*, **1979**, 52, 2451-2459.

channel structure is obtained (Figure 5b).^[54] However, the channel structure can also be obtained with low molecular weight ionic compounds.^[54,55,56]

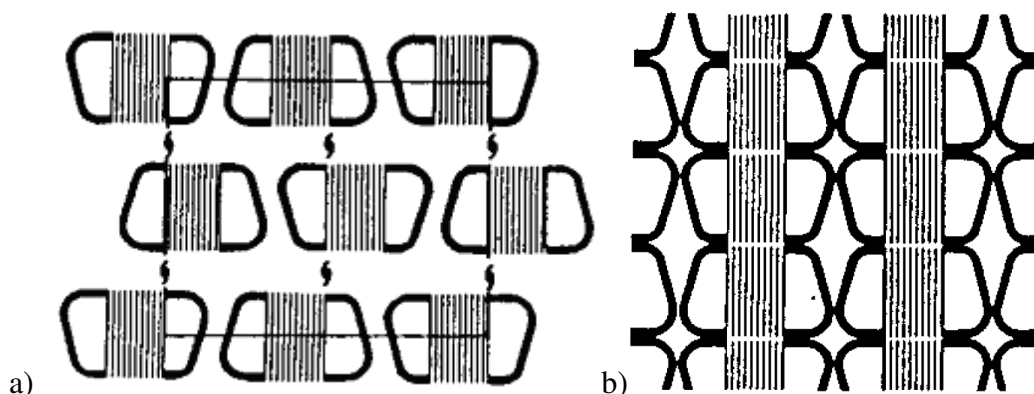


Figure 5. Schematic representations of: a) the brick structure, also called layer structure, and b) the channel structure (reproduced from reference 47).

The inclusion complexes themselves can have various stoichiometries (Figure 6), depending on the size of the guest molecules and on their physico-chemical properties (*e.g.* repartition of the hydrophilic and hydrophobic parts). Such systems should not be imagined to be static in solution. Equilibriums are found between free CDs / free guest molecules and inclusion complexes. They are characterized by binding constants which are determined using for instance microcalorimetric or potentiometric methods.^[48,57] Chemists are able to design inclusion complexes having various, more or less complex, architectures.

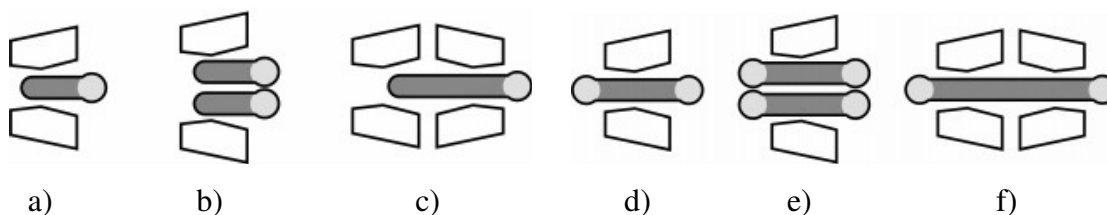


Figure 6. Schematic representations of inclusion complexes having various stoichiometries: a) 1:1, b) 1:2, c) 2:1, d) 1:1, e) 1:2 and f) 2:1. The hydrophilic part of the low molecular weight guest molecule is shown in light gray whereas the hydrophobic part is represented in dark gray (reproduced from reference 49).

[54] R. McMullan, W. Saenger, J. Fayos and D. Mootz, *Carbohydrate Research*, **1973**, 31, 37-46.

[55] A. Hybl, R. Rundle and D. Williams, *Journal of the American Chemical Society*, **1965**, 87, 2779-2788.

[56] M. Noltemeyer and W. Saenger, *Nature*, **1976**, 259, 629-632.

[57] K. Connors, *Chemical Reviews*, **1997**, 97, 1325-1357.

1.2.2.3. Catenanes and their derivatives

CD-based "catenanes" are obtained from pseudorotaxanes according to the following general strategy:^[58] Guest molecules are threaded by CDs, thus forming pseudorotaxanes, and then both ends of the guest molecules are covalently connected each other in an intramolecular way (Figure 7). The main drawback of such a synthesis strategy is the obtention of byproducts due to possible intermolecular reactions between guest molecules.^[59]

Thus, the word catenane designates a wide family of inclusion complexes in which at least two rings are topologically linked together (Figure 7). No covalent bond exists between the two or more rings forming the catenane molecule. Olympiadane is the most famous catenane since its five mechanically interlocked macrocycles resemble the Olympic rings.^[60] The ability of chemists to design complicated structures such as pretzelanes,^[61] bridged catenanes called after the Alsatian bread pastry pretzel, and handcuff-like catenanes^[62] should also be mentioned.

Catenanes have fascinating exotic forms. However, most of them are designed without any particular practical use in mind except molecular machines and switches.

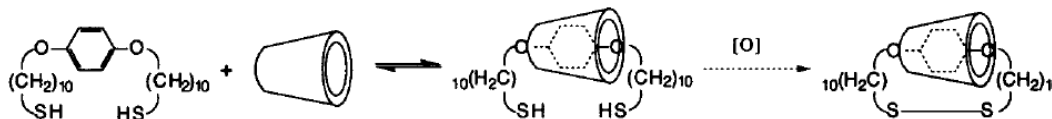


Figure 7. Representation of the general strategy used for the synthesis of CD-based catenanes (reproduced from reference 63).

1.2.2.4. Rotaxanes and their derivatives

"Rotaxanes" are also synthesized from pseudorotaxanes which are sterically capped at both ends of the guest molecules using steric stoppers, thus hindering the eventual dethreading between CDs and guest molecules (Figure 8). The word rotaxane is built from the words rotation and axis, and thus designates a structure in which a ring is able to rotate around an axis. No covalent bond exists between the ring and the axis forming

[58] A. Lüttringshaus, F. Cramer, H. Prinzbach and F. Henglein, *Liebigs Annalen der Chemie*, **1958**, 613, 185-198.

[59] S. Nepogodiev and J. Stoddart, *Chemical Reviews*, **1998**, 98, 1959-1976.

[60] D. Amabilino, P. Ashton, A. Reider, N. Spencer and J. Stoddart, *Angewandte Chemie International Edition English*, **1994**, 33, 1286-1290.

[61] C. Reuter, A. Mohry, A. Sobanski and F. Vögtle, *Chemistry: a European Journal*, **2000**, 6, 1674-1682.

[62] J. Frey, T. Kraus, V. Heitz and J.-P. Sauvage, *Chemical Communications*, **2005**, 42, 5310-5312.

[63] G. Breault, C. Hunter and P. Mayers, *Tetrahedron*, **1999**, 55, 5265-5293.

the rotaxane molecule. By the way, it should be noticed that the nomenclature of catenanes, rotaxanes and their related structures is not obvious.^[64]

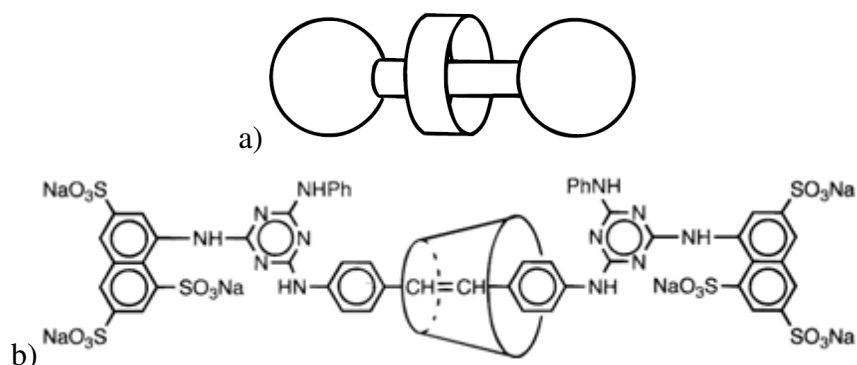


Figure 8. a) Schematic representation of a rotaxane molecule and b) example of a CD-based rotaxane molecule (reproduced from reference 59).

Different strategies can be envisaged so as to obtain rotaxanes (Figure 9). However, since CDs possess intrinsically a ring shape, the clipping approach is excluded when using CDs (Figure 9a). The slippage method consists in fact in the formation of pseudorotaxanes which are for thermodynamic and kinetic reasons stable in the threaded form in the studied medium. They can thus be called rotaxanes (Figure 9c) and be used as such. In this approach, the type of used CD (particularly its size) and the choice of the steric stopper (for instance its ionic character) are important parameters. In practice, the threading approach is the most used one (Figure 9b).

[64] O. Safarowsky, B. Windisch, A. Mohry and F. Vögtle, *Journal für Praktische Chemie*, **2000**, 342, 437-444.

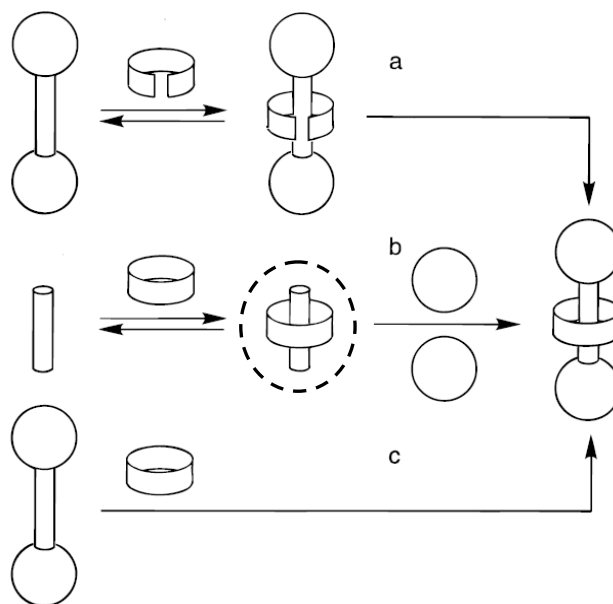


Figure 9. Schematic representations of different routes leading to rotaxanes:
 a) clipping approach, b) threading approach and c) slippage approach
 (reproduced from reference 59).

Strictly speaking, distinction is made between "polypseudorotaxane" corresponding to pseudorotaxane molecules (resulting from the threading of CDs with monomer units, like the one shown by a dashed circle in Figure 9b) which are polymerized,^[65,66] and "pseudo-polyrotaxane" corresponding to polymer chains (resulting from polymerized monomer units) which are threaded by CDs.^[67,68] In the first case, CD threading occurs with low molecular weight compounds whereas in the second case it occurs with high molecular weight compounds. However, the semantic distinction based on the way the inclusion complexes are obtained is not always made in practice. Thus, the term pseudo-polyrotaxane (PPR) is used in the following. When a PPR molecule is capped at both polymer chain ends using steric stoppers, the word "polyrotaxane" (PR) is used. Among the exotic architectures of PPR and PR molecules, it is possible to distinguish between main-chain PPRs or PRs (Figures 10a, 10b, 10e, 10f, 10g, 10h and 10i) and side-chain PPRs or PRs (Figures 10c, 10d and 10j).

[65] S. Anderson, R. Aplin, T. Claridge, T. Goodson, A. Maciel, G. Rumbles, J. Ryan and H. Anderson, *Journal of the Chemical Society, Perkin Transactions 1*, **1998**, 15, 2383-2397.

[66] C. Lagrost, J.-C. Lacroix, S. Aeiyaich, M. Jouini, K. Chane-Ching and P.-C. Lacaze, *Chemical Communications*, **1998**, 4, 489-490.

[67] I. Yamaguchi, K. Kashiwagi and T. Yamamoto, *Macromolecular Rapid Communications*, **2004**, 25, 1163-1166.

[68] H. Okumura, M. Okada, Y. Kawaguchi and A. Harada, *Macromolecules*, **2000**, 33, 4297-4298.

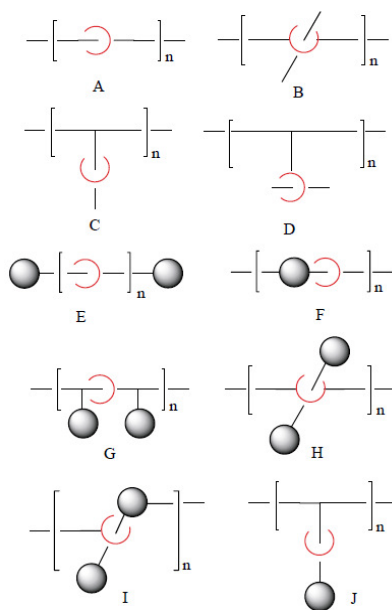


Figure 10. Schematic representations of: a, b, c, d) PPR molecules and e, f, g, h, i, j) PR molecules (reproduced from reference 69).

When pseudorotaxane molecules are polymerized, a higher coverage by CDs of the resulting polymer chains is achieved compared to a direct threading of polymer chains by CDs, although a surprising counterexample is reported in which CDs are not found on the final polymer chains.^[70] The polymerization of pseudorotaxane molecules has the characteristic to isolate more or less completely the monomer units from the exterior, to better solubilize them and thus to achieve a more efficient polymerization.

When polymer chains are aimed to be directly threaded by CDs, the experimental conditions for threading to occur are not always easily determinable. From a thermodynamic point of view, solvent molecules weakly bounded to the CD cavities^[71,72] and to the polymer chain coils are released, essentially inducing a loss of Van der Waals and hydrogen bonding stabilization, but a gain of translational and rotational motional freedom of the solvent molecules. Then, the released solvent molecules restructure and form hydrogen bonds again. Finally, CDs and polymer chains thread, principally inducing a change in the CD conformational energy and in the Van der Waals stabilization.

[69] F. Huang and H. Gibson, *Progress in Polymer Science*, **2005**, 30, 982-1018.

[70] C. Lagrost, J.-C. Lacroix, K. Chane-Ching, M. Jouini, S. Aeiyaich and P.-C. Lacaze, *Advanced Materials*, **1999**, 11, 664-667.

[71] T. Shikata, R. Takahashi and Y. Satokawa, *Journal of Physical Chemistry B*, **2007**, 111, 12239-12247.

[72] T. Shikata, R. Takahashi, T. Onji, Y. Satokawa and A. Harada, *Journal of Physical Chemistry B*, **2006**, 110, 18112-18114.

Besides the inclusion complex formation, capping PPR molecules at both polymer chain ends using steric stoppers which can be cleavable^[73] or permanent is of crucial importance as shown by the development of various end-capping reactions in the solid state^[74] and in solution (*e.g.* use of pyrene derivative as steric stopper).^[75,76,77,78,79,80] CD-based PPRs can even be capped with CDs.^[81] The choice of appropriate polymer chains and steric stoppers opens the door to the synthesis of biodegradable CD-based PRs (*e.g.* α -CD/PEO-based PR end-capped with L-phenylalanine).^[81,82,83]

The control of the CD threading and dethreading allows to tune the complexation degree *N* (*i.e.* the number of threaded CDs per PEO chain) characterizing the finally obtained PR molecules. Experimentally, in the case of α -CD/PEO polymer chains, this is made by choosing appropriate α -CD/PEO molar ratio and decreasing temperature profile during the complexation step^[75] or an adequate composition of the water/dimethyl sulfoxide (DMSO) mixture during the end-capping step.^[76]

Sliding gels

PR molecules can be physically or chemically cross-linked via the threaded CDs, thus forming macroscopic gels. These gels possess the property that the CD cross-link points are not fixed, they can potentially slide along the polymer chains. These gels are called "sliding gels" or "slide-ring gels" and the term sliding gel is used in the following.

The concept of sliding gels was introduced by de Gennes in the late 20th century.^[84] He coped with physical sliding gels in which negatively charged polymer chains (*e.g.* DNA chains) mixed with multifunctional cationic molecules (*e.g.* metal particles carrying a certain number of organic cations) can bind and form sliding bridges (Figure 11a). The polymer chains can slide on the metal particles and must maintain the contact with them for electrostatic reasons. Thus, a gel is generated in which the charged metal particles

[73] S. Loethen, T. Ooya, H. Choi, N. Yui and D. Thompson, *Biomacromolecules*, **2006**, 7, 2501-2506.

[74] N. Kihara, K. Hinoue and T. Takata, *Macromolecules*, **2005**, 38, 223-226.

[75] G. Fleury, C. Brochon, G. Schlatter, G. Bonnet, A. Lapp and G. Hadziioannou, *Soft Matter*, **2005**, 1, 378-385.

[76] N. Jarroux, P. Guégan, H. Cheradame and L. Auvray, *Journal of Physical Chemistry B*, **2005**, 109, 23816-23822.

[77] J. Araki, C. Zhao and K. Ito, *Macromolecules*, **2005**, 38, 7524-7527.

[78] H. Choi, S. Lee, K. Yamamoto and N. Yui, *Macromolecules*, **2005**, 38, 9878-9881.

[79] A. Harada, J. Li, T. Nakamitsu and M. Kamachi, *Journal of Organic Chemistry*, **1993**, 58, 7524-7528.

[80] H. Yu, Z.-G. Feng, A.-Y. Zhang, D. Hou and L.-G. Sun, *Polymer*, **2006**, 47, 6066-6071.

[81] T. Ooya, A. Ito and N. Yui, *Macromolecular Bioscience*, **2005**, 5, 379-383.

[82] T. Ooya and N. Yui, *Macromolecular Chemistry and Physics*, **1998**, 199, 2311-2320.

[83] N. Yui, T. Ooya and T. Kumeno, *Bioconjugate Chemistry*, **1998**, 9, 118-125.

[84] P.-G. de Gennes, *Physica A: Statistical Mechanics and its Applications*, **1999**, 271, 231-237.

act as physical cross-linker. Moreover, de Gennes dealt with chemical sliding gels. They consist in rings threaded by two polymer chains, also called sliding rings (Figure 11b), leading to 3D networks.

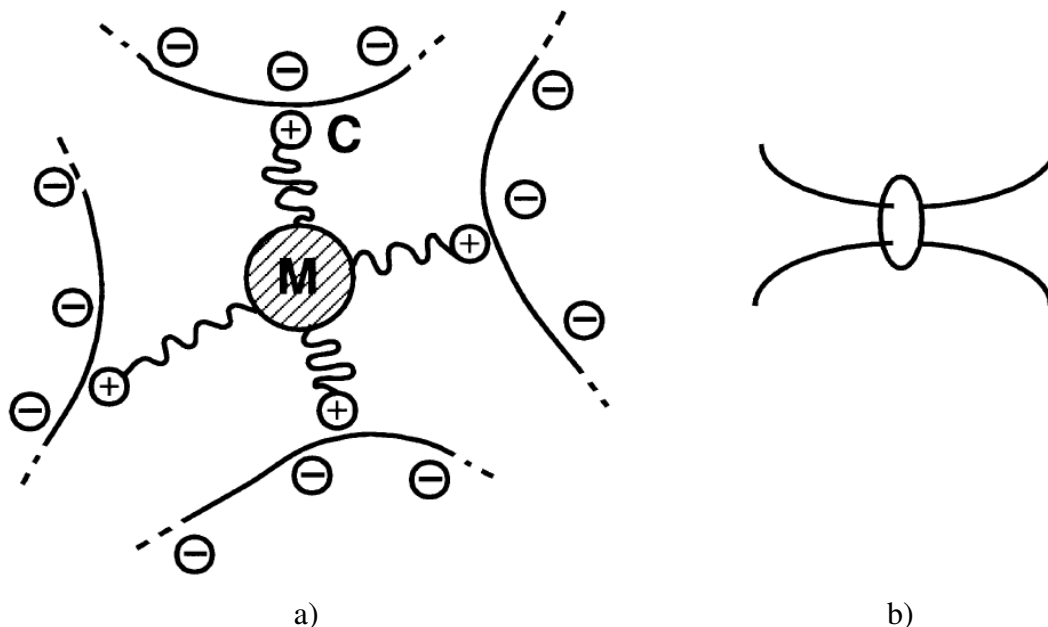


Figure 11. Schematic representations of: a) a physical sliding gel and b) a chemical sliding gel (reproduced from reference 84).

Both physical and chemical sliding gels can be obtained from α -CD/PEO-based PRs. Physical sliding gels are obtained from α -CD/PEO-based PR solutions in DMSO^[85,86] and in 40 w/w% calcium thiocyanate aqueous solution^[87] since these solutions exhibit thixotropic rheological behaviours (*i.e.* structures slowly build with time at rest, inducing a macroscopic gelation of the samples, and progressively and reversibly break down on shearing, leading to fluid mixtures).^[88] This phenomenon is observed at room temperature for concentration ranges (typically at 2.5 - 20 w/w%) depending on the PEO molar mass and on the PR complexation degree N .^[86] However, the exact origin of the gelation and the formed structures were not elucidated.

Chemical sliding gels as for them (Figure 12) were obtained for the first time from α -CD/PEO-based PR in NaOH aqueous solution using trifunctional cyanuric chloride

[85] C. Travelet, G. Schlatter, C. Brochon, P. Hébraud, D. Ivanov and G. Hadziioannou, CD-ROM congress proceedings of the EPF 2007, European Polymer Congress, Portorož, Slovenia, 2nd - 6th July 2007.

[86] J. Araki and K. Ito, *Polymer*, **2007**, 48, 7139-7144.

[87] J. Araki, T. Kataoka and K. Ito, *Journal of Applied Polymer Science*, **2007**, 105, 2265-2270.

[88] H. Barnes, *Journal of Non-Newtonian Fluid Mechanics*, **1997**, 70, 1-33.

(*i.e.* 2,4,6-trichloro-1,3,5-triazine) as cross-linker.^[89] Cross-linking occurs intermolecularly, leading to 3D networks, and also inevitably in an intramolecular way, *i.e.* between α -CDs belonging to the same PR molecule. Such gels benefit from the topological structure of PRs and consequently from the ring structure of threaded α -CDs since the cross-linker molecules are directly and covalently linked onto α -CDs *via* their hydroxyl groups, thus forming covalent bridges (Figure 12). Other chemical gels were synthesized from PRs but were not cross-linked through the threaded CDs and thus did not benefit from the originality of the PR molecules.^[90,91] Strictly speaking, the sliding gels do not belong to the chemical gel family. Indeed, the cross-link points are not fixed, they may slide. In that way, they should be considered as a new class of gels. Besides cyanuric chloride, other cross-linkers react with deprotonated CD hydroxyl groups in NaOH aqueous solution (*e.g.* difunctional divinyl sulfone at room temperature^[92]) or with protonated CD hydroxyl groups in DMSO (*e.g.* 1,1'-carbonyldiimidazole at room temperature or upon heating^[93,94]). The choice of the solvent used for PR solubilisation prior to chemical cross-linking is fundamental. Indeed, it controls the PR dissociation state and thus the homogeneity of the final sliding gels. The reactivity of the chosen cross-linker is also an important parameter. Indeed, too efficient cross-linkers induce the formation of highly cross-linked domains and thus lead to inhomogeneous systems. For instance, divinyl sulfone form sliding gels typically in one hour whereas 1,1'-carbonyldiimidazole needs typically one day. The latter gels are much more transparent than the former ones, whatever the swelling solvent. Sliding gels can reach a swelling degree in water of 40 000 % and thus may be used for superabsorbent purposes.^[89] Such a high swelling degree is assumed to originate from the fact that the cross-link points can slide along the polymer chains and thus in a certain way can adapt to the surrounding conditions. Sliding gels exhibit particular mechanical behaviours which strongly depend on the swelling solvent (DMSO or water).^[95] For instance, sliding gels show a Zener model behaviour at low

[89] Y. Okumura and K. Ito, *Advanced Materials*, **2001**, 13, 485-487.

[90] W. Hongliang, H. Jiyu, S. Ling-gang, Z. Kaiqiang and F. Zeng-guo, *European Polymer Journal*, **2005**, 41, 948-957.

[91] F. Zeng-guo and Z. Sanping, *Polymer*, **2003**, 44, 5177-5186.

[92] G. Fleury, G. Schlatter, C. Brochon and G. Hadziioannou, *Polymer*, **2005**, 46, 8494-8501.

[93] T. Sakai, H. Murayama, S. Nagano, Y. Takeoka, M. Kidowaki, K. Ito and T. Seki, *Advanced Materials*, **2007**, 19, 2023-2025.

[94] K. Karaky, C. Brochon, G. Schlatter and G. Hadziioannou, *Soft Matter*, **2008**, 4, 1165-1168.

[95] G. Fleury, G. Schlatter, C. Brochon and G. Hadziioannou, *Advanced Materials*, **2006**, 18, 2847-2851.

angular frequency over almost three decades in DMSO and not in water. Their mechanical behaviours are also studied in the present work. It should be kept in mind throughout this work that the use of the term sliding gel does not presuppose the effective sliding of the CDs. This expression insists on the *potential* cross-link point sliding in the 3D network. The above discussed chemical sliding gels synthesized from PRs (Figure 12) do not have the same structure as the one suggested by de Gennes in reference 84 (Figure 11b). Such systems based on 1:2 inclusion complexes were recently studied from an experimental point of view.^[96,97]

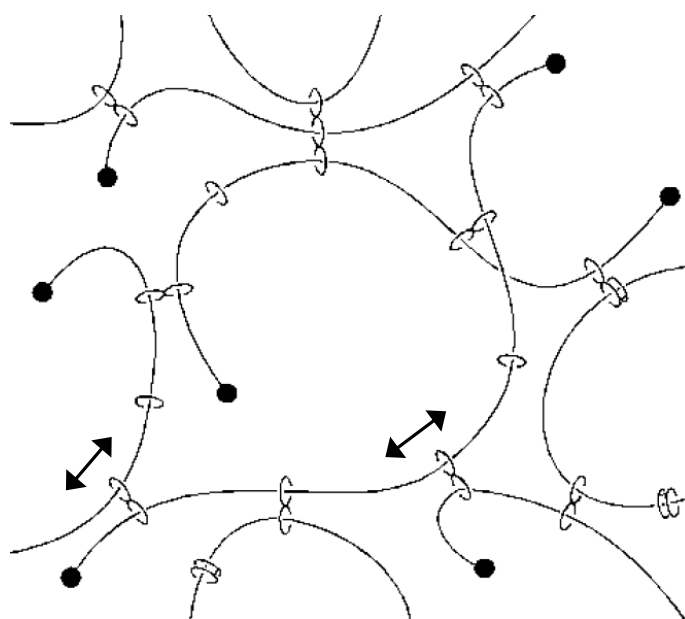


Figure 12. Schematic representation of a PR-based chemical sliding gel (reproduced from reference 89). The *potential* cross-link point sliding along the polymer chains is shown by the double arrows.

1.2.3. Applications of cyclodextrin-based rotaxanes and polyrotaxanes

Rotaxanes and their related uncapped structures are nowadays widely studied in the pharmaceutical field due to the ability of CDs to form inclusion complexes with entire drug molecules (or most of the time simply with part of them), thus increasing the solubility of drugs, enhancing their bioavailability and enhancing their stability.^[98] For instance, effective treatment for male erectile dysfunction implies the administration of

[96] R. Kawabata, R. Katoono, M. Yamaguchi and N. Yui, *Macromolecules*, **2007**, 40, 1011-1017.

[97] M.-M. Fan, Z.-J. Yu, H.-Y. Luo, S. Zhang and B.-J. Li, *Macromolecular Rapid Communications*, **2009**, doi: 10.1002/marc.200800712.

[98] M. Davis and M. Brewster, *Nature Reviews Drug Discovery*, **2004**, 3, 1023-1035.

α -CD/alprostadil inclusion complexes.^[99] CDs reduce evaporation of flavours and stabilize them. When forming inclusion complexes with the appropriate compounds, they can also reduce disgusting odours and tastes, and contribute to the elimination of bitter.^[100] CDs are also known to have a retardation effect on bread staling.^[101] CDs are also useful for separation purposes in the chromatography field due to their high selectivity towards structural isomers (constitutional isomers) and also towards spatial isomers (diastereoisomers and enantiomers).^[102] PRs and their related uncapped structures can form insulated nanowires when CDs are threaded onto semi-conducting polymer chains.^[103] CD-based PRs are also useful for drug delivery purposes (Figure 13) since they allow a more efficient binding of the drug molecules onto given receptors compared to free drug molecules.^[104] They are also used in the biology field in combination with DNA for gene delivery purposes^[105] or to facilitate DNA manipulation.^[106] The possible translational and rotational mobility of CDs gives the possibility to design molecular machines and shuttles.^[107]

[99] J. Buvat, P. Costa, D. Morlier, B. Lecocq, B. Stregmann and D. Albrecht, *Journal of Urology*, **1998**, 159, 116-119.

[100] J. Szejtli and L. Szenté, *European Journal of Pharmaceutics and Biopharmaceutics*, **2005**, 61, 115-125.

[101] Y. Tian, Y. Li, Z. Jin, X. Xu, J. Wang, A. Jiao, B. Yu and T. Talba, *Thermochimica Acta*, **2009**, doi: 10.1016/j.tca.2009.01.025.

[102] M. Asztemborska, R. Nowakowski and D. Sybilska, *Journal of Chromatography A*, **2000**, 902, 381-387.

[103] T. Shimomura, T. Akai, T. Abe and K. Ito, *Journal of Chemical Physics*, **2002**, 116, 1753-1756.

[104] T. Ooya and N. Yui, *Journal of Controlled Release*, **2002**, 80, 219-228.

[105] T. Ooya, H. Choi, A. Yamashita, N. Yui, Y. Sugaya, A. Kano, A. Maruyama, H. Akita, R. Ito, K. Kogure and H. Harashima, *Journal of the American Chemical Society*, **2006**, 128, 3852-3853.

[106] K. Tokuhisa, E. Hamada, R. Karinaga, N. Shimada, Y. Takeda, S. Kawasaki and K. Sakurai, *Macromolecules*, **2006**, 39, 9480-9485.

[107] A. Harada, *Accounts of Chemical Research*, **2001**, 34, 456-464.

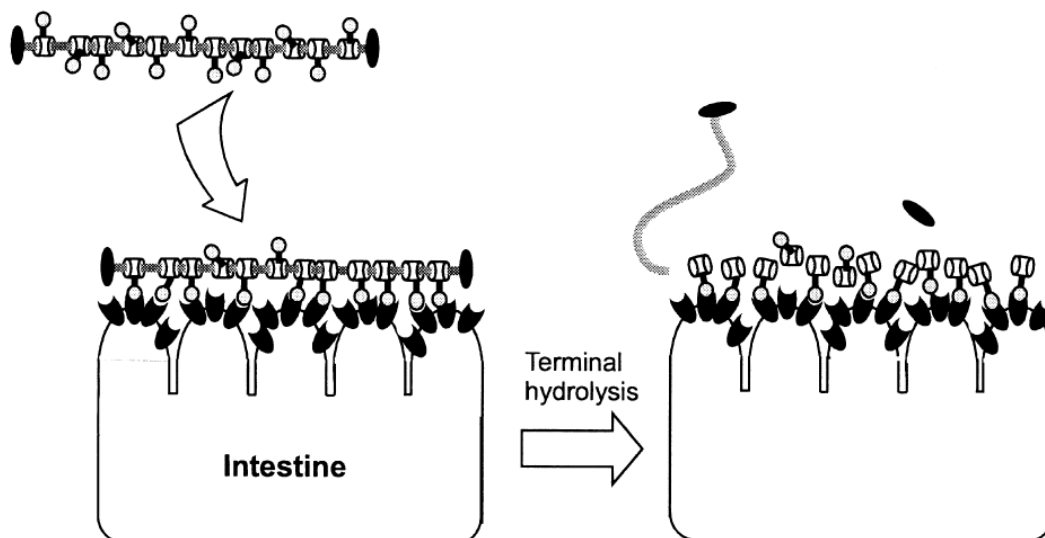


Figure 13. Schematic representation of the drug delivery process using CD-based PR molecules (reproduced from reference 104).

The general properties of CDs and particularly their inclusion properties were considered in the previous section. In the following of the present work, α -CD/PEO-based inclusion complexes and their derivatives will be studied. Thus, knowing that PEO can form intra- and/or inter-molecular associations, PEO properties and particular its association and solubility properties are now studied.

1.3. Poly(ethylene oxide) and its inclusion complexes

1.3.1. Poly(ethylene oxide): synthesis and properties

Ethylene oxide was prepared for the first time by the Alsatian scientist Würtz in the middle 19th century by the reaction of 2-chloroethanol with an aqueous solution of potassium hydroxide.^[108] The direct oxidation of ethylene to ethylene oxide over a silver catalyst was discovered and patented in the 1930's.^[109] Ethylene oxide molecules are highly reactive. The three-membered rings are opened in many reactions involving compounds carrying labile hydrogen atoms such as water or alcohols (Figure 14a). The terminal hydroxyl groups which are thus formed can react by addition to further ethylene oxide molecules, leading to oligomers of ethylene oxide or to polymers with a

[108] A. Würtz, *Annales de Chimie et de Physique*, **1859**, 55, 400-478 (available via the Internet at <http://visualiseur.bnf.fr/ark:/12148/bpt6k34796b>) (in French).

[109] T. Lefort, *Process for the Production of Ethylene Oxide*, Société Française de Catalyse Généralisée, United States Patent Number 1998878, April **1935** (available via the Internet at http://gb.espacenet.com/search97cgi/s97_cgi.exe?Action=FormGen&Template=gb/en/advanced.hts).

molecular mass below 20 kg mol^{-1} (Figure 14b) depending on the reaction conditions and particularly on the reactant ratios. High molecular weight PEO is formed from ethylene oxide by catalytic anionic or cationic polymerization. The anionic mechanism allows to obtain PEO with a low polydispersity.

The three names poly(ethylene oxide) (PEO), poly(ethylene glycol) and polyoxyethylene are from a chemical point of view synonymous. However, PEO refers historically to polymers with a molecular mass above 20 kg mol^{-1} . Poly(ethylene glycol) has the tendency to refer to oligomers and to polymers with a molecular mass below 20 kg mol^{-1} . Polyoxyethylene as for him refers to polymers of any molecular mass. The semantic distinction based on the molecular mass is presently not made and, since 22 kg mol^{-1} PEO is exclusively utilized in the following experimental chapters, the term poly(ethylene oxide) (PEO) is appropriate.

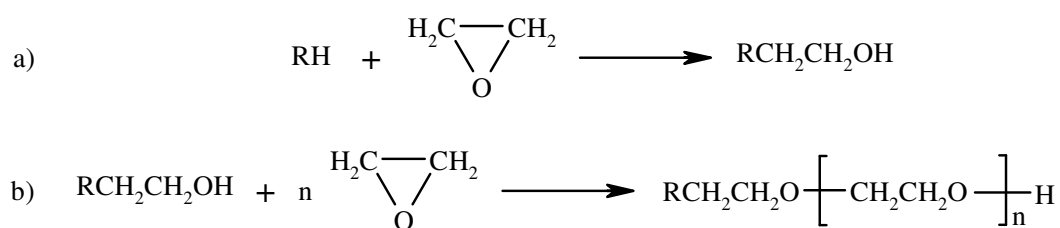


Figure 14. a) Reaction of compounds carrying labile hydrogen atoms with ethylene oxide and b) reaction with further ethylene oxide molecules, thus leading to the formation of PEO.

At room temperature, without necessitating preliminary heating, PEO do not exhibit aggregates larger than the typical light wavelength and thus is considered to be soluble in water, methanol, 2-propanol (91 w/w%), acetonitrile, N,N-dimethylformamide, tetrahydrofuran and in several chlorinated hydrocarbons such as dichloromethane, 1,2-dichloroethane or trichloroethylene.^[110] However, preliminary moderate heating (typically up to $30 - 50 \text{ }^\circ\text{C}$) is necessary so that PEO becomes soluble at room temperature in toluene, xylene, acetone, anisole, 1,4-dioxane, ethanol (dry) and 2-propanol (dry).^[110] In the above mentioned solvents except for instance water, a temperature decrease below room temperature leads to a precipitation of the system. The evaluation of the solubility parameters show that PEO is not in good solvent

[110] H. Mark, D. Othmer, C. Overberger and G. Seaborg, *Encyclopedia of Chemical Technology*, Wiley, New York (USA), **1982**, volume 18.

conditions in DMSO.^[111] Experiments confirm that moderate heating up to 30 °C is necessary to solubilize PEO in DMSO and that precipitation occurs slowly with time at room temperature. PEO is insoluble in ethylene glycol, diethylene glycol and glycerol at all temperatures.^[110]

Great attention was particularly paid on the solubility of PEO in water. The phase diagrams (temperature T , mass fraction Φ) of PEO in water are of the closed loop type.^[112] Although two phases coexist inside the closed loops, a single phase is observed outside the closed loops (Figure 15). The transition temperature between the one-phase domains and the two-phase domains depends mainly on the PEO mass fraction in the system and on the PEO polymerization degree.^[113]

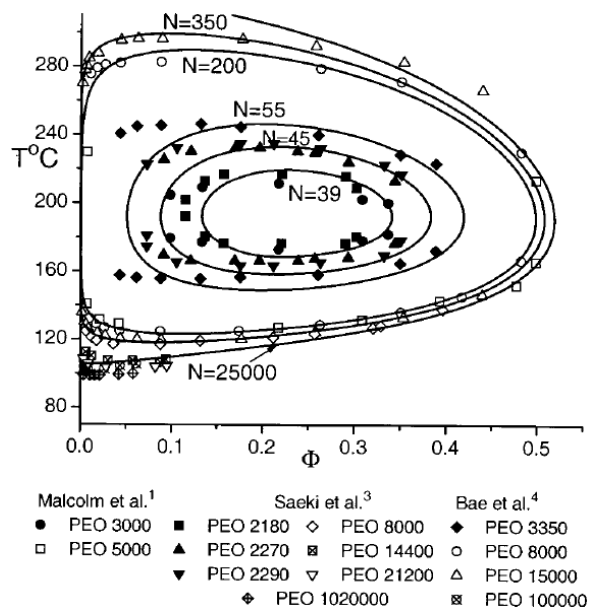


Figure 15. PEO phase diagrams (temperature T , mass fraction Φ) in water where N designates the PEO polymerization degree. Experimental data taken from references 112, 114 and 115 are shown by symbols whereas calculations correspond to the solid curves (reproduced from reference 113).

PEO phase diagrams in water are determined using turbidity measurements (UV-visible spectroscopy),^[112,115,116] PEO phase diagrams are also modelled evaluating the

[111] C. Özdemir and A. Güner, *European Polymer Journal*, **2007**, 43, 3068-3093.

[112] S. Saeki, N. Kuwahara, M. Nakata and M. Kaneko, *Polymer*, **1976**, 17, 685-689.

[113] E. Dormidontova, *Macromolecules*, **2002**, 35, 987-1001.

[114] G. Malcolm and J. Rowlinson, *Transactions of the Faraday Society*, **1957**, 53, 921-931.

[115] Y. Bae, S. Lambert, D. Soane and J. Prausnitz, *Macromolecules*, **1991**, 24, 4403-4407.

[116] F. Bailey Jr. and R. Callard, *Journal of Applied Polymer Science*, **1959**, 1, 56-62.

interaction energies PEO/PEO, PEO/water and water/water.^[113,117,118,119] Once plotted, the obtained closed loops are in agreement with the experimental curves (Figure 15). Moreover, static light scattering measurements allow to estimate the PEO aggregate size and the solubility parameter called second virial coefficient.^[120,121,122] For temperatures typically below 90 °C, PEO has the particularity to be in better solvent conditions when decreasing the temperature (Figure 16). This behaviour is explained by a solvation effect: Physical bond formation between ethylene oxide units of the PEO chains and water molecules is favoured at low temperature.^[123] When the temperature increases, hydrogen bonds break and water becomes a poorer solvent for PEO (Figure 17). It appears that the care taken in the preparation of the aqueous PEO solutions is determinant for the presence or not of aggregates within the solutions. Thus, for instance, the purity of the water used for PEO solubilization^[124,125] and the sample history^[126] are determinant. However, the time period separating the PEO/water mixing and the measurement does not influence considerably the static light scattering results.^[125] For all of these reasons, aggregation is not an inherent characteristic of the aqueous PEO solutions.^[127]

[117] S. Bekiranov, R. Bruinsma and P. Pincus, *Physical Review E: Statistical, Nonlinear and Soft Matter Physics*, **1997**, 55, 577-585.

[118] G. Karlström, *Journal of Physical Chemistry*, **1985**, 89, 4962-4964.

[119] P. Linse, *Macromolecules*, **1993**, 26, 4437-4449.

[120] H. Venohr, V. Fraaije, H. Strunk and W. Borchard, *European Polymer Journal*, **1998**, 34, 723-732.

[121] W. Polik and W. Burchard, *Macromolecules*, **1983**, 16, 978-982.

[122] S. Kawaguchi, G. Imai, J. Suzuki, A. Miyahara, T. Kitano and K. Ito, *Polymer*, **1997**, 38, 2885-2891.

[123] A. Matsuyama and F. Tanaka, *Physical Review Letters*, **1990**, 65, 341-344.

[124] K. Devanand and J. Selsler, *Macromolecules*, **1991**, 24, 5943-5947.

[125] S. Kinugasa, H. Nakahara, N. Fudagawa and Y. Koga, *Macromolecules*, **1994**, 27, 6889-6892.

[126] M. Duval and D. Sarazin, *Polymer*, **2000**, 41, 2711-2716.

[127] K. Devanand and J. Selsler, *Nature*, **1990**, 343, 739-741.

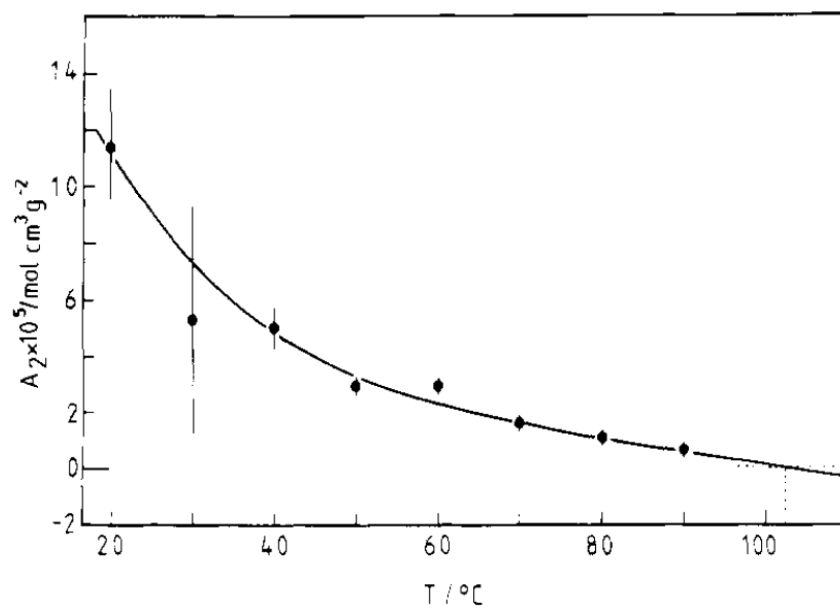


Figure 16. Second virial coefficient A_2 versus temperature T for 20 kg mol^{-1} PEO chains in water (reproduced from reference 121).

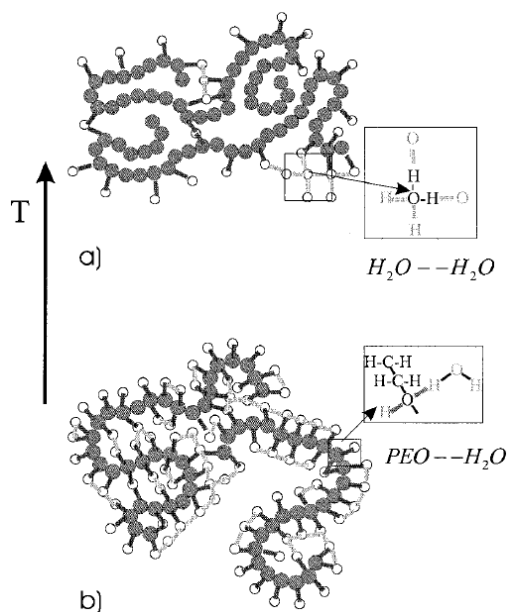


Figure 17. Schematic representations of physical bond formation in an aqueous PEO solution: a) at high temperature and b) at low temperature (reproduced from reference 113).

1.3.2. Poly(ethylene oxide)-based inclusion complexes

PEO is known to form inclusion complexes with α -CDs, although no 1:1 complex is observed with β -CDs and γ -CDs.^[128] However, 1:2 complexes are formed between PEO and γ -CDs since two PEO segments belonging to the same PEO polymer chain or not

[128] A. Harada, *Supramolecular Science*, **1996**, 3, 19-23.

need to thread the γ -CDs for steric reasons and also to favour weak interactions (Figure 18).^[129] A PEO polymerization degree equal or higher than 4 is needed for α -CDs to form inclusion complexes. The highest yields of inclusion complex formation are observed for a typical PEO polymerization degree of 45.^[128] Indeed, for longer PEO chains, the chain ends are not so easily available for the α -CDs. α -CDs can complex PEO having various architectures: linear PEO,^[130] star-like PEO,^[130] PEO comb-like grafted polymer^[131] and even PEO double-grafted polymer.^[132]

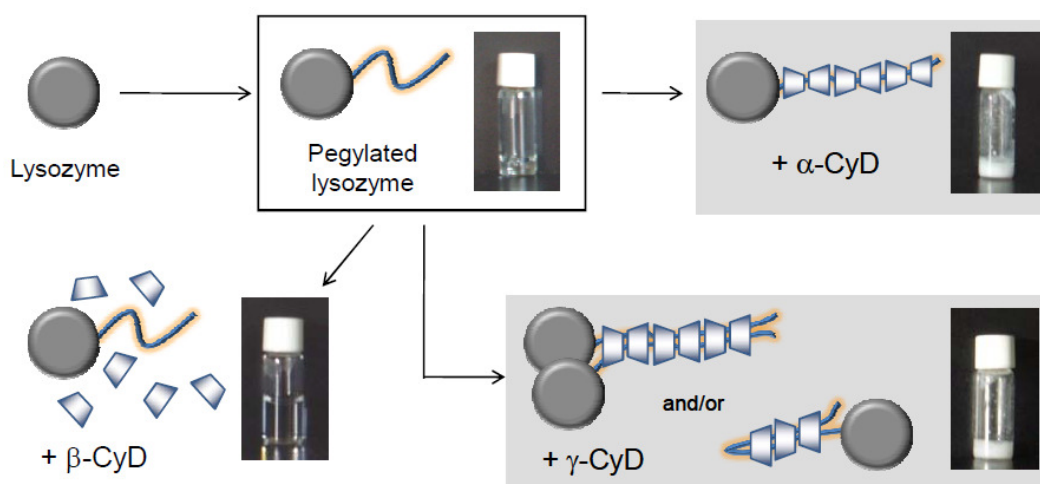


Figure 18. Schematic representations of the inclusion complex structures of PEO with α -CDs and γ -CDs in water. No inclusion complex is observed with β -CDs (reproduced from reference 129).

It is worth mentioning that α -CDs can also thread onto random,^[133] diblock^[134,135,136] or multiblock copolymers containing PEO. Surprisingly, α -CDs can directly thread onto poly(propylene oxide)-PEO-poly(propylene oxide) triblock copolymer chains (reverse Pluronic[®])^[137,138] although pure poly(propylene oxide) cannot be threaded by α -CDs.^[128]

[129] T. Higashi, F. Hirayama, S. Yamashita, S. Misumi, H. Arima and K. Uekama, *International Journal of Pharmaceutics*, **2009**, doi: 10.1016/j.ijpharm.2009.02.017.

[130] P. Lo Nostro, L. Giustini, E. Fratini, B. Ninham, F. Ridi and P. Baglioni, *Journal of Physical Chemistry B*, **2008**, 112, 1071-1081.

[131] L. He, J. Huang, Y. Chen and L. Liu, *Macromolecules*, **2005**, 38, 3351-3355.

[132] L. He, J. Huang, Y. Chen, X. Xu and L. Liu, *Macromolecules*, **2005**, 38, 3845-3851.

[133] C. Yang, X. Wang, H. Li, S. Goh and J. Li, *Biomacromolecules*, **2007**, 8, 3365-3374.

[134] J. Huang, L. Ren, H. Zhu and Y. Chen, *Macromolecular Chemistry and Physics*, **2006**, 207, 1764-1772.

[135] C. Cheng, R. Tang and F. Xi, *Macromolecular Rapid Communications*, **2005**, 26, 744-749.

[136] X. Li and J. Li, *Journal of Biomedical Materials Research, Part A*, **2008**, 86, 1055-1061.

[137] J. Li, X. Ni, Z. Zhou and K. Leong, *Journal of the American Chemical Society*, **2003**, 125, 1788-1795.

[138] C. Yang, X. Ni and J. Li, *European Polymer Journal*, **2009**, doi: 10.1016/j.eurpolymj.2009.01.020.

Similarly, β -CDs can directly thread onto PEO-poly(propylene oxide)-PEO triblock copolymer chains (Pluronic[®])^[139] although β -CDs are not able to thread onto pure PEO.^[128]

The use of block copolymers whose one block type is stimuli-sensitive (*e.g.* temperature-sensitive such as poly(propylene oxide) or pH-sensitive such as polyethyleneimine) allows to control the position of CDs on one defined block type simply by adjusting adequately the temperature^[139,140] or the pH.^[78,94,141] For instance, charging the polyethyleneimine block type by decreasing the pH-value forces the CDs which possess quite hydrophobic cavities to slide on the neutral block type. Since both polymer chain ends of the PR molecules are capped by steric stoppers, CDs cannot be expelled from the polymer chains.

[139] H. Fujita, T. Ooya and N. Yui, *Macromolecular Chemistry and Physics*, **1999**, 200, 706-713.

[140] H. Fujita, T. Ooya and N. Yui, *Macromolecules*, **1999**, 32, 2534-2541.

[141] H. Choi, A. Hirasawa, T. Ooya, D. Kajihara, T. Hohsaka and N. Yui, *ChemPhysChem*, **2006**, 7, 1671-1673.

CHAPTER 2

Formation and self-organization of pseudo-polyrotaxanes in water

In the previous chapter (**Chapter 1**), the state of the art concerning CD-based inclusion complexes, going from simple structures such as pseudorotaxanes to more complicated systems such as catenanes, rotaxanes, PPRs and PRs, was given. The bibliography about sliding gels, *i.e.* PR derivatives possessing original physico-chemical properties, was also reported. Then, the state of the art about the physico-chemical properties of PEO and its capacity to form inclusion complexes with different CD types was given.

In the present chapter (**Chapter 2**), it is shown that the temperature, the α -CD/PEO ratio and the choice of the PEO terminal group control the interactions between α -CDs and PEO and are thus of crucial importance regarding to the threading process between α -CDs and PEO in water. Concerning the temperature, quenching an α -CD/PEO mixture in water from 70 °C down to a temperature in the range from 5 °C to 30 °C leads to favourable interactions between α -CD cavities and PEO chains. Thus, threading of α -CDs onto PEO chains occurs, corresponding to the formation of PPRs. Moreover, since the formed PPR molecules are not in good solvent conditions in water, phase separation occurs, the mixture becomes milky and a physical gel forms at a typical total mass fraction in α -CD and PEO of 15 w/w%. Interactions between PPR molecules and more precisely between threaded α -CDs *via* their hydroxyl groups are put in evidence. The aggregates generated by the formation of such hydrogen bonds consist in threaded α -CD based nano-cylinders corresponding to the alignment of segments made of weakly stacked α -CDs along the PEO chains. These nano-scale aggregates precipitate and reorganize at a higher length-scale, leading to the milky aspect of the system.

Formation and self-organization kinetics of α -CD/PEO-based pseudo-polyrotaxanes in water. A specific behaviour at 30 °C

Published in *Langmuir*, 2009, doi: 10.1021/la900070v

Abstract

α -cyclodextrins (α -CDs) have the ability to form inclusion complexes with poly(ethylene oxide) (PEO) polymer chains. These pseudo-polyrotaxanes (PPRs) can be obtained by quenching an α -CD/PEO mixture in water from 70 °C down to a lower temperature (typically in the range from 5 °C to 30 °C) thanks to favorable interactions between α -CD cavities and PEO chains. Moreover, starting from a liquid α -CD/PEO mixture at a total mass fraction of 15 w/w% at 70 °C, the formation of PPRs with time at a lower temperature induces a white physical gel with time and phase separation is observed. We established that PPR molecules are exclusively found in the precipitated phase although unthreaded α -CD molecules and unthreaded PEO chains are in the liquid phase.

At 30 °C, the physical gel formation is much slower than at 5 °C. At 30 °C, we established that, in a first step, α -CDs thread onto PEO chains, forming PPR molecules which are not in good solvent conditions in water. At a higher length-scale, rapid aggregation of the PPR molecules occurs and threaded α -CD-based nano-cylinders form (cylinder length $L = 5.7$ nm and cylinder radius $R = 4.7$ nm). At a higher length-scale, α -CD-based nano-cylinders associate in a Gaussian way engendering the formation of precipitated domains which are responsible for the high turbidity of the studied system. At the end of this first step (*i.e.* after 20 min), the system still remains liquid and the PPRs are totally formed. Then, in a second step (*i.e.* after 150 min), the system undergoes its reorganization characterized by a compacity increase of the precipitated domains and forms a physical gel. We found that PPRs are totally formed after 20 min at 30 °C and that the system stays in a non-gel state up to 150 min. This opens new perspectives regarding the PPR chemical modification: between these two characteristic times, we can easily envisage an efficient chemical modification of the PPR molecules

in water, as for instance an end-capping reaction leading to the synthesis of polyrotaxanes.

2.1. Introduction

The word "cyclodextrin" refers to a large family of cyclic oligosaccharides constituted by the repetition of glucose units. These compounds were mentioned for the first time in the late 19th century.^[1] For a long time, only the molecules made by the repetition of 6, 7 and 8 glucose units were known and used. The existence of larger cyclodextrins was more recently put in evidence.^[2] For moderate numbers of glucose units, they are organized in a truncated conic form. The glucose unit cycles are more or less tangential to the conic surface whereas the hydroxyl groups point out of the surface. Most of them point outwards the outer surface, rendering the outer surface more hydrophilic, whereas the inner surface is more hydrophobic. Cyclodextrins thus realize a topological separation between the cavity and the outer part of the molecule. Playing with the different affinities of the inner and outer surface, new supramolecular assemblies can be designed.

Indeed, cyclodextrins show the ability to form inclusion complexes with low and high molecular weight compounds.^[3,4,5,6,7,8,9,10,11,12] Inclusion complexes are supramolecular structures resulting from the threading of cyclodextrins – the hosts – onto given molecules – the guests. Most of the time, they are formed in water^[5] which is, generally speaking, a good solvent for cyclodextrins.^[13] Forecasting if cyclodextrins are able to form inclusion complexes with given guest molecules is not obvious. In order to form inclusion complexes, it is necessary that the guest molecules fit cyclodextrins and exhibit an affinity with their inner surface:

[1] A. Villiers, *Comptes Rendus de l'Académie des Sciences*, **1891**, 112, 536-538.

[2] D. French, *Advances in Carbohydrate Chemistry and Biochemistry*, **1957**, 12, 189-260.

[3] A. Harada and M. Kamachi, *Macromolecules*, **1990**, 23, 2821-2823.

[4] A. Harada, J. Li and M. Kamachi, *Nature*, **1992**, 356, 325-327.

[5] M. Rekharsky and Y. Inoue, *Chemical Reviews*, **1998**, 98, 1875-1917.

[6] A. Harada, *Acta Polymerica*, **1998**, 49, 3-17.

[7] A. Harada, *Carbohydrate Polymers*, **1997**, 34, 183-188.

[8] A. Harada, *Coordination Chemistry Reviews*, **1996**, 148, 115-133.

[9] G. Wenz and B. Keller, *Angewandte Chemie International Edition English*, **1992**, 31, 197-199.

[10] K.-M. Shin, T. Dong, Y. He, Y. Taguchi, A. Oishi, H. Nishida and Y. Inoue, *Macromolecular Bioscience*, **2004**, 4, 1075-1083.

[11] L. Huang, E. Allen and A. Tonelli, *Polymer*, **1999**, 40, 3211-3221.

[12] A. Müller, *Dickenerkennung mit Cyclodextrinen und Synthese von Cyclodextrin-Rotaxanen aus Seitenkettenpolyrotaxanen*, Ph.D. Thesis, University of Saarbrücken (Germany), **2006** (available via the Internet at <http://scidok.sulb.uni-saarland.de/volltexte/2007/928/> or <http://www.d-nb.de/netzpub/index.htm>) (in German).

[13] J. Szejtli, *Cyclodextrin Technology*, Kluwer, Dordrecht (Netherlands), **1988**.

- The role played by the sizes of the cyclodextrin cavity and of the guest is indeed determinant. For instance, too large guest molecules cannot fit the cyclodextrins.^[3]
- As far as the interactions are concerned, the threading driving forces mainly consist in hydrophobic interactions.^[14] The hydrocarbon-like guest molecule reduces its water molecule surrounding by making contact with the inner surface of the cyclodextrin molecule. Besides these hydrophobic interactions, the variation of conformational energy,^[15] the change of van der Waals interactions,^[16] and the breakage and formation of hydrogen bonds participate to the formation of the inclusion complexes.

The formation of inclusion complexes is interesting for applications in the field of molecular machines and shuttles,^[17,18,19,20,21] information storage^[22] and intermembrane transfer.^[23] Yet, one of the main attracts of cyclodextrins consists in their ability to form inclusion complexes with polymer chains. For certain cyclodextrins/polymer chain systems, it is possible to control the number of threaded cyclodextrins per polymer chain over a wide range.^[24] The resulting structures find applications in insulated single-molecule nanowires^[25,26,27] or sliding gels having high swelling ratios and original viscoelastic properties.^[28,29,30] In such cyclodextrins/polymer chain systems, the

[14] I. Tabushi, *Accounts of Chemical Research*, **1982**, 15, 66-72.

[15] P. Manor and W. Saenger, *Journal of the American Chemical Society*, **1974**, 96, 3630-3639.

[16] J. Pozuelo, F. Mendicuti and W. Mattice, *Macromolecules*, **1997**, 30, 3685-3690.

[17] A. Harada, *Accounts of Chemical Research*, **2001**, 34, 456-464.

[18] Q.-C. Wang, D.-H. Qu, J. Ren, K. Chen and H. Tian, *Angewandte Chemie International Edition English*, **2004**, 43, 2661-2665.

[19] Y. Kawaguchi and A. Harada, *Organic Letters*, **2000**, 2, 1353-1356.

[20] H. Murakami, A. Kawabuchi, R. Matsumoto, T. Ido and N. Nakashima, *Journal of the American Chemical Society*, **2005**, 127, 15891-15899.

[21] H. Murakami, A. Kawabuchi, K. Kotoo, M. Kunitake and N. Nakashima, *Journal of the American Chemical Society*, **1997**, 119, 7605-7606.

[22] I. Willner, V. Pardo-Yissar, E. Katz and K. Ranjit, *Journal of Electroanalytical Chemistry*, **2001**, 497, 172-177.

[23] K. Tanhuanpää, K. Cheng, K. Anttonen, J. Virtanen and P. Somerharju, *Biophysical Journal*, **2001**, 81, 1501-1510.

[24] G. Fleury, C. Brochon, G. Schlatter, G. Bonnet, A. Lapp and G. Hadziioannou, *Soft Matter*, **2005**, 1, 378-385.

[25] P. Taylor, M. O'Connell, L. McNeill, M. Hall, R. Aplin and H. Anderson, *Angewandte Chemie International Edition English*, **2000**, 39, 3456-3460.

[26] F. Cacialli, J. Wilson, J. Michels, C. Daniel, C. Silva, R. Friend, N. Severin, P. Samorì, J. Rabe, M. O'Connell, P. Taylor and H. Anderson, *Nature Materials*, **2002**, 1, 160-164.

[27] M. van den Boogaard, G. Bonnet, P. van't Hof, Y. Wang, C. Brochon, P. van Hutten, A. Lapp and G. Hadziioannou, *Chemistry of Materials*, **2004**, 16, 4383-4385.

[28] Y. Okumura and K. Ito, *Advanced Materials*, **2001**, 13, 485-487.

[29] G. Fleury, G. Schlatter, C. Brochon and G. Hadziioannou, *Polymer*, **2005**, 46, 8494-8501.

[30] G. Fleury, G. Schlatter, C. Brochon, C. Travelet, A. Lapp, P. Lindner and G. Hadziioannou, *Macromolecules*, **2007**, 40, 535-543.

attractive hydrogen bonding interactions between adjacent cyclodextrins play an important role in the threading process.^[16,31,32] When pure cyclodextrins (without polymer chain) are recrystallized from water in controlled conditions, they can also interact weakly between adjacent cyclodextrins. Thus, they adopt a so-called columnar structure.^[33]

The structure and properties of inclusion complexes were studied in the steady state using Fourier transform infrared spectroscopy^[34,35] and nuclear magnetic resonance.^[36,37,38,39] Furthermore, the inclusion complexes exhibit higher thermal stability compared to the free cyclodextrins and polymer chains as shown by thermogravimetric experiments.^[34,35] Moreover, they show by differential scanning calorimetry measurements no endothermic peak related to the fusion of the crystalline phase of the polymer chains since the polymer chains, threaded by cyclodextrins, are not able to associate to form crystals.^[34,35] The inclusion complexes were also observed in the dried state using wide-angle X-ray scattering measurements.^[34,35,40,41,42,43] A columnar structure (also called channel or rod-like structure) was put in evidence, corresponding to the packing of the cyclodextrins along the polymer chains. On the diffractograms, such a structure is characterized by a peak at an observation angle $2\Theta = 20^\circ$. The cage structure present in native cyclodextrin and characterized by a peak at $2\Theta = 12^\circ$ vanishes when cyclodextrins are threaded onto the polymer chains.

In order to better apprehend the inclusion complex formation, their segregation was studied *in situ* (in presence of solvent to preserve the system from a possible structure modification upon drying) as a function of time by turbidity measurements^[43,44,45,46,47]

[31] Y. Okumura, K. Ito and R. Hayakawa, *Polymers for Advanced Technologies*, **2000**, 11, 815-819.

[32] K. Miyake, S. Yasuda, A. Harada, J. Sumaoka, M. Komiyama and H. Shigekawa, *Journal of the American Chemical Society*, **2003**, 125, 5080-5085.

[33] C. Rusa, T. Bullions, J. Fox, F. Porbeni, X. Wang and A. Tonelli, *Langmuir*, **2002**, 18, 10016-10023.

[34] C. Rusa, C. Luca and A. Tonelli, *Macromolecules*, **2001**, 34, 1318-1322.

[35] C. Rusa, J. Fox and A. Tonelli, *Macromolecules*, **2003**, 36, 2742-2747.

[36] H.-J. Schneider, F. Hacket and V. Rüdiger, *Chemical Reviews*, **1998**, 98, 1755-1785.

[37] J. Lu, P. Mirau and A. Tonelli, *Macromolecules*, **2001**, 34, 3276-3284.

[38] M. Ceccato, P. Lo Nostro, C. Rossi, C. Bonechi, A. Donati and P. Baglioni, *Journal of Physical Chemistry B*, **1997**, 101, 5094-5099.

[39] M. Pons and O. Millet, *Progress in Nuclear Magnetic Resonance Spectroscopy*, **2001**, 38, 267-324.

[40] I. Topchieva, A. Tonelli, I. Panova, E. Matuchina, F. Kalashnikov, V. Gerasimov, C. Rusa, M. Rusa and M. Hunt, *Langmuir*, **2004**, 20, 9036-9043.

[41] J. Chung, T. Kang and S.-Y. Kwak, *Macromolecules*, **2007**, 40, 4225-4234.

[42] I. Topchieva, I. Panova, B. Kurganov, V. Spiridonov, E. Matukhina, S. Filippov and A. Lezov, *Colloid Journal (Translation of Kolloidnyi Zhurnal)*, **2008**, 70, 356-365.

[43] P. Lo Nostro, L. Giustini, E. Fratini, B. Ninham, F. Ridi and P. Baglioni, *Journal of Physical Chemistry B*, **2008**, 112, 1071-1081.

[44] P. Lo Nostro, J. Lopes and C. Cardelli, *Langmuir*, **2001**, 17, 4610-4615.

[45] M. Ceccato, P. Lo Nostro and P. Baglioni, *Langmuir*, **1997**, 13, 2436-2439.

(UV-visible spectroscopy) and also by static and dynamic light scattering experiments.^[42] It was observed that the formation of inclusion complexes in water induces their segregation from the solvent due to the formation of large heterogeneities. The influence of the concentration, temperature, solvent composition, and molecular weight and architecture of the polymer chain was investigated. It was also found that cyclodextrins form inclusion complexes more or less rapidly, depending on the terminal group of the polymer chains.^[48] Thus, cyclodextrins can be used as recognition agents in order to separate polymer chains having different terminal groups.^[49,50] Cyclodextrins are also able to separate molecules having different architectures (*e.g.* linear *versus* cyclic molecules).^[51] Moreover, it was found that cations and anions added as salts have a considerable influence on the kinetics of inclusion complex formation and segregation from water.^[52]

Among the different types of available cyclodextrins, the one resulting from the repetition of 6 glucose units, called α -cyclodextrin (α -CD), is widely used and studied in particular due to its high water solubility.^[13] α -CDs are known to thread onto poly(ethylene oxide) (PEO).^[3,4] They form inclusion complexes which are also called pseudo-polyrotaxanes.^[53,54] In the following, the pseudo-polyrotaxanes will be denoted PPR_N where N is the α -CD/PEO mole ratio used in the mixture.

A long time after mixing α -CDs and PEO in water, it was possible to prove the formation of inclusion complexes and to get information about their structure. However, the evolution of the system structure as a function of time was not studied. Indeed, UV-visible spectroscopy and light scattering only give access to the kinetics of segregation of inclusion complexes. In the present article, this aspect, macroscopically characterized by the formation of a physical gel, is followed by mechanical dynamical

[46] C. Tait and D. Davies, *Langmuir*, **2002**, 18, 2453-2454.

[47] A. Becheri, P. Lo Nostro, B. Ninham and P. Baglioni, *Journal of Physical Chemistry B*, **2003**, 107, 3979-3987.

[48] J. Xue, L. Chen, L. Zhou, Z. Jia, Y. Wang, X. Zhu and D. Yan, *Journal of Polymer Science, Part B: Polymer Physics*, **2006**, 44, 2050-2057.

[49] J. Xue, Z. Jia, X. Jiang, Y. Wang, L. Chen, L. Zhou, P. He, X. Zhu and D. Yan, *Macromolecules*, **2006**, 39, 8905-8907.

[50] J. Xue, L. Zhou, P. He, X. Zhu, D. Yan and X. Jiang, *Journal of Inclusion Phenomena and Macrocyclic Chemistry*, **2008**, 61, 83-88.

[51] S. Singla, T. Zhao and H. Beckham, *Macromolecules*, **2003**, 36, 6945-6948.

[52] P. Lo Nostro, J. Lopes, B. Ninham and P. Baglioni, *Journal of Physical Chemistry B*, **2002**, 106, 2166-2174.

[53] F. Huang and H. Gibson, *Progress in Polymer Science*, **2005**, 30, 982-1018.

[54] Please note that, although the term "pseudo-polyrotaxane" has strictly speaking a different meaning from "polypseudorotaxane", the distinction between both substantives is not always made in the literature. Here, the use of "pseudo-polyrotaxane" is more accurate.

measurements. Complementary kinds of nuclear magnetic resonance (^1H NMR), particularly liquid-state and high-resolution magic angle spinning 2D ^1H NMR, give information on the nature of the formed structures. Neutron scattering experiments are used to follow *in situ* the kinetics of inclusion complex formation and to get direct information on the mechanism of PPR formation and on their structure and organization. Furthermore, a complete study of the system at 30 °C was carried out and showed that the PPR formation occurs in a first step which is totally separated from the physical gel formation.

2.2. Experimental section

2.2.1. Materials

Dihydroxy-terminated poly(ethylene oxide) (PEO_{OH}) was purchased from Serva Electrophoresis[®] and dried by an azeotropic distillation from toluene before use. An average number molecular weight of 22 kg mol⁻¹ and a polydispersity index of 1.03 were measured in dimethyl sulfoxide at 70 °C by gel permeation chromatography with PEO standard calibration. α -CD was supplied by Acros Organics[®] and dried over phosphorous pentoxide under reduced pressure before use. Deuterated water (D_2O) with a 99.9 % enrichment, purchased from Euriso-top[®], was used as received without further purification.

2.2.2. Synthesis

α,ω -Bis-amine-terminated poly(ethylene oxide) (PEO_{NH_2}) was synthesized from PEO_{OH} according to a three-step synthesis.^[55] α,ω -Bis-carboxyl-terminated poly(ethylene oxide) (PEO_{COOH}) was synthesized from PEO_{OH} according to a one-step synthesis.^[56] The conversion yield in amino and carboxyl groups was determined by acido-basic titration and was found to exceed 91 %. The purity of the (un)modified PEOs was determined using conventional liquid-state ^1H nuclear magnetic resonance in deuterated chloroform at room temperature ($\delta = 3.6$ ppm, singlet, CH_2 of the (un)modified PEOs) and gel permeation chromatography in dimethyl sulfoxide at 70 °C.

[55] M. Mutter, *Tetrahedron Letters*, **1978**, 19, 2839-2842.

[56] J. Araki, C. Zhao and K. Ito, *Macromolecules*, **2005**, 38, 7524-7527.

2.2.3. Characterization methods

Liquid-state ^1H Nuclear Magnetic Resonance. Liquid-state ^1H NMR measurements were carried out as 2D nuclear Overhauser enhancement spectroscopy (LS-NOESY), as 2D diffusion ordered spectroscopy (LS-DOSY) and as 1D NMR (LS-1D). All spectra were recorded on a spectrometer commercialized by Bruker[®], operating at a frequency of 500 MHz and using a 5 mm broadband inverse gradient probe. In LS-NOESY measurements, no spinning was applied to the NMR tube for B_1 inhomogeneity reasons. It is also not spun in LS-DOSY experiments since it affects the diffusion properties of the studied mixture. α -CD (275 mg, 2.83×10^{-4} mol) and PEO_{OH} (77.8 mg, 3.54×10^{-6} mol, equivalent to PPR₈₀) were mixed in D₂O (2 g, total mass fraction in α -CD and PEO_{OH} = 15 w/w%) at 70 °C for 30 min under stirring. The NMR tube was filled in with the solution, rapidly introduced in the temperature-regulated spectrometer at 5 °C or 70 °C, and measured after 15 min. The RF NMR sequence used for the LS-DOSY measurements was a pulsed field gradient limited eddy current sequence with bipolar pulsed field gradients. Thirty incremental steps were used for building the diffusion dimension. The maximum value of gradient pulses was 48 G cm⁻¹. The diffusion time was 400 ms at 5 °C (150 ms at 70 °C), and the single gradient duration was 1750 μs at 5 °C (1000 μs at 70 °C). D₂O was used as the solvent during all of the experiments. The internal lock was made on the ^2H -signal of the solvent.

High-resolution Magic Angle Spinning ^1H Nuclear Magnetic Resonance. High-resolution magic angle spinning ^1H NMR experiments were carried out as 2D nuclear Overhauser enhancement spectroscopy (HRMAS-NOESY) and as 1D NMR (HRMAS-1D). All spectra were recorded on a spectrometer commercialized by Bruker[®], operating at a frequency of 500 MHz and equipped with a 4 mm double resonance magic angle spinning probe. α -CD (275 mg, 2.83×10^{-4} mol) and PEO_{OH} (77.8 mg, 3.54×10^{-6} mol, equivalent to PPR₈₀) were mixed in D₂O (2 g, total mass fraction in α -CD and PEO_{OH} = 15 w/w%) at 70 °C during 30 min under stirring. The solution was introduced into a 4 mm zirconium oxide rotor fitted with a 50 μL cylindrical insert. The sample was rapidly introduced in the temperature-regulated spectrometer at 5 °C and 70 °C and spun at 6 kHz. At 5 °C and 70 °C, HRMAS-NOESY and HRMAS-1D spectra were measured after 15 min. D₂O was used as the solvent during all of the experiments. The internal lock was made on the ^2H -signal of the solvent.

Small-angle Neutron Scattering (SANS). SANS measurements were performed on the PAXY spectrometer^[57] at the Laboratoire Léon Brillouin (LLB, CEA, Saclay, France). The modulus of the scattering vector is denoted q and is equal to $(4\pi/\lambda) \times \sin(\theta/2)$ where θ designs the observation angle and λ represents the wavelength of the used radiation. The different used configurations consisted in a sample-to-detector distance of 3 m (respectively 1 m) and a wavelength of 1.0 nm (respectively 0.6 nm). The global probed q -range corresponding to these configurations was $8.25 \times 10^{-2} \text{ nm}^{-1} \leq q \leq 3.49 \text{ nm}^{-1}$. The signal was corrected by taking into account the contributions of the measurement cell, the solvent and the incoherent background.^[58] The incoherent scattering of poly(methyl methacrylate) was used to correct the detector efficiency. Thus, the data were brought to absolute scale. The measurement cells were made of 1 mm thick quartz windows separated by a 2 mm O-ring and equipped with a cadmium-boron carbide diaphragm whose hole diameter is 10 mm. D₂O was used as the solvent during all of the experiments. α -CD (275 mg, 2.83×10^{-4} mol) and PEO_{OH} (77.8 mg, 3.54×10^{-6} mol, equivalent to PPR₈₀) were mixed in D₂O (2 g, total mass fraction in α -CD and PEO_{OH} = 15 w/w%) at 70 °C during 30 min under stirring. The rack carrying the empty measurement cell was temperature-regulated at 30 °C. The cell was filled in with the solution and 5.5 min scans were continuously recorded during 4 h at 30 °C. It was not possible to carry out such a measurement at 10 °C, 15 °C, 20 °C or 25 °C due to the rapid evolution of the system with time. For these temperatures, only the final steady state could be measured. At 5 °C, the water contained in the air strongly condensed onto the measurement cell. Thus, no SANS measurement was possible at 5 °C.

Rheological Dynamic Analysis (RDA). RDA was performed on the Physica MCR 301 rheometer commercialized by Anton Paar[®] and equipped with the CC27 thermo-regulated Couette device. The Couette geometry had an internal diameter of 26.7 mm, an external diameter of 28.9 mm and a height of 40.0 mm. The rheometer could be strain controlled *via* a control loop or stress controlled. Water was used as the solvent during all of the experiments. α -CD and (un)modified PEO were mixed in water at 70 °C during 30 min under stirring. The empty Couette device was temperature-regulated at 5 °C, 10 °C, 20 °C, 25 °C or 30 °C. As soon as the air-gap was

[57] <http://www-llb.cea.fr/fr-en/pdf/paxy-llb.pdf>.

[58] A. Brûlet, D. Lairez, A. Lapp and J.-P. Cotton, *Journal of Applied Crystallography*, **2007**, 40, 165-177.

filled in with the solution, the elastic modulus (G') and the loss modulus (G'') were continuously recorded during few hours at an angular frequency of 10 rad s^{-1} . Due to the large variation of the mechanical response of the mixtures with time, the following procedure was automated: At the beginning of the measurement, while the system was fluid enough, a constant stress of 0.1 Pa was applied. Then, as soon as the resulting deflection angle fell below the rheometer resolution, *i.e.* $7.0 \times 10^{-5} \text{ rad}$, the strain was imposed at a value of 0.3% .

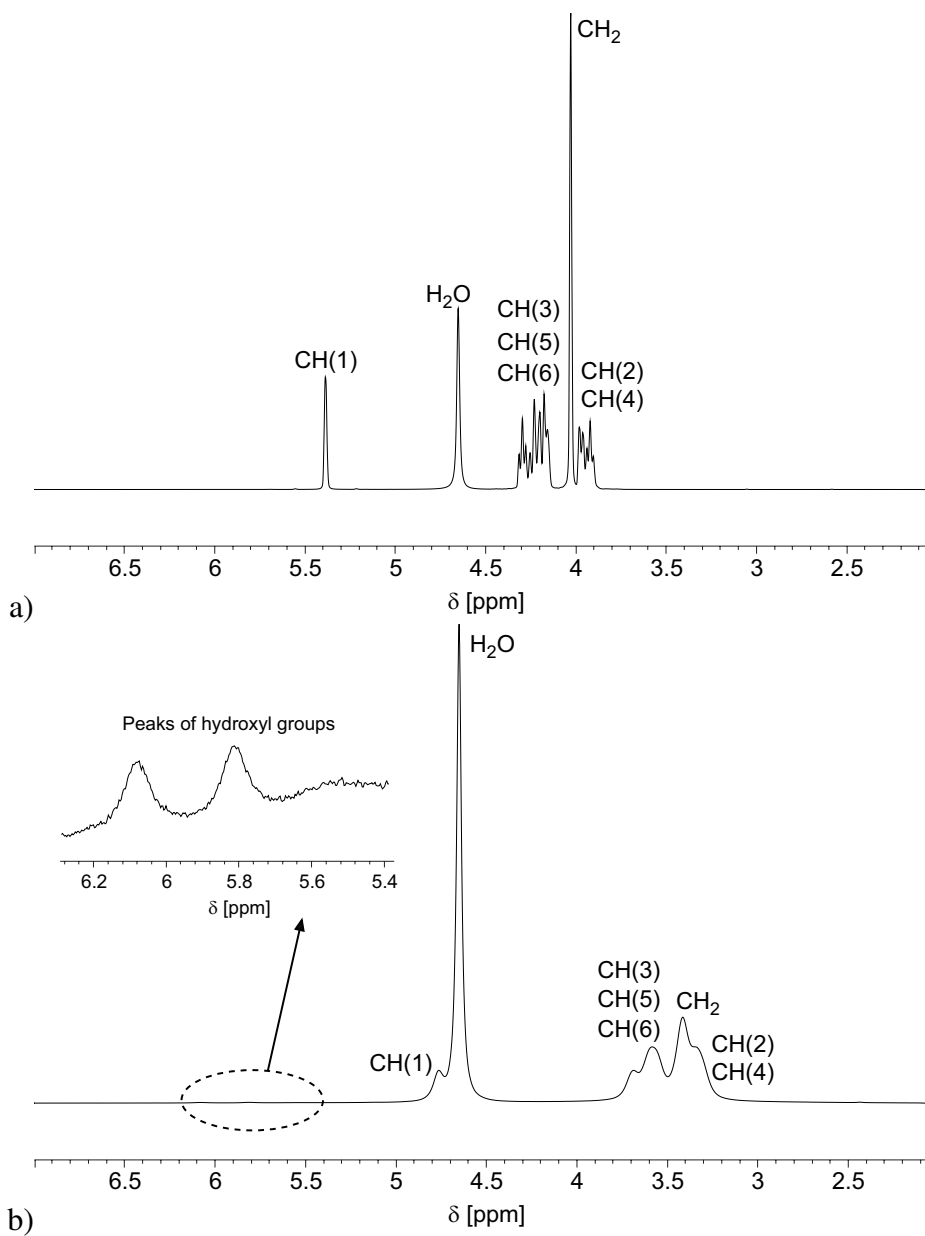
2.3. Results and discussion

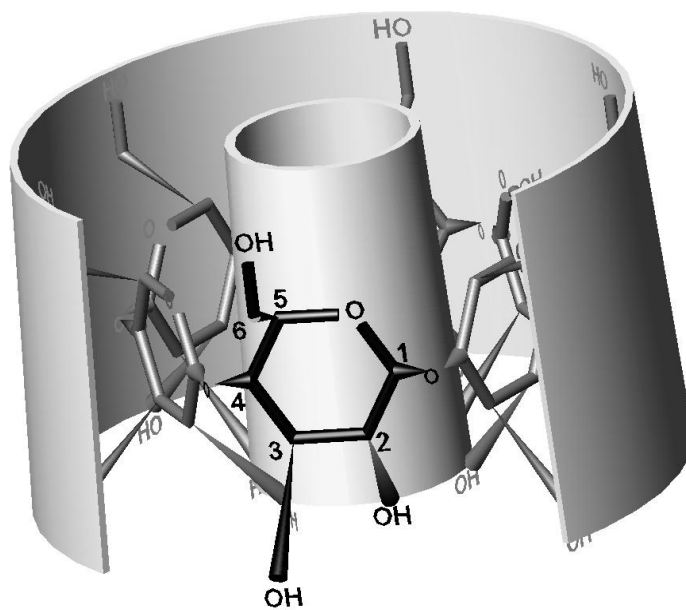
2.3.1. Interactions between α -cyclodextrins and poly(ethylene oxide): threading mechanism

An α -CD/PEO mixture, typically equivalent to PPR₈₀, with a mass fraction in α -CD and PEO of $15 \text{ w/w}\%$ forms a physical gel and becomes rapidly white when kept at $5 \text{ }^\circ\text{C}$. Thus, the obtained heterogeneities are highly segregated from water with a characteristic size in the order of magnitude of the light wavelength.

Figure 1 shows that the α -CD characteristic peaks and the PEO characteristic peak obtained in conventional LS-1D NMR experiments do not appear at the same chemical shifts (δ) at $70 \text{ }^\circ\text{C}$ and $5 \text{ }^\circ\text{C}$. Indeed, the calibration of the NMR spectra is made at $\delta = 4.65 \text{ ppm}$ on the H_2O peak whose chemical shift is known to be temperature dependent due to a change of the electronic environment of the water molecules when modifying the temperature. Thus, the other functional groups appear at different chemical shifts at $70 \text{ }^\circ\text{C}$ and $5 \text{ }^\circ\text{C}$.

The characteristic peaks obtained in conventional LS-1D NMR experiments at $70 \text{ }^\circ\text{C}$ are much sharper than those at $5 \text{ }^\circ\text{C}$ (Figure 1), indicating a much more homogeneous system in the initial state of the mixture at $70 \text{ }^\circ\text{C}$. Furthermore, the presence of α -CD-based heterogeneities at $5 \text{ }^\circ\text{C}$ is corroborated by the fact that NMR characteristic peaks of α -CD hydroxyl groups appear moderately at low temperature in conventional LS-1D NMR experiments (inset, Figure 1b). Nevertheless, they are not visible at all at $70 \text{ }^\circ\text{C}$ (Figure 1a). Indeed, rapid hydrogen/deuterium exchange between the α -CD hydroxyl groups and the D_2O molecules is favoured in the dissociated state, *i.e.* at high temperature.

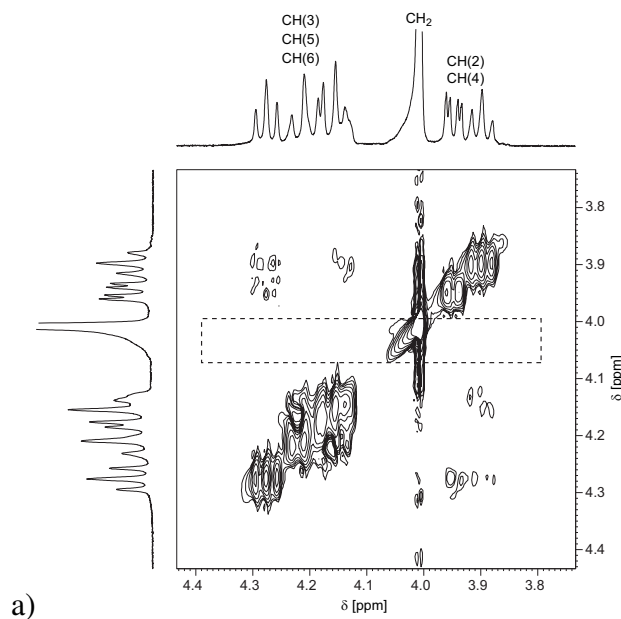




c)

Figure 1. Liquid-state-1D ^1H NMR: Spectrum of an α -CD/PEO mixture, equivalent to PPR₈₀, at 15 w/w% in D_2O : a) after 15 min at 70 °C and b) after 15 min at 5 °C. Inset: characteristic peaks of α -CD hydroxyl groups. c) Schematic 3D representation of an α -CD molecule.

Moreover, at 5 °C, the peaks are sharp and very well defined in HRMAS-1D NMR experiments (1D spectrum along the x-axis or along the y-axis, Figure 2b) compared to the LS-1D NMR experiments (Figure 1b). This shows that the smooth peaks obtained by LS-1D NMR experiments are due to the presence of heterogeneities within the system (and not to relaxation dynamics).



a)

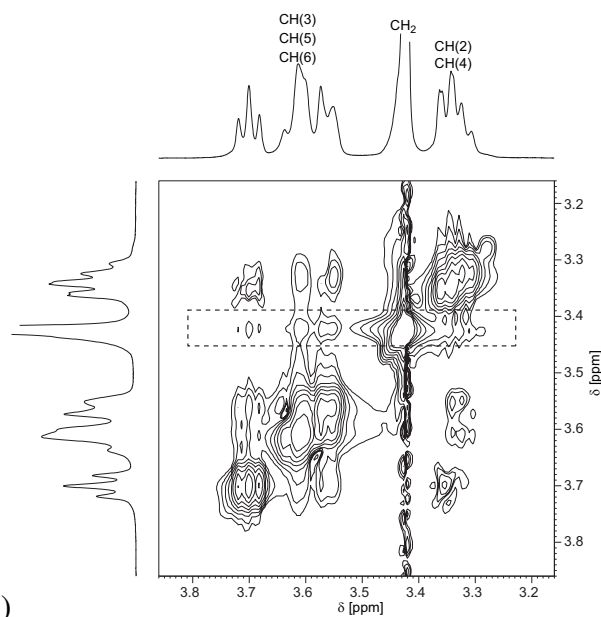


Figure 2. HRMAS-NOESY ^1H NMR: Spectrum of an α -CD/PEO mixture, equivalent to PPR₈₀, at 15 w/w% in D_2O : a) after 15 min at 70 °C and b) after 15 min at 5 °C.

Thus, there is coexistence of two phases at low temperature:

- A liquid phase which can be probed by liquid-state NMR.
- A solid phase which can be observed by high-resolution magic angle spinning NMR. This tool is appropriate for gel and colloid systems, and thus commonly used for instance for heterogeneous biological tissues^[59] and heterogeneous raw food materials.^[60]

The presence of heterogeneities is induced by the formation of PPRs. Moreover, the formation of PPRs is due to the threading of α -CDs onto PEO chains, leading to a mobility decrease of α -CDs and PEO chains. LS-DOSY^[61,62] measurements allow to determine the diffusion coefficient (D) of molecules as a function of their chemical shifts. Thus, among the different kinds of possible liquid-state experiments, LS-DOSY is of particular interest for our system. Spectra were recorded at 70 °C and 5 °C. From each measured diffusion coefficient, it is possible to deduce the hydrodynamic diameter (D_h) of the fictive corresponding hard sphere using the Stokes-Einstein equation.^[63,64]

[59] M. Swanson, K. Keshari, Z. Tabatabai, J. Simko, K. Shinohara, P. Carroll, A. Zektzer and J. Kurhanewicz, *Magnetic Resonance in Medicine*, **2008**, 60, 33-40.

[60] L. Shintu, F. Ziarelli and S. Caldarelli, *Magnetic Resonance in Chemistry*, **2004**, 42, 396-401.

[61] C. Johnson Jr., *Progress in Nuclear Magnetic Resonance Spectroscopy*, **1999**, 34, 203-256.

[62] K. Morris and C. Johnson Jr., *Journal of the American Chemical Society*, **1992**, 114, 3139-3141.

[63] G. Strobl, *The Physics of Polymers: Concepts for Understanding their Structures and Behavior*, Springer, Berlin (Germany), **1996**.

[64] K.-F. Arndt and G. Müller, *Polymercharakterisierung*, Hanser, Munich (Germany), **1996** (in German).

The viscosity of water at 5 °C (respectively 70 °C) was taken to be equal to 1.52×10^{-3} Pa s (respectively 4.04×10^{-4} Pa s).^[65] At 70 °C, convection movements are strong in the liquid α -CD/PEO mixture, such local flowing disturbing the measurements. The following spots appear at high temperature (Figure 3a):

- The spot at $D = 250 - 600 \mu\text{m}^2 \text{s}^{-1}$, corresponding to $\delta = 4.02$ ppm (chemical shift of PEO), leads to $D_h = 2.1 - 5.0$ nm. If the PEO chains are supposed to be in Θ -solvent conditions, the characteristic diameter of the coils is 8.0 nm.^[66] The difference between both values can lay on the convection movements, or on the solvent quality which is in reality lower than expected, thus reducing the 0.5 exponent given in numerator in reference 66. Nevertheless, both characteristic sizes are of the same order of magnitude. We can thus deduce that the spot at $D = 250 - 600 \mu\text{m}^2 \text{s}^{-1}$ corresponds to non-aggregated PEO chains.
- The spots observed at $D = 1000 \mu\text{m}^2 \text{s}^{-1}$, corresponding to $\delta = 4.14 - 4.31$ ppm and 3.89 - 3.98 ppm (chemical shifts of α -CD), lead to $D_h = 1.2$ nm. This corresponds to the characteristic diameter of the α -CD molecule.^[67] Thus, non-aggregated α -CDs are observed in the system. Moreover, no spot corresponding to the chemical shift of H_2O is found at $D = 1000 \mu\text{m}^2 \text{s}^{-1}$. It is attributed to a rapid exchange at 70 °C between free water molecules (which are majority in the system) and water molecules included in the α -CD cavities. A supplementary spot, corresponding to $\delta = 4.02$ ppm (chemical shift of PEO), is also observed. This sickle shaped spot is indubitably an artifact originating from the convection movements. Indeed, the fictive resulting PPR would diffuse faster than the non-aggregated PEO chains ($D = 250 - 600 \mu\text{m}^2 \text{s}^{-1}$), which is not possible.
- The spot at $D = 4500 \mu\text{m}^2 \text{s}^{-1}$, corresponding to $\delta = 4.65$ ppm (chemical shift of H_2O), leads to $D_h = 0.3$ nm. This indicates the presence of free water molecules.

When cooling down the α -CD/PEO mixture at 5 °C, the convection movements vanish. We are in favourable measurement conditions. The observed spots can thus be easily assigned from their chemical shifts. Moreover, at 5 °C, the system becomes white and is

[65] R. Weast, G. Tuve and S. Selby, *Handbook of Chemistry and Physics*, The Chemical Rubber, Cleveland (USA), **1968**.

[66] Considering the 22 kg mol^{-1} PEO chains as chains in Θ -solvent conditions, the gyration radius is given by $R_g = 499^{0.5} \times 0.44 / 6^{0.5} = 4.0$ nm.

[67] J. Szejtli, *Chemical Reviews*, **1998**, 98, 1743-1753.

not liquid anymore, inducing a global decrease of all measured diffusion coefficients. We consider the resulting spectrum at low temperature (Figure 3b):

- The spot at $D = 10 \mu\text{m}^2 \text{s}^{-1}$ corresponds to $\delta = 3.42$ ppm (chemical shift of PEO). We have thus $D_h = 27$ nm. This indicates the presence of unthreaded aggregated PEO chains which do not contain significant amount of bound water molecules. At the first site, this result seems to be surprising since PEO is almost in its free form and in better solvent conditions when cooling from 70 °C down to 20 °C.^[68,69] However, we do not deal with a simple PEO/water mixture but with a mixture containing also α -CDs at 5 °C.
- The spots observed at $D = 50 - 80 \mu\text{m}^2 \text{s}^{-1}$, corresponding to $\delta = 4.77$ ppm, 3.69 ppm and 3.59 ppm (chemical shifts of α -CD) and $\delta = 4.65$ ppm (chemical shift of H_2O), lead to $D_h = 3.4 - 5.4$ nm. This indicates the presence of α -CDs aggregates containing bound water molecules. These water molecules consist in some water molecules included in the α -CD cavities^[70] and some other situated between the aggregated α -CDs.
- The spots observed at $D = 160 \mu\text{m}^2 \text{s}^{-1}$, corresponding to $\delta = 3.65$ ppm and 3.61 ppm (chemical shifts of α -CD), lead to $D_h = 1.2$ nm. This indicates the presence of non-aggregated α -CDs. Thus, LS-DOSY reveals the coexistence of aggregated and non-aggregated α -CDs at 5 °C. Yet, this method being mainly qualitatively, it is not possible to evaluate the relative proportion of each of these two components.
- The spot at $D = 450 \mu\text{m}^2 \text{s}^{-1}$, corresponding to $\delta = 4.65$ ppm (chemical shift of H_2O), leads to $D_h = 0.6$ nm. This hydrodynamic diameter cannot correspond to totally non-interacting water molecules for which a typical value of 0.2 nm is expected. Consequently, we are in presence of a second type of water consisting in almost non-interacting water molecules.^[71]

[68] H. Venohr, V. Fraaije, H. Strunk and W. Borchard, *European Polymer Journal*, **1998**, 34, 723-732.

[69] E. Dormidontova, *Macromolecules*, **2002**, 35, 987-1001.

[70] K. Harata, *Chemical Reviews*, **1998**, 98, 1803-1827.

[71] L. Avram and Y. Cohen, *Journal of the American Chemical Society*, **2005**, 127, 5714-5719.

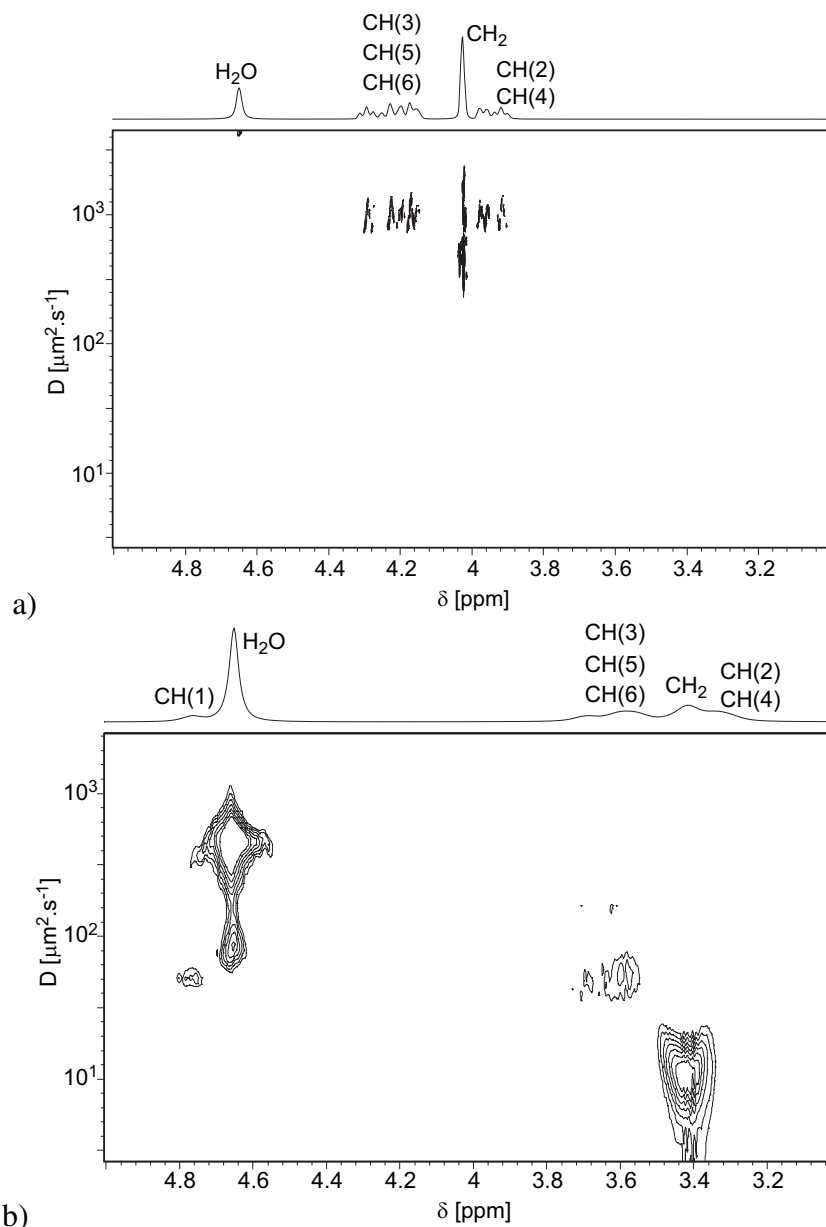


Figure 3. Liquid-state-DOSY ^1H NMR: Spectrum of an α -CD/PEO mixture, equivalent to PPR₈₀, at 15 w/w% in D_2O : a) after 15 min at 70°C and b) after 15 min at 5°C .

Furthermore, the LS-NOESY spectrum obtained at 70°C (Figure 4a) shows correlation spots between the α -CD characteristic peaks and the PEO characteristic peak. The absence of formation of PPRs at 70°C was proved by LS-DOSY measurements. Presently, the observed correlation spots do not correspond to the formation of PPRs but are attributed to weak interactions resulting from spatial proximity between α -CD molecules and PEO chains. The LS-NOESY spectrum obtained at 5°C (Figure 4b) shows large peaks which however cannot be interpreted in term of correlation between α -CDs and PEO. These measurements lead to conclusions analogous to the one

discussed above: Whereas unthreaded α -CD molecules and unthreaded PEO chains are observed at 70 °C, no PPR can be put into evidence in the liquid phase at 5 °C.

It comes from LS-DOSY and LS-NOESY experiments that no PPR is observed in the liquid phase at 5 °C.

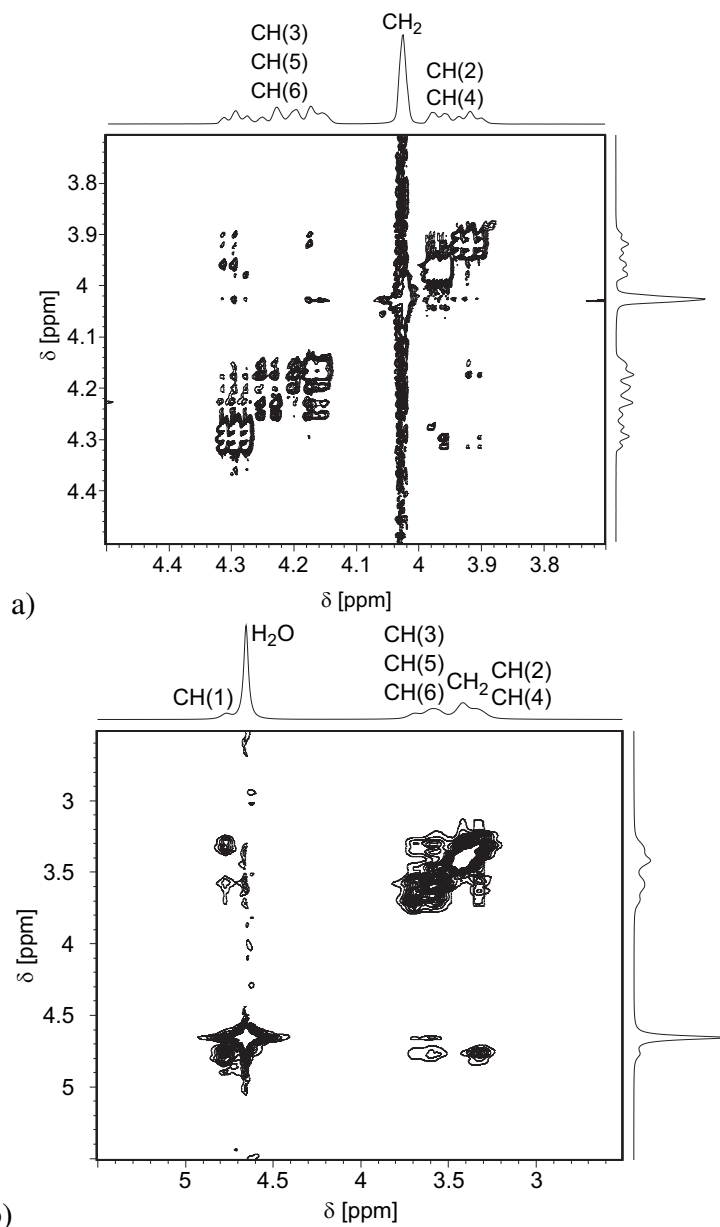


Figure 4. Liquid-state-NOESY ^1H NMR: Spectrum of an α -CD/PEO mixture, equivalent to PPR₈₀, at 15 w/w% in D_2O : a) after 15 min at 70 °C and b) after 15 min at 5 °C.

Now, we consider the solid phase of the α -CD/PEO mixture for which HRMAS-NOESY experiments were carried out at 70 °C and 5 °C (Figure 2). The spectrum of the α -CD/PEO mixture at 70 °C does not exhibit correlation between the α -CD characteristic peaks and the PEO characteristic peak, indicating that no PPR is

present (Figure 2a). On the contrary, after cooling down the α -CD/PEO mixture at 5 °C, we observe clear correlation spots between the α -CD characteristic peaks and the PEO characteristic peak (Figure 2b). Thus, PPRs are unambiguously present at 5 °C, forming large precipitated domains in their own phase.

After the α -CD/PEO mixture is kept at 5 °C, so that a physical gel containing PPRs is formed, the temperature is increased up to 70 °C. Most of the intramolecular weaker interactions fade out rapidly upon heating, the system becomes liquid again. After 5 h at 70 °C, HRMAS-NOESY experiments were carried out. The spectrum still shows correlation spots between the α -CD characteristic peaks and the PEO characteristic peak. It should also be noticed that the mixture still appears strongly milky. Thus, PPRs are still present when heating back the system up to 70 °C, forming large precipitated domains in their own phase. Heating the α -CD/PEO mixture from 5 °C up to 70 °C is not sufficient to break all the intramolecular weaker interactions and to induce a quantitative dethreading of the α -CDs. Thus, the behaviour of the studied system with the temperature is not totally reversible, a hysteresis phenomenon is observed. Urea should be added to the mixture besides heating so as to achieve a complete α -CD dethreading.^[72,73,74]

It comes from the previous experiments that:

- At 70 °C, no attractive interaction between α -CDs and PEO occurs. No PPR is formed.
- At 5 °C, such favourable interactions occur, leading to the formation of PPRs. The obtained PPRs are not in good solvent conditions in water, they thus form heterogeneities.

When an α -CD/PEO mixture is quenched from 70 °C down to 5 °C, the interactions between α -CDs and PEO become favourable, leading to the threading between both species and thus to the formation of PPRs, as followed by NMR. Yet, we observed that the formation of PPRs induces phase separation: PPR molecules are in the precipitated phase although unthreaded α -CD molecules and unthreaded PEO chains are in the liquid phase. Thus, for better understanding the interactions between PPRs and particularly between α -CDs leading to such a precipitation at high length-scale, small-angle neutron scattering (SANS) experiments were carried out.

[72] A. Harada, J. Li, S. Suzuki and M. Kamachi, *Macromolecules*, **1993**, 26, 5267-5268.

[73] H. Okumura, M. Okada, Y. Kawaguchi and A. Harada, *Macromolecules*, **2000**, 33, 4297-4298.

[74] C. Rusa and A. Tonelli, *Macromolecules*, **2000**, 33, 1813-1818.

2.3.2. Pseudo-polyrotaxane formation, aggregation and precipitation at 30 °C

In D₂O, the neutron contrast of α -CDs is almost the same as that of PEO (Annexe 2.a). Thus, SANS experiments can probe the structures constituted by α -CDs and/or PEO. Before studying the evolution with time of an α -CD/PEO mixture, equivalent to PPR₈₀, at 15 w/w% in D₂O at 30 °C, we focus on this system at 70 °C, corresponding to the dissociated state of the mixture and thus to the initial state of the system. The scattering profiles do not show any structural evolution with time at 70 °C. At this temperature, as shown by NMR measurements, unthreaded non-aggregated α -CD molecules and unthreaded non-aggregated PEO chains are observed in the system. To confirm the NMR results, the experimental curves are fitted by a superposition of the form factor of a thick cylinder $P_{cyl}^{[75]}$ of length $L_{\alpha-CD}$ and radius $R_{\alpha-CD}$ (to account for the presence of α -CDs), the form factor of a Gaussian behaviour $P_{Gauss}^{[76]}$ of gyration radius R_{gPEO} (to account for the presence of PEO) and an incoherent signal $I_{inc}^{[58]}$ (independent on q) in the following way:

$$I(q) = AP_{Gauss}(q, R_{gPEO}) + BP_{cyl}(q, L_{\alpha-CD}, R_{\alpha-CD}) + I_{inc} \quad (1)$$

With:

$$P_{Gauss}(q, R_{gPEO}) = \frac{2[\exp(-q^2 R_{gPEO}^2) + q^2 R_{gPEO}^2 - 1]}{q^4 R_{gPEO}^4} \quad (2)$$

$$P_{cyl}(q, L_{\alpha-CD}, R_{\alpha-CD}) = \int_0^{\frac{\pi}{2}} \left[\frac{2J_1(qR_{\alpha-CD} \sin \alpha)}{qR_{\alpha-CD} \sin \alpha} \frac{\sin\left(\frac{qL_{\alpha-CD} \cos \alpha}{2}\right)}{\frac{qL_{\alpha-CD} \cos \alpha}{2}} \right]^2 \sin \alpha d\alpha \quad (3)$$

Where A (respectively B) designates the weight of the Gaussian form factor (respectively cylinder form factor) and J_1 is the first-order Bessel function. The form factor P_{cyl} of length $L_{\alpha-CD}$ and radius $R_{\alpha-CD}$ is chosen to account for the presence of unthreaded and thus almost not aggregated α -CDs. Thus, the parameters $L_{\alpha-CD}$ and $R_{\alpha-CD}$ are taken equal to the characteristic dimensions of an α -CD, 0.79 nm and 0.76 nm respectively.^[67] The experimental profile is well rendered by the fitting curve obtained with equation (1) (Figure 5). We obtain $R_{gPEO} = 5$ nm, what is compatible with the PEO chain characteristic dimensions of 2.1 - 5.0 nm (hydrodynamic diameter obtained by NMR measurements at 70 °C) and of 8.0 nm (two times the gyration radius obtained by

[75] J. Pedersen, *Journal of Applied Crystallography*, **2000**, 33, 637-640.

[76] J. Pedersen and P. Schurtenberger, *Macromolecules*, **1996**, 29, 7602-7612.

calculation^[66]). It should be noticed that, although the form factor P_{cyl} is affected to smaller structures (unthreaded and thus almost not aggregated α -CDs), its use is necessary to obtain a proper fit. Thus, at 70 °C, the system is in good solvent conditions and contains unthreaded non-aggregated α -CD molecules and unthreaded non-aggregated PEO chains as shown by NMR measurements and corroborated by SANS experiments.

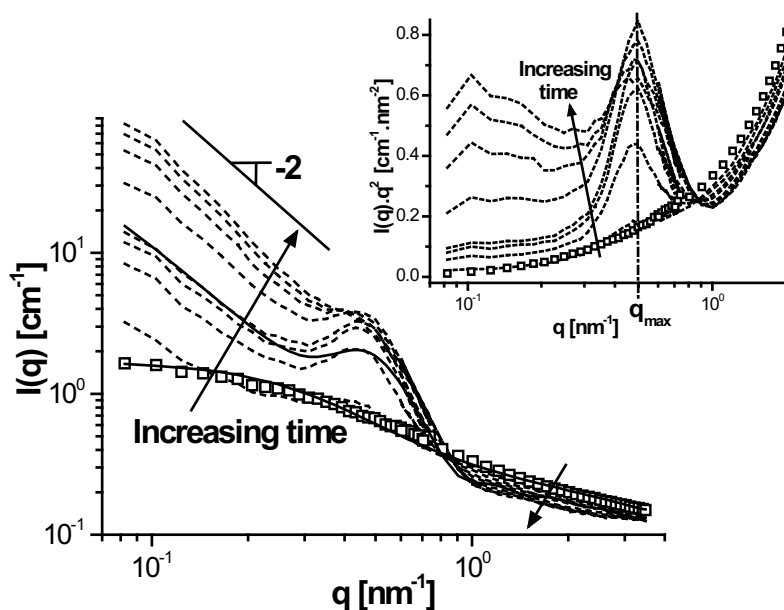


Figure 5. SANS: Absolute scattering intensity $I(q)$ versus modulus of the scattering vector q for an α -CD/PEO mixture, equivalent to PPR₈₀, at 15 w/w% in D₂O: (\square) at 70 °C, (solid line) fitting curve with equation (1) of the experimental profile at 70 °C, (dashed lines) after 5.5, 11, 16.5, 22, 71.5, 121, 170.5 and 220 min at 30 °C and (solid line) fitting curve with equation (4) of the experimental profile obtained after 22 min at 30 °C. Inset: corresponding Kratky-like plot.

The initial state of the α -CD/PEO mixture, equivalent to PPR₈₀, at 15 w/w% in D₂O at 70 °C being now well established, we focus on its temporal evolution when quenched down to 30 °C. For this, SANS scans were continuously recorded at 30 °C. The absolute scattering intensity profiles are characterized at intermediate q values by the apparition of a well-marked ripple (Figure 5). The ripple appears in the corresponding Kratky plot like a peak whose q_{max} position does not change with time and is found to be $q_{\text{max}} = 4.96 \times 10^{-1} \text{ nm}^{-1}$ (inset, Figure 5). It indicates that association takes place in the system and that the formed structures have the same characteristic sizes at any time. Indeed, such an association originates from the fact that a PPR molecule based on a 22 kg mol⁻¹ PEO guest chain exhibits a multiblock copolymer structure where one block

type is made of an α -CD rod-like tube and the other one of a naked PEO segment (*i.e.* the ethylene oxide units of the PEO chains which are not covered by α -CDs). Furthermore, the scattering intensity of the peak at q_{\max} increases with time, showing that the number of formed structures increases with time. Moreover, at low q values, the profiles exhibit the development of a q^{-2} shape, showing a Gaussian repartition of the formed structures, whose intensity increases with time.

Considering the studied experimental conditions (3.3 w/w% of PEO in water at 30°C), the observed structures are mainly based on threaded α -CDs. Indeed, on the one hand, medium molecular weight PEO (an average number molecular weight of 22 kg mol⁻¹ is currently used) at low concentration is almost in its free form in water at 30 °C as studied by different techniques.^[68,69,77,78,79,80,81,82] Thus, the naked PEO segments of the PPRs are also in good solvent conditions (*i.e.* non-aggregated) whatever their length. On the other hand, intramolecular association is known to occur (in solution or in the solid state) between α -CDs threaded onto polymer chains under the form of rod-like tubes corresponding to weakly stacked α -CDs along the polymer chains.^[24,40,41,43,83,84] Moreover, the rod-like tubes can intermolecularly aggregate to form large structures.^[40,41,43,84]

Thus, by analogy to the above reported experiments, the experimental profiles lead to interpret the threaded α -CD organization as a random association of thick cylinders which result from the aggregation of the already mentioned rod-like tubes. The experimental profiles are therefore fitted by a linear combination of the form factor of a thick cylinder $P_{\text{cyl}}^{[75]}$ of length L and radius R , the form factor of a Gaussian behaviour $P_{\text{Gauss}}^{[76]}$ of gyration radius R_g (to account for the random cylinder association) and an incoherent signal $I_{\text{inc}}^{[58]}$ (independent on q). The use of the cut-off function $f(q) = \exp\left[-(q/q_0)^\Phi\right]$ allows to weight the form factors as a function of q .^[76] Thus, P_{Gauss} dominates at low q whereas P_{cyl} is predominant at high q range. Moreover, at high q values, a decrease of the scattering intensity with time is observed, suggesting that the

[77] S. Kinugasa, H. Nakahara, N. Fudagawa and Y. Koga, *Macromolecules*, **1994**, 27, 6889-6892.

[78] K. Devanand and J. Selser, *Nature*, **1990**, 343, 739-741.

[79] S. Bekiranov, R. Bruinsma and P. Pincus, *Physical Review E: Statistical, Nonlinear and Soft Matter Physics*, **1997**, 55, 577-585.

[80] Y. Bae, S. Lambert, D. Soane and J. Prausnitz, *Macromolecules*, **1991**, 24, 4403-4407.

[81] S. Saeki, N. Kuwahara, M. Nakata and M. Kaneko, *Polymer*, **1976**, 17, 685-689.

[82] F. Bailey and R. Callard, *Journal of Applied Polymer Science*, **1959**, 1, 56-62.

[83] A. Tonelli, *Macromolecules*, **2008**, 41, 4058-4060.

[84] T. Girardeau, T. Zhao, J. Leisen, H. Beckham and D. Bucknall, *Macromolecules*, **2005**, 38, 2261-2270.

quantity of unthreaded and thus almost not aggregated α -CD decreases. Thus, the form factor of a cylinder $P_{cyl}^{[75]}$ of length $L_{\alpha-CD}$ and radius $R_{\alpha-CD}$ is introduced, allowing to account for the presence of unthreaded and thus almost not aggregated α -CDs. The resulting scattering intensity is written in the following way:

$$I(q) = A_{Gauss} \exp\left[-\left(\frac{q}{q_0}\right)^\Phi\right] P_{Gauss}(q, R_g) + B_{cyl} \left\{1 - \exp\left[-\left(\frac{q}{q_0}\right)^\Phi\right]\right\} P_{cyl}(q, L, R) \quad (4)$$

$$+ B_{\alpha-CD} P_{cyl}(q, L_{\alpha-CD}, R_{\alpha-CD}) + I_{inc}$$

Where q_0 designates the cut-off modulus (*i.e.* the crossover point between form factors), Φ represents the sharpness of the crossover region, A_{Gauss} stands for the weight of the Gaussian form factor, and B_{cyl} and $B_{\alpha-CD}$ stand for the weight of the cylinder form factors. It was shown elsewhere through a parameter optimization procedure that $\Phi = 5.33$.^[76] At any time, the fitting curves obtained with equation (4) render well the experimental profiles, as shown after 22 min at 30 °C (Figure 5), except in the crossover region. The presence of unthreaded non-aggregated PEO chains are not taken into account in equation (4), what does not prevent to obtain proper fits. We have $R_g \geq 33$ nm, $L = 5.7$ nm, $R = 4.7$ nm, $L_{\alpha-CD} = 0.79$ nm, $R_{\alpha-CD} = 0.76$ nm, $q_0 = 0.42$ nm⁻¹ and $I_{inc} = 0.1$ cm⁻¹. The observed difference between the experimental and the simulated curves in the crossover region may be due to the predominance of interaction effects between threaded α -CD-based nano-cylinders, what can be accounted for by the use of an effective structure factor S as follows:^[85]

$$I(q) = CS(q)P_{cyl}(q, L, R) + B_{\alpha-CD} P_{cyl}(q, L_{\alpha-CD}, R_{\alpha-CD}) + I_{inc} \quad (5)$$

Where C is a constant. The structure factor of equation (5) accounts by itself the interactions between the nano-cylinders in the whole q range. However, due to empirical formulations of the structure factors,^[85] it cannot be inferred that much from equation (5) and from the shape of S . Thus, the scattering intensity given by equation (4) will be used in the following.

The adequation at any time between the fitting and the experimental curves corroborates that the characteristic dimensions of the system (R_g , L , R , $L_{\alpha-CD}$, $R_{\alpha-CD}$) do not change with time. Thus, the growing with time of the forming threaded α -CD-based nano-cylinders is not observed. However, the number of threaded α -CD-based nano-cylinders should increase with time: The weighting parameters A_{Gauss} and B_{cyl} are

[85] P. Lindner and T. Zemb, *Neutron, X-rays and Light: Scattering Methods applied to Soft Condensed Matter*, Elsevier, Amsterdam (Netherlands), **2002**.

expected to increase. On the contrary, unthreaded and thus almost not aggregated α -CDs are "consumed" with time so as to form threaded α -CD-based nano-cylinders. Thus, their number should decrease with time: The weighting parameter $B_{\alpha\text{-CD}}$ is expected to decrease.

"Consumption" of unthreaded α -cyclodextrins

Since $P_{\text{cyl}}(q, L_{\alpha\text{-CD}}, R_{\alpha\text{-CD}})$ is used to account for the presence of unthreaded and thus almost not aggregated α -CDs, the parameters $L_{\alpha\text{-CD}}$ and $R_{\alpha\text{-CD}}$ are taken equal to the characteristic dimensions of an α -CD, 0.79 nm and 0.76 nm respectively.^[67] Then, the weighting $B_{\alpha\text{-CD}}$ of the form factor is determined as a function of time while the other parameters $L_{\alpha\text{-CD}}$ and $R_{\alpha\text{-CD}}$ are kept constant. The weighting parameter $B_{\alpha\text{-CD}}$ effectively decreases with time, reflecting the decreasing number of unthreaded and thus almost not aggregated α -CDs (Figure 6). At long time, $B_{\alpha\text{-CD}}$ does not go towards 0 but reaches a plateau value, showing that α -CDs still remain unthreaded and thus almost not aggregated. Consequently, the adopted notation PPR_N should not be understood as a pseudo-polyrotaxane having N threaded α -CDs per PEO chain, but as a pseudo-polyrotaxane prepared from an α -CD/PEO mixture with a molar stoichiometric ratio $N/1$. It should be noticed that the temporal evolution of $B_{\alpha\text{-CD}}$ is not rapid since roughly 75 min is needed to reach the plateau value. It indicates that the unthreaded and thus almost not aggregated α -CDs are swiftly "consumed", so as to form threaded α -CD-based nano-cylinders rapidly as confirmed latter in this article.

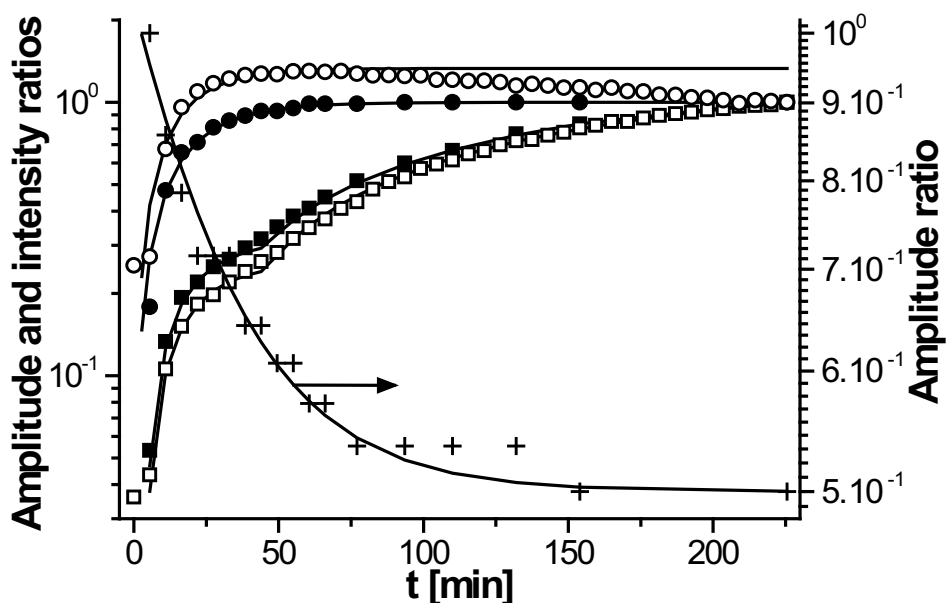


Figure 6. SANS: Amplitude ratios (■) $A_{\text{Gauss}}/A_{\infty 2}$, (●) $B_{\text{cyl}}/B_{\infty}$ and (+) $B_{\alpha\text{-CD}}/B_{\alpha\text{-CD}0}$ where $B_{\alpha\text{-CD}0}$ designates the value of $B_{\alpha\text{-CD}}$ at short times, as indicated in equation (4), and intensity ratios (□) $I(q = 1.24 \times 10^{-1} \text{ nm}^{-1})/I(q = 1.24 \times 10^{-1} \text{ nm}^{-1})_{\infty}$ where $I(q = 1.24 \times 10^{-1} \text{ nm}^{-1})_{\infty}$ represents the value of $I(q = 1.24 \times 10^{-1} \text{ nm}^{-1})$ at long times and (○) $I(q_{\text{max}} = 4.96 \times 10^{-1} \text{ nm}^{-1})/I(q_{\text{max}} = 4.96 \times 10^{-1} \text{ nm}^{-1})_{\infty}$ where $I(q_{\text{max}} = 4.96 \times 10^{-1} \text{ nm}^{-1})_{\infty}$ designates the value of $I(q_{\text{max}} = 4.96 \times 10^{-1} \text{ nm}^{-1})$ at long times *versus* time t at $30 \text{ }^{\circ}\text{C}$ for an $\alpha\text{-CD}/\text{PEO}$ mixture, equivalent to PPR_{80} , at $15 \text{ w/w}\%$ in D_2O . The solid lines are the fitting curves obtained with equations (6) and (7).

Formation of threaded α -cyclodextrin-based nano-cylinders

At any time, we obtain a gyration radius $R_g \geq 33 \text{ nm}$, a cylinder length $L = 5.7 \text{ nm}$, a cylinder radius $R = 4.7 \text{ nm}$ and an incoherent intensity $I_{\text{inc}} = 0.1 \text{ cm}^{-1}$. Moreover, the cut-off modulus q_0 is equal to 0.42 nm^{-1} . The value of R_g can only be undervalued. Indeed, the experimental data do not show a plateau in the lowest probed q region and a quasi-perfect q^{-2} behaviour without slight bend is observed (Figure 5). Except at $t = 5.5 \text{ min}$ where a q^{-1} shape substitutes the q^{-2} behaviour, corresponding to the association of the first formed threaded $\alpha\text{-CD}$ -based nano-cylinders as short chaplets. It should be noticed that the use in equation (4) of the form factor of a homogeneous sphere^[86] instead of that of a thick cylinder P_{cyl} ^[75] of length L and radius R gives similar profiles. Indeed, since the obtained parameter L does not differ strongly from $2R$, the cylinder can be viewed as a sphere. However, due to the ability of the $\alpha\text{-CD}$ s to form rod-like tubes corresponding to weakly stacked $\alpha\text{-CD}$ s along the polymer chains,^[24,40,41,43,83,84] a cylinder shape is more probable than a sphere shape. Thus, the

[86] Lord Rayleigh, *Proceedings of the Royal Society A*, **1911**, 84, 25-38.

form factor of a thick cylinder is kept in equation (4) and used in the following. Then, the weightings A_{Gauss} and B_{cyl} of the form factors are determined as a function of time while the other parameters R_g , L , R , I_{inc} and q_0 are kept constant. The evolutions with time of A_{Gauss} and B_{cyl} are studied in detail so as to have a better idea of the α -CD organization kinetics. As expected, the weighting parameters A_{Gauss} and B_{cyl} increase with time (Figure 6). The amplitude B_{cyl} which reflects the weight of the nano-cylinder form factor follows a simple-exponential law (equation (6)), indicating that the number of threaded α -CD-based nano-cylinders increases with time. The amplitude A_{Gauss} which reflects the weight of the Gaussian form factor follows a double-exponential law (equation (7)).

$$B_{\text{cyl}}(t) = B_{\infty} \left[1 - \exp\left(-\frac{t}{\tau_c^B}\right) \right] \quad (6)$$

$$A_{\text{Gauss}}(t) = A_{\infty 1} \left[1 - \exp\left(-\frac{t}{\tau_c^{A1}}\right) \right] + A_{\infty 2} \left[1 - \exp\left(-\frac{t - \tau_0^A}{\tau_c^{A2}}\right) \right] \quad (7)$$

Where $A_{\infty 1}$, $A_{\infty 2}$ and B_{∞} are constant pre-factors corresponding to long time values, τ_c^{A1} and τ_c^{A2} (respectively τ_c^B) represent the characteristic times of A_{Gauss} (respectively B_{cyl}) and τ_0^A designates the induction time of A_{Gauss} . The parameters obtained by fitting the temporal evolution of A_{Gauss} and B_{cyl} are given in Table 1.

Table 1. SANS: Characteristic times and amplitudes determined with equations (6) and (7) from the temporal evolution at 30 °C of the amplitudes A_{Gauss} , B_{cyl} , $I(q = 1.24 \times 10^{-1} \text{ nm}^{-1})$ and $I(q_{\text{max}} = 4.96 \times 10^{-1} \text{ nm}^{-1})$ for an α -CD/PEO mixture, equivalent to PPR₈₀, at 15 w/w% in D₂O.

	$A_{\infty 1} [\text{cm}^{-1}]$	$\tau_c^{A1} [\text{min}]$	$A_{\infty 2} [\text{cm}^{-1}]$	$\tau_c^{A2} [\text{min}]$	$\tau_0^A [\text{min}]$
A_{Gauss}	87.0	15.5	295	145	45.0
$I(q = 1.24 \times 10^{-1} \text{ nm}^{-1})$	9.5	15.9	45.0	160	45.0
	$B_{\infty} [\text{cm}^{-1}]$	$\tau_c^B [\text{min}]$	–	–	–
B_{cyl}	8.5	17.3	–	–	–
$I(q_{\text{max}} = 4.96 \times 10^{-1} \text{ nm}^{-1})$	3.7	14.4	–	–	–

It should be noticed that the intensity at $q_{\text{max}} = 4.96 \times 10^{-1} \text{ nm}^{-1}$, *i.e.* where the cylinder form factor dominates (respectively $q = 1.24 \times 10^{-1} \text{ nm}^{-1}$, *i.e.* where the Gaussian form factor dominates), *versus* time shows the same profile as B_{cyl} (respectively A_{Gauss}) (Figure 6) with comparable characteristic and induction times (Table 1). In the following, the evolutions with time of A_{Gauss} and B_{cyl} are studied in detail.

The values of τ_c^B and τ_c^{A1} are comparable up to the temporal resolution of the acquisitions. It shows that the formation of threaded α -CD-based nano-cylinders (aggregation step) and their association in a Gaussian way (precipitation step) are simultaneous. The increasing number of threaded α -CD-based nano-cylinders with time, leading to an increase of the scattering intensity of the peak at q_{\max} , engenders also an intensity increase in the q^{-2} region due to the need for the increasing number of threaded α -CD-based nano-cylinders to associate in a Gaussian way. Moreover, the value τ_c^{A2} characterizing the amplitude A_{Gauss} is much higher than τ_c^B and τ_c^{A1} . Furthermore, after $3\tau_c^B \sim 50$ min at 30 °C, the aggregation step is achieved and the number of threaded α -CD-based nano-cylinders remains constant. Thus, the threaded α -CD-based nano-cylinders, already associated in a Gaussian way during the first 50 min, continue to precipitate after the induction time τ_0^A . The Gaussian organization becomes much compact with time as indicating in the experimental profiles at low q values by the slight increase of the -2 slope and also by the intensity increase in the q^{-2} region. Thus, at 30 °C, α -CDs self-organize at three different length-scales in the following way:

- α -CDs thread onto PEO chains. The formed PPR molecules are not in good solvent conditions as shown by liquid-state and HRMAS NMR.
- Thus, at a higher length-scale, rapid aggregation of the PPR molecules occurs and threaded α -CD-based nano-cylinders form.
- At a higher length-scale, the threaded α -CD-based nano-cylinders which are linked together *via* naked PEO segments rapidly precipitate. They associate in a Gaussian way. This step, leading to the formation of large precipitated domains whose compacity increases at higher time-scale, may be responsible for the high turbidity of the studied system.

Consequently, the formation of PPRs, their aggregation and precipitation are not completely kinetically separated steps with respect to the time resolution of the SANS measurements. An initially liquid α -CD/PEO mixture forms a physical gel at long times. Thus, we followed the kinetics of gelation with mechanical measurements and more precisely with rheological dynamic analysis (RDA) measurements. We considered the α -CD/PEO mixture, equivalent to PPR₈₀, at 15 w/w% in water at 30 °C. The evolution with time of the elastic modulus (G') and the loss modulus (G'') at an angular frequency of 10 rad s⁻¹ is shown in Figure 7a. At short times, the elastic modulus G'_0 is smaller than the loss modulus and both are more or less constant with time up to an

induction time $\tau_1 = 17.2$ min. The mixture is liquid. Then, both moduli and particularly the elastic modulus increase strongly until $G' = G''$ at 41.7 min. G' and G'' remain equal up to $\tau_2 = 156$ min, where both again increase strongly with time before reaching asymptotic values (G'_{plateau} as far as concerns the elastic modulus). At the plateau, the elastic modulus G'_{plateau} is roughly one decade larger than the loss modulus. The mixture is thus a physical gel originating from hydrogen bonding interactions between threaded α -CD-based nano-cylinders which are linked together by naked PEO segments. As discussed above, neutron scattering experiments showed that this gelation is the result of different phenomena: the formation of PPRs and their aggregation into threaded α -CD-based nano-cylinders on a time-scale τ_c^B , and the association of the threaded α -CD-based nano-cylinders in a Gaussian way on two time-scales τ_c^{A1} and τ_c^{A2} . The formation and the association of the threaded α -CD-based nano-cylinders, on a time-scale $\tau_c^B \approx \tau_c^{A1}$, result in the first increase of the elastic modulus, and we have $\tau_1 \approx \tau_c^B \approx \tau_c^{A1}$. Then, the system undergoes its reorganization at higher time-scale τ_c^{A2} . This reorganization is associated with the increase of both moduli up to their long time plateau values on a time-scale $\tau_2 \approx \tau_c^{A2}$.

These results open new perspectives regarding the PPR chemical modification. Indeed, the fact that the system containing PPR molecules remains liquid during typically more than one hour gives enough time for PPR *in situ* chemical modification such as end-capping reaction.

Mechanical measurements thus allow to follow the PPR organization kinetics. We now use RDA measurements to study in detail the PPR organization kinetics and particularly the related energy barriers, varying the temperature.

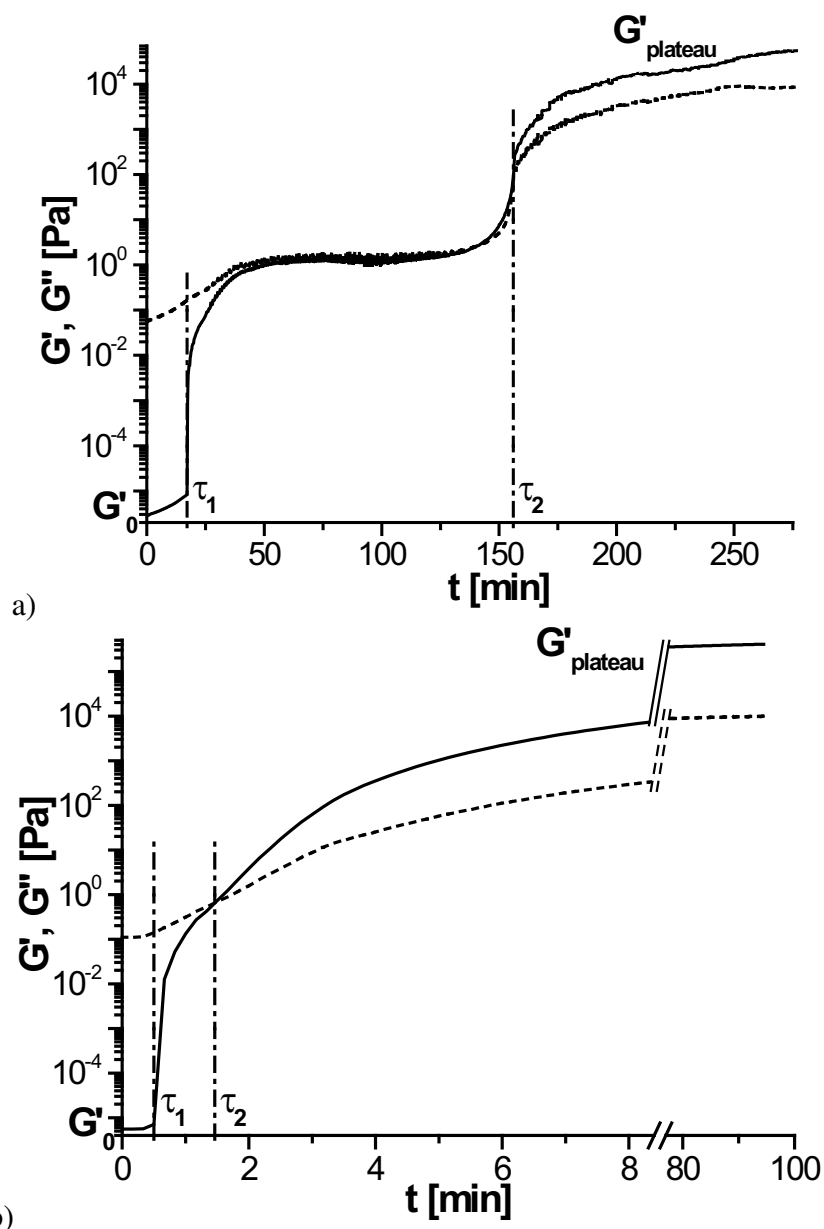


Figure 7. RDA: (solid line) Elastic modulus G' and (dashed line) loss modulus G'' at an angular frequency of 10 rad s^{-1} versus time t for an α -CD/PEO mixture, equivalent to PPR₈₀, at 15 w/w% in water: a) at 30 °C and b) at 5 °C. G'_0 is the value of the elastic modulus at an angular frequency of 10 rad s^{-1} at short times and G'_{plateau} its value at long times.

2.3.3. Pseudo-polyrotaxane formation, aggregation and precipitation at various temperatures

We carried out RDA measurements on α -CD/PEO mixtures, equivalent to PPR₈₀, at 15 w/w% in water at other temperatures (5 °C, 10 °C, 20 °C and 25 °C). The evolution with time of the elastic and the loss moduli at an angular frequency of 10 rad s^{-1} at 5 °C is shown in Figure 7b. For all studied temperatures, the temporal moduli evolution is of the same type as the one described at the end of section 2.3.2. Whatever the

temperature, the system is in the liquid state at short times and evolves towards a physical gel at $t \rightarrow \infty$. In this state, G'_{plateau} is typically 15 times higher than the loss modulus and of the order of 2×10^5 Pa. The main effect of the temperature change is a modification of the kinetics. Indeed, we observe that the induction time τ_1 decreases when the temperature decreases. A sharp increase of the elastic and the loss moduli with time is then followed by a latent regime where the evolution of the moduli slows down. The higher is the temperature, the longer is the latent regime and the smaller is the slope of the variation of the moduli with time (Figure 7a and 7b). Finally, after the time τ_2 , a second rapid increase of the moduli is observed and G' becomes higher than G'' up to their plateau values: a physical gel is formed.

The times characteristic of the evolution of the elastic and the loss moduli are thus τ_1 , corresponding to the formation of PPRs, their aggregation into threaded α -CD-based nano-cylinders and the association of the threaded α -CD-based nano-cylinders in a Gaussian way, and $\tau_2 - \tau_1$, corresponding to the final reorganization of the threaded α -CD-based nano-cylinders organized in a Gaussian way. These times increase with increasing temperature and are treated with an Arrhenius equation:

$$\frac{1}{y} = \frac{1}{y_0} \exp\left(\frac{-E_y^{\text{app}}}{RT}\right) \quad (8)$$

Where $y = \tau_1$ or $\tau_2 - \tau_1$, $1/y_0$ represents the pre-exponential factor which can also be called in the circumstances frequency factor or attempt frequency, E_y^{app} is the apparent activation energy and R designates the gas constant. The Arrhenius relationship fits well the experimental data (Figure 8) except for the extreme studied temperature (30 °C as far as concerns τ_1 and 5 °C as far as concerns $\tau_2 - \tau_1$). We obtain $E_{\tau_1}^{\text{app}} = -16.9 \text{ kJ mol}^{-1}$ and $E_{\tau_2 - \tau_1}^{\text{app}} = -75.2 \text{ kJ mol}^{-1}$. Both apparent activation energies are negative, as already reported in the case of physical gels based on schizophyllan,^[87] implying that the structure formation is more difficult and slower at high temperature. Moreover, the energy barrier of the final reorganization step is much higher than that to overcome in the previous step. Ceccato *et al.* modeled the threading mechanism of α -CDs onto PEO chains shorter (3.35 kg mol^{-1}) than the presently studied one and in more dilute aqueous mixtures (6.1 w/w%).^[45] They determine the energy related to the threading step by studying the effect of the temperature on a characteristic time called by them threading time, denoted t_{th} and corresponding to the steeply increase of the absorbance determined

[87] Y. Fang, R. Takahashi and K. Nishinari, *Biomacromolecules*, **2004**, 5, 126-136.

by UV-visible spectroscopy. In the model proposed by Ceccato *et al.*, if one substitutes t_{th} by the τ_1 values determined in the present article, it leads to an energy of $-74.9 \text{ kJ mol}^{-1}$ and an effective number of threaded α -CDs of $m = 24$. This quantitative experimental evaluation of m shows that only a small fraction of the ethylene oxide units of the PEO chains are covered by α -CDs. The obtained m value is much lower than $N = 80$ defined as the ratio of the used mole number of α -CD by that of PEO. This result, showing the presence of unthreaded α -CDs, is in agreement with SANS and NMR experiments. The energy value of $-74.9 \text{ kJ mol}^{-1}$ obtained with the model of Ceccato *et al.* is very different from the one obtained by the Arrhenius treatment $E_{\tau_1}^{app} = -16.9 \text{ kJ mol}^{-1}$. Indeed, the model proposed by Ceccato *et al.* presumes that the threading process is totally dissociated from all kinds of aggregation between PPRs. Thus, the theory reported in reference 45 is not appropriate for the characteristic time τ_1 determined by rheological measurements. A similar conclusion was also qualitatively reported by Tait et Davies,^[46] who refined the description of the complexation mechanism proposed by Ceccato *et al.* Finally, the characteristic time τ_1 and the related energy $E_{\tau_1}^{app}$ account not only for the threading of α -CDs onto PEO chains but also the aggregation of PPRs into threaded α -CD-based nano-cylinders and the association of the threaded α -CD-based nano-cylinders in a Gaussian way.

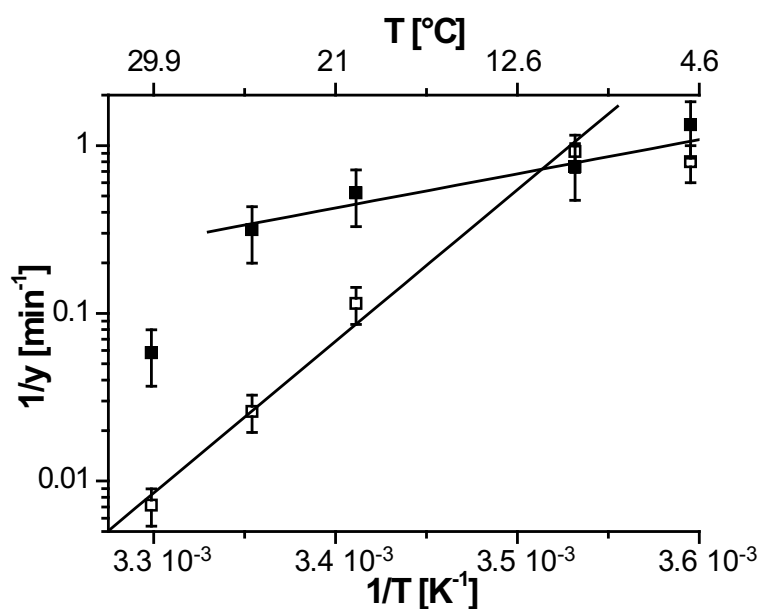


Figure 8. RDA: (■) $1/\tau_1$ versus $1/T$ and (□) $1/(\tau_2 - \tau_1)$ versus $1/T$ for an α -CD/PEO mixture, equivalent to PPR₈₀, at 15 w/w% in water.

2.3.4. Pseudo-polyrotaxane formation, aggregation and precipitation at various N values

The kinetics of gelation were followed by RDA measurements carried out on α -CD/PEO mixtures in which the ratio N of the used mole number of α -CD by that of PEO is varied (equivalent to $PPR_N = PPR_{80}, PPR_{65}, PPR_{50}, PPR_{35}, PPR_{20}$ and PPR_{10}), at a total mass fraction in α -CD and PEO of 15 w/w% in water at 5 °C. For all studied N values, the evolutions with time of the elastic and the loss moduli at an angular frequency of 10 rad s⁻¹ are similar and look like the one shown in Figure 7b in the case of PPR_{80} . PEO in water has the particularity to be in better solvent conditions when decreasing the temperature.^[68,69] Since PEO is almost in its free form (*i.e.* non-aggregated) in water at 30 °C, it is also aggregate-free in the studied experimental conditions at 5 °C. Moreover, α -CDs threaded onto polymer chains can associate as rod-like tubes^[24,40,41,43,83,84] and even as larger structures.^[40,41,43,84] Thus, the threaded α -CD-based structures observed by SANS at 30 °C and studied in section 2.3.2 are also present in the studied systems at 5 °C.

Both times characteristic of the evolution of the elastic and the loss moduli, τ_1 and $\tau_2 - \tau_1$, decrease when N increases and possess similar evolutions with N. The characteristic time $\tau_2 - \tau_1$, corresponding to the reorganization of the threaded α -CD-based nano-cylinders organized in a Gaussian way, exhibits a power law behaviour with N (Figure 9). The exponent characteristic of the Gaussian reorganization is -1.5 ± 0.9 , except for the point at N = 10. The other characteristic time τ_1 , corresponding to the formation of PPRs, their aggregation into threaded α -CD-based nano-cylinders and the association of the threaded α -CD-based nano-cylinders in a Gaussian way, exhibits also a power law behavior with N (Figure 9) whose exponent is -2.6 ± 0.8 , except for the point at N = 10. Between $t = 0$ and τ_1 , the evolution of the system can be described as follows:



Where $(PPR_N)_{cylinder}$ represents the threaded α -CD-based nano-cylinder and $[(PPR_N)_{cylinder}]_{Gauss}$ designates the threaded α -CD-based nano-cylinders organized in a Gaussian way. If we assume that the kinetics of equations (9), (10) and (11) is imposed by the first one, we have:

$$-\frac{d[PEO]}{dt} = K[PEO][\alpha - CD]^N \quad (12)$$

Thus, since at any time $[\alpha\text{-CD}] = N [PEO]$, we obtain after variable separation and integration between 0 and t:

$$[PEO] = \frac{[PEO]_0}{\left(1 + K[PEO]_0^N N^{N+1} t\right)^{\frac{1}{N}}} \quad (13)$$

Where $[PEO]_0$ is the initial PEO concentration. The characteristic time τ of the formation of PPRs can be deduced from equation (13):

$$\tau = \frac{2^N - 1}{K[PEO]_0^N N^{N+1}} \quad (14)$$

When we plot the characteristic time τ as a function of N (equation (14)), characterizing the formation of PPRs, it appears that this expression cannot account for the observed $N^{-2.6 \pm 0.8}$ decrease of τ_1 in the range from $N = 20$ up to $N = 80$, whatever K and $[PEO]_0$. Thus, the kinetics of the evolution of the system between $t = 0$ and τ_1 is not dominated by the formation of PPRs, and thus by the threading of α -CDs, but by the aggregation of the PPRs into threaded α -CD-based nano-cylinders and/or the association of the threaded α -CD-based nano-cylinders in a Gaussian way, what cannot be easily mathematically modeled. It should be remembered that, analogously, the kinetics of the evolution of the system at times $t > \tau_1$ is dominated by the Gaussian reorganization of the threaded α -CD-based nano-cylinders.

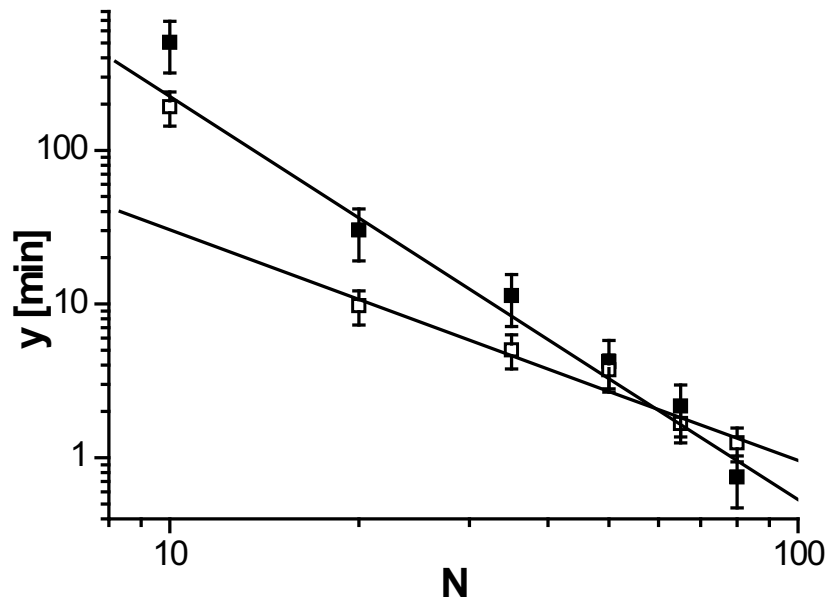


Figure 9. RDA: (■) τ_1 versus N and (□) $\tau_2 - \tau_1$ versus N for α -CD/PEO mixtures, equivalent to PPR_N , at 15 w/w% in water at 5 °C.

2.4. Conclusion

Currently, α -CDs are mainly used in the industry for their capacity to form inclusion complexes with a large variety of compounds, improving for instance the solubility of pharmaceutical products. Among the wide range of compounds which can be threaded by α -CDs, polymer chains and particularly PEO are good candidates. The appropriate experimental conditions leading to such a threading are of crucial importance. Thus, when an α -CD/PEO mixture in water is quenched from 70 °C down to a lower temperature (typically in the range from 5 °C to 30 °C), the interactions between α -CDs and PEO become favourable, leading to the threading between both species and thus to the formation of PPRs. We observed that the formation of PPRs from an α -CD/PEO mixture at a typical total mass fraction in α -CD and PEO of 15 w/w% induces phase separation and a white physical gel forms: PPR molecules are exclusively found in the precipitated phase although unthreaded α -CD molecules and unthreaded PEO chains are in the liquid phase.

At 30 °C, the physical gel formation is much slower than at 5 °C and the α -CD self-organization was studied as a function of time. We observed that, in a first step, α -CDs thread onto PEO chains, forming PPR molecules which are not in good solvent conditions in water. Thus, at a higher length-scale, rapid aggregation of the PPR molecules occurs and threaded α -CD-based nano-cylinders form (cylinder length $L = 5.7$ nm and cylinder radius $R = 4.7$ nm). At a higher length-scale, the threaded α -CD-based nano-cylinders rapidly precipitate. They associate in a Gaussian way, engendering the formation of large precipitated domains which are responsible for the high turbidity of the studied system. In a second step, at higher time-scale, the system undergoes its reorganization characterized by a compacity increase of the large precipitated domains.

Finally, our work which focused on the PPR formation at 30 °C leads to a new way to apprehend the α -CD/PEO-based polyrotaxane synthesis. Indeed, PPRs, the polyrotaxane precursors, are used to be obtained at low temperature (typically 5 °C) at high total mass fraction in water (ensuring a good yield of the synthesis). Unfortunately, this procedure induces the formation of a physical gel when intermediate or high molecular weight PEO chains are used and thus makes difficult to chemically modify *in situ* the formed PPRs (*e.g.* for end-capping or other functionalizations). Yet, for a total mass fraction of 15 w/w% at 30 °C, PPRs are totally formed after 15-20 min and the system stays in a

non-gel state up to 150 min. Thus, between these two characteristic times, we can easily envisage an efficient chemical modification of the PPRs in water.

Annexes

Annexe 2.a: Sensitivity of small-angle neutron scattering measurements in deuterated water

Characteristic quantities, such as the dimensions, the shape or the compacity of aggregated species, and the crystal perfectness or the type of crystal phase of organized assemblies, can be determined using scattering methods. Light, X-ray and neutron are classically used radiations. Different physical phenomena are responsible for the scattering of these radiations:

- For light scattering, the scattering cross-section is related to the polarizability variation between the solute and the solvent.^[88] In the case of dilute systems, this variation can be related to the difference between the indexes of refraction of the solution and that of the pure solvent.
- For X-ray scattering, the scattering cross-section is due to the electron density difference between the solute and the solvent.^[88]
- For neutron scattering, the determinant condition for scattering to occur concerns the scattering length density of the solute with respect to the solvent.^[89]

The scattering length density δ_i can be estimated as follows:

$$\delta_i = \frac{a_i N_A}{V_i} \quad (15)$$

$$a_i = \sum_m a_{i,m} \quad (16)$$

Where the index i stands for the α -CD, the PEO or the D_2O molecule and the index m represents the constitutive atoms of the molecule i . a_i designates the coherent diffusion length of the molecule i , N_A the Avogadro constant and V_i the molar volume of the molecule i . The so-called contrast length density ${}^v b_i$ with respect to the solvent is equal to:

$${}^v b_i = \delta_i - \delta_{solvent} \quad (17)$$

[88] G. Strobl, *The Physics of Polymers: Concepts for Understanding their Structures and Behavior*, Springer, Berlin (Germany), **1996**.

[89] J.-P. Cotton, *Journal de Physique IV (France)*, **1999**, 9, 21-49 (in French).

The obtained values are given in Table 2. The comparison of the obtained contrast length density ${}^v b_i$ values shows that α -CD and PEO scatter neutrons in an equivalent way in D_2O . Thus, SANS measurements are not sensitive to a particular species as far as concerns α -CD or PEO in D_2O .

Table 2. SANS: Molar volume V_i , coherent diffusion length a_i , scattering length density δ_i and contrast length density ${}^v b_i$ with respect to the solvent for $i = \alpha$ -CD, PEO and D_2O .

i	V_i [$cm^3 mol^{-1}$]	a_i [cm]	δ_i [cm^{-2}]	${}^v b_i$ [cm^{-2}]
α -CD	973	1.89×10^{-11} #	1.17×10^{10}	-5.22×10^{10}
PEO	40.1	4.13×10^{-13} #	6.20×10^9	-5.77×10^{10}
D_2O	18.1 ¶	1.92×10^{-12} #	6.39×10^{10}	0

¶: calculated with reference 90

#: calculated with equation (16) and reference 91

Annexe 2.b: Influence of the poly(ethylene oxide) terminal group on the kinetics of gelation

The kinetics of gelation were followed by RDA measurements carried out at 5 °C on α -CD/PEO mixtures using the following (un)modified PEOs: PEO_{OH} , PEO_{NH_2} and PEO_{COOH} . The mixtures were equivalent to PPR₅₀ at 15 w/w% in water. The evolution with time of the elastic and the loss moduli at an angular frequency of 10 rad s⁻¹ is similar to the one shown in Figure 7b. At short times, the mixture is liquid, the elastic modulus is smaller than the loss modulus and both remain constant with time up to τ_1 . Then, both moduli increase strongly and cross over each other at τ_2 before reaching asymptotic values, the elastic modulus being larger than the loss modulus. A physical gel is formed. The parameters τ_1 and $\tau_2 - \tau_1$ are plotted on a histogram as a function of the PEO chain end (Figure 10).

[90] A. Vértes, S. Nagy, Z. Klencsár and G. Molnár, *Handbook of Nuclear Chemistry. Elements and Isotopes: Formation, Transformation, Distribution*, Kluwer, Dordrecht (Netherlands), **2003**, volume 2.

[91] A.-J. Dianoux and G. Lander, *Neutron Data Booklet*, OCP Science, Philadelphia (USA), **2003**.

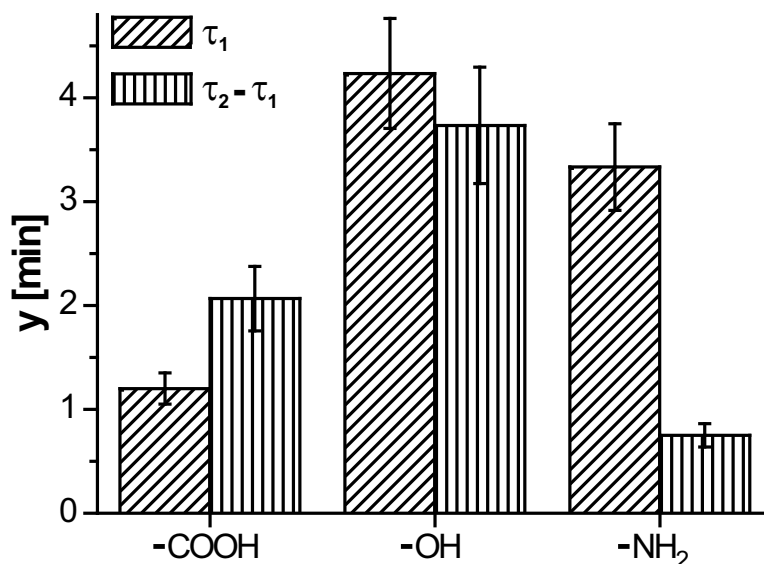


Figure 10. RDA: τ_1 and $\tau_2 - \tau_1$ versus PEO terminal group for α -CD/PEO mixtures, equivalent to PPR₅₀, at 15 w/w% in water.

The characteristic time τ_1 corresponds to the formation of PPRs, their aggregation into threaded α -CD-based nano-cylinders and the association of the threaded α -CD-based nano-cylinders in a Gaussian way. The most polar PEO terminal group -COOH among the studied one induces the formation of attractive hydrogen bonding interactions with α -CDs, thus favouring the surrounding of the terminal group by α -CDs. Thus, in spite of the bulkiness of the PEO terminal group -COOH, the shortest characteristic time τ_1 is observed for the polar PEO terminal group -COOH, in contrast with previously reported experiments.^[92,93,94] Indeed, in the presently carried out measurements as well as in those previously reported, inherently to such experiments, not only the polarity but also the size of the PEO terminal groups vary, leading to experiments in which two parameters vary simultaneously.

The parameter $\tau_2 - \tau_1$ corresponds to the reorganization of the threaded α -CD-based nano-cylinders organized in a Gaussian way. A priori, the reorganization step is not directly influenced by the PEO terminal group. Nevertheless, we observe that $\tau_2 - \tau_1$ varies by a factor 5 when the PEO terminal group is changed from -NH₂ to -OH. It may be assumed that this modification of kinetics is due to a change in the effective number

[92] J. Xue, L. Chen, L. Zhou, Z. Jia, Y. Wang, X. Zhu and D. Yan, *Journal of Polymer Science, Part B: Polymer Physics*, **2006**, 44, 2050-2057.

[93] J. Xue, Z. Jia, X. Jiang, Y. Wang, L. Chen, L. Zhou, P. He, X. Zhu and D. Yan, *Macromolecules*, **2006**, 39, 8905-8907.

[94] J. Xue, L. Zhou, P. He, X. Zhu, D. Yan and X. Jiang, *Journal of Inclusion Phenomena and Macrocyclic Chemistry*, **2008**, 61, 83-88.

of formed threaded α -CD-based nano-cylinders and thus in the effective number of threaded α -CDs per PEO chain.

CHAPTER 3

Physical gels based on polyrotaxanes in dimethyl sulfoxide

In the previous chapter (**Chapter 2**), it was shown that the experimental conditions, particularly the temperature but also the α -CD/PEO ratio or the choice of the PEO terminal group, controlling the interactions between α -CDs and PEO, are of crucial importance regarding to the threading process between α -CDs and PEO in water. As far as concerns the temperature, quenching an α -CD/PEO mixture in water from 70 °C down to a temperature in the range from 5 °C to 30 °C leads to favourable interactions between α -CD cavities and PEO chains. Thus, threading of α -CDs onto PEO chains occurs, corresponding to the formation of PPRs. Additionally, the formed PPR molecules are not in good solvent conditions in water. Phase separation occurs, the mixture becomes milky and a physical gel forms at a typical total mass fraction in α -CD and PEO of 15 w/w%. Interactions between PPR molecules and more precisely between threaded α -CDs *via* their hydroxyl groups were put in evidence. The aggregates generated by the formation of such hydrogen bonds consist in threaded α -CD based nano-cylinders corresponding to the alignment of segments made of weakly stacked α -CDs along the PEO chains. These nano-scale aggregates precipitate and reorganize at a higher length-scale, leading to the milky aspect of the system. Now, when the obtained PPRs are capped at both PEO chain ends using steric stoppers, PRs are obtained.^[A] It is empirically found that α -CD/PEO-based PRs are soluble in few solvents, such as DMSO,^[B,C] aqueous NaOH solution,^[B,C] halogen-containing ionic liquids,^[D] concentrated aqueous solutions of calcium thiocyanate^[E] and N,N-dimethylacetamide/lithium halogenide mixtures.^[F] Among them, DMSO is the most investigated in the literature. Yet, DMSO is found to be strictly speaking a solvent not as good as expected since it can lead at room temperature to a thixotropic rheological behaviour.^[G] Thus, it is wondered which types of weak interaction are present between PRs in DMSO and how they influence the PR structure. For this, PR solutions in DMSO will be studied in the concentrated regime.

The present chapter (**Chapter 3**) is dedicated to the study of the physical gelation of α -CD/PEO-based PRs in DMSO.

[A] F. Huang and H. Gibson, *Progress in Polymer Science*, **2005**, 30, 982-1018.

[B] A. Harada, J. Li, T. Nakamitsu and M. Kamachi, *Journal of Organic Chemistry*, **1993**, 58, 7524-7528.

[C] A. Harada, J. Li and M. Kamachi, *Journal of the American Chemical Society*, **1994**, 116, 3192-3196.

[D] S. Samitsu, J. Araki, T. Kataoka and K. Ito, *Journal of Polymer Science, Part B: Polymer Physics*, **2006**, 44, 1985-1994.

[E] J. Araki, T. Kataoka and K. Ito, *Journal of Applied Polymer Science*, **2007**, 105, 2265-2270.

[F] J. Araki and K. Ito, *Journal of Polymer Science, Part A: Polymer Chemistry*, **2006**, 44, 532-538.

[G] J. Araki and K. Ito, *Polymer*, **2007**, 48, 7139-7144.

More precisely, in the next subchapter (**Subchapter 3.1**), it is shown using rheological measurements that PRs in concentrated solution in DMSO form a physical gel with time at room temperature. Moreover, the interactions responsible for the physical gelation of PRs are precisely identified. Thermal analysis, nuclear magnetic resonance and X-ray scattering demonstrate that two distinct contributions lead to the formation of a physical gel: the crystallization of naked PEO segments (*i.e.* the ethylene oxide units of the PEO chains which are not covered by α -CDs) and the regular aggregation of α -CDs due to hydrogen bonding. The first mentioned contribution dominates at low complexation degree (*i.e.* the number of threaded α -CDs per PEO chain) value whereas the second one is present at high complexation degree value.

3.1. Physical gels based on polyrotaxanes: kinetics of the gelation, and relative contributions of α -cyclodextrin and poly(ethylene oxide) to the gel cohesion

Submitted to Macromolecular Symposia

Abstract

Polyrotaxanes (PRs) based on α -cyclodextrins (α -CDs) threaded onto 22 kg mol^{-1} poly(ethylene oxide) (PEO) chains in concentrated solution in dimethyl sulfoxide (DMSO) have shown the particularity to form physical gel when resting at $21 \text{ }^\circ\text{C}$. The wide range of studied complexation degrees N (from 7 up to 176), where N is the number of threaded α -CDs per PEO chain, allowed to better understand the molecular origin of the physical gelation. The non-monotonous evolution of the mechanical properties of the gels with the complexation degree can be attributed to the crystallization of naked PEO segments and the aggregation of α -CDs. In fact, differential scanning calorimetry (DSC) measurements carried out on these physical gels have shown two distinct endothermic peaks. The first peak at $29.4 \text{ }^\circ\text{C}$ has been attributed to the crystals of naked PEO segments (the PR molecule parts which are not covered by α -CDs). The second peak at $32.0 \text{ }^\circ\text{C}$ has been attributed to α -CD aggregates. It was observed that the dissolution enthalpy of the low temperature peak decreases monotonously with increasing N and the dissolution enthalpy of the high temperature peak increases monotonously with increasing N . These results were confirmed by X-ray scattering and ^1H nuclear magnetic resonance (^1H NMR) measurements showing the two contributions to the gelation.

From the above the cohesion of the physical gel is, on the one hand, due to the crystallization of the naked PEO segments and, on the other hand, to the regular aggregation of the α -CDs driven by intra- and inter-molecular hydrogen bonding interactions of their hydroxyl groups.

3.1.1. Introduction

Polyrotaxane (PR) is a pearl necklace shape supramolecule in which many macrocycles are threaded onto a single guest polymer chain whose ends are capped with bulky groups to prevent dethreading.^[1] Among them, PRs formed with α -cyclodextrins (α -CDs) as macrocycles have been widely studied.^[1] α -CDs are composed by the repetition of 6 glucose units organized in a truncated conic form. Among the 18 hydroxyl groups carried by an α -CD, 12 of them point outside the molecule, whereas the 6 other ones are directed towards the inner cavity. Favorable hydrophobic interactions between the inner cavity of the α -CDs and guest polymer chains such as poly(ethylene oxide) (PEO) can be tuned by choosing for instance an appropriate temperature^[2] or an adequate composition of the solvent mixture.^[3] Thus, PEO thread into the α -CDs in a controlled way forming PRs characterized by a given number of threaded α -CDs per PEO chain which can be varied over a wide range.

In the present study, we show that PRs based on α -CD and PEO in concentrated solution in DMSO form a physical gel with time at room temperature. Moreover, we precisely identify the interactions responsible for the physical gelation of PRs. For this, we studied PRs based on α -CD and PEO with molecular weight of 22 kg mol⁻¹ and varied complexation degree N (*i.e.* the number of threaded α -CDs per PEO chain) from 7 up to 176. From complementary experimental techniques, the origin of the physical gelation of PR solutions is elucidated. We demonstrate that two distinct contributions lead to the formation of physical gels:

- the crystallization of naked PEO segments (*i.e.* the ethylene oxide units of the PEO chains which are not covered by α -CDs),
- the aggregation of α -CDs due to intra- and inter-molecular hydrogen bonding.

3.1.2. Experimental section

3.1.2.1. Materials and polyrotaxane synthesis

Dihydroxy-terminated PEO was purchased from Serva Electrophoresis[®] and dried by an azeotropic distillation from toluene before use. An average number molecular weight

[1] G. Wenz, B.-H. Han and A. Müller, *Chemical Reviews*, **2006**, 106, 782-817.

[2] G. Fleury, C. Brochon, G. Schlatter, G. Bonnet, A. Lapp and G. Hadziioannou, *Soft Matter*, **2005**, 1, 378-385.

[3] N. Jarroux, P. Guégan, H. Cheradame and L. Auvray, *Journal of Physical Chemistry B*, **2005**, 109, 23816-23822.

of 22 kg mol^{-1} and a polydispersity index of 1.03 were measured in DMSO at $70 \text{ }^\circ\text{C}$ by gel permeation chromatography (GPC) with PEO standard calibration. DMSO (from Riedel de Haën[®]) was distilled over potassium hydroxide under reduced pressure. Deuterated dimethyl sulfoxide with a 99.9 % enrichment (DMSO- d_6) (from Aldrich[®]) was used as received without any further purification steps.

PRs based on α -CD as macrocycles, α,ω -bis-amine-terminated PEO (synthesized from dihydroxy-terminated PEO according to an adaptation of the procedure of Mutter^[4]) as guest chains and 2,4-dinitro-1-fluorobenzene as bulky groups were synthesized according to an adaptation of the procedure of Fleury.^[2] The PRs were obtained with a yield relative to the mole number of α,ω -bis-amine-terminated PEO ranging between 3 and 24 %. The values of the complexation degree were estimated using ^1H NMR in DMSO- d_6 and the efficiency of the capping step using GPC in HPLC grade DMSO at $70 \text{ }^\circ\text{C}$.^[2]

3.1.2.2. Characterization methods

^1H Nuclear Magnetic Resonance (^1H NMR). ^1H NMR spectra were recorded on a spectrometer commercialized by Bruker[®] and operating at a frequency of 400 MHz with 24 scans per spectrum. Each spectrum measured on a non-turning sample needed roughly 2.5 min to be measured. The PR solutions in DMSO- d_6 were introduced in the NMR tubes and heated up at $43 \text{ }^\circ\text{C}$ in a water bath during 5 min. Then, the tubes were rapidly introduced in the spectrometer pre-cooled at $21.0 \pm 0.5 \text{ }^\circ\text{C}$ and spectra were continuously recorded during 100 min. The internal lock was made on the ^2H -signal of the solvent.

Rheological Dynamic Analysis (RDA). RDA was performed on the Physica MCR 301 rheometer commercialized by Anton Paar[®] and equipped with the P-PTD 200 + H-PTD 200 Peltier system allowing heating or cooling in the range of -40 to $200 \text{ }^\circ\text{C}$. The rheometer could be strain controlled *via* a control loop or stress controlled. The used configuration was the CP 25-2 cone-plate geometry supplied by Anton Paar[®] with a cone angle of 2 ° , a diameter of 25 mm and a cone truncation of $49 \text{ }\mu\text{m}$. In order to achieve an initial state as reproducible as possible, the PR solutions in DMSO were heated up at $43.0 \pm 0.1 \text{ }^\circ\text{C}$ while continuously sheared at a shear rate

[4] M. Mutter, *Tetrahedron Letters*, **1978**, 19, 2839-2842.

of 40 s^{-1} . After 10 min in these conditions, the solutions were cooled down at $21.0 \pm 0.1 \text{ }^\circ\text{C}$. When this temperature was reached, the elastic modulus (G') and the loss modulus (G'') were continuously recorded during few hours at an angular frequency of 1 rad s^{-1} . Due to the large variation of the mechanical response of the mixtures with time, the following procedure was automated: At the beginning of the measurement, while the system was fluid enough, a constant stress of 0.1 Pa was applied. Then, as soon as the resulting deflection angle fell below the rheometer resolution, *i.e.* $7.0 \times 10^{-5} \text{ rad}$, a constant strain of 0.3 % was imposed.

Differential Scanning Calorimetry (DSC). DSC thermograms were recorded on the DSC 2910 calorimeter commercialized by TA Instruments[®] and equipped with a liquid nitrogen cooling accessory allowing continuous programmed cooling in the range of -150 to $725 \text{ }^\circ\text{C}$. The pressure DSC cells supplied by TA Instruments[®] were filled in with the PR solutions in DMSO. Afterwards, they were heated up to $43 \text{ }^\circ\text{C}$ and immediately cooled down at $21 \text{ }^\circ\text{C}$ at a heat/cooling rate of $\pm 5.0 \pm 0.1 \text{ }^\circ\text{C min}^{-1}$. Then, the cells were kept at $21.0 \pm 0.1 \text{ }^\circ\text{C}$ inside the DSC apparatus during a given aging time t_a varying between 1 min and 52 h and finally heated up to $43 \text{ }^\circ\text{C}$ at a heat rate of $5.0 \pm 0.1 \text{ }^\circ\text{C min}^{-1}$. A supplementary measurement point at $t_a = 16$ days (384 h) was obtained after keeping the cells in a room at $21 \pm 2 \text{ }^\circ\text{C}$.

Wide-angle X-ray Scattering (WAXS). WAXS measurements were made on the BM26 and ID02 beamlines at the European Synchrotron Radiation Facility (ESRF, Grenoble, France). The energies of X-ray photons were 10 keV for BM26 and 12 keV for ID02, which correspond respectively to wavelengths of 0.12 nm and 0.10 nm. The modulus of the scattering vector ($q = 4\pi \sin(\theta/2)/\lambda$) was calibrated using several diffraction orders of silver behenate. The solutions were first heated up at $43 \text{ }^\circ\text{C}$. Then, they were cooled down at $21 \text{ }^\circ\text{C}$. The samples were measured after a long aging time (typically 24 h) at this temperature. The total volume crystallinity at a given time is defined as the ratio of intensity of all crystalline peaks over the total intensity corrected by the background and the Lorentz factor. The volume crystalline ratios are given with respect to the whole PR system volume.

3.1.3. Results and discussion

PRs with well defined complexation degrees (N) (*i.e.* the number of threaded α -CDs per PEO chain) ranging from 7 to 176 are obtained thanks to the methodology previously reported.^[2] In the following, the PRs will be denoted PR_N where N is the complexation degree. Since PEO with a molecular weight of 22 kg mol⁻¹ is used, the α -CD overlap ratio (*i.e.* the percentage of ethylene oxide units of the PEO chains which are covered by α -CDs) ranges from 3 to 70 %. A concentrated PR solution in DMSO heated up at 43 °C is fluid. When cooled down at 21 °C, it gelifies slowly with time. This process is fully thermo-reversible as the formed gel returns to its original fluid state and remains fluid when heated up at 43 °C. Thus, we have chosen to follow the evolution with time of the mechanical properties of the PR solutions when they are quenched from 43 °C down to 21 °C, *i.e.* 3 °C above the crystallization temperature of pure DMSO.

3.1.3.1. Macroscopic signature of the gelation

Rheological dynamic analysis (RDA) measurements were performed on PR₇, PR₃₇, PR₈₅ and PR₁₅₇ concentrated solutions (19.6 w/w%) in DMSO. The typical evolution of the elastic (G') and the loss (G'') moduli at an angular frequency of 1 rad s⁻¹ with time at 21 °C in the case of PR₇ is given in Figure 1a. Three distinct time domains are observed: At first, the system is liquid, the elastic modulus G'_0 is smaller than the loss modulus and both remain constant with time during a so-called induction time. Afterwards, the two moduli cross-over each other and increase strongly. Finally, the elastic modulus is one order of magnitude larger than the loss modulus and both moduli evolve slowly with time to an asymptotic value (G'_{plateau} as far as concerns the elastic modulus). In the last regime, the elastic modulus no longer depends on the angular frequency between 10² and 10⁻² rad s⁻¹ (inset of Figure 1a): A physical gel is formed.

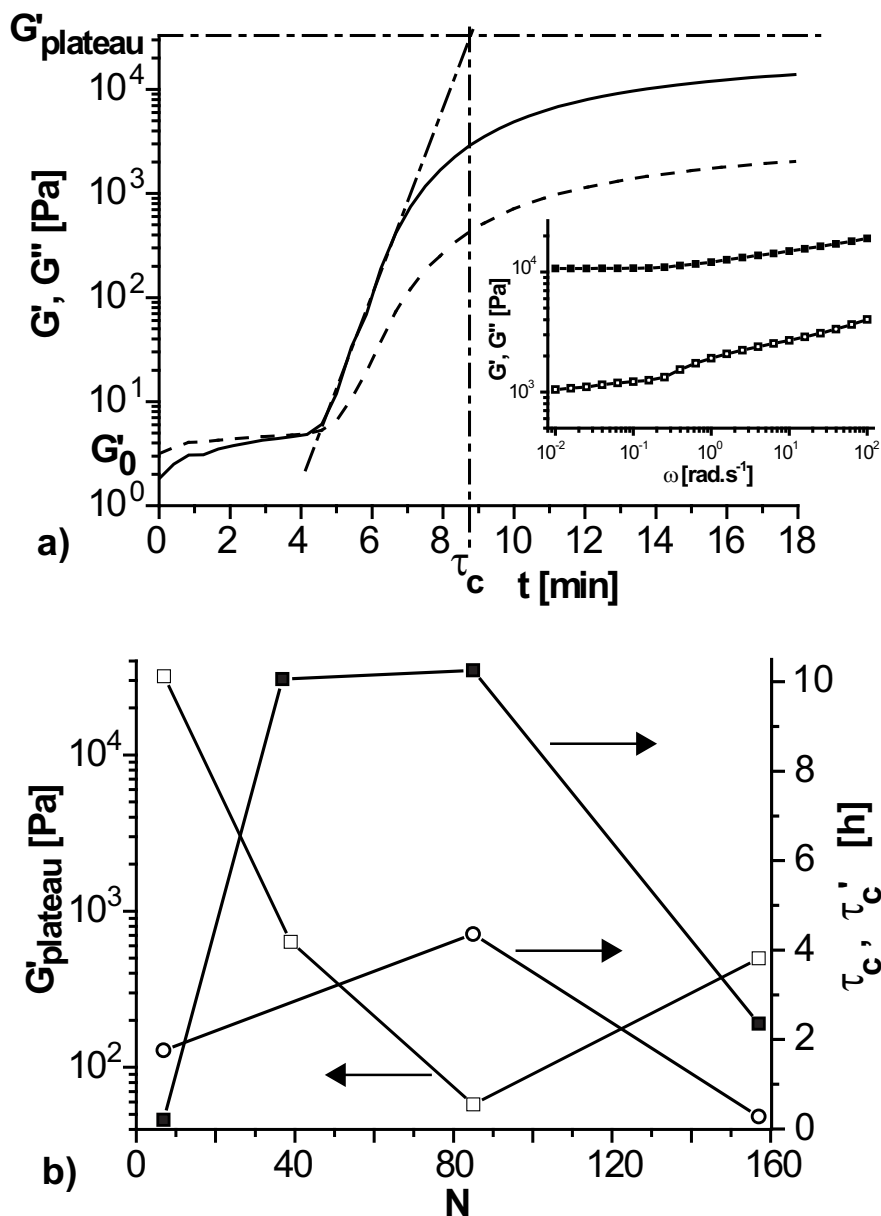


Figure 1. RDA: a) (solid line) Elastic modulus G' and (dashed line) loss modulus G'' at an angular frequency of 1 rad s^{-1} versus time t at $21 \text{ }^\circ\text{C}$ for PR_7 at $19.6 \text{ w/w}\%$ in DMSO. G'_0 is the value of the elastic modulus at an angular frequency of 1 rad s^{-1} at short times and G'_{plateau} its value at long times. Inset: (■) elastic modulus G' and (□) loss modulus G'' versus angular frequency ω for PR_7 at $19.6 \text{ w/w}\%$ in DMSO after 18 min at $21 \text{ }^\circ\text{C}$. b) (□) Elastic modulus G'_{plateau} at long times at an angular frequency of 1 rad s^{-1} , (■) characteristic time τ_c determined through RDA measurements and (○) characteristic time τ_c' determined through DSC measurements versus complexation degree N for PRs at $19.6 \text{ w/w}\%$ in DMSO at $21 \text{ }^\circ\text{C}$.

Different mechanisms can be proposed for the existence of the observed induction time:

- It could correspond to the time necessary for physical cross-link points to self-organize in a 3D percolated structure. Links may be formed prior to the

global gelation of the solution and play the role of nucleation points. In the general case, these pre-gel structures consist in weakly branched polymer chains, clusters^[5,6] or nucleation sites.^[7] Theoretical studies also reported that a thermo-reversible behaviour is due to weak junctions between associating groups or segments in an intra- and/or inter-molecular way. These junctions can have various functionalities.^[8,9,10] In our case, these structures consist both in α -CD clusters and PEO nucleation sites. When the percolation step is achieved, the viscoelastic moduli increase abruptly. Usually, the induction time of physical gelations is much higher than the one of chemical gelations due to the possibility of reformation of the physical links.

- It could also correspond to the time needed to overcome the energy barrier leading to the formation of one cross-link point. Such an induction time is known for physical gelation of sugar derivative polymers such as agarose,^[11] konjac glucomannan^[12] and methylcellulose^[11] having semi-rigid structure. On the contrary, galactomannan^[13] and poly(vinyl alcohol)^[14] have very flexible coil type structure and consequently can easily and rapidly change their conformations so as to find the most adequate position for association and gelation to occur. Thus, they do not show any induction time before their physical gelation.^[13,14]

PRs in solution in DMSO have different structures as a function of the number of threaded α -CDs per PEO chain.^[2] Indeed, PR₇ is much more flexible than PRs with higher complexation degrees. These differences may thus be responsible for the very low value of the induction time for PR₇ and the higher ones observed with higher complexation degrees.

Furthermore, the kinetics of the moduli evolution for the different complexation degrees are compared by considering a characteristic time τ_c . This time is defined as the

[5] Y. Fang, R. Takahashi and K. Nishinari, *Biomacromolecules*, **2004**, 5, 126-136.

[6] M. Takahashi, K. Yokoyama, T. Masuda and T. Takigawa, *Journal of Chemical Physics*, **1994**, 101, 798-804.

[7] M. Williams, T. Foster, D. Martin, I. Norton, M. Yoshimura and K. Nishinari, *Biomacromolecules*, **2000**, 1, 440-450.

[8] A. Semenov and M. Rubinstein, *Macromolecules*, **1998**, 31, 1373-1385.

[9] F. Tanaka and W. Stockmayer, *Macromolecules*, **1994**, 27, 3943-3954.

[10] M. Gordon and S. Ross-Murphy, *Pure and Applied Chemistry*, **1975**, 43, 1-26.

[11] K. Nishinari, *Colloid and Polymer Science*, **1997**, 275, 1093-1107.

[12] M. Yoshimura and K. Nishinari, *Food Hydrocolloids*, **1999**, 13, 227-233.

[13] E. Pezron, A. Ricard and L. Leibler, *Journal of Polymer Science, Part B: Polymer Physics*, **1990**, 28, 2445-2461.

[14] R. Schultz and R. Myers, *Macromolecules*, **1969**, 2, 281-285.

intersection point between the tangent at the inflexion point and the asymptote at long times of the G' profiles (Figure 1a). The characteristic time τ_c as well as the plateau elastic modulus G'_{plateau} (Figure 1b) are not monotonous functions of the complexation degree. At low complexation degrees N , τ_c increases with the complexation degree. It then decreases at high N values. G'_{plateau} shows the opposite tendencies. The decrease of G'_{plateau} for $N \leq 85$ is attributed to the decrease of the number of cross-linked domains formed by naked PEO segments which are in bad solvent.^[15] The increase of G'_{plateau} for $N \geq 85$ is attributed to two origins: the increase of the concentration of α -CD aggregates on the one hand and the increase of the PR stiffness on the other hand at high N values. Indeed, the α -CD mole number does not increase significantly to explain by itself the strong increase of G'_{plateau} . However, it has been demonstrated that with increasing N the stiffness of PR increases significantly.^[2]

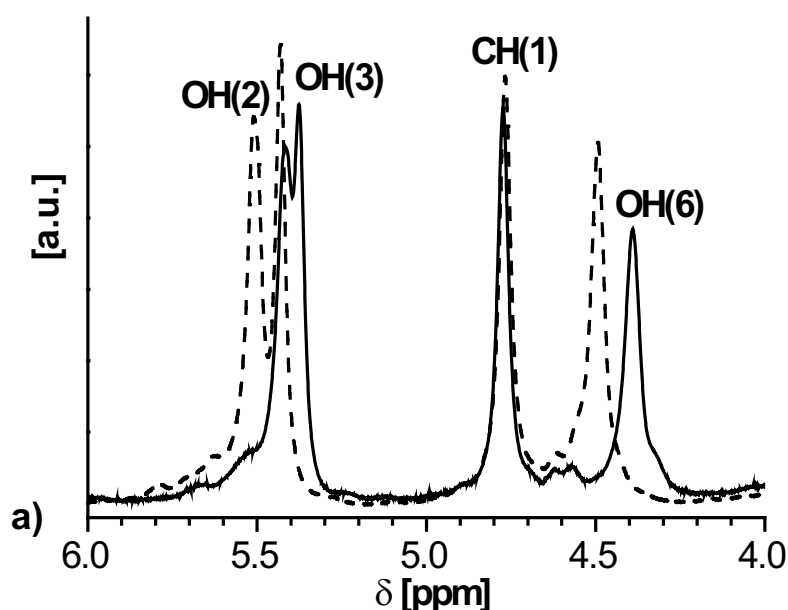
Thus, two different gelation phenomena occur. At low N , a large fraction of the PEO chains is not covered by α -CDs, and local precipitation of naked PEO segments form the physical cross-linked domains of the gel. At high N , α -CD aggregates participate to the gel cohesion. This implies a phase separation between the aggregated domains (made of α -CDs and naked PEO segments) and the solvent, the non-aggregated PR molecule parts forming the strands of the gel network.

3.1.3.2. Role of α -cyclodextrin and poly(ethylene oxide) in the gelation

To identify the implication of α -CD and PEO functional groups in the gelation, ^1H nuclear magnetic resonance (^1H NMR) measurements were carried out on PR_{85} at 19.6 w/w% in DMSO-d_6 . The signals of diluted PR solutions have already been assigned.^[2] The same characteristic peaks are also found, a bit broader, on the performed measurement in the concentrated regime. The signals of all α -CD hydroxyl groups – OH(2), OH(3) and OH(6) (Figure 2c) – are significantly shifted during gelation whereas the signals of other α -CD functional groups such as the tertiary proton CH(1) are almost not affected (Figure 2a). Thus, it suggests that the formation of hydrogen bonds between α -CDs contributes to the gelation. During the gelation process, the electronic environment of the α -CD hydroxyl group OH(3) is a bit less affected than that of the α -CD hydroxyl groups OH(2) and OH(6). On the one hand, the α -CD hydroxyl group OH(2) is directed inside the α -CD cavity (Figure 2c) and can thus only

[15] C. Özdemir and A. Güner, *European Polymer Journal*, **2007**, 43, 3068-3093.

interact in an intramolecular way. The shift of this characteristic peak cannot be due to the formation of α -CD tubes resulting from the stacking of few α -CD units along the PEO chain since they are already present in the pre-gel system.^[2,16] From our point of view, the only realistic explanation of this shift is the change of the electronic environment along the α -CD tubes resulting from the modification of the equilibrium distance between adjacent stacked α -CDs, *i.e.* belonging to the same tube. On the other hand, the α -CD hydroxyl group OH(3) is directed outside the α -CD cavity and OH(6) is a mobile secondary hydroxyl group (Figure 2c). Both groups can thus be involved in the gelation in an intra- and/or inter-molecular way. The shift of their characteristic peaks is thus responsible for the formation of aggregates resulting from the association of the α -CD tubes as well as in the modification of the equilibrium distance between adjacent stacked α -CDs coming from the formation of aggregates. The signal of the PEO group CH₂ is much less, but still, shifted compared to the α -CD hydroxyl groups (Figure 2b). Indeed, the carbon atoms are located in the external corona of the crystal helix.^[17] Consequently, the carbon atoms belonging to neighbouring PEO chains face one another. Thus, the observed upfield shift of the CH₂ peak is consistent with a crystalline state of naked PEO segments. Whereas the chemical shift of CH₂ is weak and should be considered with prudence, this result indicates that naked PEO segments contribute to the gelation of the PR₈₅ solution.



[16] G. Fleury, G. Schlatter, C. Brochon and G. Hadziioannou, *Polymer*, **2005**, 46, 8494-8501.

[17] Y. Takahashi and H. Tadokoro, *Macromolecules*, **1973**, 6, 672-675.

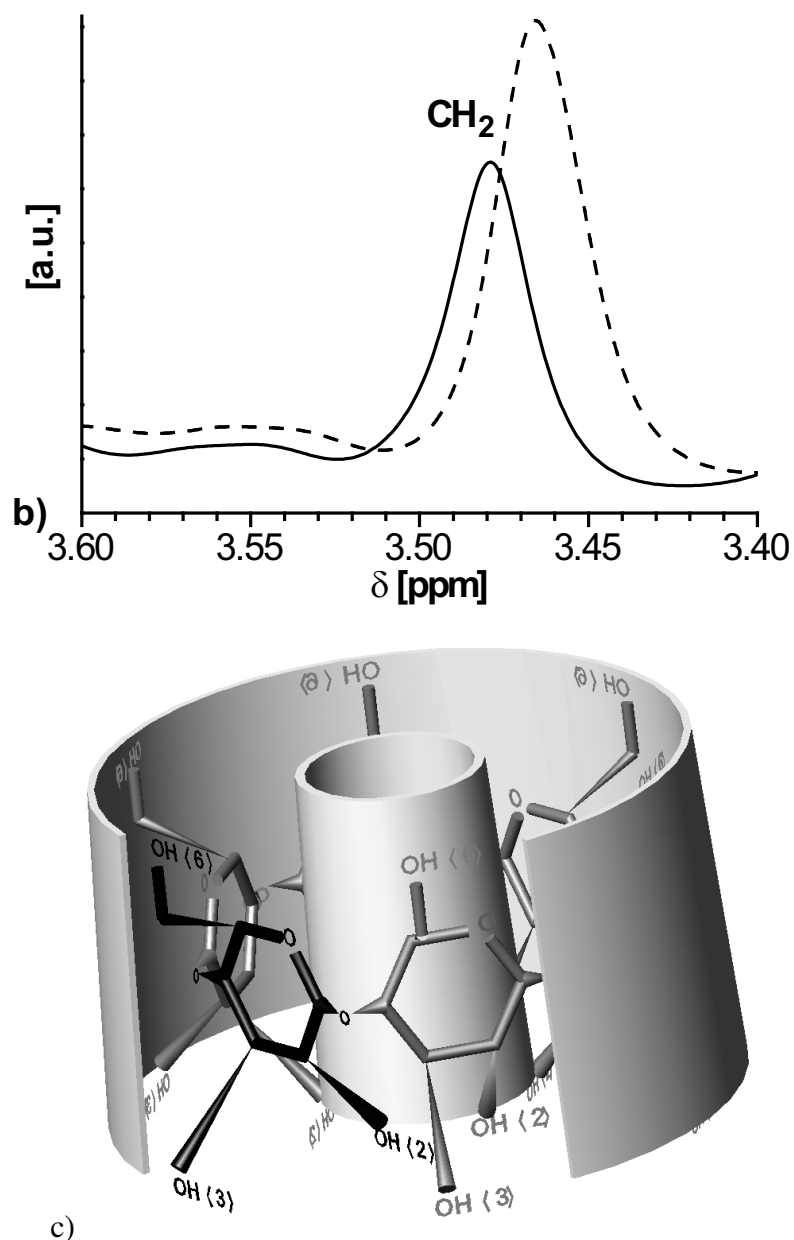
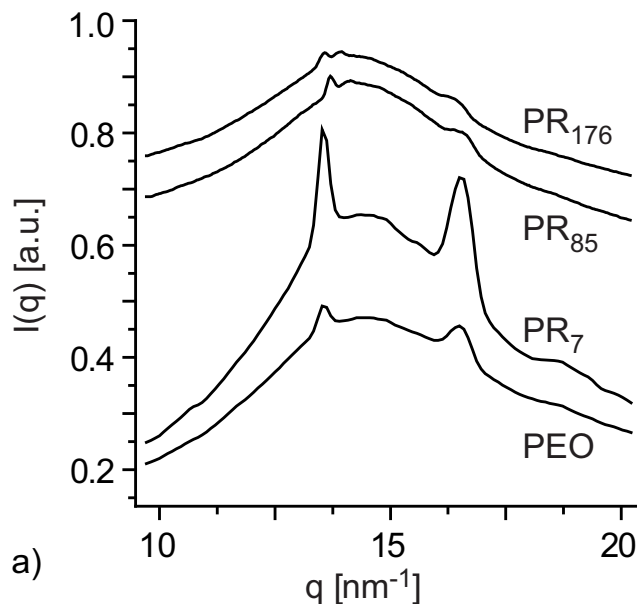


Figure 2. ^1H NMR: Spectra showing some characteristic peaks of: a) the α -CD macrocycle of the PR molecule and b) the PEO chain of the PR molecule for PR₈₅ at 19.6 w/w% in DMSO- d_6 after: (solid line) $t = 0$ and (dashed line) $t = 100$ min at 21 °C. c) Schematic 3D representation of an α -CD molecule.

During the gelation, local α -CD demixion with regard to the naked PEO segments and DMSO is suggested by RDA and ^1H NMR. Thus, it is interesting to study if such a demixion leads to crystallization. Indeed, wide-angle X-ray scattering (WAXS) patterns exhibit two intense quite narrow peaks together with a number of broader much less intense ones (Figure 3a). The positions of the peaks at $q = 13.5 \text{ nm}^{-1}$ (corresponding to the Miller indices^[17] $(hkl) = (120)$), 16.5 nm^{-1} ((112) , (032) and $(13-2)$),

18.5 nm⁻¹ (024), 19.5 nm⁻¹ (22-4) and 25.5 nm⁻¹ ((124) and (044)) are not influenced by the complexation degree. They are also found on the pattern of pure PEO at 4.5 w/w% in DMSO and are identical to the conventional monoclinic crystalline phase of PEO. Thus, DMSO being a bad solvent for PEO at 21 °C,^[15] crystallization of the naked PEO segments of the PR molecules in DMSO is observed at this temperature. For all studied PR_N and even for the pure PEO, the lateral size of the crystals formed by the naked PEO segments in the (120) direction is estimated with the Scherrer equation^[18] to be 27 ± 5 nm. In addition to the PEO peaks, a weak peak at q = 14.0 nm⁻¹ is visible in the patterns at high N values (N ≥ 85, Figure 3b) whose relative intensity increases with the complexation degree. It can be attributed to the (210) peak of the α-CD crystal structure.^[19] This structure can be due to the formation of α-CD tubes originating from attractive intramolecular hydrogen bonding interactions^[20,21] followed by the regular aggregation of these tubes due to attractive intermolecular hydrogen bonding. Thus, for lower N values, the formation of naked PEO segment crystallites is predominant whereas at higher N a second contribution due to well-organized α-CD aggregates participates to the gel cohesion.



[18] H. Klug and L. Alexander, *X-Ray Diffraction Procedures for Polycrystalline and Amorphous Materials*, Wiley, New York (USA), **1974**.

[19] I. Topchieva, A. Tonelli, I. Panova, E. Matuchina, F. Kalashnikov, V. Gerasimov, C. Rusa, M. Rusa and M. Hunt, *Langmuir*, **2004**, 20, 9036-9043.

[20] T. Girardeau, T. Zhao, J. Leisen, H. Beckham and D. Bucknall, *Macromolecules*, **2005**, 38, 2261-2270.

[21] A. Tonelli, *Macromolecules*, **2008**, 41, 4058-4060.

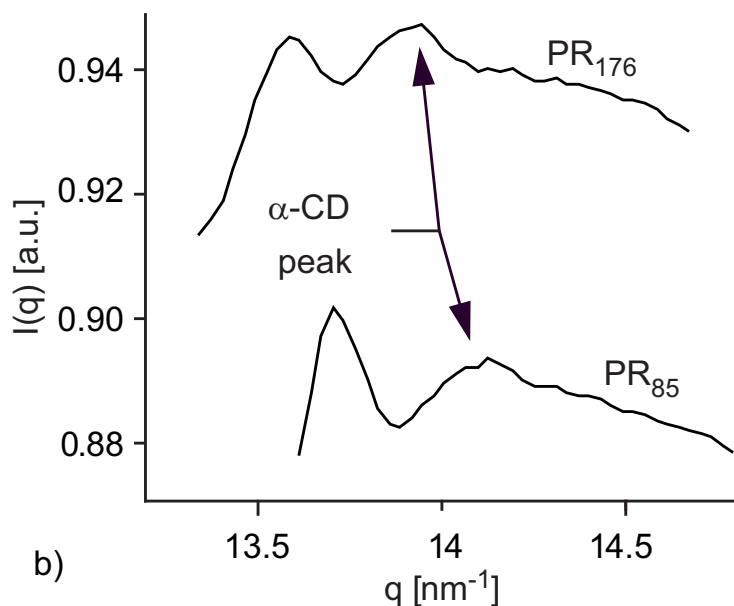


Figure 3. WAXS: Scattering intensity $I(q)$ versus modulus of the scattering vector q for PRs at 19.6 w/w% in DMSO after a long aging time at 21 °C and for PEO at 4.5 w/w% in DMSO after a long aging time at 21 °C.

In order to distinguish between the two contributions and quantify them, we used differential scanning calorimetry (DSC) to follow the association between α -CDs and between naked PEO segments with time at 21 °C.

DSC experiments performed on PR_N , with $N \geq 37$, in solution at 19.6 w/w% in DMSO show the development of two dissolution peaks with increasing aging time t_a for which the mixture is kept at 21 °C (example in Figure 4a for PR_{85}). The temperature position of the peaks, obtained after deconvolution of the mass heat flow curves using two Gaussian functions, is independent on the aging time and on the complexation degree N : 29.4 ± 0.2 °C and 32.0 ± 0.2 °C. In the case of PR_7 , DSC thermograms show monomodal profiles with a peak at 29.4 ± 0.2 °C. Furthermore, DSC measurements carried out on pure PEO at 4.5 w/w% in DMSO reveals a monomodal thermogram with a dissolution peak at 29 ± 0.2 °C. Thus, the low temperature peak at 29.4 °C is assigned to the dissolution of the PEO crystals whereas the high temperature peak at 32.0 °C corresponds to the dissolution of the organized α -CD aggregates.

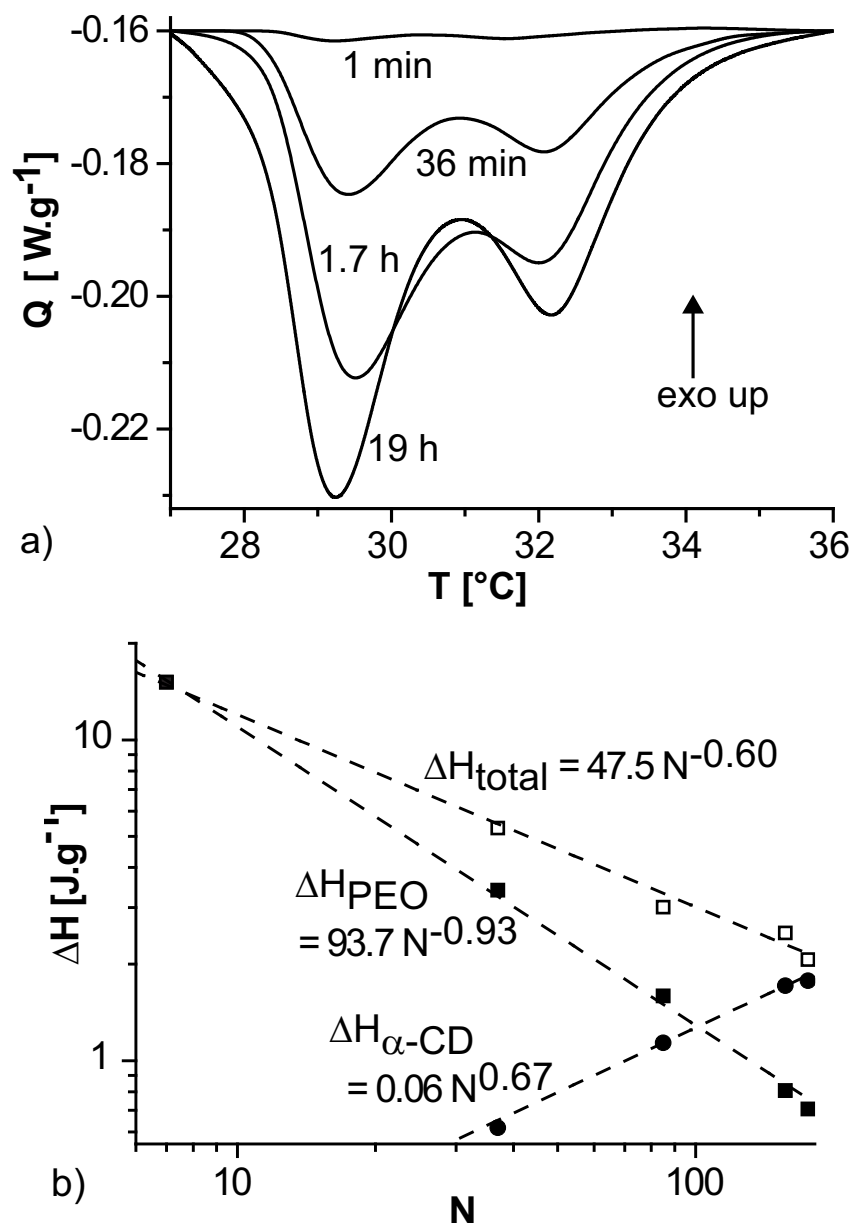
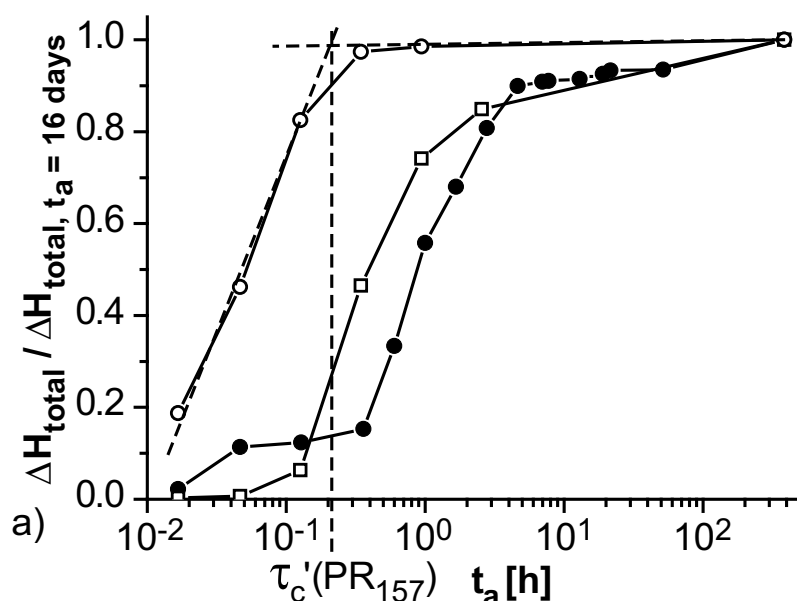


Figure 4. DSC: a) Heat flow Q versus temperature T for PR₈₅ at 19.6 w/w% in DMSO after different aging times (1 min, 36 min, 1.7 h and 19 h) at 21 °C. The heat flows are given in W g⁻¹ of PR solution. b) (\square) Total dissolution enthalpy ΔH_{total} calculated from the experimental curve, (\blacksquare) naked PEO segment dissolution enthalpy ΔH_{PEO} obtained after deconvolution and (\bullet) α -CD dissolution enthalpy $\Delta H_{\alpha\text{-CD}}$ obtained after deconvolution after a long aging time (typically 24 h) versus complexation degree N for PR solutions at 19.6 w/w% in DMSO.

The deconvolution of the mass heat flows Q results in two dissolution enthalpies ΔH_{PEO} and $\Delta H_{\alpha\text{-CD}}$. At long aging time, *i.e.* when the gel formation is achieved, a decrease of ΔH_{PEO} and an increase of $\Delta H_{\alpha\text{-CD}}$ with N are observed in Figure 4b. When N increases from 7 to 176, the number of naked PEO units and ΔH_{PEO} decrease by the same factor of 22. However, when N increases from 37 to 176, the number of α -CDs increases by a

factor of 1.4 whereas $\Delta H_{\alpha\text{-CD}}$ increases by a factor of 2.9. These results indicate that $\alpha\text{-CDs}$, contrary to PEO, favour efficiently their own aggregation due to the presence of 18 hydroxyl groups per $\alpha\text{-CD}$, each of them can bind with numerous neighbouring $\alpha\text{-CDs}$. However, Figure 4a shows that the variation of the total dissolution enthalpy with N is dominated by the content of naked PEO units. All these results show the relative contribution of each domain of PRs (*i.e.* the rotaxane blocks and the naked polymer segments of the PR) on the cohesion of the physical gels.

For all N , the total dissolution enthalpies are normalized by their values at the equilibrium state (*i.e.* when the gels are formed, at least 24 h) and plotted *versus* the aging time t_a (Figure 5a). At low t_a , the normalized dissolution enthalpy remains low before suddenly increasing with t_a till reaching a plateau value. We define the characteristic time τ_c' as the intersection point between the tangent at the inflexion point and the asymptote at long times. The resulting characteristic times depend on the complexation degree in a non-monotonous way as the characteristic times of gelation determined by RDA measurements (Figure 1b). The fastest kinetics are obtained for the lowest and the highest complexation degree values, when one contribution is predominant over the other one, whereas the intermediate complexation degree leads to a slower gelation. For high N , the absolute values of the time obtained by DSC differ strongly from that obtained by RDA since these characterization methods exhibit different sensitivities to the generating structures.



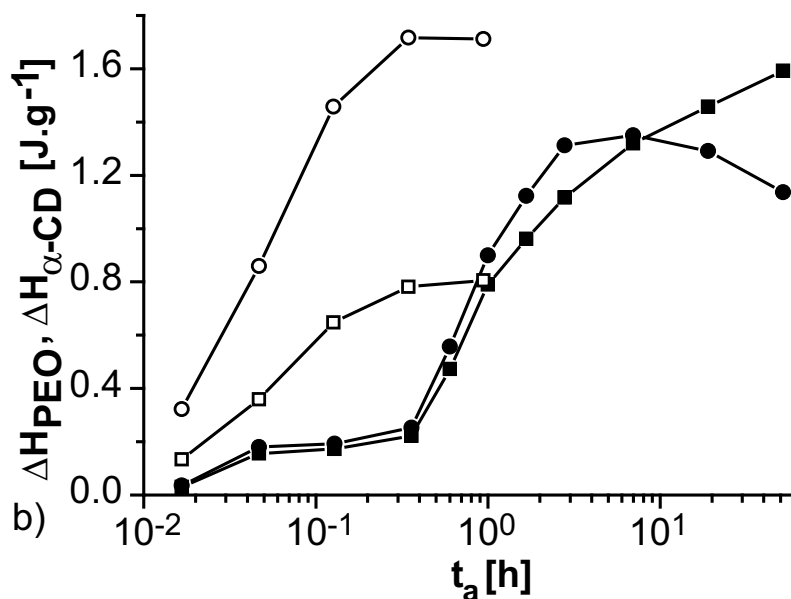


Figure 5. DSC: a) Normalized total dissolution enthalpy ΔH_{total} versus aging time t_a at 21 °C for PRs at 19.6 w/w% in DMSO: (□) PR₇, (●) PR₈₅ and (○) PR₁₅₇. The geometric construction leading to the estimation of the characteristic time τ_c' in the case of PR₁₅₇ is shown on the graphic. b) (■) Naked PEO segment dissolution enthalpy ΔH_{PEO} in the case of PR₈₅, (●) α -CD dissolution enthalpy $\Delta H_{\alpha\text{-CD}}$ in the case of PR₈₅, (□) naked PEO segment dissolution enthalpy ΔH_{PEO} in the case of PR₁₅₇ and (○) α -CD dissolution enthalpy $\Delta H_{\alpha\text{-CD}}$ in the case of PR₁₅₇ obtained after deconvolution versus aging time t_a at 21 °C for PRs at 19.6 w/w% in DMSO. The absolute values of the dissolution enthalpies are presented here. They are given in J g^{-1} of PR solution.

The quantitative estimation of the α -CD contribution to the total dissolution enthalpy can be now discussed. For instance, a PR₃₇ solution at 19.6 w/w% in DMSO exhibits a dissolution enthalpy after 52 h at 21 °C equal to 4.5 J g^{-1} of PR solution. Making the hypothesis that only α -CD hydroxyl groups are involved in the gelation process and thus contribute to the dissolution enthalpy and taking a hydrogen bond dissociation enthalpy of 1780 J mol^{-1} of hydroxyl group,^[22,23,24] it leads to a percentage of hydroxyl groups participating to hydrogen bonding equal to 112 %. This result suggests that every 18 hydroxyl group of every α -CD participates to the association which is not realistic for steric reasons. Thus, it confirms that another contribution to the gelation originating from local precipitation of PEO units has to be taken into account.

[22] J. Szejtli, *Cyclodextrins and their Inclusion Complexes*, Akadémiai Kiadó, Budapest (Hungary), **1982**.

[23] R. Gelb, L. Schwartz, J. Bradshaw and D. Laufer, *Bioorganic Chemistry*, **1980**, 9, 299-304.

[24] R. Gelb, L. Schwartz and D. Laufer, *Bioorganic Chemistry*, **1982**, 11, 274-280.

Moreover, $\Delta H_{\alpha\text{-CD}}$ and ΔH_{PEO} , obtained after deconvolution of the mass heat flows, are plotted as a function of the aging time t_a (Figure 5b). As soon as the gelation begins, the ratio of ΔH_{PEO} over $\Delta H_{\alpha\text{-CD}}$ is constant up to 3 h. Thus, the generation of the naked PEO segment crystallites and this of the $\alpha\text{-CD}$ aggregates are simultaneous: Locally, the generation of one type of domain is induced by the other one.

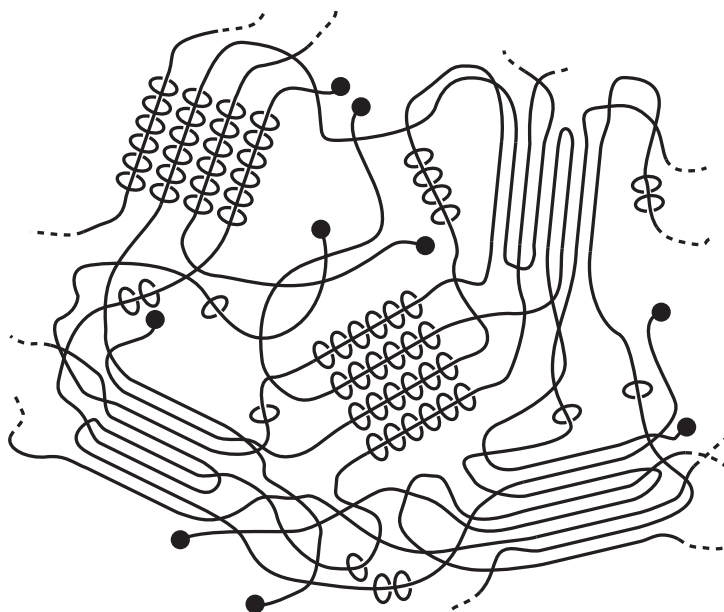


Figure 6. Schematic view of the PR physical gel showing the two kinds of cross-linked domains: the crystals of naked PEO segments and the well-organized $\alpha\text{-CD}$ aggregates more or less swollen in DMSO. The physical cross-linked domains are separated by amorphous domains made of non-aggregated rotaxane or naked PEO blocks immersed in DMSO.

3.1.4. Conclusion

PRs based on $\alpha\text{-CD}$ s threaded onto 22 kg mol^{-1} PEO chains in concentrated solution in DMSO have shown the particularity to form physical gel when let at rest at a temperature less than $25 \text{ }^\circ\text{C}$. A wide range of complexation degree has been studied (from $N = 7$ to $N = 176$ $\alpha\text{-CD}$ s threaded onto each PEO chain) which has allowed us to identify unambiguously the origins of the gelation (Figure 6):

- The cohesion of such physical gels is due on the one side to the crystallization of the naked PEO segments (the PR molecule parts which are not covered by $\alpha\text{-CD}$ s). Indeed, naked PEO segments are in bad solvent conditions in DMSO at room temperature and thus form crystal like structures which dissolve at $29.4 \text{ }^\circ\text{C}$.

- On the other side, the cohesion of these physical gels is also due to the aggregation of α -CDs through their hydroxyl groups in an intra- and inter-molecular way. These well-organized structures dissolve at 32.0 °C.

The elastic modulus of the formed gels has shown a non-monotonous dependence with N. Indeed, the elastic modulus is related to the concentration of physical cross-linked domains whose evolution with N has two distinct origins: The concentration of naked PEO segments forming crystals is high at low N whereas the concentration of aggregated α -CD domains is higher at high N. Furthermore, the increase of the elastic modulus at high N is due to the increase of the PR stiffness and consequently to the stiffness of the strands between the physical cross-linked domains. Furthermore, the gelation kinetics was followed by mechanical and calorimetric experiments. Both techniques showed the same trend of the characteristic time *versus* N. The characteristic time of the kinetics exhibits a non-monotonous evolution with N. The fastest characteristic times are reached in the case of PRs with low complexation degree values due to their high flexibility and also in the case of PRs with high complexation degree values due to the presence of numerous α -CDs per PEO chain. At intermediate complexation degree values, the kinetics is much slower. The characteristic times determined through RDA are higher than those obtained by DSC. Indeed, RDA measurements probe the elasticity of the gel and thus are little sensitive to the first stages of the aggregation, before percolation is reached. On the opposite, DSC measurements are sensitive to all types of aggregation events, whatever their size or structure, and lead thus to the fastest kinetics.

With this study we have shown that, even though DMSO can be considered as one of the best solvents for PRs based on PEO and α -CDs, physical gels form at room temperature. The cohesion of these gels is due on the one hand to the crystallization of naked PEO segments of the PRs and on the other hand to the formation of well-organized α -CD aggregates driven by the intra- and inter-molecular hydrogen bonding interactions of their hydroxyl groups. Thus, in order to observe the dynamic behaviour of the PRs due to the free sliding of α -CDs along the guest polymer chain, one needs to use PR/DMSO solutions at temperatures higher than 40 °C.

Annexe 3.1.a: Influence of the polyrotaxane concentration on the gelation

DSC experiments performed on PR₈₅ solutions at different concentrations in DMSO show the development of two dissolution peaks with increasing aging time t_a for which

the mixture is kept at 21 °C. Their temperature positions are independent on the PR concentration: 29.4 ± 0.2 °C and 32.0 ± 0.2 °C. The evolution of the total dissolution enthalpy with the aging time t_a when changing the PR₈₅ concentration is roughly equal to zero before suddenly increasing till reaching a plateau corresponding to the gel state (Figure 7). An increase of the PR concentration leads to a decrease of the characteristic time of association and to an increase of the dissolution enthalpy at any probed t_a . This behaviour is a consequence of the increase of the meeting probability per unit time between two reacting species. Since the gelation becomes too slow at concentrations lower than 14 w/w% and since PRs are not soluble at concentrations higher than 22.2 w/w%, the probed PR concentrations range between 14 w/w% and 22.2 w/w%. Furthermore, the equilibrium state is not reached for the two lowest concentrations (14 w/w% and 16.9 w/w%). Yet, in the studied concentration domain, there is a linear relation between the total dissolution enthalpy after 16 days at 21 °C and the PR concentration. Moreover, the total dissolution enthalpy relative to the PR concentration $\Delta H_{\text{total}}/C$ increases slightly with the PR concentration C which suggests that the aggregation is more efficient at higher concentrations.

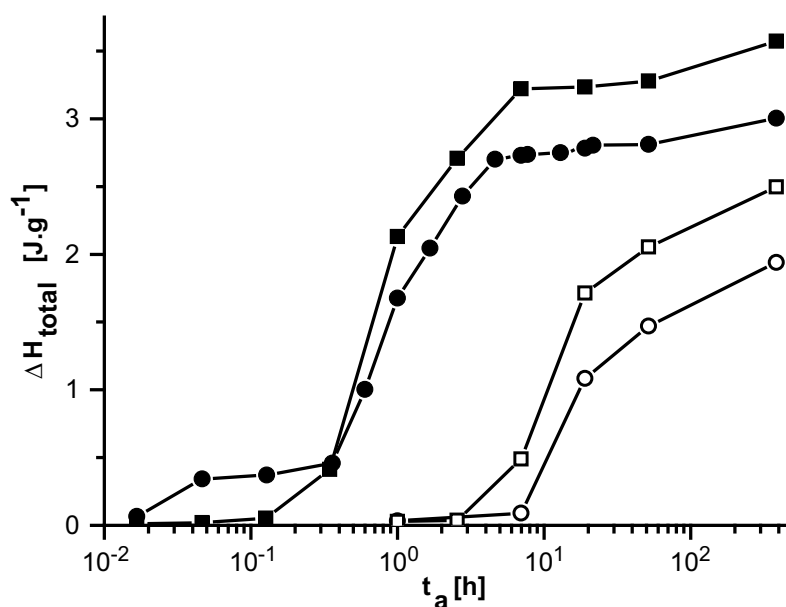


Figure 7. DSC: Total dissolution enthalpy ΔH_{total} versus aging time t_a at 21 °C for PR₈₅ in DMSO: (■) 22.2 w/w%, (●) 19.6 w/w%, (□) 16.9 w/w% and (○) 14 w/w%. The absolute values of the dissolution enthalpies are presented here. They are given in J g⁻¹ of PR solution.

In the previous subchapter (**Subchapter 3.1**), it was shown that α -CD/PEO-based PRs in solution in DMSO form physical gels when kept at room temperature. A concentrated PR/DMSO mixture at 43 °C is liquid and gelifies slowly with time at 21 °C. Thanks to the study of a wide range of complexation degrees (*i.e.* the number of threaded α -CDs per PEO chain), it was demonstrated that gelation is due to both the crystallisation of naked PEO segments (*i.e.* the ethylene oxide units of the PEO chains which are not covered by α -CDs) and the aggregation of threaded α -CDs *via* their hydroxyl groups. The crystallisation of PEO, originating from the fact that DMSO becomes a bad solvent for PEO at room temperature,^[A] is predominant at low complexation degrees. Thus, two aggregation phenomena are responsible for the gelation.

In the next subchapter (**Subchapter 3.2**), we use neutron scattering to observe *in situ* the associations at different length-scales in the concentrated regime. Naked PEO segments are found to form PEO crystallites with time. α -CD rod-like tubes consisting of weakly stacked α -CDs along the PEO chains self-organize due to the formation of hydrogen bonding between α -CD hydroxyl groups, forming α -CD nano-cylinders. The formation of PEO crystallites is predominant at low complexation degree values. The structure formation originates from the multiblock copolymer behaviour of PRs and their nano-scale sizes do not evolve with time and complexation degree. In its equilibrium state, the system still contains a fraction of non-aggregated rod-like tubes. Moreover, direct microscopic observations of the formed structures are carried out.

[A] C. Özdemir and A. Güner, *European Polymer Journal*, **2007**, 43, 3068-3093.

3.2. Structure of physical gels based on polyrotaxanes: multiblock copolymer behaviour and nano-scale self-organization

Submitted to *Physical Chemistry, Chemical Physics*

Abstract

The structure of polyrotaxanes (PR) based on α -CDs threaded onto 22 kg mol^{-1} PEO chains in concentrated solution ($\approx 20 \text{ w/w\%}$) in DMSO was studied by SANS measurements as a function of the temperature and the complexation degree N (*i.e.* the number of threaded α -CDs per PR which ranged from 7 up to 157). A multiblock copolymers behaviour was revealed for PRs in DMSO. This multiblock behaviour of PRs at $43 \text{ }^\circ\text{C}$ is due to the presence of two kinds of blocks which alternate along the PR. One block type is rigid and corresponds to α -CD rod-like tubes with a length $L_{\text{rod}} \approx 7 \text{ nm}$. The other block type corresponds to flexible naked PEO segments. When the PR mixtures are cooled down to $21 \text{ }^\circ\text{C}$, they gelify slowly with time and form transparent physical gels. The gel structure is due to the multiblock copolymer behaviour of PRs leading to the formation of regular bundles for which the characteristic sizes ($L = 14 \text{ nm}$ and $R = 5.7 \text{ nm}$) are constant during the gelification process and are independent with N . These regular bundles contain naked PEO segment crystallites surrounded by α -CD rod-like tube aggregates at their extremities. Indeed, α -CD rod-like tubes, which are present in the initial state at $43 \text{ }^\circ\text{C}$ act like a compatibilizer and thus lead to the nano-scale bundle sizes and thus to the transparency of the physical PR-based gels. Furthermore, we showed that the kinetics of the bundle formation is N -dependent. Indeed, at constant PR weight fraction in DMSO, the N value is a crucial parameter controlling the intrinsic flexibility of PRs (flexibility favoured at low N values) and their pre-alignment (pre-alignment favoured at high N values), and thus controlling the self-organization.

3.2.1. Introduction

Polyrotaxane (PR) is a pearl necklace shape supramolecule in which many macrocycles (the pearls) are threaded onto a single template polymer chain (the necklace). The ends

of the template chain are capped with steric functional groups to prevent dethreading of the macrocycles.^[1,2] The translational and rotational mobility of the macrocycles along the template chains confer new dynamical, physico-chemical and mechanical properties on the PRs. These macromolecules open the door to the realization of new functional materials. Among them, high swelling gels exploit the mobility of the macrocycles along the template chains. The macrocycles are covalently cross-linked in an intermolecular way and form a chemical gel whose cross-link points may freely slide along the template chains. This supplementary degree of freedom leads to high swelling ratios and to original viscoelastic properties of the gels.^[3,4,5,6,7,8,9] Nanowires, as for them, utilize the topological separation induced by the macrocycles between their interior and exterior. Indeed, their aligning along template polymer chains creates transient tubes. PRs with semi-conducting polymers as template chains have thus been synthesized and used as single-molecule nanowires.^[10,11] Finally, drug delivery systems based on PRs have been synthesized. A high number of proteins, covalently linked onto the macrocycles, are conveyed to the appropriate biological receptors and then released after hydrolysis of the template chains.^[12]

Many types of macrocycles and template chains can be used, leading to a huge number of different PRs. Among them, PRs formed with α -cyclodextrins (α -CDs) as macrocycles and poly(ethylene oxide) (PEO) as template chains have been widely studied.^[13] α -CDs consist in the repetition of 6 glucose units organized in a truncated-conic way. The threading between α -CDs and PEO is possible due to a negative Gibbs free energy change during the threading process. The difference of

[1] A. Harada, J. Li and M. Kamachi, *Nature*, **1992**, 356, 325-327.

[2] G. Wenz and B. Keller, *Angewandte Chemie International Edition English*, **1992**, 31, 197-199.

[3] Y. Okumura and K. Ito, *Advanced Materials*, **2001**, 13, 485-487.

[4] G. Fleury, G. Schlatter, C. Brochon and G. Hadziioannou, *Polymer*, **2005**, 46, 8494-8501.

[5] T. Sakai, H. Murayama, S. Nagano, Y. Takeoka, M. Kidowaki, K. Ito and T. Seki, *Advanced Materials*, **2007**, 19, 2023-2025.

[6] G. Fleury, G. Schlatter, C. Brochon, C. Travelet, A. Lapp, P. Lindner and G. Hadziioannou, *Macromolecules*, **2007**, 40, 535-543.

[7] G. Fleury, G. Schlatter, C. Brochon and G. Hadziioannou, *Advanced Materials*, **2006**, 18, 2847-2851.

[8] T. Karino, M. Shibayama and K. Ito, *Physica B: Condensed Matter*, **2006**, 385-386, 692-696.

[9] K. Ito, *Polymer Journal*, **2007**, 39, 489-499.

[10] T. Shimomura, T. Akai, T. Abe and K. Ito, *Journal of Chemical Physics*, **2002**, 116, 1753-1756.

[11] M. van den Boogaard, G. Bonnet, P. van't Hof, Y. Wang, C. Brochon, P. van Hutten, A. Lapp and G. Hadziioannou, *Chemistry of Materials*, **2004**, 16, 4383-4385.

[12] T. Ooya and N. Yui, *Journal of Controlled Release*, **2002**, 80, 219-228.

[13] G. Wenz, B.-H. Han and A. Müller, *Chemical Reviews*, **2006**, 106, 782-817.

Gibbs free energy, determined both theoretically and experimentally, is equal to -50 kJ mol^{-1} .^[14,15]

Nevertheless, the representation of PRs as molecular pearl necklaces in which the macrocycles freely slide along the template chains is much too simplistic. It ignores the numerous interactions that develop between each component of PRs when put into solution. The complexity introduced by the interplay of the interactions between the components manifests itself by the difficulty to solubilize PRs. Thus, PRs based on α -CDs and PEO are insoluble in neutral water or N,N-dimethylformamide, even though both are good solvents of the macrocycles and the template chains. Limited solubility has been empirically observed in few solvents, such as dimethyl sulfoxide (DMSO),^[16,17] aqueous NaOH solution (thanks to the ionization of α -CD hydroxyl groups whose $\text{pK}_a \sim 12$),^[16,17] halogen-containing ionic liquids,^[18] concentrated aqueous solutions of calcium thiocyanate^[19] and N,N-dimethylacetamide/lithium halogenide mixtures.^[20] Among them, DMSO has been the most used.

Nevertheless, although a concentrated mixture of PR in DMSO is fluid at high temperature, when it is cooled down to room temperature, it becomes a physical gel (Figure 1).^[21] Moreover, at room temperature, mixtures of PR in DMSO exhibit a thixotropic rheological behaviour.^[22,23] These observations indicate that microscopic physical aggregates are formed and may be broken by heating or by the application of a shear.

We have already studied the self-organization of PRs in DMSO at room temperature in the steady state and shown that association between α -CDs as well as between naked PEO segments (*i.e.* the ethylene oxide units of the PEO chains which are not covered by α -CDs) is present.^[21] In this paper, we study the gelation kinetics of mixtures of PR in

[14] M. Ceccato, P. Lo Nostro and P. Baglioni, *Langmuir*, **1997**, 13, 2436-2439.

[15] B. Mayer, C. Klein, I. Topchieva and G. Köhler, *Journal of Computer-Aided Molecular Design*, **1999**, 13, 373-383.

[16] A. Harada, J. Li, T. Nakamitsu and M. Kamachi, *Journal of Organic Chemistry*, **1993**, 58, 7524-7528.

[17] A. Harada, J. Li and M. Kamachi, *Journal of the American Chemical Society*, **1994**, 116, 3192-3196.

[18] S. Samitsu, J. Araki, T. Kataoka and K. Ito, *Journal of Polymer Science, Part B: Polymer Physics*, **2006**, 44, 1985-1994.

[19] J. Araki, T. Kataoka and K. Ito, *Journal of Applied Polymer Science*, **2007**, 105, 2265-2270.

[20] J. Araki and K. Ito, *Journal of Polymer Science, Part A: Polymer Chemistry*, **2006**, 44, 532-538.

[21] C. Travelet, G. Schlatter, P. Hébraud, C. Brochon, D. Anokhin, D. Ivanov and G. Hadziioannou, subchapter 3.1, submitted to *Macromolecular Symposia*.

[22] C. Travelet, G. Schlatter, C. Brochon, P. Hébraud, D. Ivanov and G. Hadziioannou, CD-ROM congress proceedings of the EPF 2007, European Polymer Congress, Portorož, Slovenia, 2nd - 6th July **2007**.

[23] J. Araki and K. Ito, *Polymer*, **2007**, 48, 7139-7144.

DMSO and more particularly the formation of α -CD aggregates and naked PEO segment crystallites by means of neutron scattering experiments.

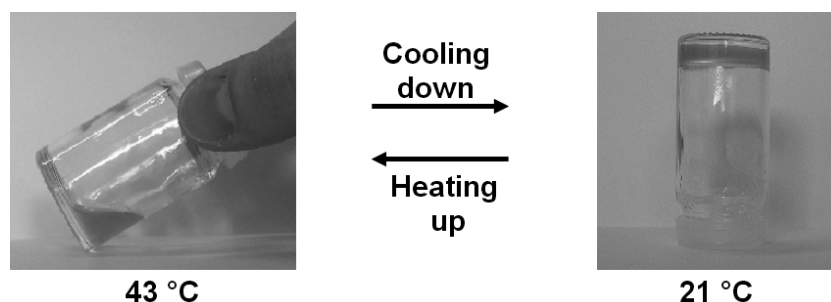


Figure 1. Thermo-reversible gelation of PR₈₅ at 19.6 w/w% in DMSO: liquid state at 43 °C and gel state after 24 h at 21 °C.

3.2.2. Experimental section

3.2.2.1. Materials

Dihydroxy-terminated PEO was purchased from Serva Electrophoresis[®] and dried by an azeotropic distillation from toluene before use. An average number molecular weight of 22 kg mol⁻¹ and a polydispersity index of 1.03 were measured in DMSO at 70 °C by gel permeation chromatography (GPC) with PEO standard calibration. α -CD was supplied by Acros Organics[®] and dried over phosphorus pentoxide under reduced pressure before use. N,N-dimethylformamide (DMF) (from Fluka[®]), DMSO (from Riedel de Haën[®]) were distilled over potassium hydroxide under reduced pressure. Triethylamine (from Acros Organics[®]) was distilled over potassium hydroxide. 2,4-dinitro-1-fluorobenzene (DNFB) (from Lancaster Synthesis[®]), deuterated dimethyl sulfoxide with a 99.9 % enrichment (DMSO-d₆) (from Aldrich[®]) and all other chemicals were used as received without any further purification step.

3.2.2.2. Polyrotaxane synthesis

α,ω -Bis-amine-terminated poly(ethylene oxide) (BA-PEO) was synthesized from dihydroxy-terminated PEO according to an adaptation of the procedure of Mutter.^[24] Then, an α -CD solution stirred at 70 °C was mixed with a BA-PEO solution stirred at 70 °C. The resulting mixture, which has the desired ratio α -CD/BA-PEO, was stirred during 30 min at 70 °C and then during 48 h at 35 °C. Then, the solution was cooled

[24] M. Mutter, *Tetrahedron Letters*, **1978**, 19, 2839-2842.

down at 5 °C until a white precipitate was obtained. The mixture was freeze dried. Afterwards, the resulting inclusion complexes – together with unthreaded α -CDs and naked BA-PEO chains – were grinded and suspended at 800 rpm in distilled DMF under nitrogen atmosphere at 30 °C. Triethylamine and DNFB (100 aliquots each, relative to the mole number of the theoretically formed inclusion complexes) were added to the suspension which became dark yellow. After 48 h, in order to eliminate the unreacted DNFB molecules, the mixture was precipitated in ether, filtered and washed with ether. The solid was three times more suspended in a minimum of DMF, precipitated in ether, filtered and washed with ether. In order to eliminate the unthreaded α -CDs and the naked PEO chains, the product was washed with distilled water. The PR fraction, which was slightly soluble in water, was recovered by centrifugation at 7000 rpm during 30 min. These washing and centrifuging steps in water were carried out two times more. The solid was freeze dried. The PRs were obtained with a yield relative to the mole number of BA-PEO ranging between 3 % and 24 %. The values of the complexation degree were estimated using ^1H nuclear magnetic resonance in DMSO-d_6 ^[25] and the efficiency of the capping step using GPC in HPLC grade DMSO at 70 °C.^[25]

3.2.2.3. Characterization method

Small-angle Neutron Scattering (SANS). SANS measurements were performed on the PAXY spectrometer at the Laboratoire Léon Brillouin (LLB, CEA, Saclay, France). The modulus of the scattering vector is denoted q and is equal to $(4\pi/\lambda) \times \sin(\theta/2)$ where θ designs the observation angle and λ represents the wavelength of the used radiation. The first (respectively second) used configuration consisted in a sample-to-detector distance of 3 m (respectively 1 m) and a wavelength of 1.0 nm (respectively 0.6 nm). The global probed q range corresponding to these configurations was $8.0 \times 10^{-2} \text{ nm}^{-1} \leq q \leq 3.5 \text{ nm}^{-1}$. The signal was corrected by taking into account the contributions of the measurement cell, the solvent and the incoherent background.^[26] The incoherent scattering of poly(methyl methacrylate) was used to correct the detector efficiency. Thus, the data were brought to absolute scale. The measurement cells were made of 1 mm thick quartz windows separated by a 2 mm O-ring and equipped with a

[25] G. Fleury, C. Brochon, G. Schlatter, G. Bonnet, A. Lapp and G. Hadziioannou, *Soft Matter*, **2005**, 1, 378-385.

[26] A. Brûlet, D. Lairez, A. Lapp and J.-P. Cotton, *Journal of Applied Crystallography*, **2007**, 40, 165-177.

cadmium/boron carbide diaphragm whose hole diameter is 10 mm. DMSO-d₆ was used as the solvent during all of the experiments. The temperature regulated rack carrying the measurement cells filled in with the PR solutions was heated up at 43 ± 1 °C and one 30 min scan was measured at that temperature. Then, the solutions were cooled down at 21 ± 1 °C and 30 min scans were continuously recorded during few hours at this temperature.

3.2.3. Results and discussion

PRs with well defined complexation degrees (N) (*i.e.* the number of threaded α -CDs per PEO chain) ranging from 7 to 157 (Table 1) are obtained thanks to the methodology previously reported.^[25] In this paper, the PRs will be denoted PR_N where N is the complexation degree. PEO with a molecular weight of 22 kg mol⁻¹ is used. Thus, the α -CD overlap ratio (*i.e.* the percentage of ethylene oxide units of the PEO chains which are covered by α -CDs) ranges from 3 % to 63 % (Table 1). A concentrated PR mixture in DMSO heated up at 43 °C is fluid. When cooled down to 21 °C, it gelifies slowly with time (Figure 1). This process seems to be fully thermo-reversible as the formed gel returns to its original fluid state and remains fluid when heated up at 43 °C. Before considering the gelation of the PR solutions at 21 °C, we determine first the initial structure of the systems out of the gel state, *i.e.* at 43 °C.

Table 1. Chemical characteristics of the PEO solution at 5.9 w/w% and of PR solutions at 19.6 w/w% in DMSO. The given mole numbers refer to 100 g of solution.

PR _N	α -CD overlap ratio [%]	n(PR _N) [mmol]	n(PR _N)/n(PR ₁₅₇)	n(α -CD) [mmol]	n(α -CD)/n(α -CD)PR ₇	n(naked PEO units) [mmol]	n(naked PEO units)/n(naked PEO units) _{PR157}
PEO = PR ₀	0	0.28	–	–	–	142	–
PR ₇	2.80 §	0.68	6.06	4.76	1	330 §	15.9 §
PR ₃₇	14.8 §	0.34	3.01	12.5	2.63	144 §	6.91 §
PR ₈₅	34.0 §	0.19	1.67	15.9	3.34	61.7 §	2.97 §
PR ₁₅₇	62.9 §	0.11	1	17.6	3.70	20.8 §	1 §

§: calculated taking into account that one α -CD covers exactly two ethylene oxide units of PEO,^[27,28] although a higher α -CD coverage was recently reported^[29]

[27] A. Harada, *Coordination Chemistry Reviews*, **1996**, 148, 115-133.

[28] A. Harada, *Carbohydrate Polymers*, **1997**, 34, 183-188.

3.2.3.1. Structure of polyrotaxanes in concentrated solution at high temperature

Before studying PRs themselves at 43 °C, we first focus on pure PEO (*i.e.* PR₀) in solution in DMSO-d₆. A 5.9 w/w% PEO solution was chosen so as to have the same mole number of naked ethylene oxide units as in a PR₃₇ solution at 19.6 w/w% (Table 1). Small-angle neutron scattering (SANS) measurements do not show any structural evolution of the PEO solution with time at 43 °C. A perfect Gaussian behaviour is observed (Figure 2) and the corresponding gyration radius is $R_g = 2.6$ nm. SANS measurements do not show any structural evolution of all PR solutions with time at 43 °C. The scattering profiles of the PR solutions, except PR₁₅₇, exhibit several features (Figure 2):

- For the highest q values (up to 3.5 nm^{-1}), a q^{-1} -like behaviour of the scattering intensity without oscillation is obtained. This suggests the presence of thin α -CD rod-like tubes.
- For the lowest q values (down to $8.0 \times 10^{-2} \text{ nm}^{-1}$), an excess of scattering intensity is observed. This behaviour is due to the presence, at the molecular level, of regions more or less concentrated in naked PEO segments (*i.e.* the ethylene oxide units of the PEO chains which are not covered by α -CDs) and/or in α -CD rod-like tubes depending on the N value. Furthermore, these regions exhibit a fractal characteristic dimension close to 2 (*i.e.* close to a Gaussian arrangement).

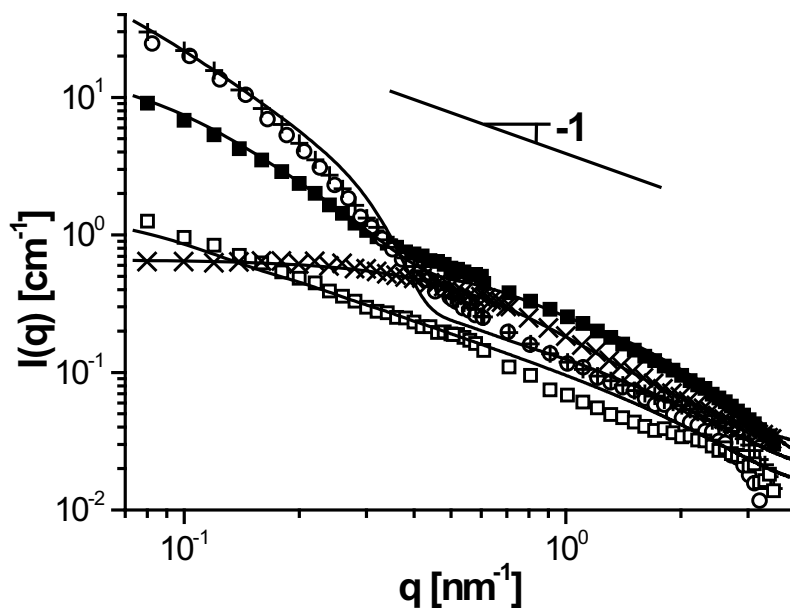


Figure 2. SANS: Absolute scattering intensity $I(q)$ versus modulus of the scattering vector q for: (\times) pure PEO (*i.e.* PR₀) at 5.9 w/w% in DMSO-d₆ at 43 °C, and PR solutions at 19.6 w/w% in DMSO-d₆ at 43 °C: (\blacksquare) PR₇, (\circ) PR₃₇, ($+$) PR₈₅ and (\square) PR₁₅₇. The solid line corresponding to PEO is the fitting curve obtained with a Gaussian form factor. The solid lines corresponding to PRs are the fitting curves obtained with equation (1).

To confirm this interpretation, the experimental curves have been fitted with the following model which is a linear combination of a cylinder form factor $P_{\text{cyl}}^{[30,31]}$ and a Gaussian form factor $P_{\text{Gauss}}^{[31,32]}$

$$\begin{aligned}
 I(q) = & A_{\text{rod}} \exp\left[-\left(\frac{q}{q_0}\right)^{5.33}\right] P_{\text{Gauss}}(q, R_{\text{ghot}}) \\
 & + B_{\text{rod}} \left\{1 - \exp\left[-\left(\frac{q}{q_0}\right)^{5.33}\right]\right\} P_{\text{cyl}}(q, L_{\text{rod}}, R_{\text{rod}}) + I_{\text{inc}}
 \end{aligned} \tag{1}$$

Where $I(q)$ is the scattering intensity at the modulus of the scattering vector q and I_{inc} is the constant intensity of a reminiscent incoherent signal. L_{rod} and R_{rod} respectively designate the cylinder length and radius, and R_{ghot} designates the gyration radius of the Gaussian distribution of α -CD rod-like tubes (the cylinders) and/or naked PEO segments. The weighting of each form factor is a cut-off function so that P_{cyl} dominates at $q > q_0$ and P_{Gauss} dominates at $q < q_0$. Figure 2 shows a good accuracy between the

[30] G. Fournet, *Bulletin de la Société Française de Minéralogie et de Cristallographie*, **1951**, 74, 37-167 (in French).

[31] P. Lindner and T. Zemb, *Neutron, X-rays and Light: Scattering Methods applied to Soft Condensed Matter*, Elsevier, Amsterdam (Netherlands), **2002**.

[32] P. Debye, *Journal of Physical and Colloid Chemistry*, **1947**, 51, 18-32.

experimental and the calculated profiles with $L_{\text{rod}} \geq 7$ nm and $R_{\text{rod}} = 0.73 \pm 0.1$ nm (Table 2) which corresponds to the radius of one α -CD.^[33] Only a minimum value of L_{rod} can be estimated due to the predominance of the Gaussian part of the intensity at the lowest measured q values. The obtained parameters L_{rod} and R_{rod} confirm that PRs in concentrated solution at 43 °C contain rod-like tubes consisting of weakly stacked α -CDs along the PEO chains (Figure 3). This is in agreement with a study carried out on chemically linked α -CD tubes^[34] where it is found both theoretically and experimentally that α -CD tubes are constituted by 2 to 7 α -CDs. This is also consistent with a SANS observation of uncapped PRs in the solid state.^[35] This is likewise in agreement with a recent theoretical study^[36] in which it is shown using Monte-Carlo simulations that α -CDs are stacked by groups of 3 to 4 α -CDs. Thus, knowing that the length of an α -CD is 0.79 nm,^[33] the value of L_{rod} is relatively high compared to the above given data taken from the literature. Nevertheless, this is explained by the presence of ethylene oxide units between α -CD rod-like tubes, both being observed by SANS (Annexe 3.2.a). Furthermore, the dynamic character of the α -CD rod-like tubes at high temperature (43 °C) can explain the high value of L_{rod} . Indeed, the dynamic character is due to the mobility of the α -CDs along the PEO chains in DMSO,^[7,37] and to continuously forming and breaking weak connections between two neighbouring α -CDs belonging to the same PR or not (Figure 3). Such dynamics was not observed for similar systems in the semi-dilute regime.^[38] However, PRs were studied at room temperature and modified with hydroxypropyl groups weakening hydrogen bonds between α -CDs. Moreover, a solvation effect due the fact that α -CD hydroxyl groups are not naked but surrounded by bounded DMSO molecules increases the L_{rod} value. Finally, the α -CD dynamics of our PR systems leads to quite a high L_{rod} value.

[33] J. Szejtli, *Chemical Reviews*, **1998**, 98, 1743-1753.

[34] M. van den Boogaard, *Cyclodextrin-containing Supramolecular Structures: from Pseudo-polyrotaxanes Towards Molecular Tubes, Insulated Molecular Wires and Topological Networks*, Ph.D. Thesis, University of Groningen (Netherlands), **2003** (available via the Internet at <http://irs.ub.rug.nl/ppn/24276326X> or <http://dissertations.ub.rug.nl/search.php>).

[35] T. Girardeau, T. Zhao, J. Leisen, H. Beckham and D. Bucknall, *Macromolecules*, **2005**, 38, 2261-2270.

[36] A. Tonelli, *Macromolecules*, **2008**, 41, 4058-4060.

[37] C. Zhao, Y. Domon, Y. Okumura, S. Okabe, M. Shibayama and K. Ito, *Journal of Physics: Condensed Matter*, **2005**, 17, S2841-S2846.

[38] K. Mayumi, N. Osaka, H. Endo, H. Yokoyama, Y. Sakai, M. Shibayama and K. Ito, *Macromolecules*, **2008**, 41, 6480-6485.

Table 2. Fitting parameters obtained for PR_N solutions at 43 °C.

PR _N	q ₀ [nm ⁻¹]	R _{ghot} [nm]	L _{rod} [nm]	R _{rod} [nm]
PR ₇	0.45	18	7	0.73
PR ₃₇	0.35	30	10	0.73
PR ₈₅	0.35	30	10	0.73
PR ₁₅₇	–	–	50	0.73

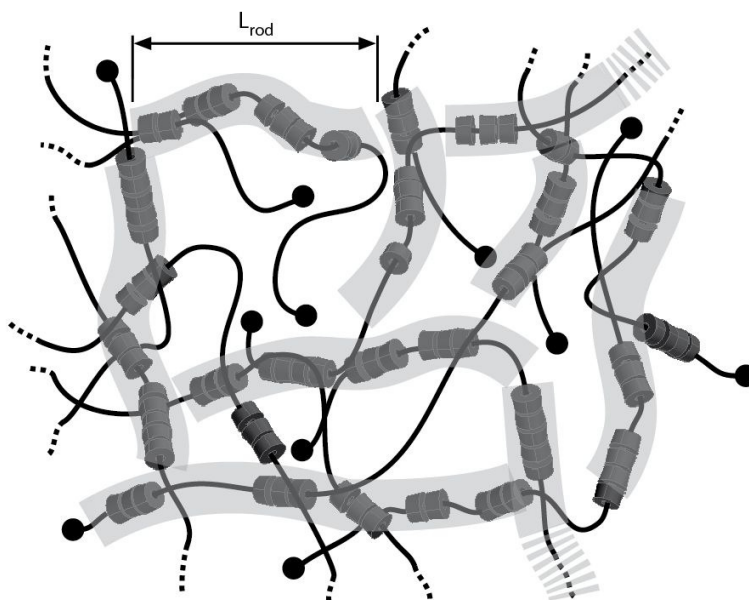


Figure 3. Schematic representation of the liquid state at 43 °C of a concentrated PR_N solution in DMSO for intermediate N values. The transparent thick lines represent the α -CD rod-like tubes of length L_{rod} as shown by SANS. The figure shows isolated α -CD rod-like tubes and also regions more dense in α -CD rod-like tubes.

For the less threaded PR (PR₇), the fitting shows a very good accuracy with the experimental curve. This confirms the cohabitation of isolated α -CD rod-like tubes surrounded by DMSO (intensity contribution for $q > q_0$) and long naked PEO segments organized in a Gaussian way (intensity contribution for $q < q_0$). Indeed, PR₇ has an α -CD overlap ratio of 3 % and its solution contains 16 times more naked PEO units compared to PR₁₅₇ (Table 1). The obtained results show that regions, with a characteristic radius of $R_{ghot} = 18$ nm, contain few long naked PEO segments belonging to different PR₇ molecules. However, such regions contain a high amount of solvent and cannot be seen as compact aggregates.

The scattering profile of the PR₁₅₇ solution is different from the scattering profiles of the three other solutions discussed above. Indeed, the expected excess of scattering intensity does not appear in Figure 2 but should be observed at smaller q values than the probed

ones. Furthermore, it exhibits a q^{-1} -like behaviour in the whole probed q range (Figure 2). Fitting with equation (1) confirms these observations and leads to $L_{\text{rod}} > 45$ nm, $R_{\text{rod}} = 0.73$ nm and a very low cut-off value $q_0 < 0.08$ nm $^{-1}$. As for the other studied PRs, PR₁₅₇ contains rod-like tubes consisting of weakly stacked α -CDs along its PEO chain. Nevertheless, the structures formed by the α -CDs are much more rigid than those formed in the PR₇, PR₃₇ and PR₈₅ solutions due to the presence of smaller naked PEO segments between the rod-like tubes.

Consequently, all these SANS observations of PRs in solution in DMSO at 43 °C confirm that PRs can be considered as multiblock copolymers where one block type is made of an α -CD rod-like tube and the other one of a naked PEO segment. The state at 43 °C corresponds to the initial state of the physical gelation observed with time at room temperature. Now, starting from a liquid PR/DMSO mixture at 43 °C, we are going to discuss the PR structure evolution with time at 21 °C, *i.e.* during the physical gelation.

3.2.3.2. Structure formation with time of polyrotaxanes in concentrated solution at room temperature

SANS measurements were used to resolve the structure of the system as a function of time. It should be remembered at that point that SANS measurements in DMSO- d_6 probe α -CD and PEO in an equivalent way (Annexe 3.2.a).

Before studying PRs themselves, we first focus on pure PEO (*i.e.* PR₀) in solution in DMSO- d_6 . The initial transparent PEO/DMSO solution observed at 43 °C in the previous section is not liquid anymore and appears opaque and heterogeneous to the eye (with aggregate characteristic size less than 1 mm) after a long time (typically 24 h) at 21 °C. After gelation, the SANS profile of the PEO/DMSO mixture shows three ripples (Figure 4). In the corresponding Kratky plot, the two main shoulders appear like two peaks indicating the presence of PEO-based structures within the system. The q positions of the low q and high q peaks, respectively q_{max} and q'_{max} , are $q_{\text{max}} = 4.31 \times 10^{-1}$ nm $^{-1}$ and $q'_{\text{max}} = 8.89 \times 10^{-1}$ nm $^{-1}$ (inset, Figure 4). Moreover, the scattering intensity exhibits a q^{-4} -like behaviour for the lowest q values (Figure 4). Such a Porod behaviour^[39,40,41] shows that the sample is highly heterogeneous and contains large PEO-based aggregates having sharp boundaries, *i.e.* small interphases between

[39] J. Teixeira, *Journal of Applied Crystallography*, **1988**, 21, 781-785.

[40] D. Williamson, D. Marr, J. Yang, B. Yan and S. Guha, *Physical Review B: Condensed Matter and Materials Physics*, **2003**, 67, 075314-1-075314-13.

[41] H. Bale and P. Schmidt, *Physical Review Letters*, **1984**, 53, 596-599.

the aggregates, on the one hand, and the solvent and few non-aggregated PEO molecules, on the other hand. Less sharp interphases would induce smoother q dependences.^[42] This result confirms calorimetric and X-ray scattering measurements showing the presence of PEO crystallites.^[21] Furthermore, the large aggregates are constituted by the gathering of smaller entities characterized by the structural peaks observed at q_{\max} and q'_{\max} (*i.e.* corresponding to a typical characteristic size of $2\pi/q_{\max} \approx 14.6$ nm as far as concerns q_{\max}).

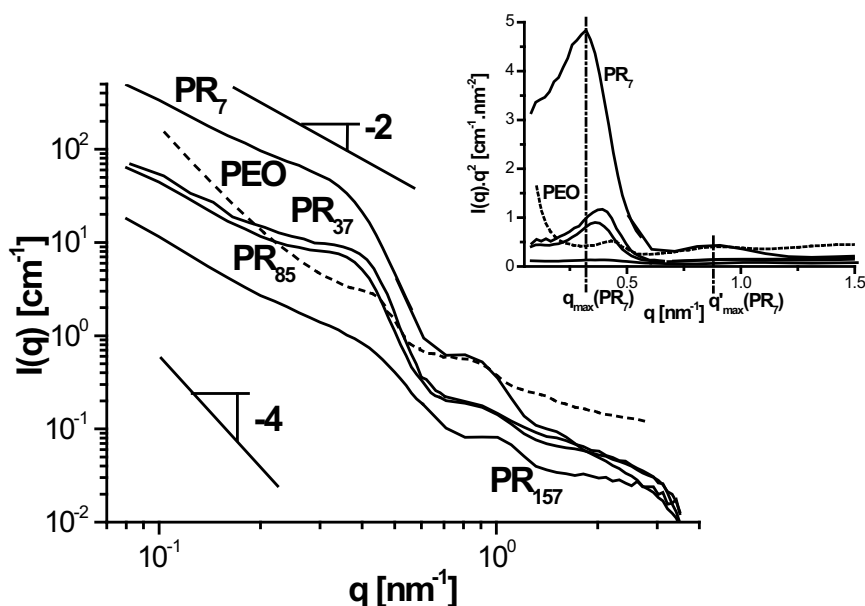


Figure 4. SANS: Absolute scattering intensity $I(q)$ versus modulus of the scattering vector q for pure PEO (*i.e.* PR_0) at 5.9 w/w% in DMSO- d_6 after 24 h at 21 °C, and PRs at 19.6 w/w% in DMSO- d_6 after 8 h at 21 °C: PR_7 , PR_{37} , PR_{85} and PR_{157} . Inset: corresponding Kratky plot.

The SANS signature of pure PEO at 21 °C being now well established, we focus on PRs. It should be first mentioned that, contrary to pure PEO, the physical gels based on PRs are homogeneous to the eye. In our SANS setup, the thermal inertia of the sample rack and of the water bath allows us to decrease the sample temperature from 43 °C to 21 °C in 10 min. Nevertheless, the scattering intensity profiles at 43 °C coincide exactly with the profiles obtained once the temperature 21 °C is reached (■ and dashed line, Figure 5a). It indicates that, during cooling, no structure based on α -CDs or on PEO forms. Thus, the origin of the times is chosen at the moment when the temperature 21 °C is reached. SANS experiments were performed on PR_7 , PR_{37} , PR_{85} and PR_{157}

[42] L. Auvray, *Comptes Rendus de l'Académie des Sciences*, **1986**, 302, 859-862.

solutions at 19.6 w/w% in DMSO-d₆ and the resulting gels were observed with time at 21 °C.

At lower complexation degree N

As far as concerns the PR₇ solution, from a qualitative point of view, the SANS profiles exhibit the development with time of three ripples during gelation (Figure 5a). In the corresponding Kratky plot, the two main shoulders appear like two peaks. The q positions of the low q and high q peaks, respectively q_{\max} and q'_{\max} , are $q_{\max} = 3.20 \times 10^{-1} \text{ nm}^{-1}$ and $q'_{\max} = 8.75 \times 10^{-1} \text{ nm}^{-1}$ and do not evolve with time as soon as the gelation starts (inset, Figure 5a). It suggests that association takes place in the form of structures having the same characteristic sizes at any time. However, the q_{\max} value obtained with PR₇ is different from the one obtained with pure PEO suggesting that the presence of few threaded α -CDs (overlap ratio of PR₇ ≈ 3 %, Table 1) considerably influences the structure size and thus the self-organization behaviour itself. Moreover, it should be noticed that the solubilisation of PR₇ at room temperature is very easy to carry out although a PEO/DMSO mixture at equivalent concentration cannot be solubilised at room temperature. Thus, the threaded α -CDs play an important role on the formed structure and the macroscopic behaviour. For the lowest q values, an increase of the scattering intensity with time and a q^{-2} -like Gaussian behaviour are observed. Furthermore, the intensity of the peaks at q_{\max} and q'_{\max} increases with time. This indicates that the number of structures increases with time. However, a decrease of the scattering intensity with time is observed at the highest q values, *i.e.* in the region where a q^{-1} -like behaviour of the scattering intensity appears. This latter result tends to show that the proportion of isolated α -CD rod-like tubes decreases with time. All these observations suggest that regular structures containing naked PEO segment crystallites surrounded by α -CD aggregates are formed during gelation and organized in a Gaussian way.

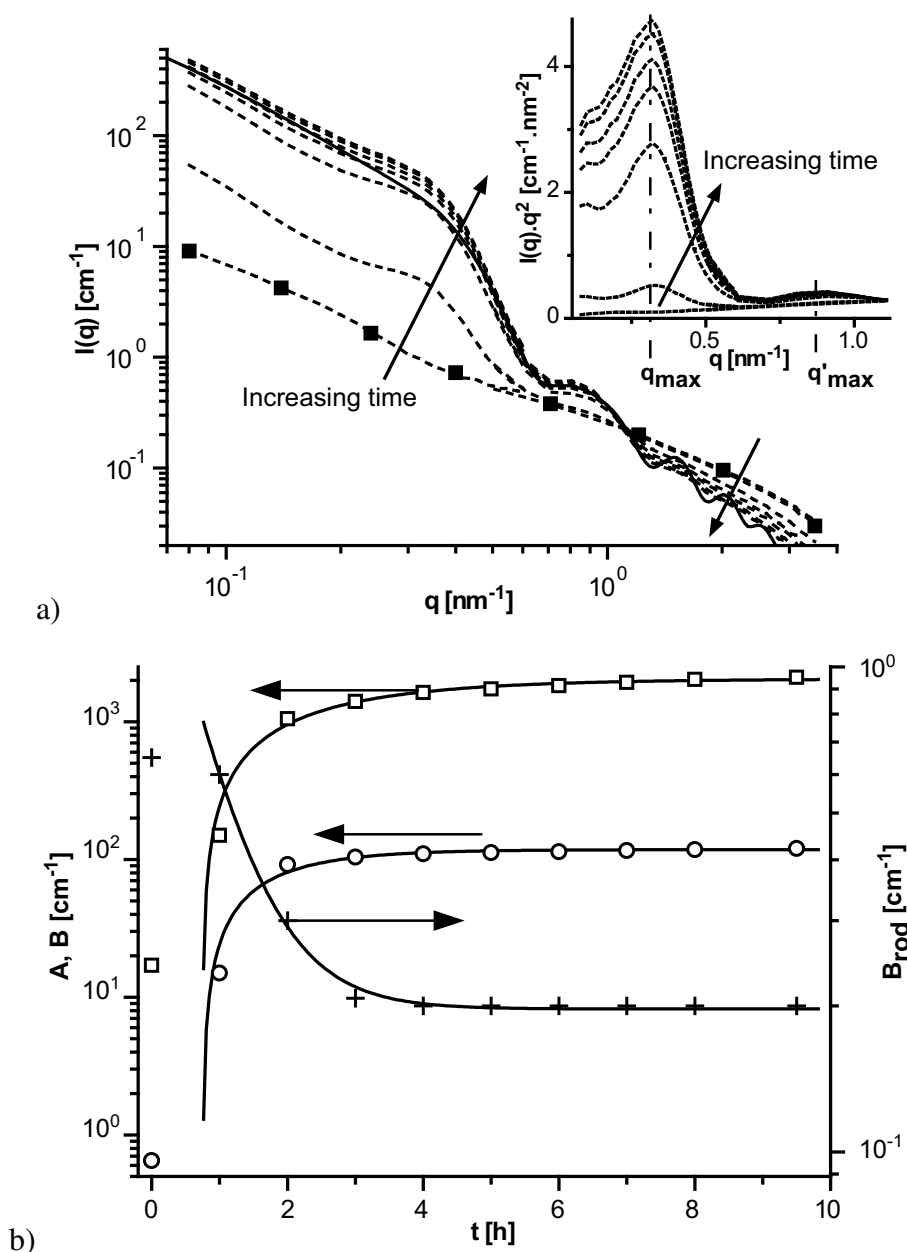


Figure 5. SANS: a) Absolute scattering intensity $I(q)$ versus modulus of the scattering vector q for PR₇ at 19.6 w/w% in DMSO-d₆: (■) at 43 °C, (dashed lines) after 0, 1, 2, 3, 4, 6 and 8 h at 21 °C and (solid line) fitting curve with equation (2) of the experimental profile obtained after 4 h at 21 °C. For clarity reasons, only 4 points per decade are shown in the curve at 43 °C. Inset: corresponding Kratky plot. b) (□) Parameter A which reflects the weight of the Gaussian form factor, (○) parameter B which reflects the weight of the cylinder form factor and (+) parameter B_{rod} which reflects the weight of the rod-like tube form factor as indicated in equation (2) versus time t at 21 °C for PR₇ at 19.6 w/w% in DMSO-d₆. The solid lines are the fitting curves obtained with equation (4).

To have more insight into formed structures during time, we propose to model the scattering intensity curves. We showed that during gelation the system can be viewed as

a blend of regular structures (called in the following bundles) containing naked PEO segment crystallites surrounded by α -CD aggregates, and both isolated naked PEO segments and α -CD rod-like tubes. Thus, the scattering intensity is the sum of the intensity scattered by the isolated entities (naked PEO segments and α -CD rod-like tubes) and the one scattered by the bundles organized in a Gaussian way:

$$I(q) = I_{bundle}(q) + B_{rod} \left\{ 1 - \exp \left[- \left(\frac{q}{q_0} \right)^{5.33} \right] \right\} P_{cyl}(q, L_{rod}, R_{rod}) + I_{inc} \quad (2)$$

Where I_{bundle} is defined as follows:

$$I_{bundle}(q) = A \exp \left[- \left(\frac{q}{q_0} \right)^{5.33} \right] P_{Gauss}(q, R_g) + B \left\{ 1 - \exp \left[- \left(\frac{q}{q_0} \right)^{5.33} \right] \right\} P_{cyl}(q, L, R) \quad (3)$$

It should be noticed that experimental curves cannot be fitted by any model of spherical symmetry (either a homogeneous sphere model, a spherical core-shell particle model or a spherical shell particle model). The parameters L_{rod} , R_{rod} and q_0 are kept equal to the values given by the fitting with equation (1) of the experiments carried out at 43 °C, corresponding to $t = 0$ at 21 °C. Regarding I_{bundle} , the parameters L , R and R_g are kept equal to the values given by the fitting with equation (3) of the steady state SANS profiles: the bundle length is $L = 14$ nm, the bundle radius is $R = 5.7$ nm, the gyration radius R_g is estimated to be higher than 33 nm and the cut-off modulus q_0 . Then, the fit consists in determining the weighting of each form factor A , B and B_{rod} at any given time, all other parameters being kept constant.

Figure 5a shows a good agreement between the fitting curves obtained with the help of equation (2) and the experimental data. This confirms that the structural parameters do not evolve with time. Consequently, the characteristic bundle length L and radius R are constant at any time. In other words, SANS measurements do not allow to observe the growing of the aggregating bundles with time. On the contrary, the absolute value of the scattering intensity, as the weighting parameters A and B , increase with time (Figure 5b) reflecting the increasing number of aggregated bundles. We conclude the time necessary to form one bundle is much lower than the scan duration of SANS measurements, *i.e.* 30 min. Furthermore, Figure 5b shows a decrease of B_{rod} with time pointing out the decreasing number of α -CD rod-like tubes with a kinetics having the

same characteristic time as for parameters A and B. It should be noticed that introducing the form factor of isolated α -CD rod-like tubes in equation (2) improves significantly the fitting of the experimental data, especially for $q > 1 \text{ nm}^{-1}$. At long aging time, *i.e.* once the steady state is reached, $B_{\text{rod}} > 0$ suggesting that a fraction of α -CD rod-like tubes is not aggregated and is still present in the system.

The fitting procedure led to estimate the bundle sizes ($L = 14 \text{ nm}$ and $R = 5.7 \text{ nm}$). From the literature, an α -CD rod-like tube consists of 2 to 7 α -CDs^[7,34,35,36] and its length goes from 1.6 nm to 5.5 nm which is much less than the bundle length L . Thus, a possible structure of the bundles is a naked PEO segment crystallite bounded to its extremities with aggregated α -CD rod-like tubes. The α -CD rod-like tubes are oriented towards DMSO and play the role of a compatibilizer inducing the nano-scale bundle size and in that way the transparency to the eye of the physical PR-based gels. It is worth mentioning that fitting the experimental curve of pure PEO with equation (2) is not possible. This indicates that the formed structures in pure PEO in the gel state are very different from those of PR₇. This confirms the primordial role of α -CD rod-like tubes on the self-organization of PR₇.

To get more insight into the kinetics, both parameters A (which reflects the weight of the Gaussian form factor) and B (which reflects the weight of the bundle form factor) are studied. Figure 5b shows that A and B evolve according to the same temporal law:

$$y(t) = y_0 + y_\infty \left[1 - \exp\left(-\frac{t - \tau_0}{\tau_c}\right) \right] \quad (4)$$

Where y designates A or B, y_0 and y_∞ are values at short and long times respectively, τ_0 is an induction time and τ_c is a time characteristic of the evolution of the bundle number. The fitting values of τ_0 and τ_c are identical up to the temporal resolution of the acquisitions: $\tau_0 = 1.02 \text{ h}$ for A and 0.98 h for B, and $\tau_c = 1.52 \text{ h}$ for A and 1.33 h for B. This behaviour suggests that the formation of aggregated α -CD rod-like tube domains is induced by the crystallization of naked PEO segments.

At higher complexation degree N

At higher complexation degree, the physical gelation of PR solutions implies indubitably structures based on α -CD rod-like tubes and naked PEO segments as shown by differential scanning calorimetry (DSC), ¹H nuclear magnetic resonance (¹H NMR) and wide-angle X-ray scattering (WAXS).^[21] Moreover, we demonstrated that the

contribution of α -CD rod-like tubes to the association is more pronounced at higher N value.^[21] However, as studied above, the contribution of α -CD rod-like tubes to the self-organization at the nano-scale exists for the lowest studied N value ($N = 7$).

The SANS profiles of PR₃₇, PR₈₅ and PR₁₅₇ are similar to the one obtained for PR₇ (Figure 6). Whatever the complexation degree N , equation (2) well fits the experimental intensity profiles with the same bundle sizes ($L = 14$ nm and $R = 5.7$ nm) as the ones obtained for PR₇. These values are consistent with direct observations carried out by microscopy (Annexe 3.2.b). For all studied PRs, the values of q_{\max} and q'_{\max} are constant. Moreover, whatever N , the most pronounced evolution with time of the Kratky plot consists in the growing of the peak at q_{\max} as shown in Figure 5a. The profiles of the scattering intensity at $q_{\max} = (3.63 \pm 0.3) \times 10^{-1} \text{ nm}^{-1}$ versus time at 21 °C are of the same type for all studied PRs (Figure 6) and have the same shape as those shown in Figure 5b. The evolution of $I(q_{\max})$ as a function of time is also well described by equation (4) (Figure 6). For all PR solutions, the times τ_0 and τ_c are in agreement with those obtained when fitting the time dependent parameter B reflecting the weight of the bundle form factor of equation (2).

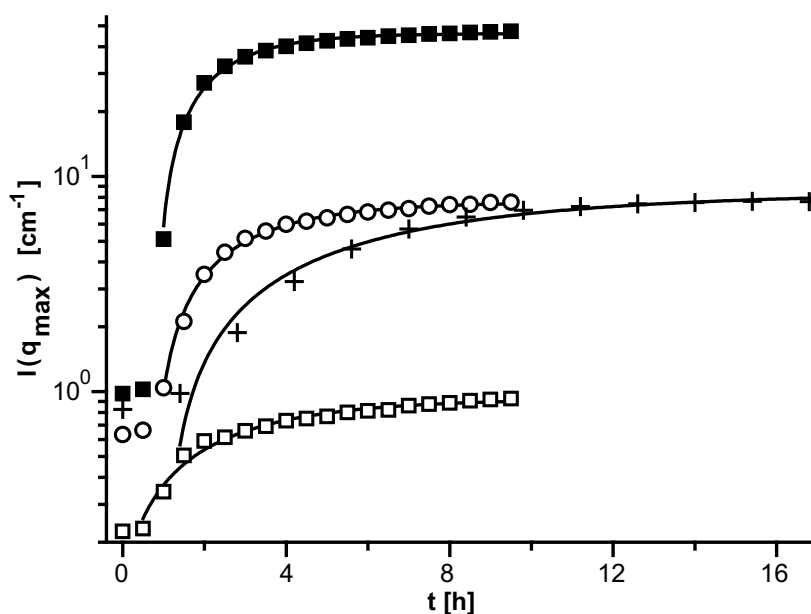


Figure 6. SANS: Absolute scattering intensity I at $q_{\max} = 3.63 \times 10^{-1} \text{ nm}^{-1}$ versus time t at 21 °C and fitting curves obtained with equation (4) for PRs at 19.6 w/w% in DMSO- d_6 :

(■) PR₇, (○) PR₃₇, (+) PR₈₅ and (□) PR₁₅₇.

In the following, we consider the evolution of the characteristic time τ_c as a function of the complexation degree N (Figure 7). The time τ_c does not show a monotonous

evolution with N . At low N values, the intrinsic flexibility of PRs is high due to long naked PEO segments leading to a self-organization which is kinetically favoured. Furthermore, at constant PR weight fraction, the number of PR molecules is the highest at the lowest N value (Table 1), increasing the bundle number. At high N values, PRs are more rigid, as observed for PR₁₅₇, leading to rapid pre-alignment of the PR molecules.

The characteristic times determined through RDA are higher than those obtained by DSC and SANS. Indeed, RDA measurements probe the elasticity of the gel and thus are little sensitive to the first stages of the aggregation, before percolation is reached. On the opposite, DSC measurements are sensitive to all types of aggregation events, whatever their size or structure, and lead thus to the fastest kinetics. SANS measurements which highlight the formation of well-defined structures lead to intermediate characteristic times.

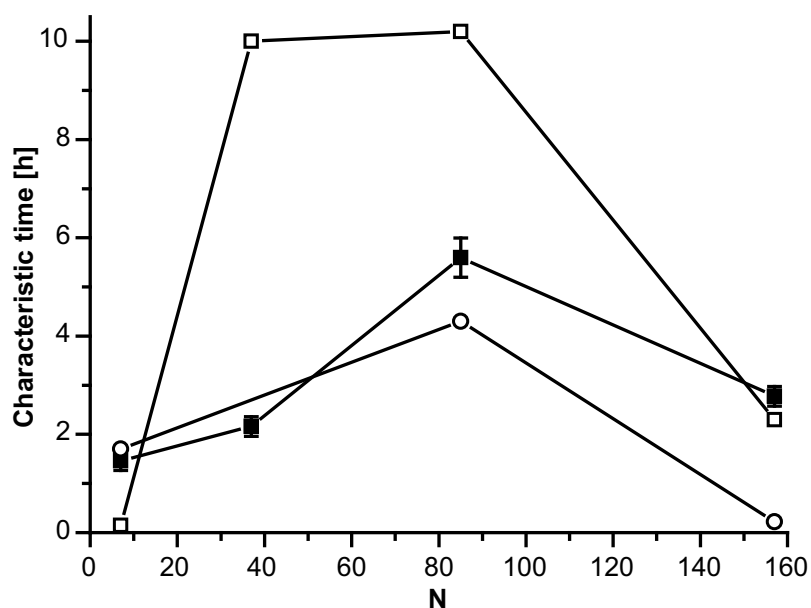


Figure 7. (■) Characteristic time τ_c determined through SANS measurements, (□) characteristic time τ_c determined through RDA measurements and (○) characteristic time τ_c' determined through DSC measurements *versus* complexation degree N for PRs at 19.6 w/w% in DMSO(-d₆) at 21 °C.

3.2.4. Conclusion

The structure of PRs based on α -CDs threaded onto 22 kg mol⁻¹ PEO chains in concentrated solution (≈ 20 w/w%) in DMSO was studied by SANS measurements as a function of the temperature and the complexation degree N which ranged from 7 up to

157. Furthermore, the behaviour of a pure PEO solution in DMSO (at 5.9 w/w%) was also compared with the one of PRs. At 43 °C, the PEO and all PR solutions stay liquid. Whereas SANS showed isolated flexible Gaussian chains in the pure PEO/DMSO mixture, a multiblock copolymers behaviour was revealed for PRs in DMSO. This multiblock behaviour of PRs at 43 °C is due to the presence of two kinds of blocks which alternate along the PR. One block type is rigid and corresponds to α -CD rod-like tubes with a length $L_{\text{rod}} \approx 7$ nm. The other block type corresponds to flexible naked PEO segments. For the highest N value (*i.e.* 157 corresponding to an α -CD overlap ratio ≈ 63 %), the polyrotaxane is much more rigid and showed rods longer than 45 nm which is in the same order as the developed length of the 22 kg mol⁻¹ PEO chain.

When the PEO or the PR mixtures are cooled down to 21 °C, they gelify slowly with time. Whereas the PEO/DMSO forms a macroscopic heterogeneous gel, the PR/DMSO physical gels are homogeneous and transparent to the eye at room temperature. For the PEO/DMSO system, gelification is due to large aggregates constituted by the gathering of small nano-scale crystallites. For the PR/DMSO systems, the gel structure is due to the multiblock copolymer behaviour of PRs leading to the formation of regular bundles for which the characteristic sizes ($L = 14$ nm and $R = 5.7$ nm) are constant during the gelification process and are independent with N. These regular bundles contain naked PEO segment crystallites surrounded by α -CD rod-like tube aggregates at their extremities. Indeed, α -CD rod-like tubes, which are present in the initial state at 43 °C act like a compatibilizer and thus lead to the nano-scale bundle sizes and, in contrast with the PEO/DMSO system, to the transparency of the physical PR-based gels. Furthermore, we showed that the kinetics of the bundle formation is N-dependent. Indeed, at constant PR weight fraction in DMSO, the N value is a crucial parameter controlling the intrinsic flexibility of PRs (flexibility favoured at low N values) and their pre-alignment (pre-alignment favoured at high N values), and thus controlling the self-organization.

Annexes

Annexe 3.2.a: Sensitivity of small-angle neutron scattering measurements in deuterated dimethyl sulfoxide

For neutron scattering, the determinant condition for scattering to occur concerns the scattering length density of the solute with respect to the solvent.^[43] The scattering length density δ_i can be estimated as follows:

$$\delta_i = \frac{a_i N_A}{V_i} \quad (5)$$

$$a_i = \sum_m a_{i,m} \quad (6)$$

Where the index i stands for the α -CD, the PEO or the DMSO- d_6 molecule and the index m represents the constitutive atoms of the molecule i . a_i designates the coherent diffusion length of the molecule i , N_A the Avogadro constant and V_i the molar volume of the molecule i . The so-called contrast length density ${}^v b_i$ with respect to the solvent is equal to:

$${}^v b_i = \delta_i - \delta_{\text{solvent}} \quad (7)$$

The obtained values are given in Table 3. The comparison of the obtained contrast length density ${}^v b_i$ values shows that α -CD and PEO scatter neutrons in an equivalent way in DMSO- d_6 . Thus, SANS measurements are not sensitive to a particular species as far as concerns α -CD or PEO in DMSO- d_6 .

Table 3. SANS: Molar volume V_i , coherent diffusion length a_i , scattering length density δ_i and contrast length density ${}^v b_i$ with respect to the solvent for $i = \alpha$ -CD, PEO and DMSO- d_6 .

i	V_i [$\text{cm}^3 \text{mol}^{-1}$]	a_i [cm]	δ_i [cm^{-2}]	${}^v b_i$ [cm^{-2}]
α -CD	973	1.89×10^{-11} #	1.17×10^{10}	-4.11×10^{10}
PEO	40.1	4.13×10^{-13} #	6.20×10^9	-4.66×10^{10}
DMSO- d_6	70.7	6.20×10^{-12} #	5.28×10^{10}	0

#: calculated with equation (6) and reference 44

[43] J.-P. Cotton, *Journal de Physique IV (France)*, **1999**, 9, 21-49 (in French).

[44] A.-J. Dianoux and G. Lander, *Neutron Data Booklet*, OCP Science, Philadelphia (USA), **2003**.

Annexe 3.2.b: Transmission electron microscopy and atomic force microscopy observations

Transmission Electron Microscopy (TEM). TEM observations were carried out at the Institut National de la Recherche Agronomique (INRA, Nantes, France) using a JEM 1230 microscope commercialized by Jeol[®], equipped with a LaB₆ filament and operating at 80 kV. The images were collected with a ES500W Erlangshen CCD camera commercialized by Gatan[®]. For a few minutes, the PR solutions in DMSO were heated up at 43 °C while being mechanically stirred. A drop of about 50 µL was placed on a carbon-coated TEM copper grid commercialized by Quantifoil[®] and then stored at 21 °C for 10 h. The solvent was wiped off with filter paper and the samples were negatively stained with 2 w/w% uranyl acetate so as to enhance the contrast of the organic material with its surrounding. The grids were then air-dried before introducing them to the electron microscope. It should be noted that the stain was applied after the samples were deposited and fixed on the TEM grids so that the aggregation phenomena should not have been induced by the stain.

Cryo-TEM observations were tried in order to observe the samples in presence of DMSO. This technique consisted in quenching the TEM grids, on which a drop of the PR/DMSO samples was placed, into liquid ethane with a high enough cooling rate so as to get vitreous DMSO. However, the cryo-TEM experiments were not successful. It can be explained by the fact that DMSO crystallization could not be avoided (DMSO is generally used as a cryo-protectant) and also that DMSO was partially soluble in liquid ethane, as numerous organic solvents. Moreover, no examples of cryo-TEM observations of DMSO-based samples are found in the literature.

Atomic Force Microscopy (AFM). AFM observations were made on a Nanoscope IV commercialized by Veeco[®] in tapping mode using topography and phase imaging. Silicon microcantilevers with a spring constant of 21 N m⁻¹ and a resonance frequency of 146 kHz were used. The PR solutions in DMSO were heated for a few minutes at 43 °C while being mechanically stirred. A drop was placed on a mica wafer and then stored at 21 °C for 12 h. The wafer was dried under vacuum at 21 °C in order to keep the integrity of the self-organized structures before the AFM investigation.

A direct observation of the formed structures is possible by TEM and AFM. The TEM observations were carried out after negative staining (Figure 8a). Thus, appearing with a

dark contrast, the negative stain moulds round the PR molecules outlining their structure which appears with a brighter contrast. The initial PR concentration and the sample preparation method are such that the structure density is high enough to induce percolation of the objects. The observed percolation can be due to the presence of stain surrounding the bundles. Furthermore, a dense network of cylinder-like structures having one characteristic dimension of about 15 nm and the other one less than 10 nm is observed. The AFM image was obtained in tapping mode. The topography image was relatively smooth whereas the phase image showed heterogeneities (Figure 8b) indicating that the mechanical properties are not uniform at the surface of the sample. It is reasonable to think that mechanical properties between bundles and non-aggregated PR molecules (or PR molecule parts) are different. Thus, the observed dark domains with a characteristic size of 6.6 ± 2 nm correspond to tilted bundles plunging more or less into the thickness of the sample. All morphologies and sizes observed by TEM and AFM are consistent with the previous results.

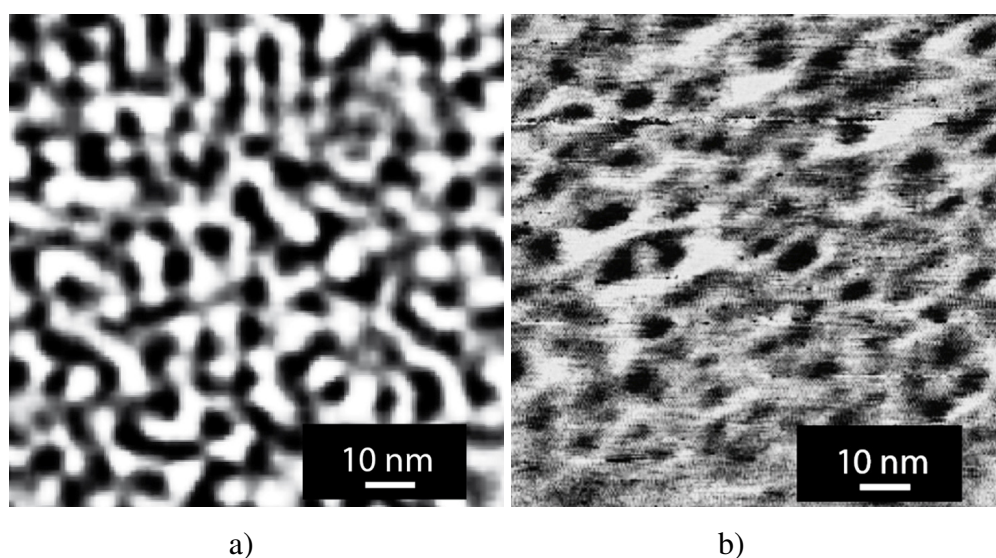


Figure 8. PR₈₅ at 19.6 w/w% in DMSO after a long aging time at 21 °C and then dried under vacuum at 21 °C: a) TEM image after negative staining and b) AFM phase image.

CHAPTER 4

Chemical gels based on polyrotaxanes in dimethyl sulfoxide and water: "sliding gels"

In the previous chapter (**Chapter 3**), it was shown that α -CD/PEO-based PRs in solution in DMSO form physical gels at room temperature. Starting from a liquid PR/DMSO mixture at high temperature (typically 43 °C) containing rod-like tubes consisting of weakly stacked α -CDs along the PEO chains, the system at a typical concentration of 19.6 w/w% forms slowly a physical gel with time at room temperature. With increasing time, naked PEO segments (*i.e.* the ethylene oxide units of the PEO chains which are not covered by α -CDs) are consumed, forming PEO crystallites due to the fact that PEO is in bad solvent conditions in DMSO at room temperature.^[A] Moreover, rod-like tubes are consumed with time, self-organizing into α -CD nano-cylinders due to the formation of numerous hydrogen bonds between α -CD hydroxyl groups. As expected, the formation of PEO crystallites is predominant at low complexation degree (*i.e.* the number of threaded α -CDs per PEO chain) values. The structure formation is due to the multiblock copolymer behaviour of PRs and their nano-scale sizes do not evolve with time and complexation degree. Typically after few hours at 21 °C, the system reaches an equilibrium state in which a fraction of non-aggregated rod-like tubes still remains present. Chemical gels (*i.e.* gels in which the cross-link points are permanent) are of high interest for their high swelling properties^[B,C] and for the wide variety of applications they can be used for.^[D,E,F] When α -CDs are intermolecularly chemically cross-linked, chemical gels of a new type are formed. It may be expected that the α -CD cross-link points freely slide along the PEO chains, leading to an increased swelling behaviour. Nevertheless, the studies carried out in the previous chapters (**Chapters 2 and 3**) on physical gels showed that numerous associations having varied origins take place between PPRs in water and between PRs in DMSO. It is wondered whether such associations still exist in the chemical gels obtained from the already synthesized PRs and if a sliding character of the α -CD cross-link points is observed in the chemical gels in spite of such interactions.

In the present chapter (**Chapter 4**), it is shown that the well-organized structures based on PEO and α -CDs observed in PR physical gels are not put in evidence in PR chemical gels. This can be explained by the lower degree of freedom of the PR molecules within

[A] C. Özdemir and A. Güner, *European Polymer Journal*, **2007**, 43, 3068-3093.

[B] Y. Okumura and K. Ito, *Advanced Materials*, **2001**, 13, 485-487.

[C] W.-F. Lee and L.-G. Yang, *Journal of Applied Polymer Science*, **2006**, 102, 927-934.

[D] M. Bonini, S. Lenz, R. Giorgi and P. Baglioni, *Langmuir*, **2007**, 23, 8681-8685.

[E] K. Kamath and K. Park, *Advanced Drug Delivery Reviews*, **1993**, 11, 59-84.

[F] N. Bhattarai, H. Ramay, J. Gunn, F. Matsen and M. Zhang, *Journal of Controlled Release*, **2005**, 103, 609-624.

the chemical gels (since short cross-linker molecules are used) and also by the quite uncontrolled chemical gel synthesis (since the PR dissociation state prior to cross-linking is not guarantee and since the cross-linking reaction is rapid leading to densely cross-linked domains). Neutron scattering exhibits micro-scale less-organized aggregates. Furthermore, rheological measurements carried out on chemical gels swollen in DMSO show a particular mechanical behaviour consisting in the existence of a relaxation mode at low frequencies. This can be reasonably interpreted in term of α -CD sliding along the PEO chains. Thus, such gels are called "sliding gels". However, this peculiar behaviour is not observed when the chemical gels are swollen in water due to a strong increase of the number of physical cross-link points which hinder the α -CD sliding.

Topological polymer networks
with sliding cross-link points: the "sliding gels".
Relationship between their molecular structure and
the viscoelastic as well as the swelling properties

Published in *Macromolecules*, 2007, 40, 535-543

Abstract

Topological polymer networks with sliding cross-link points, the "sliding gels" (also called slide-ring gels), are a new class of supramolecular networks based on intermolecularly cross-linked α -cyclodextrin/poly(ethylene oxide)-based (α -CD/PEO) polyrotaxane (PR) precursors. The cross-link points of such networks are not fixed but can slide along the template chain of the PRs. The main parameters governing the sliding gel properties are the number of α -CDs per PR molecule, the cross-linking density, and the nature of the swelling solvent. Small-angle neutron scattering, swelling measurements, and mechanical spectrometry were used to understand the unusual physical properties and their relation to the molecular structure of the sliding gels. The swelling as well as the viscoelastic properties are found to be solvent dependent reflecting the structural changes of the network. Indeed, in water, the number of cross-link points (topological and physical) increases as opposed to dimethyl sulfoxide (DMSO) leading to higher modulus values, while the persistence length of the sliding gel strands increases in DMSO as opposed to water leading to a shift of the $\tan(\delta)$ peak, the transition point between the two observed viscoelastic regimes, toward higher frequencies.

4.1. Introduction

Polymer gels are often classified following the type of cross-link points. Until recently only two main classes of polymer gels have been considered: the one with chemical bonds (permanent cross-link points) and the other with physical bonds (reversible cross-link points). A novel class of gel materials, so-called topological network, has

been recently proposed by de Gennes^[1] and was characterized by the sliding character of the cross-link points (also called slide-ring cross-link points). The topological network architecture is obtained by the intermolecular cross-linking reaction of polyrotaxane (PR) precursors.^[2,3,4,5] The main characteristic of the sliding cross-link points is to allow a sliding motion of the constitutive template network chains through the figure-of-eight junctions. The sliding network architecture was, for the first time, experimentally realized by the use of high molecular weight PRs, with chemical structures based on α -cyclodextrin (α -CD) macrocycles threaded along a poly(ethylene oxide) (PEO) template chain^[6,7,8] and their intermolecular bridging with a cross-linker through the hydroxyl groups of the α -CDs, forming thus the cross-linking network points in the form of figure-of-eight. Figure 1 shows schematically the molecular architecture of the studied gels where only few α -CDs participate to the formation of the cross-link points. The sliding gels are expected to have unusual chemical, physical, and mechanical properties due to the theoretical ability of the cross-linking points to slide along the template polymer chain.

[1] P.-G. de Gennes, *Physica A: Statistical Mechanics and its Applications*, **1999**, 271, 231-237.

[2] Y. Okumura and K. Ito, *Advanced Materials*, **2001**, 13, 485-487.

[3] Y. Okumura and K. Ito, *Polymer Preprints*, **2003**, 44, 614-615.

[4] Y. Okumura and K. Ito, *Macromolecular Symposia*, **2003**, 201, 103-110.

[5] G. Fleury, G. Schlatter, C. Brochon and G. Hadziioannou, *Polymer*, **2005**, 46, 8494-8501.

[6] A. Harada, J. Li and M. Kamachi, *Macromolecules*, **1993**, 26, 5698-5703.

[7] A. Harada and M. Kamachi, *Macromolecules*, **1990**, 23, 2821-2823.

[8] A. Harada and M. Kamachi, *Chemical Communications*, **1990**, 1322-1323.

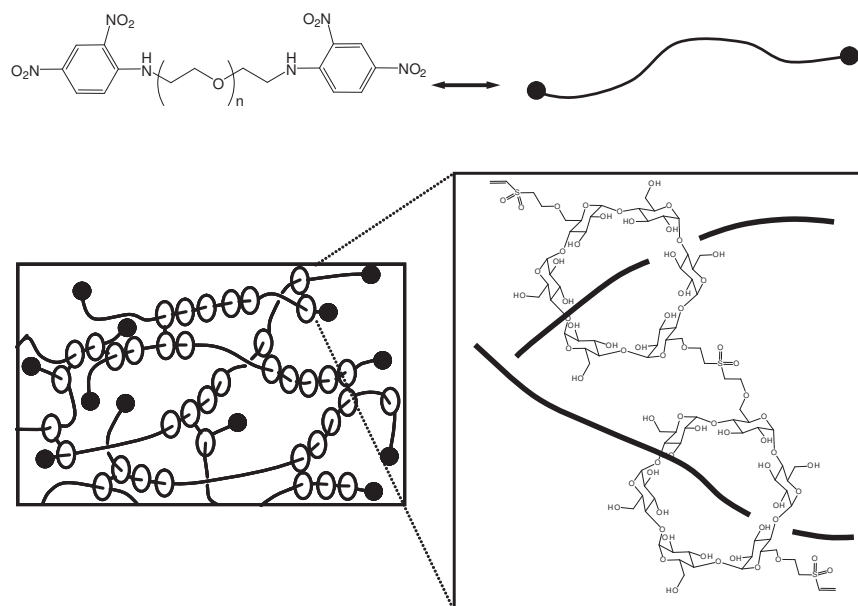


Figure 1. Schematic representation of the molecular architecture of a sliding gel obtained by reaction between α -CD/PEO-based PR and divinyl sulfone (DVS).

Three pertinent parameters governing the unusual properties of this new class of topological materials are the complexation degree (N) defined as the number of α -CDs per template PEO chain, the cross-linker fraction (K) defined as the ratio of the cross-linker mole number (n_C) on the α -CD mole number (n_{CD}), and the interactions between the swelling solvent and the constitutive parts of the network.

The aim of this work was to systematically study the physical, chemical and mechanical properties as well as their relation to the molecular structure of this new class of topological networks as a function of the three previously mentioned parameters governing their structure. For this study, swelling measurements, small-angle neutron scattering (SANS) and mechanical spectrometry were used.

4.2. Experimental section

4.2.1. Material preparation, polyrotaxane precursor synthesis and sliding gel formation

Material preparation, PR precursor synthesis and sliding gel formation are reported in Annexe 4.a and have been extensively described in previous publications.^[5,9]

[9] G. Fleury, C. Brochon, G. Schlatter, G. Bonnet, A. Lapp and G. Hadziioannou, *Soft Matter*, **2005**, 1, 378-385.

4.2.2. Characterization methods

^1H Nuclear Magnetic Resonance (^1H NMR). ^1H NMR spectra were recorded in deuterated dimethyl sulfoxide (DMSO- d_6) on a spectrometer commercialized by Bruker[®] and operating at a frequency of 300 MHz. The internal lock was made on the ^2H -signal of the solvent. The complexation degree was determined by comparison of the integrations of the CH(1) signal of α -CD at 4.8 ppm to the signal between 3.4 and 3.9 ppm, which corresponds to CH(3), CH(6), and CH(5) of α -CD and the CH_2 of the α,ω -bis-amine-terminated poly(ethylene oxide) (BA-PEO).

Swelling measurements. The swelling degrees (S) were determined by a gravimetric technique, and the calculations were based on the gel weight according to the equation:

$$S[\%] = \frac{W_S - W_D}{W_D} \times 100 \quad (1)$$

Where W_S and W_D are, respectively, the weights of the swollen and dried gel. For SANS study, the swelling volume ratio (Q) was determined by a volumetric technique and calculated according to the following equation:

$$Q = \frac{V_S}{V_D} \quad (2)$$

Where V_S and V_D are, respectively, the volumes of the swollen and dried gel. These experiments were realized in distilled water and dimethyl sulfoxide (DMSO) and the swelling capacity of the gels was measured at room temperature (22 ± 1 °C). For the weight measurements of completely swollen gels, the excess of water or DMSO on the surface of the gel was wiped off with filter paper. The dried gel measurements were obtained after 48 h in an oven at 50 °C.

Small-angle Neutron Scattering (SANS). SANS measurements were carried out at the Laboratoire Léon Brillouin (LLB, CEA, Saclay, France) and at the Institut Laue-Langevin (ILL, CEA, Grenoble, France). The use of two diffractometers allows the study of the sliding gels by SANS on a large range of scattering vector (q). The PAXY instrument was used at the LLB to study the sliding gel structure in the intermediary domain. The sample-to-detector distance was fixed at 5 m with a wavelength of $\lambda = 1.2$ nm (5×10^{-2} nm $^{-1} \leq q \leq 4 \times 10^{-1}$ nm $^{-1}$). Absolute intensities corrected for detector sensitivity were obtained by normalization to the scattering from Plexiglas with reference to the direct beam. For the sliding gel study at very low q , the

D11 diffractometer at the ILL was used using an incident wavelength of $\lambda = 1.2$ nm. The sample-to-detector distance was prone to 36.7 m and the resulting explored q range was $7.4 \times 10^{-3} \text{ nm}^{-1} \leq q \leq 6.7 \times 10^{-2} \text{ nm}^{-1}$. The scattered neutron intensity calibration was performed using the signal from a 1 mm thick water sample. Heavy water (D_2O) was used as swelling solvent during all the experiments. The sample cell for all the experiments carried out on the PAXY and D11 diffractometers consisted of 1 mm thick quartz windows separated by a 2.5 mm O-ring. Corrections for incoherent background, detector response and cell window scattering were applied to all measurements.

Dynamic Mechanical Analysis (DMA). The experimental used setup is the RSA II strain controlled spectrometer commercialized by Rheometrics[®]. This spectrometer is equipped with one normal force transducer that can detect normal forces within the range 0.001-10 N. The instrument is equipped with a STD motor having a strain resolution corresponding to 0.05 μm and an angular frequency range between 10^{-3} and 10^2 rad s^{-1} . The configuration chosen for mechanical spectrometry was the parallel plate configuration. The samples, with a typical diameter of 12.8 mm and a thickness of 3 mm, were immersed in distilled water or DMSO during all the experiments in order to maintain the same state of solvent content in the material, thus avoiding sample drying and deswelling during the time of the experiments. Mechanical spectrometry was carried out at angular frequencies from 10^{-3} up to 10^2 rad s^{-1} with a strain amplitude of 2.5 %. A pre-strain of 5 % was applied to the sample before the start of the test in order to ensure that the sample was always in compression during the experiments.

4.3. Results

The physical, chemical and mechanical properties of the topological networks and their relation to their molecular architecture, which is governed by the complexation degree N and the cross-linker fraction K were recognized in an earlier work.^[5] These promising results led us to consider a more systematic study of the properties and the internal structure of the sliding gels as a function of these two relevant parameters. Moreover, a third parameter had to be considered in order to properly apprehend the molecular mechanisms underpinning the sliding gels in view of their topological architecture: the swelling solvent quality. Hence the swelling behaviour of the sliding gel as a function of two different kind of swelling solvents – one poor (water) and one good solvent (DMSO) of the PR precursors – has been studied to understand the network/solvent

interactions and their influence on the molecular structure of the sliding gel. For this purpose, PR precursors with a well-defined degree of complexation N have been synthesized according to the procedure reported previously.^[9] These syntheses allowed us to obtain PRs with a controlled N by varying the initial ratio R_0 between the α -CDs and PEO and the thermal cycle during the complexation process. The complexation degree N of each PR used in this work was in the range 22-90 as reported in Annexe 4.a (Table 3). The intermolecular cross-linking reaction between the PR chains was carried out with divinyl sulfone (DVS) as cross-linking agent according to the procedure already described.^[5] More precisely, the topological cross-link points were formed by bridging *via* the DVS molecule the hydroxyl groups of two α -CDs threaded on different PRs. This reaction allowed us to synthesize swollen topological networks of PRs. By control of the cross-linking density, soft to hard sliding gel materials could be obtained. The degree of cross-linking density is related to the cross-linker fraction K defined following the equation:

$$K = \frac{n_C}{n_{CD}} \quad (3)$$

Where n_C and n_{CD} are, respectively, the cross-linker and α -CDs mole numbers introduced in the pre-gel solutions. All characteristics of the sliding gels prepared for this study are reported in Annexe 4.a (Table 3). For the rest of this study, the sliding gels are denoted by G_xR_y , where x represents the complexation degree N and y the volume V in microliters of cross-linker incorporated in the pre-gel solution.

4.3.1. Influence of the cross-linker fraction K in water

In Figure 2, the influence of the cross-linker fraction ($3.25 \leq K \leq 9.43$) as a function of the swelling degree S in water of several sliding gels prepared from PRs with different complexation degrees ($22 \leq N \leq 80$) is presented. For all the sliding gels, the swelling behaviour shows the same tendencies with the cross-linker fraction K . Two swelling regimes appear with increasing cross-linker fraction K in water. For low K , a quasi-linear decrease of the swelling degree is observed. The highest swelling degree for these sliding gels is reached for the G80R40 gel with S about 1200 %. For higher K , a quasi-stationary regime is achieved with a plateau close to 500 % for all sliding gel series.

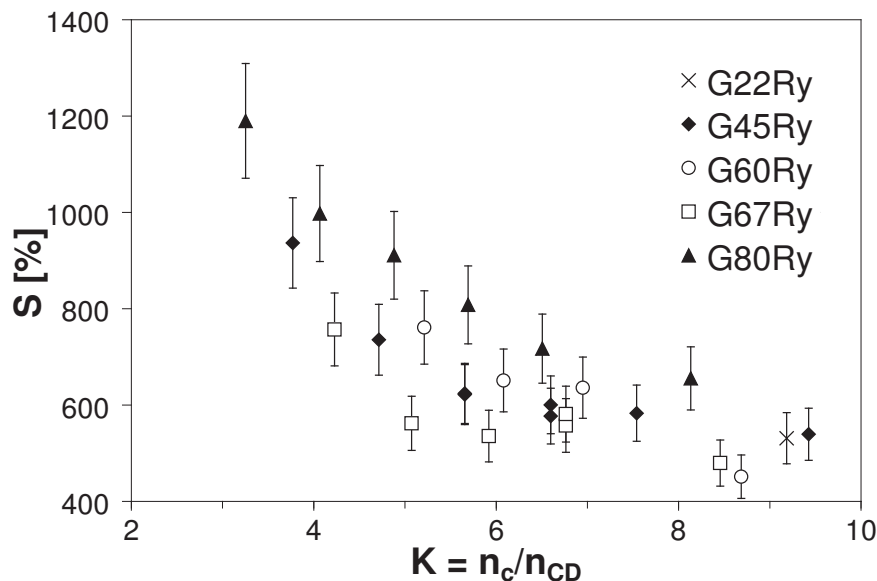


Figure 2. Influence of the cross-linker fraction K on the swelling degree S in water for: (×) G22Ry, (◆) G45Ry, (○) G60Ry, (□) G67Ry and (▲) G80Ry.

Small-angle neutron scattering (SANS) on the PAXY diffractometer at LLB was performed in a series of the sliding gels with increasing cross-linker fraction. The experiments were done with sliding gels in an isotropic equilibrium swollen state in D_2O as swelling solvent and in a q range visualizing the network mesh size as well as large structural heterogeneities. In Figure 3, the SANS data obtained for sliding gels series G70Ry are presented. The scattering intensities of the sliding gels are clearly dependent on the cross-linker fraction K . With increasing K , the scattering intensities increase. Moreover an excess of scattering intensities is also observed for the lowest q values. This result is attributed to the presence of large heterogeneities: the so-called Benoît-Picot effect.^[10] The fitting of the scattering intensities with a single squared Lorentzian function was not possible for the lowest q because of the excess scattering, a signature of large structural heterogeneities in the swollen network. In an attempt to relate the scattering data with the molecular structure of swollen gels with large structural heterogeneities, the form factor (equation (4)) developed by Mallam *et al.*^[11,12] has been adopted. This form factor introduces two scattering contributions: a Lorentzian, $I_F(q)$, comparable to that of semi-dilute solutions and a

[10] H. Benoît and C. Picot, *Pure and Applied Chemistry*, **1966**, 12, 545-561.

[11] S. Mallam, A. Hecht, E. Geissler and P. Pruvost, *Journal of Chemical Physics*, **1989**, 91, 6447-6454.

[12] F. Horkay, A. Hecht, S. Mallam, E. Geissler and A. Rennie, *Macromolecules*, **1991**, 24, 2896-2902.

stretched exponential representing a "solid-like" contribution, $I_S(q)$, arising from the static fluctuations due to the structural heterogeneities in the gel.

$$I(q) = I_S(q) + I_F(q) = I_S \exp[-(q\Xi)^{0.7}] + \frac{I_F}{1 + q^2 \xi^2} \quad (4)$$

Where the correlation lengths ξ and Ξ are associated with a molecular characteristic correlation length of the topological network and a characteristic correlation length related to the heterogeneity size respectively.

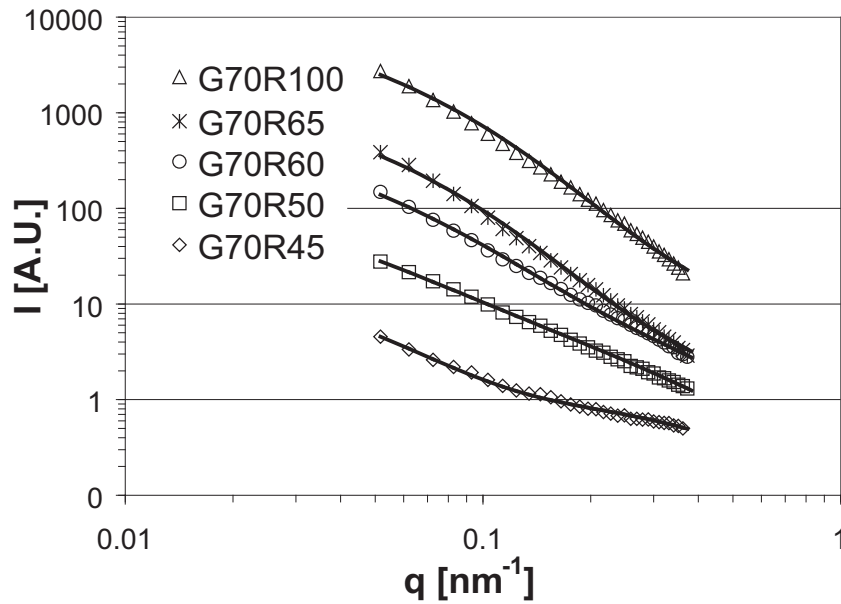


Figure 3. SANS: Neutron scattering functions and their fitting curves for sliding gels prepared from a 70 α -CD PR precursor with different cross-linker fractions K for:
 (\diamond) G70R45 ($K = 3.76$), (\square) G70R50 ($K = 4.18$), (\circ) G70R60 ($K = 5.02$),
 (\times) G70R70 ($K = 5.86$) and (Δ) G70R100 ($K = 8.37$).

In Table 1, a summary of the fitting of the SANS data is presented. The correlation length ξ was found to have values ranging from 6.5 to 5 nm for the less to the most cross-linked gels respectively and is related to the persistence length of the network. The correlation length Ξ also depends clearly on the cross-linker fraction K. It was found in the range 85-61 nm for the less to the most cross-linked gels respectively and corresponds to the characteristic length scale of the large structural heterogeneities. It clearly appears that the correlation lengths ξ and Ξ decrease with increasing K, implying that the mesh size as well as the distance between the heterogeneities decreases (*i.e.* the density of heterogeneities increases) with an increase in the cross-linking density of the network.

Table 1. SANS: Correlation lengths, ξ and Ξ , for the G70Ry sliding gels obtained from equation (4).

	ξ [nm]	Ξ [nm]
G70R45	6.5	85.0
G70R50	6.5	79.0
G70R60	5.8	70.0
G70R70	5.3	67.5
G70R100	5.0	61.0

In Figure 4, the SANS data obtained for sliding gels series G80Ry in D₂O as swelling solvent and in a very low q range ($7.4 \times 10^{-3} \text{ nm}^{-1} \leq q \leq 6.7 \times 10^{-2} \text{ nm}^{-1}$) are presented. For the highest scattering vector region (Figure 4a), the scattering intensity increases with increasing K , a similar behaviour observed with the series of G70Ry gels. In this very low q range a crossover in the scattering intensities with a value close to $q = 1.7 \times 10^{-2} \text{ nm}^{-1}$ was observed. For q values beyond this crossover point, the tendency of the scattering intensities are reversed with respect to cross-linking densities of the network and the lowest cross-linked system scatters more. This observation is attributed to the swelling degree evolution with the cross-linking density of the network. Previously, in the case of non-topological swollen gels including heterogeneities, Bastide *et al.*^[13] have shown that the scattering intensity for $q \rightarrow 0$ is directly related to the volume concentration of elementary strands and to the concentration differences between strongly cross-linked zones (the heterogeneities named frozen aggregates) and the homogeneous matrix of the network. Assuming this treatment is valid in the case of topological swollen gels, we can transpose this analysis to the sliding gels. In topological networks with heterogeneities, this dilution effect, produced by increasing the swelling degree, leads to an increase of the concentration fluctuations between the frozen aggregates and the homogeneous network matrix. This effect is more pronounced for the low cross-linked sliding gels and explains the higher level of scattering intensity at $q \rightarrow 0$ for the sliding gels exhibiting the highest swelling degrees. Moreover a second contribution must be taken into account to explain fully the observed scattering intensities with increasing K at $q \rightarrow 0$. At low q values, the spatial correlations between the heterogeneities become weaker. Thus, the scattering contribution due to the heterogeneities in the total scattering intensity is weaker at $q \rightarrow 0$. In order to rationalize these observations, a scaling law (equation (5)) was proposed by Bastide *et al.*^[13] and

[13] J. Bastide, L. Leibler and J. Prost, *Macromolecules*, **1990**, 23, 1821-1825.

Daoud *et al.*^[14] to correlate the volume concentration of elementary ϕ strands (or the volume swelling ratio Q) with the scattering intensity for $q \rightarrow 0$:

$$I(q \rightarrow 0) \propto \phi^{-t} \propto Q^t \quad (5)$$

Where $I(q \rightarrow 0)$ is the experimental scattering intensity for $q \rightarrow 0$.

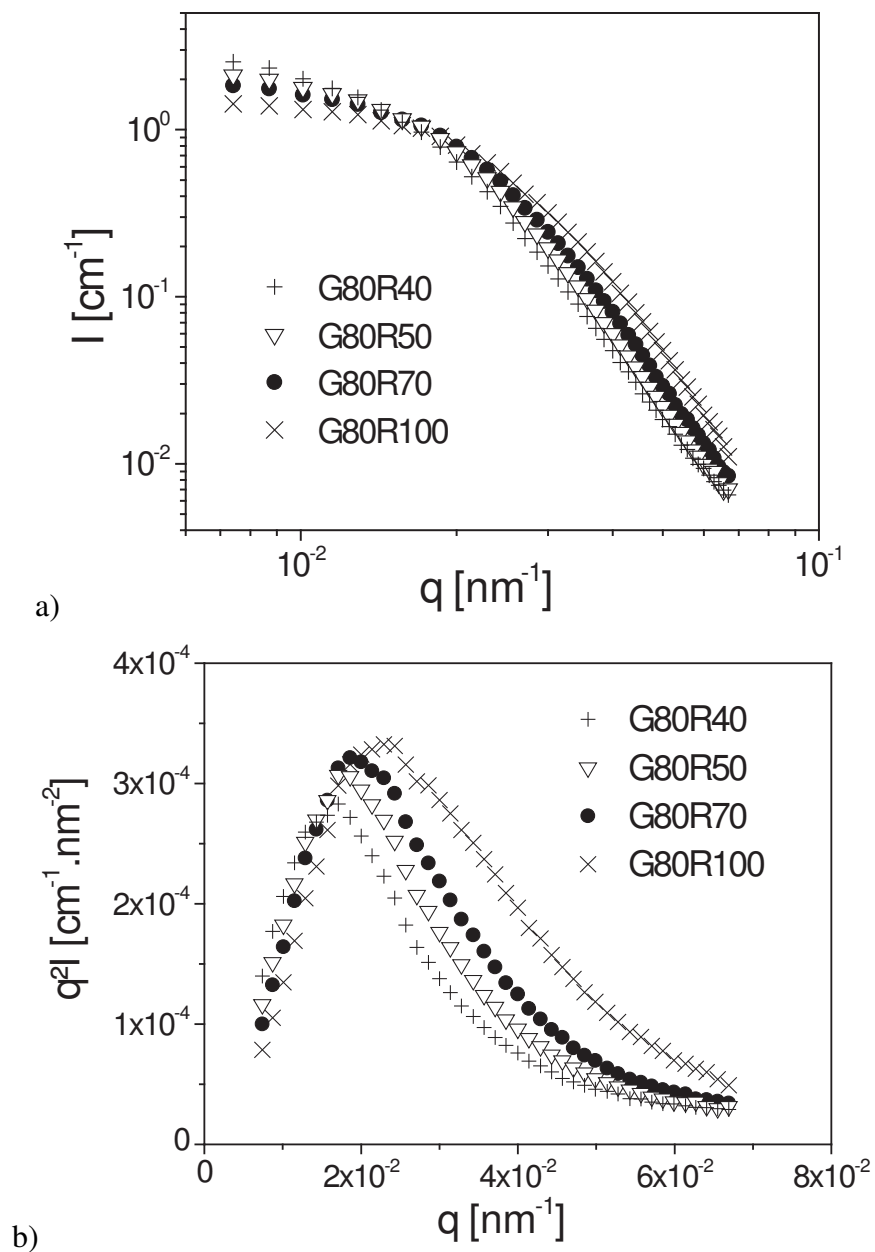


Figure 4. SANS: Neutron scattering functions for the G80Ry sliding gels: (+) G80R40 ($K = 3.25$), (∇) G80R50 ($K = 4.07$), (\bullet) G80R70 ($K = 5.69$) and (\times) G80R100 ($K = 8.13$). Key: a) $I(q) = f(q)$ and b) Kratky plot $I(q) \times q^2 = f(q)$.

[14] M. Daoud and L. Leibler, *Macromolecules*, **1988**, 21, 1497-1501.

In Table 2, the summary of the experimental data for the sliding gel series of G80Ry is presented, and Figure 5 shows the correlation between the scattering intensity for $q \rightarrow 0$ and the swelling ratio Q . The exponent of the scaling law is comparable to that observed before for chemical cross-linked gel systems^[15] and corresponds fairly well with the theoretical exponent value of $5/3$ predicted by Daoud *et al.*^[14] The high value of this exponent reveals the dilution effects for gels with a high swelling capacity. In Figure 4b a treatment of the scattering data for the gel series of G80Ry in the Kratky representation is presented. A correlation peak is observed for a scattering vector value q_{\max} which is attributed to a characteristic correlation length related to the density fluctuations in the sliding gel. The position of the correlation peak has an obvious relationship with the cross-linker fraction K . With decreasing K , the correlation peak is shifted toward the low q values. In fact the observed maximum is due to the presence of heterogeneities in the form of particles the size of which decreases with increasing K . Several previous workers^[16,17,18] used the Guinier and Fournet^[19] analysis to obtain an indication for the inter-particle distances D_{app} between the heterogeneities. Strictly speaking this treatment is only valid for uniform spherical particles on a face-centred cubic lattice. Indeed, the average distance between the centres of the particles was correlated with the q_{\max} position according to the equation:

$$D_{\text{app}} = 1.22 \times \frac{2\pi}{q_{\max}} \quad (6)$$

Where D_{app} is the average distance between the centres of the particles.

Table 2. SANS: Experimental data for the G80Ry sliding gels.

	n_C [mmol]	K	Q	$I(q \rightarrow 0)$ [cm^{-1}]	q_{\max} [nm^{-1}]	D_{app} [nm]	R_P [nm]
G80R40	0.40	3.25	12.90	3.92	2.29×10^{-2}	448	224.0
G80R50	0.50	4.07	10.97	3.03	2.00×10^{-2}	412	206.0
G80R70	0.68	5.69	9.08	2.21	1.86×10^{-2}	383	191.5
G80R100	0.95	8.13	7.55	1.66	1.71×10^{-2}	335	187.5

[15] M. Adam, J. Bastide, S. Candau, J.-P. Cohen Addad, J.-F. Joanny, D. Lairez, W. Oppermann and U. Schröder, *Physical Properties of Polymeric Gels*, Wiley, Chichester (Great Britain), **1996**.

[16] A. Ramsi, R. Scherrenberg, J. Brackman, J. Joosten and K. Mortensen, *Macromolecules*, **1998**, 31, 1621-1626.

[17] A. Topp, B. Bauer, T. Prosa, R. Scherrenberg and E. Amis, *Macromolecules*, **1999**, 32, 8923-8931.

[18] S. Plentz-Meneghetti, J. Kress, F. Peruch, A. Lapp, M. Duval, R. Muller and P. Lutz, *Polymer*, **2005**, 46, 8813-8825.

[19] A. Guinier and G. Fournet, *Small-Angle Scattering of X-Rays*, Wiley, London (Great Britain), **1955**.

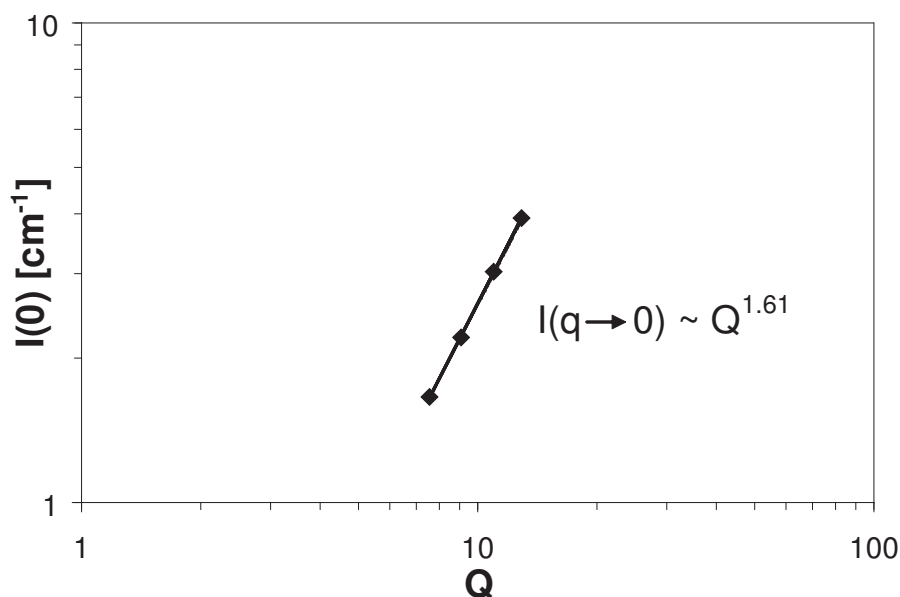


Figure 5. SANS: Scaling law $I(0) = f(Q)$ established for the G80Ry sliding gels.

A reasonable approximation in estimating the radii of the particles, R_p , is to consider them being equal to $D_{app}/2$. In Table 2 are reported the results obtained according to the approximation above. The values of R_p indicate the presence of clusters of highly physically cross-linked PR chain stacks formed via the hydrogen bonds between the α -CDs. The size of these clusters is directly related to the increase of the cross-linker fraction which prevents the swelling of these clusters by the solvent. These arguments can be confirmed by the results presented in Figure 6, where the variation of R_p with the swelling ratio Q of the studied sliding gels clearly shows the cross-linker fraction effect on the swelling ability of the heterogeneities. Indeed, the higher K is, the lower the swelling ratio Q of the sliding gel.

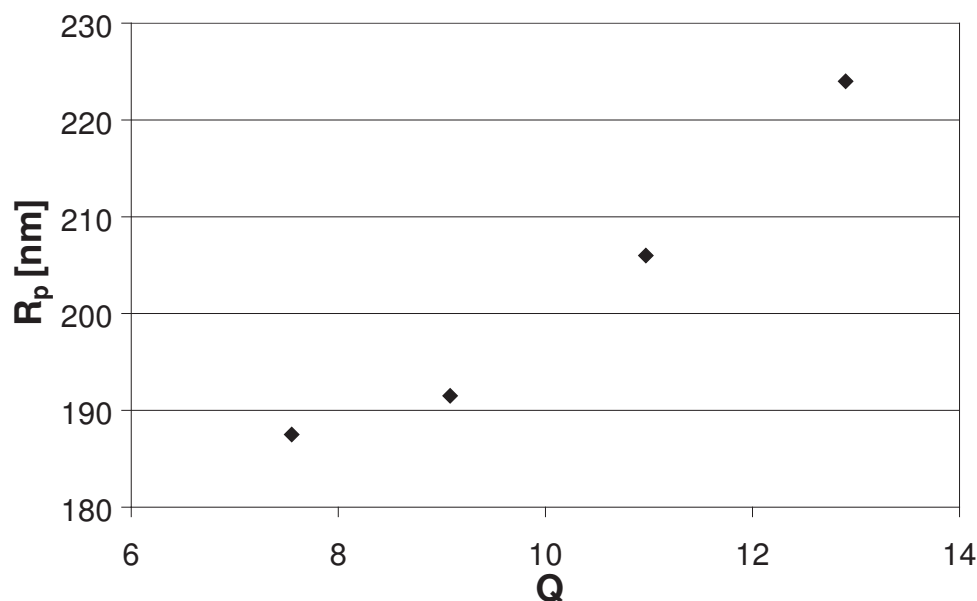
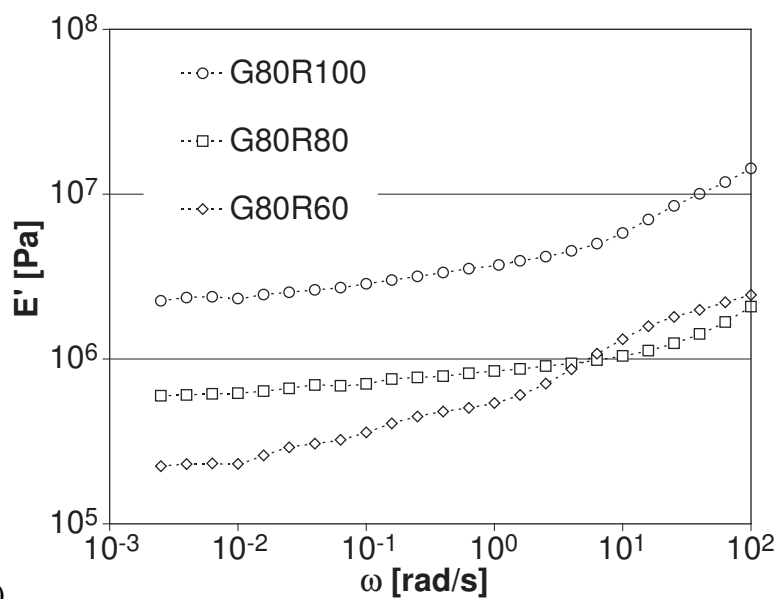
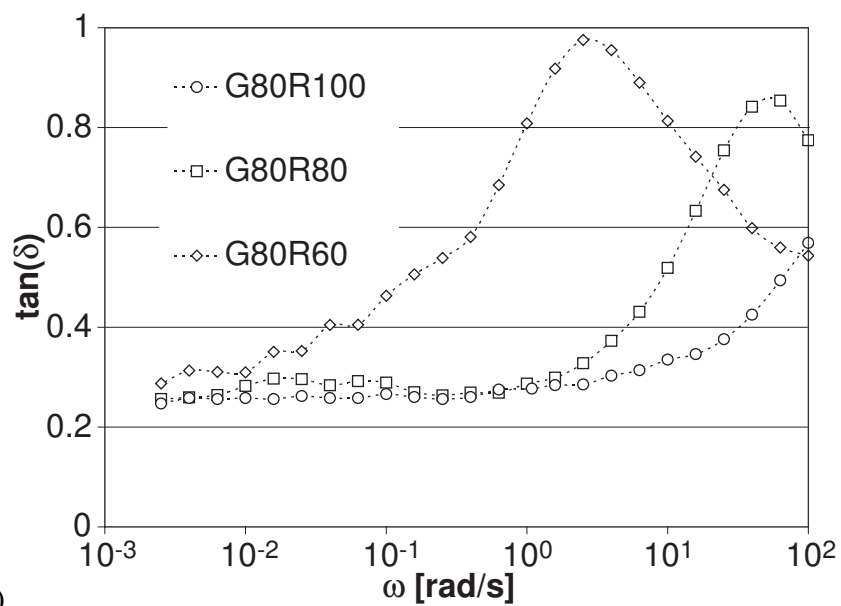


Figure 6. SANS: Evolution of the particle radius R_p with the swelling ratio Q for the G80Ry sliding gels.

The mechanical spectrometry in compression was performed in order to evaluate the cross-linker fraction influence on the viscoelastic properties of these topological materials. Figure 7 shows the viscoelastic spectra for the G80Ry sliding gel series. With increasing K , the elastic and loss moduli increase but the frequency dependence of the moduli appears more complex. In Figure 7c, the E' and E'' do not show a unique plateau but rather two corresponding to two different viscoelastic regimes. The transition between these regimes is clearly observable with the loss angle δ evolution with a pronounced $\tan(\delta)$ peak at the transition region (Figure 7b). It can be noticed that, with an increase in the cross-linker fraction K and thus the cross-linking density, the transition shifts from a low to a higher frequency even though the global moduli values are higher. These experimental observations have been found on all the tested sliding gels whatever the PR complexation degree N was.



a)



b)

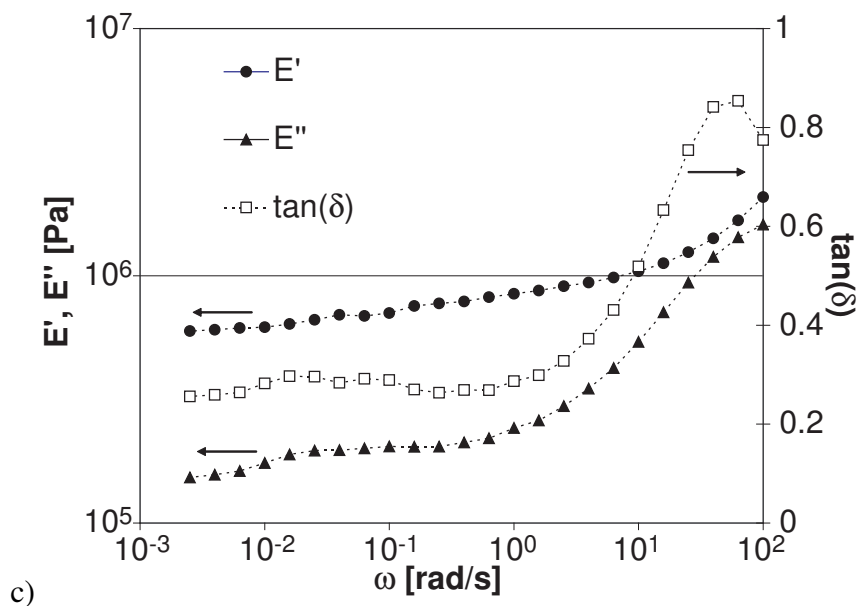


Figure 7. DMA: Frequency sweep tests for the G80Ry sliding gels in water: a) E' versus ω for: (\diamond) G80R60, (\square) G80R80 and (\circ) G80R100. b) $\tan(\delta)$ versus ω for: (\diamond) G80R60, (\square) G80R80 and (\circ) G80R100. c) Viscoelastic spectra of G80R80: (\bullet) E' , (\blacktriangle) E'' and (\square) $\tan(\delta)$.

4.3.2. Influence of the complexation degree N in water

The complexation degree N is another parameter controlling the conformation of the PRs and as a consequence also the properties of the sliding gels. Assuming that two monomer units of BA-PEO are covered by one α -CD,^[20] the complexation degrees for the PRs used in this study are in the range of 10 % to 35 % with respect to the theoretical full coverage for a template BA-PEO chain of 20 kg mol^{-1} . In fact, the increasing complexation degree N plays a considerable role in the conformation evolution of the PR precursor chain going from a Gaussian chain behaviour (low N) with excluded volume to a rod-like chain (high N) with a high persistence length.^[9] It should be expected that sliding networks synthesized with PR precursor chains with various complexation degrees will lead to topological network materials with different viscoelastic properties and various swelling behaviours. However, the swelling degree S , for a given weight fraction $\Phi = 0.15$ of the gel, appears to be slightly dependent on the complexation degree N as shown in Figure 8. This unexpected result can be attributed to the high level of cross-linking density of the series of gels studied in this work which have been designed for viscoelastic characterization experiments. The high

[20] A. Harada, *Coordination Chemistry Reviews*, **1996**, 148, 115-133.

level of cross-linking density seems to overshadow the influence of the complexation degree on the swelling behaviour of the sliding gels.

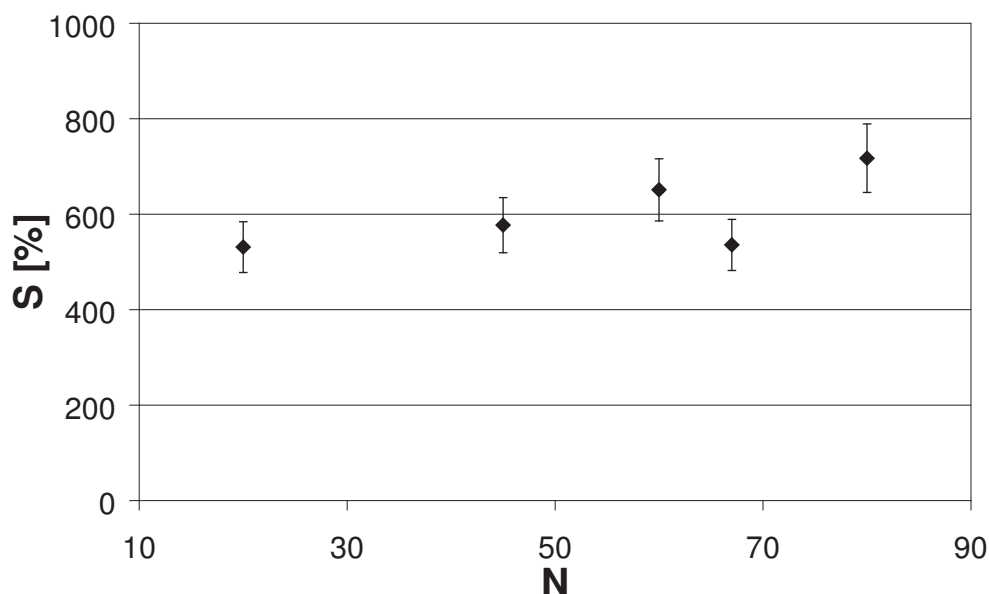


Figure 8. Influence of the complexation degree N on the swelling degree S in water of the GxR70 sliding gels at a fixed cross-linker volume $V = 70 \mu\text{L}$.

The influence of the complexation degree on the sliding gel viscoelastic properties was also explored by mechanical spectrometry. Dynamical frequency sweep experiments in compression were carried out in order to evaluate the $E'_{\max(\tan(\delta))}$ which was defined as the elastic moduli value at the $\tan(\delta)$ peak. $E'_{\max(\tan(\delta))}$ is related to a specific dynamic state of the sliding network and allows to describe the same state of relaxation for all studied sliding gels. Figure 9 shows $E'_{\max(\tan(\delta))}$ versus the complexation degree N for six sliding gels prepared with a cross-linker mole number $n_C = 0.7 \text{ mmol}$. The $E'_{\max(\tan(\delta))}$ values at constant cross-linker mole number do not follow a monotonous dependence with the complexation degree N . An experimental minimum was observed for the complexation degree $N = 67$ and is attributed to two antagonist effects. With increasing N , the number of topological cross-link points decreases due to more probable intramolecular bridging between the α -CDs threaded on a same PR while the persistence length of the network strands increases due to the formation of molecular channels promoted by this intermolecular chemical bridging and the physical interactions between the α -CDs belonging to the same template chain. Thus, on the one hand, the average number of cross-link points is higher at low complexation degree, leading to high moduli levels. On the other hand, the formation of α -CD tubes around

the template chains is promoted with the increase of N , leading to an increase of the rigidity of the elementary elastic strands of the sliding network, resulting to higher moduli levels.

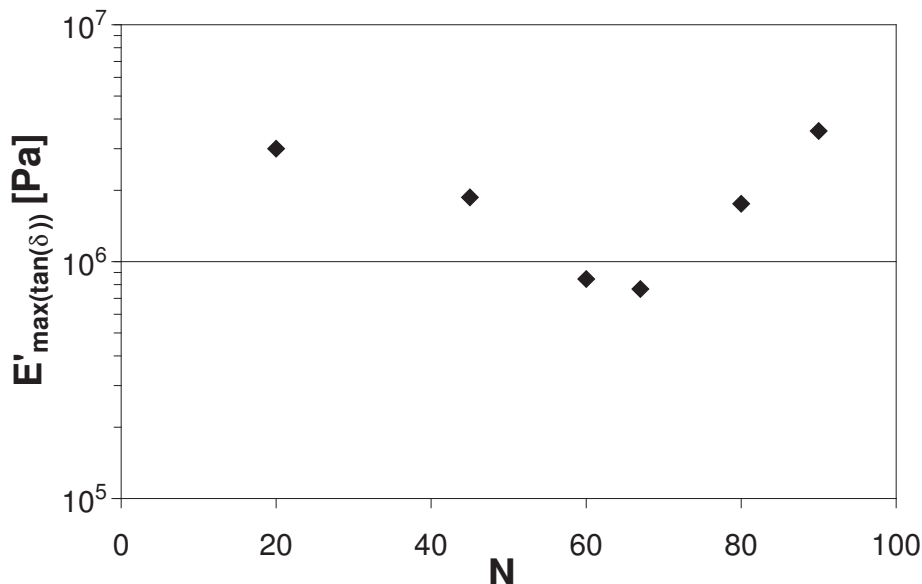


Figure 9. DMA: $E'_{\max(\tan(\delta))}$ versus complexation degree N for the GxR70 sliding gels in water.

4.3.3. Influence of the cross-linker fraction K in dimethyl sulfoxide

The influence of the solvent on the PR conformation is also noticeable. Karino *et al.*^[21] have shown that the conformation of the same PR in sodium deuteroxide (NaOD) is characterized by a Gaussian conformation with excluded volume while in DMSO- d_6 the PR chain adopts a more rigid rod-like conformation. This difference was rationalized by the fact that the electrostatic repulsions between charged α -CDs present in NaOD prevent thus the attractive interactions and as a consequence hinder the establishment of α -CD transient tubes around the template chain. It should be expected that this PR conformation could be preserved on the sliding gels synthesized with the same PR precursor chains when swollen in different solvents having each a different quality with the PR chain.

[21] T. Karino, Y. Okumura, K. Ito and M. Shibayama, *Macromolecules*, **2004**, 37, 6177-6182.

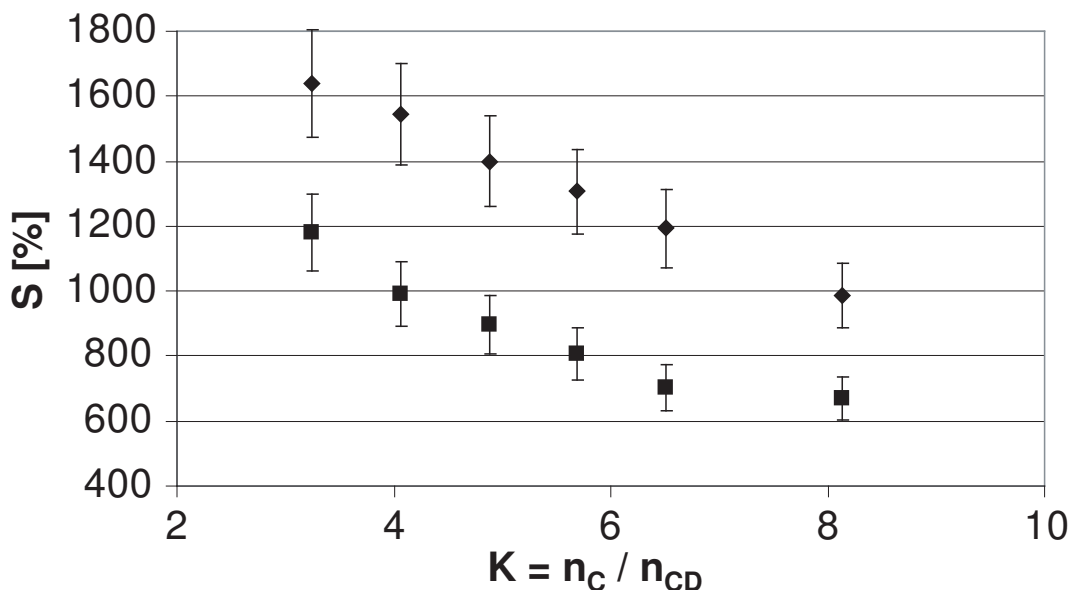


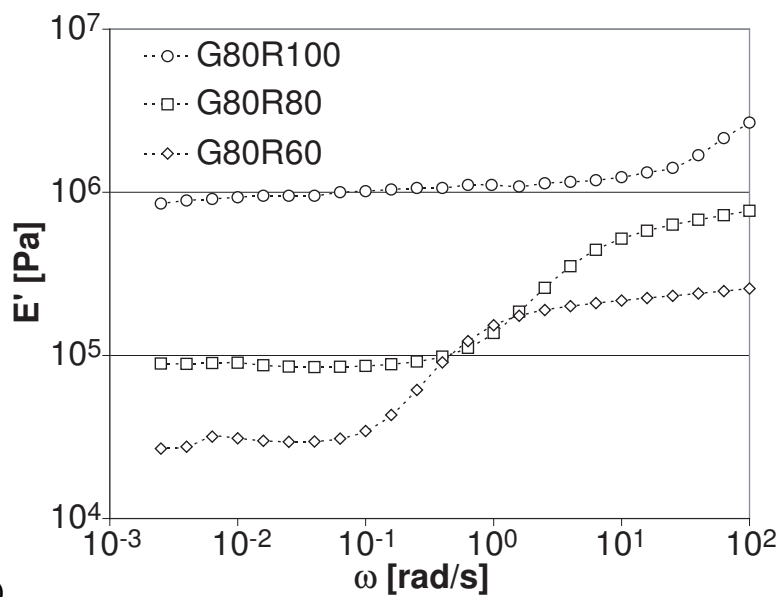
Figure 10. Swelling degree S evolution with regard to the cross-linker fraction K for the G80Ry sliding gels: (■) in water and (◆) in DMSO.

Figure 10 shows the swelling degree S of the G80Ry sliding gel series for various K in distilled water and in DMSO. The swelling degree S appears higher in DMSO than in water and reaches values almost twice as high in the region of low K sliding gels. Two viscoelastic regimes, separated with a transition marked by $\tan(\delta)$ peak, are observed in DMSO as well (Figure 11). Furthermore, increasing the cross-linker fraction K leads to the same tendencies as in water:

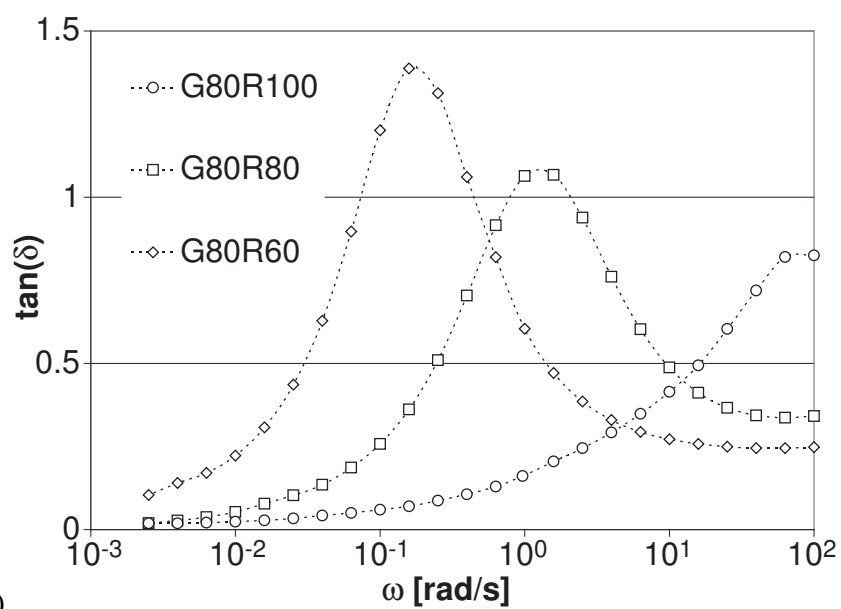
- an increase of the complex moduli,
- a shift of the $\tan(\delta)$ peak toward the highest frequencies.

Nevertheless, as compared to measurements in water, the behaviour in DMSO has shown much lower moduli and a $\tan(\delta)$ peak shift toward the lower frequencies. The two viscoelastic regimes found in DMSO are characterized by two plateaus for E' as already observed in water. However, as opposed to the E'' behaviour observed in water, E'' increases monotonically in DMSO at low frequencies until a maximum corresponding to the transition between the two viscoelastic regimes. This original behaviour, as previously reported,^[22] is more pronounced for the less cross-linked gels where the E'' power-law dependence is close to the value 1, characteristic of low viscous dissipations.

[22] G. Fleury, G. Schlatter, C. Brochon and G. Hadziioannou, *Advanced Materials*, **2006**, 18, 2847-2851.



a)



b)

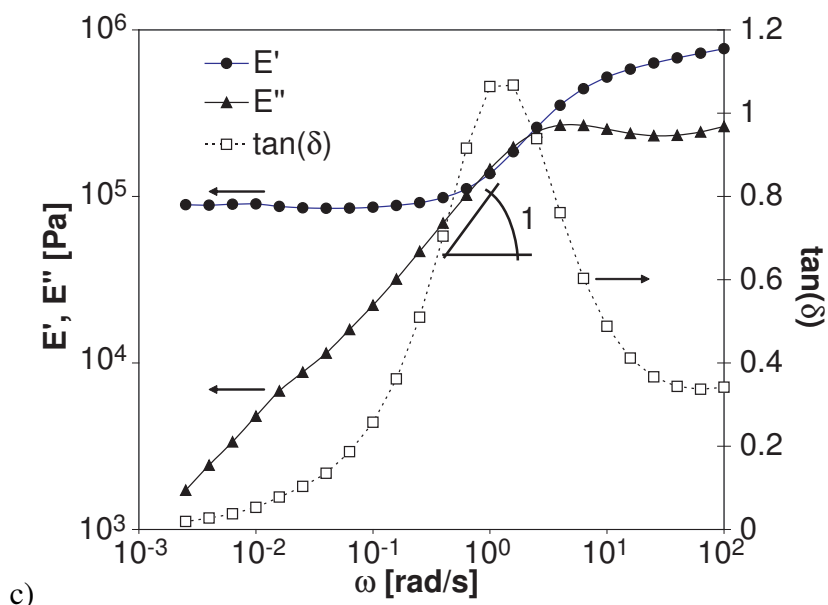


Figure 11. DMA: Frequency sweep tests for the G80Ry sliding gels in DMSO:

- a) E' versus ω for: (\diamond) G80R60, (\square) G80R80 and (\circ) G80R100. b) $\tan(\delta)$ versus ω for: (\diamond) G80R60, (\square) G80R80 and (\circ) G80R100. c) Viscoelastic spectra of G80R80: (\bullet) E' , (\blacktriangle) E'' and (\square) $\tan(\delta)$.

4.4. Discussion

The internal structure of the sliding gels, characterized with SANS, is complex with molecular and supramolecular organization length scales. At the molecular level, a correlation length close to 5 nm was measured and was assigned to a characteristic correlation length of the sliding network strands. At the submicroscopic scale, non-homogeneous huge aggregates of about 0.1 μm have been evidenced as a consequence of a statistical cross-linking reaction.^[15] These heterogeneous aggregates, composed essentially from stacks of hydrogen-bonded α -CDs threaded on PEO segments, are due to the collapse of the PR network strands in water. The size and the density of the aggregates depend on the quality of the swelling solvent. Indeed, an opaque sliding gel in water becomes translucent when it is swollen in DMSO. Thus, the swelling solvent has a considerable influence on the internal structure of the sliding gels, particularly on the heterogeneities. The use of DMSO as swelling solvent, due to its better affinity with the PR network strands, helps to swell the collapsed part of the network and prevents the stacks of hydrogen-bonded α -CDs and consequently the establishment of extra intermolecular hydrogen bond bridges between the PR chains. Consequently, the heterogeneities fade out leading to a more homogeneous gel where the intermolecular hydrogen bond bridges between the PR chains are significantly

attenuated. However, the intramolecular hydrogen bond interactions between the α -CDs belonging on the same PR chain are always effective both in water and DMSO^[9,12] and lead to the formation of α -CDs transient molecular tubes. Figure 12 shows a molecular model for the internal structure of the sliding gels where both chemical and physical intramolecular bonds are considered as cross-link points between the α -CDs belonging to the same or to different PR network strands. Also, the presence of α -CD molecular tubes around the PR network strands, due to the physical or chemical bonding between intra-PR α -CDs, is also envisaged. The number, the nature and the ratio between all these types of bonds considered above depend strongly on the cross-linker fraction, the swelling solvent and the complexation degree.

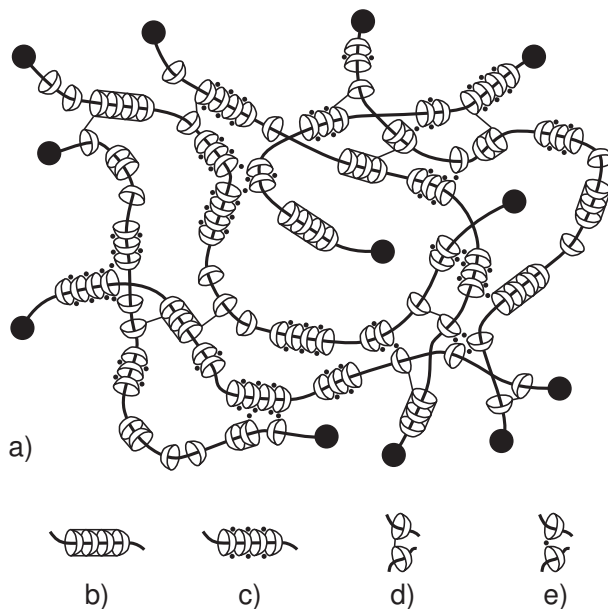


Figure 12. a) Schematic view of the sliding gel at the molecular level showing:
 b) chemically bonded α -CD tube, c) physically bonded α -CD tube, d) chemical cross-link
 between α -CDs and e) physical cross-link between α -CDs.

The proposed molecular model of the sliding gels (Figure 12) allows to explain their specific viscoelastic properties as a function of the cross-linker fraction. The viscoelastic characterization of the sliding gels swollen in water or DMSO has led to two main observations: with increasing K , the modulus levels increase and the $\tan(\delta)$ peak related to the transition between the two E' plateaus shifts toward the highest frequencies. The observed transition between the two plateaus is similar to a

rubber-glass transition of elastomeric materials.^[23] This behaviour is also known for end-linked star-polymer structures^[24] and multicomponent associative polymer networks.^[25] At the molecular level, this transition corresponds to a mobility decrease of the constitutive strands of the network with the increase of the frequency. This transition is attributed to different strand dynamics of the sliding gel network as a function of the frequency. At low frequencies, an efficient relaxation of the network strands is possible, while, at higher frequencies, this relaxation is slowed down due to the presence of α -CD tubes increasing the persistence length of the strands and thus leading to the higher modulus plateau. The explanation of the $\tan(\delta)$ peak shift toward the higher frequencies with increasing K is less obvious at first sight. This shift can be rationalized as follows (Figure 13). For the low cross-linker fraction (Figure 13a), the attractive hydrogen bond interactions between the intra-PR α -CDs lead to the formation of transient α -CD tubes around the PR network strands. Thus, the network strands exhibit a high persistence length which contributes unfavourably to the relaxation processes while the establishment of low number of cross-link points results in low moduli levels. For the high cross-linker fraction (Figure 13b), the hydrogen bonding interactions between the intra-PR α -CDs are prevented due to the modification of the hydroxyl functions with the cross-linker molecules. This chemical modification produces PR strands with a lower persistence length contributing favourably to the relaxation processes. As already pointed out by SANS experiments, a high cross-linker fraction introduces a high number of aggregates and cross-link points which lead to high moduli levels.

[23] J. Ferry, *Viscoelastic Properties of Polymers*, Wiley, New York (USA), **1980**.

[24] C. Satmarel, C. von Ferber and A. Blumen, *Journal of Chemical Physics*, **2005**, 123, 034907-1-034907-13.

[25] D. Loveless, S. Lan Jeon and S. Craig, *Macromolecules*, **2005**, 38, 10171-10177.

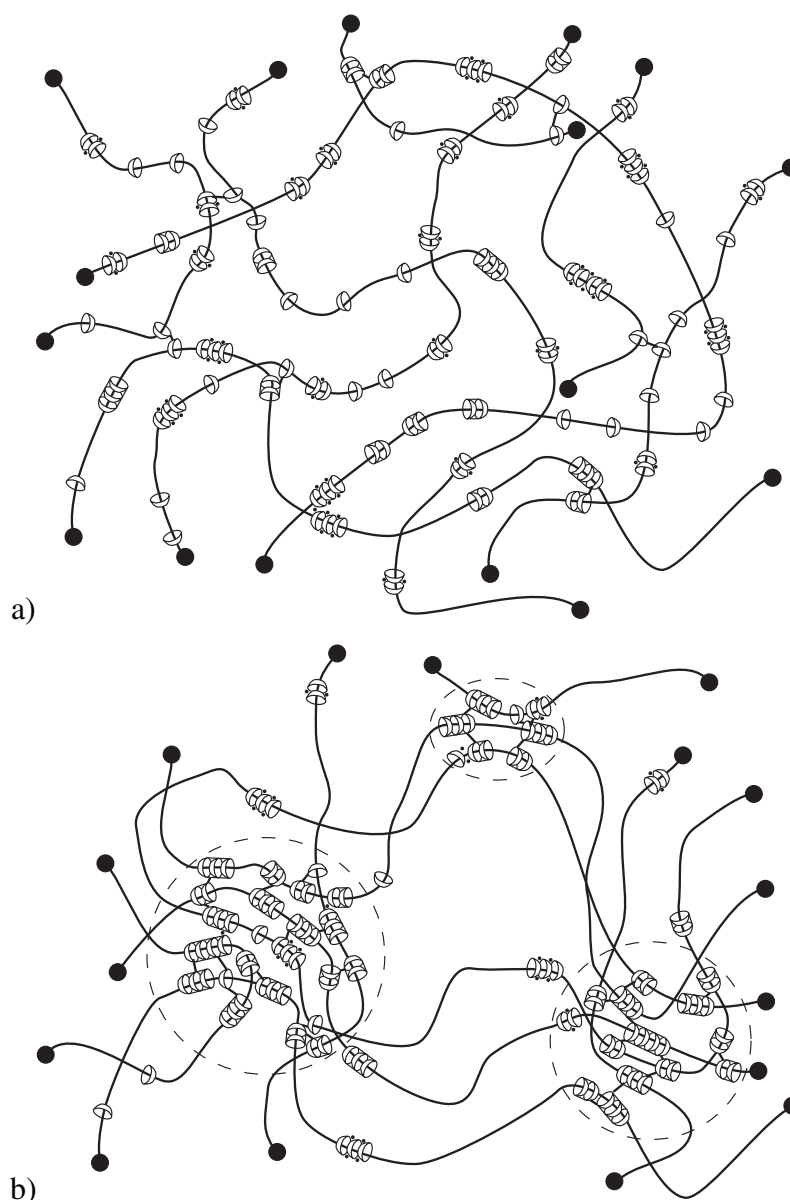


Figure 13. Schematic view of the sliding gel at its equilibrium swelling in the same solvent for: a) low cross-linker fraction K and b) for high K . The dashed lines highlight the aggregates which are favoured at high K .

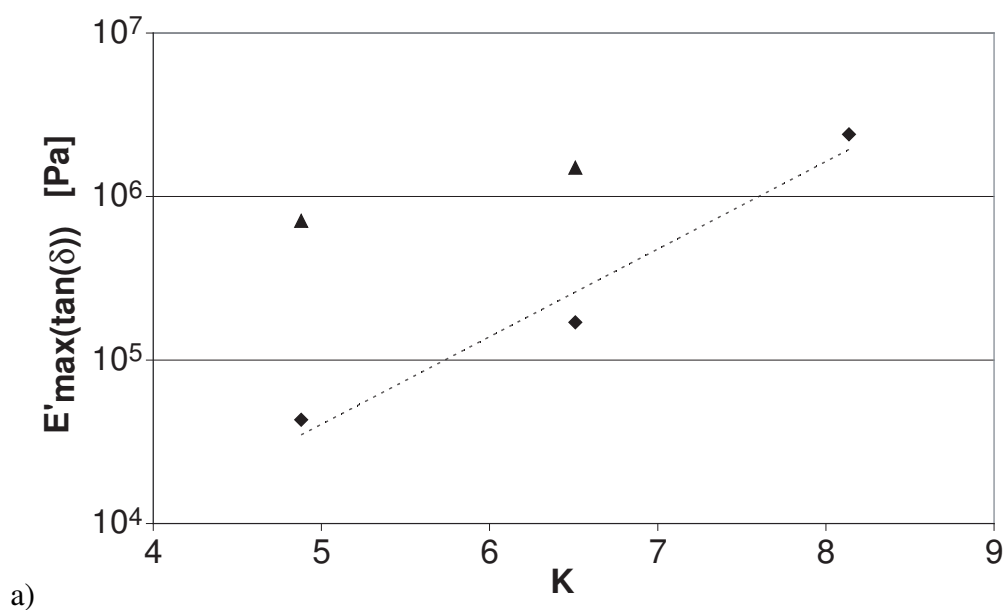
The proposed molecular model of the sliding gels also allows to explain the difference of swelling behaviour between the two solvents (water and DMSO). The swelling behaviour of the sliding gels studied in water and DMSO have led to two main observations:

- the presence of different hydrogen-bonding densities and intramolecular/intermolecular hydrogen-bonding ratios in DMSO and water,
- the sliding gels had a more pronounced ability to swell in DMSO, as opposed to water, leading to a network expansion.

These observations are related to the different solvent interactions of the PR chains in DMSO and water. Indeed, the establishment of the hydrogen bonding interactions between inter-PR α -CDs is more favourable in water, inducing a collapse of the PR network resulting in large heterogeneities which can explain the different swelling behaviour of the sliding gels in the two solvents. DMSO, as a better solvent than water for the PR precursors, is more able to swell the heterogeneities as can be indirectly seen by the quasi-linear decrease of the swelling degree with increasing K (Figure 10). In the case of water, however, a plateau is obtained for the highest K values due to the lesser ability for this solvent to swell the cross-linked aggregates. These aggregates were certainly present at the time of dissolution of the PR precursors in sodium hydroxide solution, just before the cross-linking reaction step for the preparation of the sliding gels. The use of a dissociating solvent such as DMSO or DMAC/LiH, as reported by Araki *et al.*^[26] for the high molecular weight PRs, during the cross-linking reaction step should prevent the aggregate formation in the sliding gels. The viscoelastic properties are also dependent on the swelling solvent. In DMSO, viscoelastic measurements at low frequencies have shown for E'' a power-law dependence with an exponent close to 1 and E' higher than E'' . It results a dominant elastic response over the viscous component at low frequencies. This peculiar behaviour can be attributed to the sliding motions of α -CD cross-link points. In fact, in DMSO, sliding motions of α -CDs are favoured in comparison to water since hydrogen bonds between α -CDs belonging to two different PRs mostly vanish in DMSO. Consequently, in this swelling solvent, the network expansion as well as the sliding motion of α -CDs are enhanced. The effective sliding motion is overshadowed in water where the chains collapse due to the formation of numerous hydrogen bonds. Frozen aggregates are formed slowing down the sliding motion. To have more insight into the different viscoelastic behaviours of the sliding gels in water and DMSO, the dependence of the $E'_{\max(\tan(\delta))}$ values and the positions of the $\tan(\delta)$ peak in the frequency range as a function of the cross-linker fraction K for the G80Ry sliding gels both in water and DMSO were analyzed (Figure 14). The dependence of $E'_{\max(\tan(\delta))}$ with K follows an exponential law for both swelling solvents. The absolute values of the moduli are higher in water than in DMSO for all the sliding gels. For high K, $E'_{\max(\tan(\delta))}$ in water and DMSO seem to converge to a same value. Thus, $E'_{\max(\tan(\delta))}$ does not depend on the swelling solvent for the highest K, which is due

[26] J. Araki and K. Ito, *Journal of Polymer Science, Part A: Polymer Chemistry*, **2006**, 44, 532-538.

to the fact that the high density of cross-links prevents all motions and overshadows the sliding mobility in the topological network. For a given gel, the $\tan(\delta)$ transition shifts toward the lowest frequencies in DMSO as opposed to water. Indeed, in water, the network collapse increases the probability of intermolecular hydrogen bonding interactions between the α -CDs threaded along different PR chains while the larger swelling degree in DMSO results in a large network expansion and favours the hydrogen bonding interactions between the intra-PR α -CDs. Thus, for a given sliding gel at a fixed cross-linker fraction, the persistence length of the PR strands is higher in DMSO than in water, due to the formation of transient α -CD tubes, leading to a $\tan(\delta)$ peak shift toward the low frequencies.



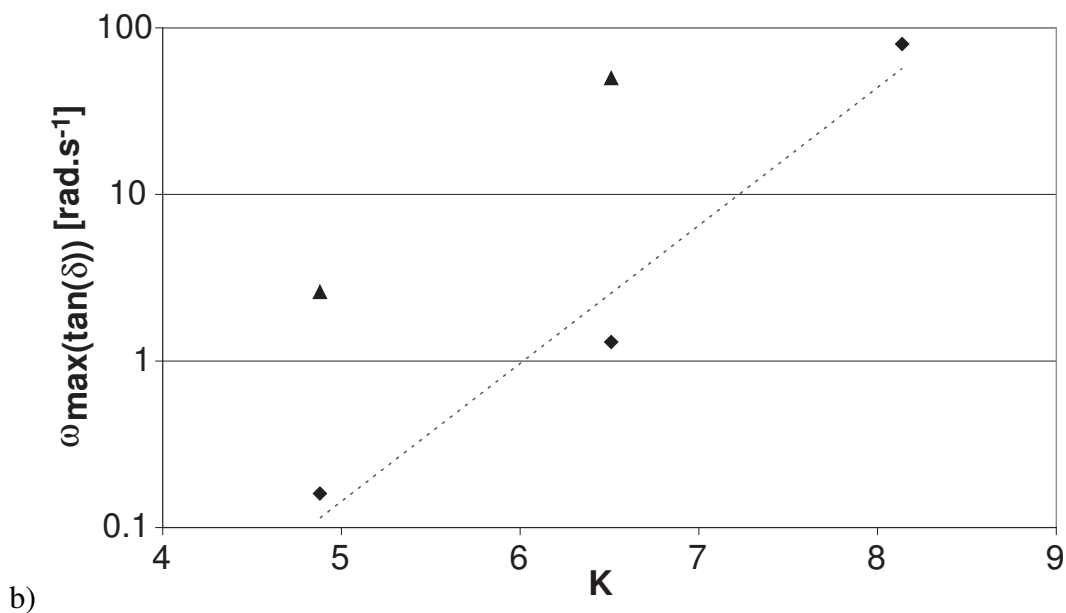


Figure 14. DMA: Evolution of $E'_{\max(\tan(\delta))}$ and $\omega_{\max(\tan(\delta))}$ for the G80Ry sliding gels:

a) $E'_{\max(\tan(\delta))}$ versus K: (◆) in DMSO and (▲) in water.

b) $\omega_{\max(\tan(\delta))}$ versus K: (◆) in DMSO and (▲) in water.

4.5. Conclusion

In summary the sliding gel molecular structure is complex and strongly influenced by three main parameters: the complexation degree N , the cross-linker fraction K and the swelling solvent interactions with the constitutive components of the sliding network. The SANS study reported in this paper has firmly established the heterogeneous structure in water of the sliding gels as previously observed by Karino *et al.*^[21] and recently reported by Shinohara *et al.*^[27] Aggregates of PR network strands are formed during the statistical cross-linking reaction in sodium hydroxide solution which mostly are promoted by the stacks of hydrogen bonded α -CDs. These aggregates are dispersed in a diluted network matrix. It was demonstrated that the presence of the heterogeneities is greatly dependent on the swelling solvent. In DMSO, a good solvent, the heterogeneities fade out rendering the gel more homogeneous and then the sliding cross-link points contribute mainly to the peculiar viscoelastic properties of the sliding gels. Thus, the sliding motion of the cross-link points along the template chain particularly at low frequencies in DMSO revealed the sliding characteristics of the topological networks. This sliding characteristic motion is a unique signature of the molecular dynamics encountered in topological polymer networks with sliding

[27] Y. Shinohara, K. Kayashima, Y. Okumura, C. Zhao, K. Ito and Y. Amemiya, *Macromolecules*, **2006**, 39, 7386-7391.

cross-link points. This sliding motion is expressed in the viscoelastic behaviour by weak viscous dissipation underlining the very effective relaxation mechanism on this new class of materials: the "sliding gels".

Annexe 4.a: Materials, polyrotaxane precursor synthesis and sliding gel formation

Materials

PEO with a number molecular weight of 20 kg mol^{-1} and a polydispersity of 1.05 was supplied by Serva Electrophoresis[®] and dried by an azeotropic distillation from toluene before use. α -CDs were purchased from Acros[®] and dried over phosphorus pentoxide under reduced pressure before use. 2,4-dinitro-1-fluorobenzene (DNFB) was purchased from Lancaster[®] and used as received. Triethylamine (from Lancaster[®]) was distilled over potassium hydroxide before use. DVS was purchased from Aldrich[®] and used as received. N,N-dimethylformamide (DMF) (from Fluka[®]) and DMSO (from Acros[®]) were distilled over potassium hydroxide before use. All other chemicals were purchased from Lancaster[®], Sigma[®] or Aldrich[®] and used as received.

Polyrotaxane precursor synthesis

Solutions of α -CD and BA-PEO in distilled water were mixed together in different ratios as reported in Table 3. After the complexation process, a white paste of α -CD/BA-PEO-based pseudo-polyrotaxanes was obtained. This paste was recovered by centrifugation (9000 rpm) and washed two times by distilled water in order to eliminate free α -CDs and unthreaded BA-PEO chains. This product was dried under reduced pressure and the dried pseudo-polyrotaxanes were then dispersed under nitrogen atmosphere at $25 \text{ }^\circ\text{C}$ in distilled DMF. DNFB and triethylamine were added in large excess and the solution was stirred at $25 \text{ }^\circ\text{C}$ during 24 h. The resulting PRs were precipitated in ether, washed three times with 100 mL ether and dried under reduced pressure at $30 \text{ }^\circ\text{C}$. To further eliminate the free α -CDs and the unthreaded polymer chains, the PRs were purified by dialysis with a membrane (cut-off of 16000 g mol^{-1}) in distilled water for three weeks. The product was dried, re-dissolved in DMSO, precipitated in ether, washed again three times with 100 mL ether and dried under reduced pressure at $30 \text{ }^\circ\text{C}$ for 48 h. The complexation degree N, defined as the average number of threaded α -CDs per template polymer chain, was determined for all PRs (Table 3) by $^1\text{H NMR}$ as previously described.^[7]

Sliding gel formation

Various gels were obtained by varying the amount of cross-linking agent (*i.e.* DVS) and the type of PR (Table 3). The PRs ($m_{\text{PR}} = 150 \text{ mg}$) were dissolved in 0.75 mL of a sodium hydroxide molar aqueous solution at 5 °C. The PR weight fraction in the pre-gel solution was also fixed at $\Phi = 0.15$. The cross-linking agent (typically $V = 40\text{-}100 \text{ }\mu\text{L}$) was dissolved in 0.2 mL of distilled water at 5° C. After the complete dissolution of the PRs, the cross-linker solution was added to the PR solution, which was vigorously mixed during a few seconds. The pre-gel solution was poured in a cylindrical shaped mould in order to obtain a piece of gel of a cylindrical form. After this step, the gel was carefully removed from the mould and washed by changing the water several times during a few days in order to eliminate the non-reacted cross-linker and PR precursors.

Table 3. Parameters for the synthesis and characterization of the sliding gels.

	PR			DVS		K #
	N ¶	m _{PR} [mg]	n _{PR} [mmol]	V [µL]	n _C [mmol]	
G22R70	22 ± 3	150	3.80 × 10 ⁻³	70	0.7	9.18
G45R40	45 ± 5	150	2.35 × 10 ⁻³	40	0.4	3.77
G45R50	45 ± 5	150	2.35 × 10 ⁻³	50	0.5	4.71
G45R60	45 ± 5	150	2.35 × 10 ⁻³	60	0.59	5.66
G45R70	45 ± 5	150	2.35 × 10 ⁻³	70	0.68	6.60
G45R80	45 ± 5	150	2.35 × 10 ⁻³	80	0.77	7.54
G45R100	45 ± 5	150	2.35 × 10 ⁻³	100	0.95	9.43
G60R50	60 ± 6	150	1.91 × 10 ⁻³	50	0.5	4.34
G60R60	60 ± 6	150	1.91 × 10 ⁻³	60	0.59	5.21
G60R70	60 ± 6	150	1.91 × 10 ⁻³	70	0.68	6.08
G60R80	60 ± 6	150	1.91 × 10 ⁻³	80	0.77	6.95
G60R100	60 ± 6	150	1.91 × 10 ⁻³	100	0.95	8.67
G67R50	67 ± 7	150	1.76 × 10 ⁻³	50	0.5	4.23
G67R60	67 ± 7	150	1.76 × 10 ⁻³	60	0.59	5.07
G67R70	67 ± 7	150	1.76 × 10 ⁻³	70	0.68	5.92
G67R80	67 ± 7	150	1.76 × 10 ⁻³	80	0.77	6.76
G67R100	67 ± 7	150	1.76 × 10 ⁻³	100	0.95	8.45
G70R45	70 ± 7	150	1.70 × 10 ⁻³	45	0.45	3.77
G70R50	70 ± 7	150	1.70 × 10 ⁻³	50	0.5	4.19
G70R70	70 ± 7	150	1.70 × 10 ⁻³	70	0.68	5.86
G70R100	70 ± 7	150	1.70 × 10 ⁻³	100	0.95	8.37
G80R40	80 ± 8	150	1.53 × 10 ⁻³	40	0.4	3.25
G80R50	80 ± 8	150	1.53 × 10 ⁻³	50	0.5	4.07
G80R60	80 ± 8	150	1.53 × 10 ⁻³	60	0.59	4.88
G80R70	80 ± 8	150	1.53 × 10 ⁻³	70	0.68	5.69
G80R80	80 ± 8	150	1.53 × 10 ⁻³	80	0.77	6.51
G80R100	80 ± 8	150	1.53 × 10 ⁻³	100	0.95	8.13
G90R70	90 ± 9	150	1.39 × 10 ⁻³	70	0.68	5.56

¶: defined as the average number of threaded α -CDs per template polymer chain determined by ¹H NMR

#: defined as n_C/n_{CD}

CHAPTER 5

Static and dynamic behaviour of polyrotaxanes in solution in dimethyl sulfoxide

In the previous chapter (**Chapter 4**), it was shown that chemical gels resulting from the inter- and intra-molecular cross-linking of threaded α -CDs do not contain well-organized nano-scale structures due to the fact that the cross-linking conditions are not that much controlled. On the contrary, neutron scattering exhibits micro-scale less-organized aggregates. Furthermore, rheological measurements carried out on chemical gels showed a particular mechanical behaviour in the case where the chemical gels are swollen in DMSO. It consists in the existence of a relaxation mode at low frequencies what is not observed when the chemical gels are swollen in water. This peculiar behaviour observed in DMSO can be reasonably interpreted in term of α -CD sliding along the PEO chains. Thus, such gels are called "sliding gels".

In the present chapter (**Chapter 5**), it is investigated whether the α -CD sliding property observed in chemical gels swollen in DMSO is also present in more simple systems such as PR solutions in the dilute regime in DMSO. A good solvent for α -CD/PEO-based PRs, DMSO, is chosen since it allowed to observe the α -CD sliding in the case of chemical gels, and the dilute regime is chosen so as to avoid the interactions between PR molecules which could lower the α -CD mobility. However, large PR aggregates with a characteristic size of 320-500 nm are found within PR solutions by static scattering measurements of light. The aggregates contain rod-like tubes corresponding to weakly stacked α -CDs along the PEO chains as found by static scattering measurements of neutrons, and remain in the mixtures even upon heating at 43 °C and diluting down to 0.02 w/w%. The presence of the aggregates hinders the observation by dynamic scattering measurements of light of an eventual α -CD sliding along the PEO chains, such a sliding was reported elsewhere for PRs in NaOH aqueous solution.^[A] However, in DMSO, the self-diffusion of large PR aggregates and the self-diffusion of almost independent PR molecules are observed by light scattering. Moreover, the relaxation mode relative to the threaded α -CDs, to the naked PEO segments or to both is also attributed.

[A] C. Zhao, Y. Domon, Y. Okumura, S. Okabe, M. Shibayama and K. Ito, *Journal of Physics: Condensed Matter*, **2005**, 17, S2841-S2846.

Static and dynamic behaviour of α -CD/PEO-based polyrotaxanes in dilute solution in dimethyl sulfoxide

Submitted to *Journal of Physics: Condensed Matter*

Abstract

Polyrotaxanes (PRs) based on α -cyclodextrins (α -CDs) and poly(ethylene oxide) (PEO) are usually considered to be well soluble in dimethyl sulfoxide (DMSO). However, large PR aggregates with a characteristic radius of $160 \text{ nm} \leq R \leq 250 \text{ nm}$ containing rod-like tubes corresponding to weakly stacked α -CDs along the PEO chains are found within PR solutions by static scattering measurements of radiations such as light and neutron. The aggregates remain in the mixtures even upon heating at $43 \text{ }^\circ\text{C}$ and diluting down to $0.02 \text{ w/w}\%$. The presence of the aggregates hinders the observation by dynamic light scattering (DLS) of an eventual α -CD sliding along the PEO chains, such a sliding was reported elsewhere for PRs in NaOH aqueous solution. However, in DMSO, the self-diffusion of large PR aggregates and the self-diffusion of almost independent PR molecules are observed by DLS. Moreover, the relaxation mode relative to the threaded α -CDs, to the naked PEO segments (*i.e.* the ethylene oxide units of the PEO chains which are not covered by α -CDs) or to both is also reasonably attributed.

5.1. Introduction

The term "polyrotaxane" (PR) designates a class of supramolecular structures consisting in ring molecules threaded onto polymer chains. The ends of the polymer chains are capped with steric stoppers to hinder dethreading of the ring molecules.^[1,2] One typical and widely studied PR type is made of α -cyclodextrins (α -CDs) and poly(ethylene oxide) (PEO).^[3] α -CDs consist in the repetition of 6 glucose units with a hollow truncated cone shape.^[4] The potential translational and rotational mobility of the α -CDs

[1] C. Gong and H. Gibson, *Current Opinion in Solid State and Materials Science*, **1997**, 2, 647-652.

[2] N. Yui and T. Ooya, *Journal of Artificial Organs*, **2004**, 7, 62-68.

[3] G. Wenz, B.-H. Han and A. Müller, *Chemical Reviews*, **2006**, 106, 782-817.

[4] S. Li and W. Purdy, *Chemical Reviews*, **1992**, 92, 1457-1470.

along the PEO chains confer new dynamical, physico-chemical and mechanical properties on the PRs. These macromolecules open the door to the realization of new functional materials such as molecular machines and shuttles.^[5,6] Nevertheless, the representation of PRs as supramolecules in which the α -CDs freely slide along the PEO chains is much too simplistic. Indeed, it ignores the numerous interactions that can develop between each component of PRs when put into solution in a given solvent. α -CD/PEO-based PRs are soluble in NaOH aqueous solution.^[7,8] In that solvent, the sliding of α -CDs along the PEO chains was observed by dynamic light scattering (DLS) with a typical decay time of 0.5 ms.^[9] Thus, it can be concluded that the dissociation state of PRs is enough for α -CD sliding to be observed. In the present paper, we study the behaviour of α -CD/PEO-based PRs in dimethyl sulfoxide (DMSO). Although DMSO is generally considered as a good solvent,^[7,8] an aggregative behaviour was reported at room temperature for concentrated PR solutions^[10] and also for solutions of PRs based on low molecular weight PEO.^[11] Static scattering of radiations such as light and neutron (static light scattering, SLS, and small-angle neutron scattering, SANS) is performed on PR solutions in DMSO(-d₆). We show that, even at high temperature, the PR solutions in DMSO contain large aggregates for all studied PR concentrations down to 0.02 w/w%. The presence of such PR aggregates hinders the observation by DLS of an eventual α -CD sliding along the PEO chains.

5.2. Experimental section

5.2.1. Material preparation and polyrotaxane synthesis

Material preparation and α -CD/PEO-based PR synthesis were carried out thanks to the procedure given in reference 12. α,ω -bis-carboxyl-terminated poly(ethylene oxide) was synthesized from commercial PEO with an average number molecular weight of 22 kg mol⁻¹ and a polydispersity of 1.03, equivalent PEO, as reported in reference 12.

[5] A. Harada, *Accounts of Chemical Research*, **2001**, 34, 456-464.

[6] H. Murakami, A. Kawabuchi, R. Matsumoto, T. Ido and N. Nakashima, *Journal of the American Chemical Society*, **2005**, 127, 15891-15899.

[7] A. Harada, J. Li, T. Nakamitsu and M. Kamachi, *Journal of Organic Chemistry*, **1993**, 58, 7524-7528.

[8] A. Harada, J. Li and M. Kamachi, *Journal of the American Chemical Society*, **1994**, 116, 3192-3196.

[9] C. Zhao, Y. Domon, Y. Okumura, S. Okabe, M. Shibayama and K. Ito, *Journal of Physics: Condensed Matter*, **2005**, 17, S2841-S2846.

[10] C. Travelet, G. Schlatter, P. Hébraud, C. Brochon, A. Lapp, D. Anokhin, D. Ivanov, C. Gaillard and G. Hadziioannou, *Soft Matter*, **2008**, 4, 1855-1860.

[11] J. Araki and K. Ito, *Polymer*, **2007**, 48, 7139-7144.

[12] J. Araki, C. Zhao and K. Ito, *Macromolecules*, **2005**, 38, 7524-7527.

1-aminoadamantane was used as steric stopper. PRs with well defined complexation degrees (N) (*i.e.* the number of threaded α -CDs per PEO chain) were obtained thanks to the methodology previously reported.^[13] In the following, the PRs are denoted PR_N where N is the complexation degree. All solutions were prepared with distilled DMSO(-d₆). The solutions were stirred at 43 °C or in a thermoregulated room at 21 °C during one week, then filtered through 0.45 μ m nylon filters and finally characterized.

5.2.2. Characterization methods

Static/Dynamic Light Scattering (SLS/DLS). Light scattering measurements were performed on a home-made apparatus equipped with an argon laser at a wavelength of 514 nm and a power of 100 mW. The cylindrical measurement cells (intern diameter = 13 mm) filled in with the PR solutions in DMSO were immersed in a toluene bath temperature regulated at 21 °C or 43 °C. The scattered photons were detected by a photomultiplier. In this study, the modulus of the scattering vector in light scattering experiments is denoted q and is equal to $(4\pi n/\lambda) \times \sin(\theta/2)$ where n represents the refractive index of pure DMSO, θ is the scattering angle and λ designates the used light wavelength in vacuum. In SLS measurements, the detection angle ranged between 20 ° and 150 ° by a step of 1 °. This corresponds to the q -range $6.3 \times 10^{-3} \text{ nm}^{-1} \leq q \leq 3.5 \times 10^{-2} \text{ nm}^{-1}$. The duration of each measuring point is equal to 2.5 min. The scattering intensity was corrected by taking into account the contributions of the measurement cell, the solvent and the toluene as well as the change of the scattering volume with the detection angle. In DLS measurements, the measured time-intensity correlation functions were processed using the Contin software package.^[14]

The refractive index increments of the constitutive parts of the PR molecules are found to be equal to $3.7 \times 10^{-4} \text{ w/w}\%^{-1}$ for PEO in DMSO and $5.3 \times 10^{-4} \text{ w/w}\%^{-1}$ for α -CD in DMSO. Thus, the components of the PR solutions scatter light in an equivalent way with a slight predominance of the signal originating from the α -CDs if making the hypothesis that the free α -CDs have the same scattering cross-section as the threaded ones. Contrary to 2,4-dinitro-1-fluorobenzene, the use of 1-aminoadamantane as steric stopper guarantees the obtention of PRs which are inactive in the visible light spectrum

[13] G. Fleury, C. Brochon, G. Schlatter, G. Bonnet, A. Lapp and G. Hadziioannou, *Soft Matter*, **2005**, 1, 378-385.

[14] S. Provencher, *Journal of Chemical Physics*, **1976**, 64, 2772-2777.

and thus particularly at the wavelength used in the light scattering experiments, *i.e.* 514 nm.

Small-angle Neutron Scattering (SANS). SANS measurements were performed on the LOQ spectrometer^[15] at the Rutherford Appleton Laboratory (RAL, ISIS, Didcot, Great Britain). In this study, the modulus of the scattering vector in SANS experiments is denoted q and is equal to $(4\pi/\lambda) \times \sin(\theta/2)$ where θ designates the observation angle and λ represents the wavelength of the used radiation. The global probed q -range was $9.0 \times 10^{-2} \text{ nm}^{-1} \leq q \leq 2.9 \text{ nm}^{-1}$. The PR solutions in deuterated DMSO (DMSO- d_6) were measured in 2 mm thick quartz Hellma[®] cells. DMSO- d_6 was used as the solvent during all of the experiments which were carried out at 21 °C. The signal was corrected by taking into account the contributions of the measurement cell, the solvent and the incoherent background in order to obtain the absolute scattering intensity.^[16]

5.3. Results and discussion

5.3.1. Static behaviour of polyrotaxanes in solution

DMSO is reported to be a good solvent for α -CD/PEO-based PRs.^[7,8] However, we will show that large aggregates exist within PR solutions in DMSO at 21 °C, *i.e.* 3 °C above the crystallization temperature of pure DMSO. For this, we studied in detail PR₃₇ solutions at different concentrations in DMSO and carried out SLS experiments at concentrations between 0.02 w/w% and 3 w/w%. Measurements at higher concentrations were impossible due to strong scattering of the solutions. At 3 w/w%, measurements were not possible at the lowest q -values due to a saturation of the photomultiplier. In order to have access to a more extended q -range and thus to get more information about the morphology of the present aggregates, SANS measurements were complementarily carried out on the PR₃₇ solutions at 21 °C. In that way, a global q -range from $6.3 \times 10^{-3} \text{ nm}^{-1}$ up to 2.9 nm^{-1} is reached. However, experimental points at q -values ranging from $3.5 \times 10^{-2} \text{ nm}^{-1}$ up to $9.0 \times 10^{-2} \text{ nm}^{-1}$ are lacking since the q -ranges accessible by SLS and SANS do not overlap.

[15] <http://www.isis.rl.ac.uk/largescale/LOQ/loq.htm>.

[16] A. Brûlet, D. Lairez, A. Lapp and J.-P. Cotton, *Journal of Applied Crystallography*, **2007**, 40, 165-177.

For intermediate q -values between $1.0 \times 10^{-2} \text{ nm}^{-1}$ and $2.0 \times 10^{-1} \text{ nm}^{-1}$, both SLS and SANS intensities exhibit at $21 \text{ }^\circ\text{C}$ a q^{-2} behaviour for all studied PR_{37} concentrations (Figure 1a). Furthermore, the scattering intensity globally increases with increasing PR_{37} concentration at any given probed q -value as shown at $q = 2.5 \times 10^{-2} \text{ nm}^{-1}$ (Figure 2). A power-law behaviour of the scattering intensity as a function of the PR_{37} concentration is approximately obtained and we have $I(q = 2.5 \times 10^{-2} \text{ nm}^{-1}) = I_{21 \text{ }^\circ\text{C}} \times C^\beta = (9.27 \pm 4.64) \times C^{1.20 \pm 0.33}$. This almost power-law increase of the scattering intensity with the PR_{37} concentration characterized by a positive power value close to one shows that the overlap concentration of PR_{37} is not reached, even at 3 w/w%, and that an increase of the concentration simply increases the number of non-interacting aggregates. We thus observe a Gaussian organization of smaller structures that may be revealed by considering higher q -values. For the higher q -values, SANS exhibits an intensity decrease as q^{-1} for all studied PR_{37} concentrations (Figure 1a). Furthermore, it should be noticed that a mixture at 13.8 w/w% was also measured by SANS (Figure 1a). A profile different from those obtained at lower concentrations was registered, which one exhibits a strong structural peak at $q = 2.5 \times 10^{-1} \text{ nm}^{-1}$. Such a higher concentration, engendering the formation of structural peaks, was previously studied.^[10] Whatever in solution or in the solid state, association is known to occur between α -CDs threaded onto polymer chains under the form of rod-like tubes corresponding to weakly stacked α -CDs along the polymer chains.^[13,17,18,19,20,21] Thus, since α -CDs are as much observed by SANS as naked PEO segments (*i.e.* the ethylene oxide units of the PEO chains which are not covered by α -CDs) in DMSO- d_6 (Annexe 3.2.a), the observed q^{-1} behaviour of the scattering intensity at the highest q -values is due to the presence of rod-like tubes which are organized at a higher length-scale within the aggregates in a Gaussian way as shown by the q^{-2} behaviour observed at lower q -values. At low q -values, the slope of the scattering intensity changes from -2 to almost 0 (Figure 1b). Thus, for q -values smaller than $q_0 = (1.0 \pm 0.2) \times 10^{-2} \text{ nm}^{-1}$, the PR_{37} solutions can be considered as homogeneous. Furthermore, the radius R of the non-interacting aggregates can be estimated using the following Gaussian model which gives the scattering intensity $I(q)$:

[17] A. Tonelli, *Macromolecules*, **2008**, 41, 4058-4060.

[18] T. Girardeau, T. Zhao, J. Leisen, H. Beckham and D. Bucknall, *Macromolecules*, **2005**, 38, 2261-2270.

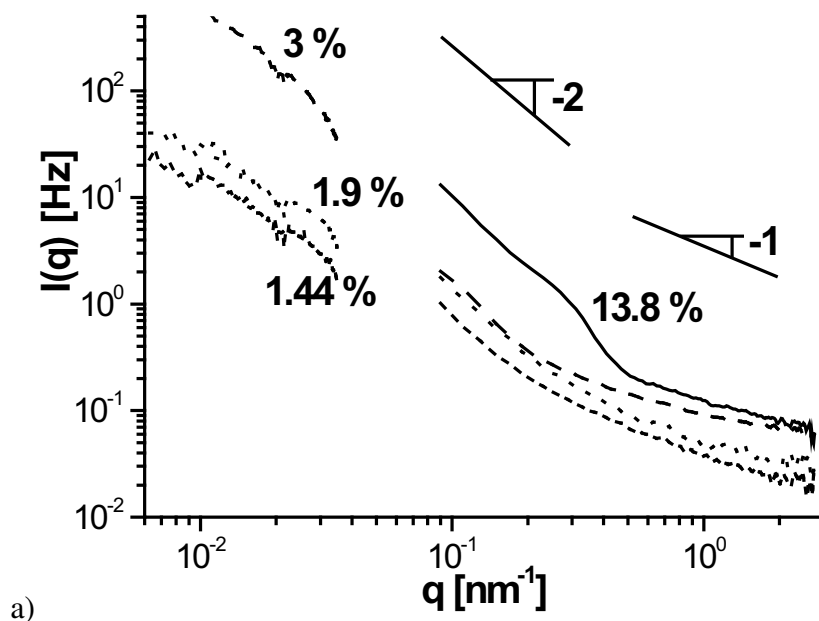
[19] P. Lo Nostro, L. Giustini, E. Fratini, B. Ninham, F. Ridi and P. Baglioni, *Journal of Physical Chemistry B*, **2008**, 112, 1071-1081.

[20] I. Topchieva, A. Tonelli, I. Panova, E. Matuchina, F. Kalashnikov, V. Gerasimov, C. Rusa, M. Rusa and M. Hunt, *Langmuir*, **2004**, 20, 9036-9043.

[21] J. Chung, T. Kang and S.-Y. Kwak, *Macromolecules*, **2007**, 40, 4225-4234.

$$I(q) = AS(q)P(q) \approx A \frac{2[\exp(-q^2 R^2) + q^2 R^2 - 1]}{q^4 R^4} \quad (1)$$

Where A designates a constant, S represents the structure factor and P designates the form factor of the aggregates. Since the aggregates are non-interacting, we have $S(q) \approx 1$. The fitting of the experimental data obtained at 21 °C, corresponding to different PR₃₇ concentrations ranging from 0.02 w/w% to 1.9 w/w%, gives an aggregate characteristic radius of $160 \text{ nm} \leq R \leq 250 \text{ nm}$, even in the most dilute solution at 0.02 w/w%. The origin of such large aggregates may be due, on the one hand, to crystallization of the naked PEO segments and, on the other hand, to α -CD aggregation driven by intra- and inter-molecular hydrogen bonding interactions between the α -CD hydroxyl groups.^[10]



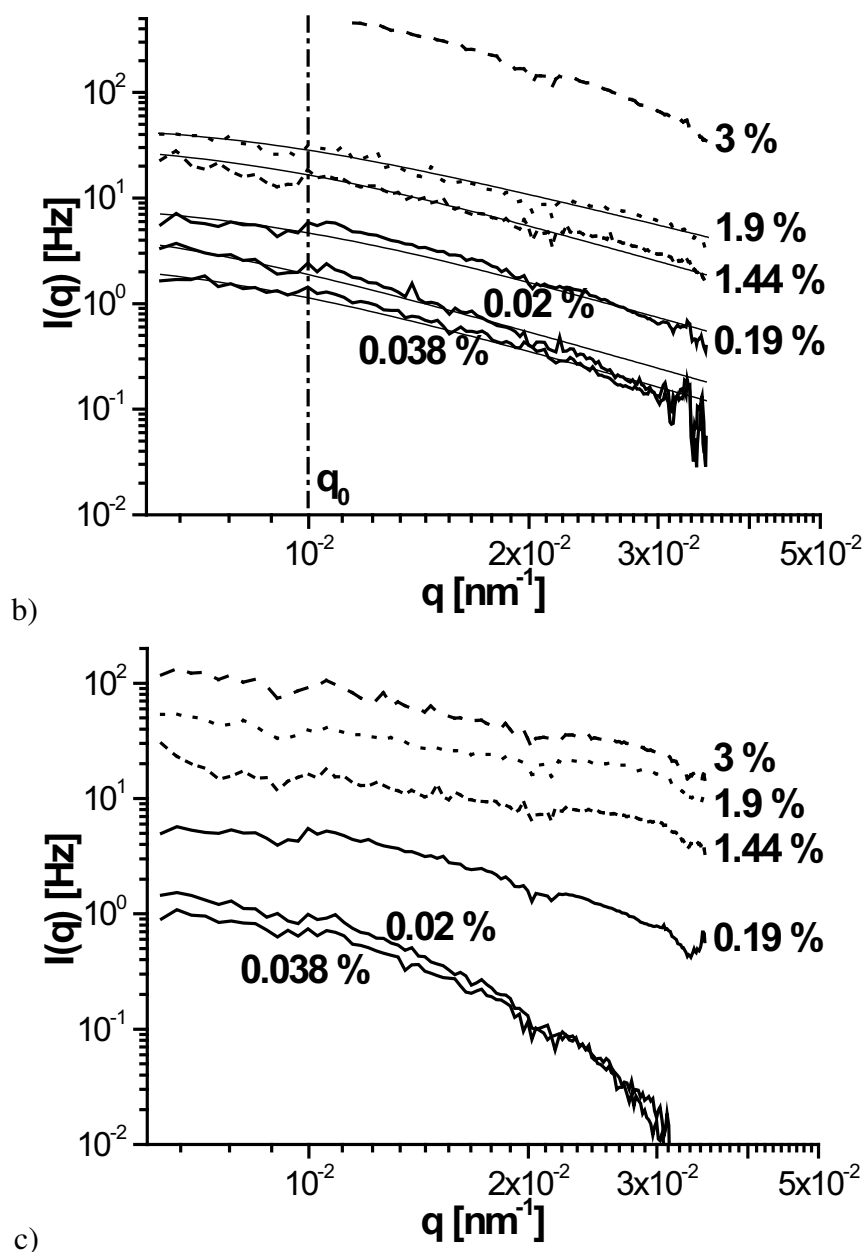


Figure 1. SLS and SANS: Scattering intensity $I(q)$ versus modulus of the scattering vector q for PR₃₇ solutions in DMSO(-d₆): a) $I(q)$ at 21 °C: 1.44 w/w%, 1.9 w/w%, 3 w/w% obtained by SLS and SANS, and 13.8 w/w% obtained by SANS only. b) $I(q)$ at 21 °C: 0.02 w/w%, 0.038 w/w%, 0.19 w/w%, 1.44 w/w%, 1.9 w/w%, 3 w/w% obtained by SLS only. The thin solid lines correspond to the fits obtained with equation (1). c) $I(q)$ at 43 °C: 0.02 w/w%, 0.038 w/w%, 0.19 w/w%, 1.44 w/w%, 1.9 w/w% and 3 w/w% obtained by SLS.

Now, the question is to know if heating the PR₃₇ solutions allows to reduce drastically the size or the number of aggregates. For this, SLS measurements were performed at 43 °C. The scattering intensity is much less q dependent than at low temperature, particularly at high concentration (Figure 1c). The fact that the curves are smoother

indicates the presence of a more homogeneous mixture. Moreover, the scattering intensity increases with increasing PR₃₇ concentration at any given probed q -value, as shown at $q = 2.5 \times 10^{-2} \text{ nm}^{-1}$ (Figure 2), what indicates that the overlap concentration of PR₃₇ is not reached at 43 °C, even at 3 w/w%. A power-law behaviour is obtained and we have $I(q = 2.5 \times 10^{-2} \text{ nm}^{-1}) = I_{43 \text{ °C}} \times C^\gamma = (4.38 \pm 1.97) \times C^{1.28 \pm 0.25}$. The power-law behaviours of the scattering intensity as a function of the PR₃₇ concentration at 21 °C and 43 °C lead to the same power value $\beta \approx \gamma$. Moreover, since the value of $I_{21 \text{ °C}}$ is higher than that of $I_{43 \text{ °C}}$, the intensity scattered at 43 °C is lower than that scattered at 21 °C. Consequently, at 43 °C, the PR₃₇ solutions are more homogeneous and the aggregates are less numerous than at 21 °C.

Thus, in order to have a better comprehension of the dynamic behaviour of PRs in solution, we performed DLS experiments at 43 °C, *i.e.* in the most dissociated state. Indeed, at 21 °C, we observed that huge fluctuations of the intensity did not allow us to compute properly the time-intensity correlation functions of the scattering intensity.

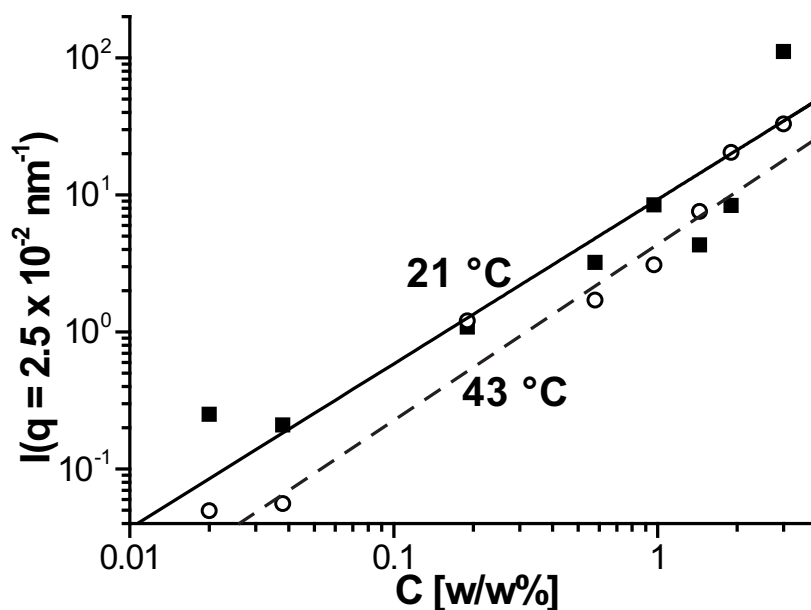


Figure 2. SLS: Scattering intensity $I(q = 2.5 \times 10^{-2} \text{ nm}^{-1})$ versus PR concentration C for PR₃₇ solutions in DMSO: (■) at 21 °C and (○) at 43 °C.

5.3.2. Dynamic behaviour of polyrotaxanes in solution

DLS measurements were performed on 0.75 w/w% solutions of PR₃₇, PR₉₃ and PR₁₂₉ in DMSO at 43 °C. After treatment of the time-intensity correlation functions (Figure 3a) using the Contin software package,^[14] three main decay times Γ^{-1}_1 , Γ^{-1}_2 and Γ^{-1}_3 ($\Gamma^{-1}_1 > \Gamma^{-1}_2 > \Gamma^{-1}_3$) are obtained from the maxima of the decay time distribution

functions (Figure 3b). Considering all of the studied samples, at $\theta = 90^\circ$ (Table 1), we have typically $\Gamma^{-1}_1 = 2.6$ ms, $\Gamma^{-1}_2 = 0.18$ ms and $\Gamma^{-1}_3 = 0.02$ ms.

Table 1. DLS: Decay times Γ^{-1}_i for PR_N at 0.75 w/w% in DMSO at 43 °C at $\theta = 90^\circ$.

PR_N	Γ^{-1}_1 [ms]	Γ^{-1}_2 [ms]	Γ^{-1}_3 [ms]
PR_{37}	2.55	0.178	0.0269
PR_{93}	2.73	0.166	0.00762
PR_{129}	2.55	0.205	0.0234

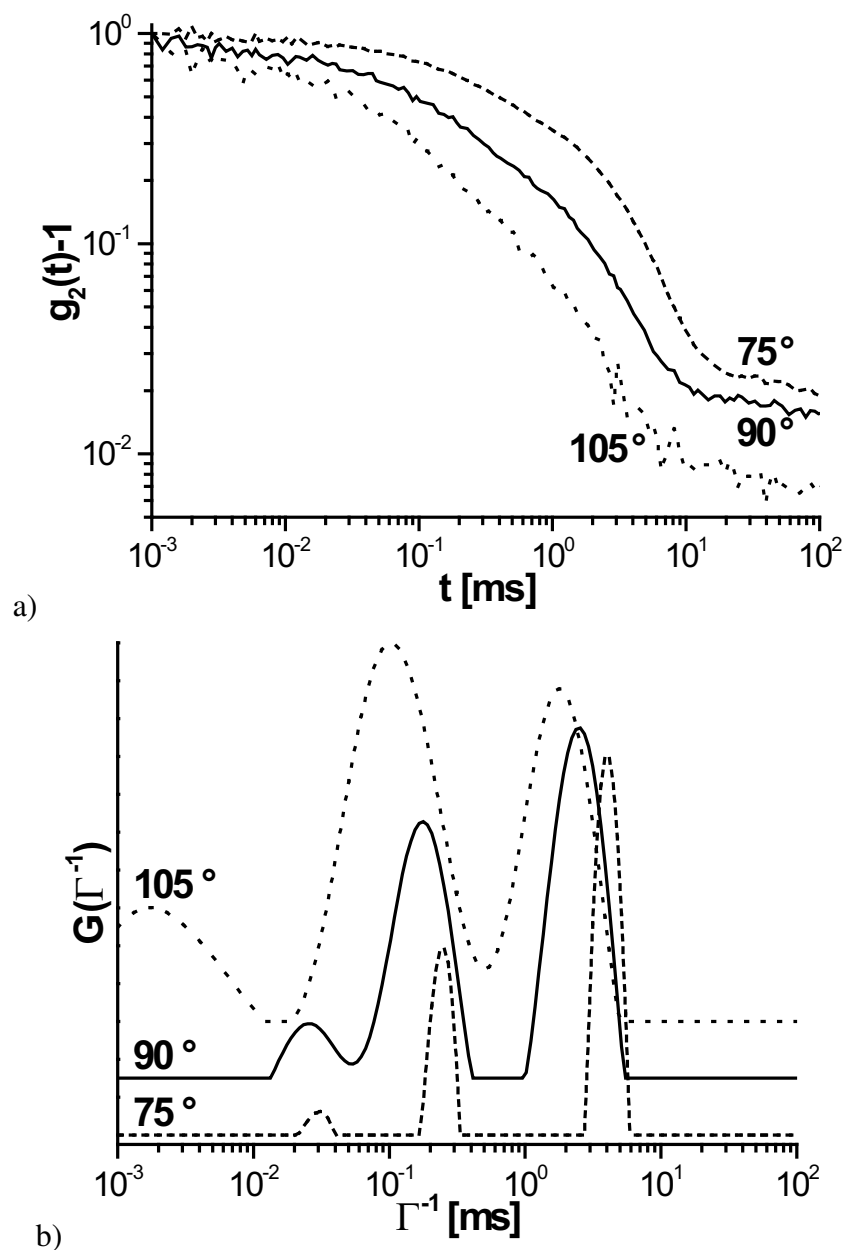


Figure 3. DLS: a) Time-intensity correlation function $g_2(t)-1$ and b) decay time distribution function $G(\Gamma^{-1})$ for PR_{37} at 0.75 w/w% in DMSO at 43 °C at $\theta = 75^\circ, 90^\circ$ and 105° .

As far as concerns α -CD/PEO-based PRs in NaOH aqueous solution, it was also reported that three decay times were observed at concentrations ranging from 2.5 w/w% to 10 w/w%.^[9] The three decay times were assigned to the self-diffusion mode for the highest Γ^{-1} -value, to the sliding mode of α -CDs for the intermediate Γ^{-1} -value and to the cooperative mode for the lowest Γ^{-1} -value.^[9] In reference 9, the experiments were performed at a fixed observation angle and the diffusive character of the observed modes was thus not proven. Furthermore, the associative or non-associative character of PR in NaOH aqueous solution was not deeply discussed. In DMSO, the hypothesis that PR molecules do not interact together cannot be made even at 43 °C as shown by SLS in section 5.3.1. Such interactions between PR molecules in DMSO may hinder the sliding of α -CDs observed in the PR mixtures in NaOH aqueous solution. Presently, angle dependence measurements were carried out on each sample, so that the three obtained decay times reveal for most of the studied samples a q^{-2} behaviour (Figure 4), indicating that the observed modes are diffusive. Consequently, the observed modes cannot be assigned to transient aggregation between PR molecules. Indeed, such modes are expected to be independent of q .^[22] Thus, the observed modes cannot consist in transient sticking between threaded α -CDs *via* their hydroxyl groups, or between naked PEO segments, or between threaded α -CDs and naked PEO segments (this interaction type was observed in blend for other polysaccharide/PEO mixtures^[23]). Furthermore, the modes cannot be attributed either to transient sticking between steric stoppers (this interaction type was observed in solution for other PEO end groups^[24,25,26]). For PR₃₇ at 0.75 w/w% in DMSO at 43 °C, at $\theta = 90^\circ$, we have $\Gamma^{-1}_1 = 2.55$ ms, $\Gamma^{-1}_2 = 0.178$ ms and $\Gamma^{-1}_3 = 0.0269$ ms. Knowing that:^[27,28]

$$\Gamma^{-1}_i = \frac{1}{D_i q^2} \quad (2)$$

Where D_i represents the diffusion coefficient, we obtain $D_1 = 0.60 \mu\text{m}^2 \text{s}^{-1}$, $D_2 = 8.6 \mu\text{m}^2 \text{s}^{-1}$ and $D_3 = 57 \mu\text{m}^2 \text{s}^{-1}$. From each diffusion coefficient D_i , the

[22] E. Michel, L. Cipelletti, E. d'Humières, Y. Gambin, W. Urbach, G. Porte and J. Appell, *Physical Review E: Statistical, Nonlinear and Soft Matter Physics*, **2002**, 66, 031402-1-031402-7.

[23] T. Kondo, C. Sawatari, R. Manley and D. Gray, *Macromolecules*, **1994**, 27, 210-215.

[24] E. Alami, M. Almgren, W. Brown and J. François, *Macromolecules*, **1996**, 29, 2229-2243.

[25] O. Vorobyova, A. Yekta, M. Winnik and W. Lau, *Macromolecules*, **1998**, 31, 8998-9007.

[26] F. Laffèche, D. Durand and T. Nicolai, *Macromolecules*, **2003**, 36, 1331-1340.

[27] B. Berne and R. Pecora, *Dynamic Light Scattering with Applications to Chemistry, Biology and Physics*, Wiley, New York (USA), **1976**.

[28] K.-F. Arndt and G. Müller, *Polymercharakterisierung*, Hanser, Munich (Germany), **1996** (in German).

Stokes-Einstein equation gives the hydrodynamic diameter D_{hi} of the fictive corresponding hard sphere.^[29] The viscosity of DMSO was measured at 43 °C and found to be equal to 1.45×10^{-3} Pa s. Thus, we have $D_{h1} = 420$ nm, $D_{h2} = 29$ nm and $D_{h3} = 4.4$ nm. These values estimated for PR₃₇ are the same as those obtained for PR₉₃ and PR₁₂₉ as shown by the quasi-constant decay times with N (Table 1). The characteristic dimensions of the studied system are a typical diameter of 1 nm for the unique α -CD,^[30] and a typical diameter larger than 8 nm for the whole PR molecule (more than twice the gyration radius of the PEO chain obtained by calculation^[31]). Since the hydrodynamic diameter $D_{h1} \approx 2R$ (where R is the aggregate radius previously obtained at 21 °C with equation (1)), the decay time Γ^{-1}_1 is attributed to the self-diffusion mode of large PR aggregates. Thus, it seems that all the aggregates observed at 21 °C are not broken upon heating as discussed in section 5.3.1. D_{h2} is in the order of magnitude of the characteristic size of a PR molecule, the decay time Γ^{-1}_2 is thus attributed to the self-diffusion mode of almost independent PR molecules. D_{h3} corresponds to the length of few monomers, the decay time Γ^{-1}_3 is thus reasonably attributed to the relaxation mode of the chains.^[32] However, it is not possible to determine whether the relaxation mode is relative to the threaded α -CDs, to the naked PEO segments or to both.

[29] G. Strobl, *The Physics of Polymers: Concepts for Understanding their Structures and Behavior*, Springer, Berlin (Germany), **1996**.

[30] J. Szejtli, *Chemical Reviews*, **1998**, 98, 1743-1753.

[31] Considering the 22 kg mol^{-1} PEO chains as chains in Θ -solvent conditions, the gyration radius is given by $R_g = 499^{0.5} \times 0.44 / 6^{0.5} = 4.0$ nm.

[32] M. Doi and S. Edwards, *The Theory of Polymer Dynamics*, Clarendon, Oxford (Great Britain), **1986**.

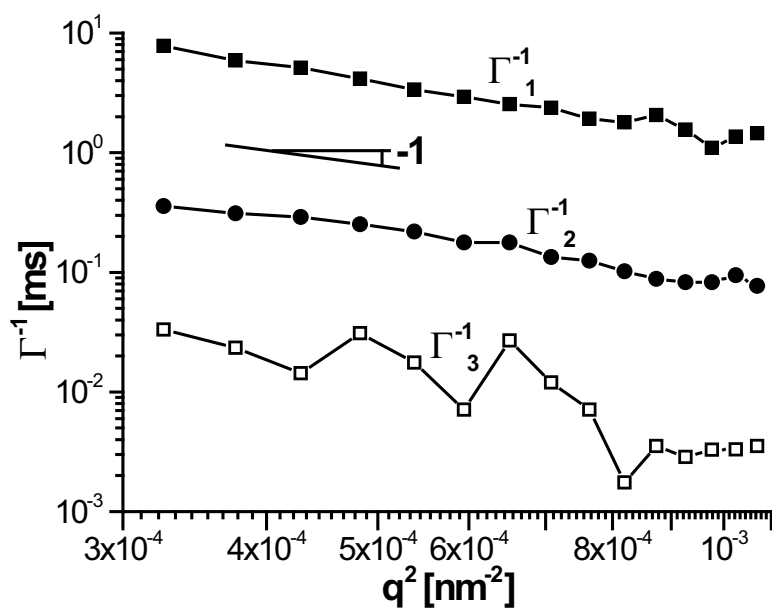


Figure 4. DLS: Decay times Γ^{-1} , Γ^{-2} and Γ^{-3} versus q^2 for PR₃₇ at 0.75 w/w% in DMSO at 43 °C.

5.4. Conclusion

α -CD/PEO-based PRs are known to be soluble in DMSO. However, large PR aggregates with a characteristic radius of $160 \text{ nm} \leq R \leq 250 \text{ nm}$ containing rod-like tubes corresponding to weakly stacked α -CDs along the PEO chains are found by SLS and SANS measurements within PR solutions. The aggregates remain in the mixtures even upon heating at 43 °C and diluting down to 0.02 w/w%. The presence of the aggregates hinders the observation by DLS of an eventual α -CD sliding along the PEO chains, such a sliding was reported elsewhere for PRs in NaOH aqueous solution.^[9] However, in DMSO, the self-diffusion of large PR aggregates and the self-diffusion of almost independent PR molecules are observed by DLS. Moreover, the relaxation mode relative to the threaded α -CDs, to the naked PEO segments or to both is also reasonably attributed.

GENERAL CONCLUSION AND PERSPECTIVES

"Il faut bien quitter l'amour un jour, pour peu qu'on vieillisse, et ce jour doit être celui où il cesse de nous rendre heureux. Enfin, songeons à cultiver le goût de l'étude, ce goût qui ne fait dépendre notre bonheur que de nous-mêmes. Préservons-nous de l'ambition, et surtout sachons bien ce que nous voulons être ; décidons-nous sur la route que nous voulons prendre pour passer notre vie, et tâchons de la semer de fleurs."

Madame du Châtelet (1706 - 1749), Discours sur le bonheur

General conclusion

In the present PhD work, we studied the threading process between α -cyclodextrins (α -CDs) and poly(ethylene oxide) (PEO) in water, thus leading to the formation of inclusion complexes called pseudo-polyrotaxanes (PPRs) (Figure 1) (**Chapter 2**).

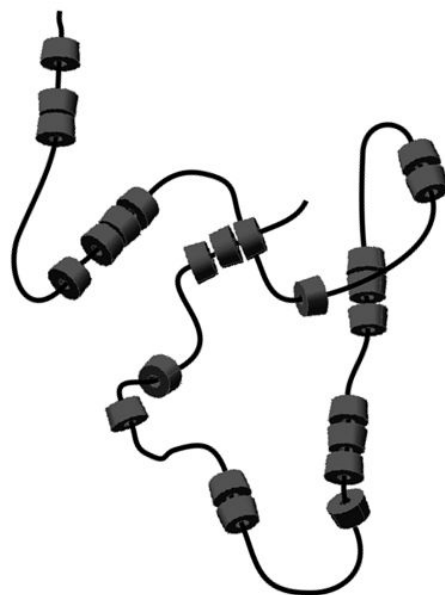


Figure 1. Schematic representation of a PPR molecule showing α -CD rod-like tubes and naked PEO segments

The nanostructures resulting from the self-organization of PPRs were also investigated *in situ*. Starting from a liquid α -CD/PEO mixture in water at a typical total mass fraction of 15 w/w% at 70 °C, the formation of PPRs with time at a lower temperature (typically in the range from 5 °C to 30 °C) induces a white physical gel with time and phase

separation was observed. We established that PPR molecules are exclusively found in the precipitated phase although unthreaded α -CD molecules and unthreaded PEO chains are in the liquid phase. At 30 °C, the physical gel formation is much slower than at 5 °C. At 30 °C, we established that, in a first step, α -CDs thread onto PEO chains, forming PPR molecules (Figure 1) which are not in good solvent conditions in water. At a higher length-scale, rapid aggregation of the PPR molecules occurs and threaded α -CD-based nano-cylinders form (cylinder length $L = 5.7$ nm and cylinder radius $R = 4.7$ nm) (Figure 2a). At a higher length-scale, α -CD-based nano-cylinders associate in a Gaussian way (Figure 2b) engendering the formation of precipitated domains which are responsible for the high turbidity of the studied system. At the end of this first step (*i.e.* after 20 min), the system still remains liquid and the PPRs are totally formed. Then, in a second step (*i.e.* after 150 min), the system undergoes its reorganization characterized by a compacity increase of the precipitated domains and forms a physical gel.

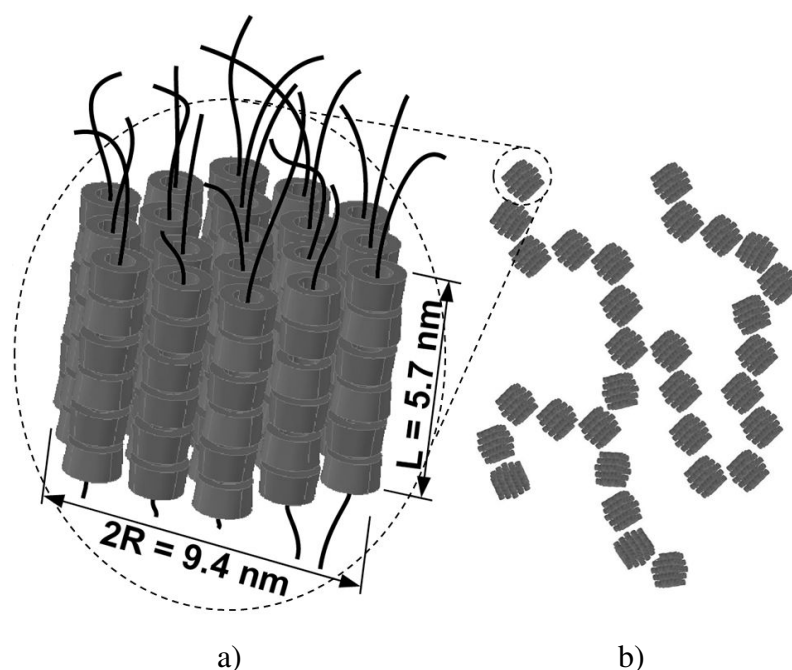


Figure 2. Schematic representation of: a) a threaded α -CD-based nano-cylinder and b) threaded α -CD-based nano-cylinders associated in a Gaussian way (for clarity reason, free α -CDs and naked PEO segments, which connect the nano-cylinders, are not shown in this view).

Then, we investigated polyrotaxanes (PRs), *i.e.* end-capped α -CD/PEO-based PPRs, in concentrated solution in dimethyl sulfoxide (DMSO) and established that they have the particularity to form physical gels with time when resting at room temperature

(typically 21 °C) (**Chapter 3**). The molecular origin of the self-organization is, on the one hand, the crystallization of naked PEO segments (*i.e.* the ethylene oxide units of the PEO chains which are not covered by α -CDs) (Figure 3) and, on the other hand, the regular aggregation of threaded α -CDs driven by intra- and inter-molecular hydrogen bonding interactions of their hydroxyl groups (Figure 3). The first contribution to the physical gel cohesion dominates at low complexation degree (*i.e.* the number of threaded α -CDs per PEO chain) value whereas the second one is present at high complexation degree value.

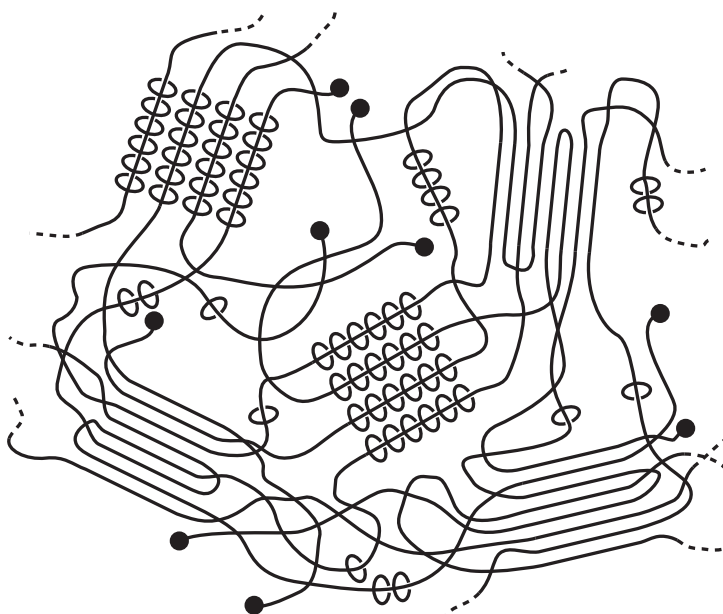


Figure 3. Schematic view of the PR physical gel showing the two kinds of cross-linked domains: the crystals of naked PEO segments and the well-organized α -CD aggregates more or less swollen in DMSO. The physical cross-linked domains are separated by amorphous domains made of non-aggregated rotaxane or naked PEO blocks immersed in DMSO.

Then, we studied chemical gels obtained by cross-linking PRs *via* their α -CDs in an inter- and intra-molecular way (**Chapter 4**). The chemical intramolecular cross-linking leads to the formation of rod-like tubes corresponding to stacked α -CDs along the PEO chains whereas the chemical intermolecular cross-linking engenders the 3D network formation. The chemical cross-linking reaction with divinyl sulfone (DVS) does not occur in soft conditions so that highly cross-linked domains cohabit with less cross-linked ones (Figure 4). The gels swell in water and DMSO, and were found to be more heterogeneous in water. In DMSO, the gels have weak viscous dissipation at low frequencies underlining a very effective relaxation mechanism. From the existence of a

relaxation mode at low frequencies, we can reasonably conclude that chemical gels swollen in DMSO possess sliding cross-link points, *i.e.* α -CDs can slide along the PEO chains. They are thus called "sliding gels". This behaviour was not observed in water since in that swelling solvent the number of physical cross-link points increases drastically compared to DMSO, hindering the sliding.

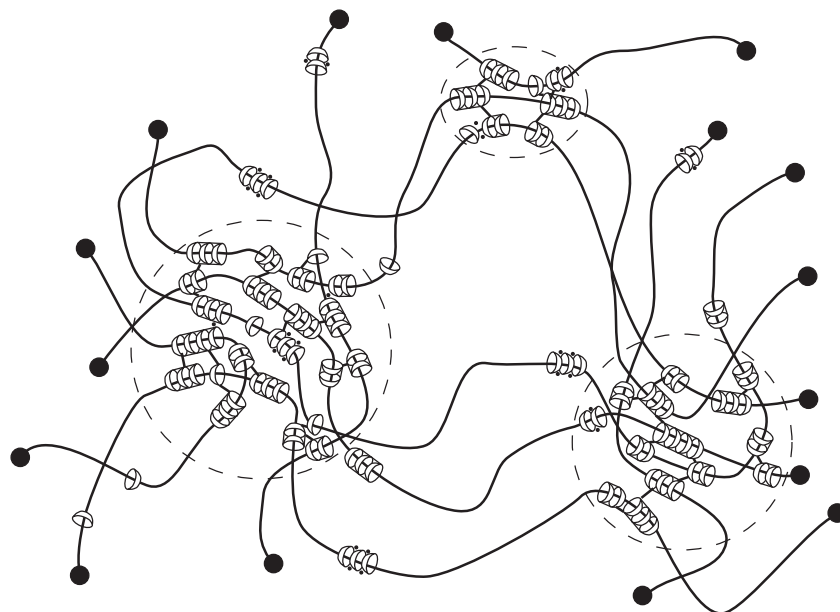


Figure 4. Schematic view of the swollen PR chemical gel showing structural heterogeneities, in the circumstances domains more cross-linked than other ones.

To finish, we investigated whether the α -CD sliding along the PEO chains can be observed in PRs in dilute solution in DMSO (**Chapter 5**). DMSO is usually considered to be a good solvent for α -CD/PEO-based PRs, and thus should lower the weak intra- and inter-molecular PR interactions and favour the α -CD sliding. However, large PR aggregates with a characteristic size of 320-500 nm containing rod-like tubes corresponding to weakly stacked α -CDs along the PEO chains were found within PR solutions even upon heating at 43 °C and diluting down to 0.02 w/w%. The presence of the aggregates hinders the observation of an eventual α -CD sliding along the PEO chains. Such a sliding was reported elsewhere for PRs in NaOH aqueous solution.^[A] However, in DMSO, the self-diffusion of large PR aggregates and the self-diffusion of almost independent PR molecules were observed. Moreover, the relaxation mode

[A] C. Zhao, Y. Domon, Y. Okumura, S. Okabe, M. Shibayama and K. Ito, *Journal of Physics: Condensed Matter*, **2005**, 17, S2841-S2846.

relative to the threaded α -CDs, to the naked PEO segments or to both was also attributed.

Among the three main types of system studied along the present PhD work, *i.e.* PPRs as physical gel in water, PRs as physical gel in DMSO and PRs as chemical gel in water or DMSO, we observed different types of association using various characterization methods principally based on radiation scattering. The less organized system is indubitably the PR-based chemical gel. It contains micro-scale aggregates based on α -CDs what is inherent to the used chemical gel formation procedure. The PPR-based physical gel in water, and particularly the one formed at 30 °C, was deeply studied and exhibits as for him well-organized structures made of threaded α -CDs. The PR-based physical gel in DMSO contains also well-organized structures. However, they consist of naked PEO segment crystallites surrounded by aggregated threaded α -CDs.

Perspectives

The image of PRs as pearl necklaces is very simplistic and does not take into account the diversity of interactions that occur between α -CDs and between naked PEO segments, leading to physical gel or aggregate formation, depending on the PR concentration. This is the same for PPRs whose organization is considerably influenced by such interactions. Perspectives for further work consist in reaching non-interacting pearl necklaces in which neither the pearls nor the necklaces interact together. It necessitates to chemically modify the α -CDs and the PEO, and/or to find a more adequate solvent, what would open the door to interesting dynamic systems. Basic water may be such a solvent.

Moreover, during the PPR formation and self-organization in water at 30 °C, we found that PPRs are totally formed after 20 min and that the system stays in a non-gel state up to 150 min. This opens perspectives regarding the PPR chemical modification: between these two characteristic times, we can easily envisage an efficient end-capping reaction leading to the synthesis of PRs or generally speaking an *in situ* chemical modification of the PPR molecules in water.

Other perspectives consist in better controlling the structure of the chemical gels based on PRs by controlling the dissociation state of PRs prior to cross-linking and the cross-linking reaction between α -CDs itself. As far as concerns the cross-linking reaction with DVS, this cross-linker is found to be soluble in water but not in NaOH aqueous solution which is the medium where the cross-linking with PR molecules

effectively occurs. It leads thus to the formation of micro-scale heterogeneities in the final gel.

The use of 1,1'-carbonyldiimidazole as cross-linker^[B,C] does not seem to be the ideal solution. Although it leads to the gel formation in typically one day upon heating (at 70-80 °C) or in typically one month at room temperature, a high amount of cross-linker is needed for cross-linking to occur ($m_{1,1'\text{-carbonyldiimidazole}} \approx m_{\text{PR}}$). The dissociation state of PRs, a crucial parameter regarding the final gel homogeneity, is thus not guaranteed. Indeed, the homogeneous mixture 1,1'-carbonyldiimidazole/DMSO plays the role of solvent instead of DMSO. However, considering the transparency to the eye of the obtained gel, a softer cross-linking reaction seems to be achieved with 1,1'-carbonyldiimidazole.

In order to better control the cross-linking reaction of PRs, the following procedure was studied during the present PhD work. Instead of using a low molecular weight cross-linker molecule whose compatibility (and particularly solubility) with the PR/DMSO mixture is not guaranteed, synthons were chosen and grafted onto the PR molecules. The following synthons were synthesized:

- 2-(2-azidoethoxy)ethyl-4-methylbenzenesulfonate which is an azide/tosyl derivative,
- prop-2-ynyl-2-bromoacetate which is an alkyne/bromide derivative.

Certain steps used for the synthesis of both synthons were taken from reference D. Then, the synthons were separately grafted onto the PR molecules *via* their tosyl and their bromide extremities, reacting with deprotonated hydroxyl groups of the threaded α -CDs. To finish, the side chain and more precisely the hanging functional groups (azide and alkyne) are covalently linked together *via* a click chemistry reaction (*i.e.* a variation of the Huisgen 1,3-dipolar cycloaddition reaction).^[E,F,G,H,I]

However, such a procedure could not be successfully achieved probably due to the difficulty to properly graft small amount of synthons onto the PR molecules. Indeed, the

[B] T. Sakai, H. Murayama, S. Nagano, Y. Takeoka, M. Kidowaki, K. Ito and T. Seki, *Advanced Materials*, **2007**, 19, 2023-2025.

[C] K. Karaky, C. Brochon, G. Schlatter and G. Hadziioannou, *Soft Matter*, **2008**, 4, 1165-1168.

[D] W. Agut, D. Taton and S. Lecommandoux, *Macromolecules*, **2007**, 40, 5653-5661.

[E] D. Fournier, R. Hoogenboom and U. Schubert, *Chemical Society Reviews*, **2007**, 36, 1369-1380.

[F] J. Moses and A. Moorhouse, *Chemical Society Reviews*, **2007**, 36, 1249-1262.

[G] W. Binder and R. Sachsenhofer, *Macromolecular Rapid Communications*, **2008**, 29, 952-981.

[H] W. Binder and R. Sachsenhofer, *Macromolecular Rapid Communications*, **2007**, 28, 15-54.

[I] P. Lecomte, R. Riva, C. Jérôme and R. Jérôme, *Macromolecular Rapid Communications*, **2008**, 29, 982-997.

threaded α -CDs contains high amount of bound water molecules, disfavours the grafting step.

Such an optimized procedure could lead to well-organized and well-distributed α -CD chemically cross-linked domains with a high functionality (*i.e.* a high number of PEO chain links going outwards the α -CD chemically cross-linked domains) in the gels. They are viewed as highly functional permanent nano-fillers and used to form nanocomposite gels. From a mechanical point of view, such nanocomposite gels are expected to exhibit enhanced mechanical properties such as the modulus, the elongation at break and the fracture energy.^[J,K]

[J] K. Haraguchi and H.-J. Li, *Macromolecules*, **2006**, 39, 1898-1905.

[K] K. Haraguchi, *Macromolecular Symposia*, **2007**, 256, 120-130.

CHRISTOPHE ALEXANDRE FRANÇOIS TRAVELET

Né le 21 octobre 1982 à Dijon (Côte d'Or)

CURSUS ET DIPLOMES

- Janvier 2006/
décembre 2008** Thèse de doctorat au laboratoire d'ingénierie des polymères pour les hautes technologies (université de Strasbourg), sous la direction du Professeur Georges HADZHOANNOU et du Professeur Guy SCHLATTER
Sujet : Systèmes supramoléculaires à base d' α -cyclodextrines et de poly(oxyéthylène) : structure et propriétés des pseudo-polyrotaxanes, polyrotaxanes et gels glissants
- Novembre 2005**
- Diplôme d'ingénieur de l'école européenne de chimie, polymères et matériaux de Strasbourg (promotion Jean-Pierre Sauvage)
 - Diplôme de chimiste de l'université de Dresde (Allemagne)
- Septembre 2000/
juin 2002** Classes préparatoires aux grandes écoles au lycée Carnot de Dijon

PUBLICATIONS, CONFERENCES ET POSTERS

DSM science and technology awards, 2008

- Publications
parues et
soumises**
- *Langmuir*, **2009**, doi : 10.1021/la900070v, Formation and self-organization kinetics of α -CD/PEO-based pseudo-polyrotaxanes in water. A specific behavior at 30 °C
 - *Soft Matter*, **2008**, 4, 1855-1860, Multiblock copolymer behaviour of α -CD/PEO-based polyrotaxanes : towards nano-cylinder self-organization of α -CDs
 - *Macromolecules*, **2007**, 40, 535-543, Topological polymer networks with sliding cross-link points : the "sliding gels". Relationship between their molecular structure and the viscoelastic as well as the swelling properties
 - *Macromolecular Symposia*, soumise
 - *Physical Chemistry, Chemical Physics*, soumise
 - *Journal of Physics : Condensed Matter*, soumise
 - "Diplomarbeit", université de Dresde (Allemagne), 2005

**Conférences
présentées**

- 37^{ème} colloque national du GFP, groupe français d'études et d'applications des polymères, 27-29 novembre 2007, Strasbourg
- 35^{èmes} journées d'études des polymères, JEPO 35, 16-21 septembre 2007, La Colle-sur-Loup
- European polymer congress 2007, EPF 2007, 2-6 juillet 2007, Portorož (Slovénie)
- Trends in materials and nanosciences 2006, TMN 2006, 21-24 novembre 2006, Strasbourg
- European mechanics society, EUROMECH colloquium 487, 10-13 octobre 2006, Strasbourg

**Posters
présentés**

- 2^{ème} journée scientifique du PMNA, 18 septembre 2008, Strasbourg
- 3rd international conference "smart materials, structures and systems", CIMTEC 2008, 8-13 juin 2008, Acireale (Italie)
- 6^{èmes} rencontres scientifiques de Saint-Aubin LLB-SOLEIL, 18-19 mars 2008, Saint-Aubin
- 114th BASF summer course, 20-30 août 2007, Ludwigshafen (Allemagne)

Supramolecular systems based on α -cyclodextrins and poly(ethylene oxide): structure and properties of pseudo-polyrotaxanes, polyrotaxanes and sliding gels

Abstract: We studied the threading process between α -cyclodextrins (α -CDs) and poly(ethylene oxide) (PEO) in water, thus leading to the formation of inclusion complexes called pseudo-polyrotaxanes (PPRs). At 30 °C, we established that, in a first step, α -CDs thread onto PEO chains, forming PPR molecules. At a higher length-scale, rapid aggregation of the PPR molecules occurs and threaded α -CD-based nano-cylinders form. At a higher length-scale, α -CD-based nano-cylinders associate in a Gaussian way engendering the formation of precipitated domains. Then, in a second step, the system undergoes its reorganization characterized by a compacity increase of the precipitated domains and forms a physical gel.

Then, we investigated polyrotaxanes (PRs), *i.e.* end-capped α -CD/PEO-based PPRs, in concentrated solution in dimethyl sulfoxide (DMSO) and established that they have the particularity to form physical gels with time when resting at room temperature. The molecular origin of the self-organization is the crystallization of naked PEO segments and the regular aggregation of threaded α -CDs driven by hydrogen bonding interactions of their hydroxyl groups.

Then, we studied chemical gels obtained by cross-linking PRs *via* their α -CDs. The chemical cross-linking reaction with divinyl sulfone (DVS) does not occur in soft conditions so that highly cross-linked domains cohabit with less cross-linked ones.

Systèmes supramoléculaires à base d' α -cyclodextrines et de poly(oxyéthylène) : structure et propriétés des pseudo-polyrotaxanes, polyrotaxanes et gels glissants

Résumé : Nous avons étudié le processus de complexation entre les α -cyclodextrines (α -CD) et le poly(oxyéthylène) (PEO) dans l'eau, conduisant ainsi à la formation de complexes d'inclusion appelés pseudo-polyrotaxanes (PPR). A 30 °C, nous avons établi que, dans une première étape, les α -CD complexent les chaînes de PEO, formant des molécules de PPR. A plus grande échelle, une agrégation rapide des molécules de PPR a lieu et des nano-cylindres à base d' α -CD complexées se forment. A plus grande échelle encore, les nano-cylindres à base d' α -CD s'associent de manière gaussienne, engendrant la formation de domaines précipités. Ensuite, dans une seconde étape, le système subit une auto-réorganisation caractérisée par une augmentation de la compacité des domaines précipités, et il se forme un gel physique.

Nous avons ensuite investigué les polyrotaxanes (PR), c'est-à-dire les PPR à base d' α -CD et de PEO bouchonnés stériquement aux extrémités, en solution concentrée dans le diméthylsulfoxyde (DMSO) et avons établi qu'ils ont la particularité de former des gels physiques au cours du temps à température ambiante. L'origine moléculaire de l'auto-organisation est la cristallisation des segments de PEO nus et l'agrégation régulière des α -CD complexées provenant de liaisons hydrogène par l'intermédiaire de leurs groupements hydroxyles.

Ensuite, nous avons étudié les gels chimiques obtenus par réticulation des PR par l'intermédiaire de leurs α -CD. La réaction de réticulation chimique avec la divinylsulfone (DVS) n'a pas lieu dans des conditions douces si bien que des domaines hautement réticulés cohabitent avec d'autres qui sont moins réticulés.

Mots-clefs : α -cyclodextrine ; poly(oxyéthylène) ; pseudo-polyrotaxane ; polyrotaxane ; auto-organisation ; gel physique ; gel chimique ; gel glissant.